# THE MOLECULAR BASIS OF CHILDHOOD NEPHROTIC SYNDROME

**Ania Barbara Koziell**

Thesis submitted for the degree of

Doctor of Philosophy

at the University of London

March 2002

Institute of Child Health,

London





ProQuest LLC
789 East Eisenhower Parkway
P.O. Box 1346
Ann Arbor, MI 48106-1346

## Abstract

Childhood nephrotic syndrome results from massive leakage of protein into the urine, a low plasma albumin and oedema. Disease may be kidney-specific, occur as part of a malformation syndrome, or may complicate systemic diseases such as diabetes mellitus. Despite the apparent heterogeneity, the underlying defect is loss of the normal permselective characteristics of the glomerular filtration barrier (GFB). Clues for a molecular basis came from observation of occasional autosomal dominant or recessive inheritance, and the detection of *WT1* mutations in Denys Drash syndrome (DDS), a triad of intersex, nephrotic syndrome and Wilms' tumour (Pelletier *et al*, 1991).

The role of three glomerular genes *WT1*, *NPHS1* and *NPHS2* in the pathogenesis of glomerular protein leak was investigated. *WT1* mutations were not detected in non-syndromic diffuse mesangial sclerosis (DMS) and focal segmental glomerulosclerosis (FSGS), despite their association with DDS. However, subsequent analysis established that *WT1* mutations cause Frasier syndrome, a triad of FSGS, intersex and gonadoblastoma, by reversing the normal +(KTS)/-(KTS) WT1 isoform ratio. Unfortunately, yeast 2-hybrid screens failed to ascertain any WT1 protein binding partners with clear roles in glomerular function, and through which the effects of mutations might be mediated.

A wide range of *NPHS1* mutations was detected in Finnish type congenital nephrotic syndrome (CNF) in non-Finns, and a novel mild CNF phenotype described. *NPHS2* mutations affected some CNF cases, and an overlap in the *NPHS1/NPHS2* mutation spectrum was confirmed by the discovery of a unique di-genic inheritance of mutations. This modified the phenotype from CNF to congenital FSGS, providing the first evidence for a functional inter-relationship between these genes. Finally, disrupted protein-DNA binding to an area of the *NPHS1* promoter containing a G→C base substitution was identified, suggesting the location of a transcription factor binding site and underscoring the importance of appropriate transcriptional control of *NPHS1* for correct gene function.

## Acknowledgements

First and foremost I thank Pete Scambler, for taking me on as a "free transfer" to Molecular Medicine, and without whose support there simply would have been no PhD. Of equal importance are my Mum and Dad, my husband Rod, my children Alex and Katie, and our nanny Editha, to whom I will be eternally grateful for everything. I would also like to thank Professor Martin Barratt and Dr Richard Grundy for introducing me to research, and Professor Karl Tryggvason, Dr Ulla Lenkkeri and past members of MMU especially Roy, Nora, Helen, Paola, Harry, Hannah and Robin for their helpful advice. Particular thanks goes to Catherine who has been instrumental in teaching me the "art of science", has kept me sane and who continues to provide an invaluable source of discussion and direction. Finally, I would like to thank my team, Abi and Sugi, for their suggestions, support and hard work, and for putting up with me – especially over the last 3 months. This PhD was funded by a Twistington Higgins Fellowship from the National Kidney Research Fund.

# TABLE OF CONTENTS

# LIST OF TABLES

# LIST OF FIGURES

## Abbreviations

| | |
|---|---|
| A | Absorbance |
| Å | Angstrom unit |
| AA | Afferent arteriole |
| aa | Amino Acid |
| Ac | Acetate |
| ACTN4 | alpha-actinin 4 gene |
| AD | Activation domain |
| ADS | Amplification dilution solution |
| APS | Ammonium persulphate |
| AFP | Alpha fetoprotein |
| 3-AT | 3 ammino triazole |
| BC | Bowman's capsule |
| BD | Binding domain |
| β-Gal | B-galactosidase |
| BMP | Bone morphogenic protein |
| bp | Base pair |
| BSA | Bovine serum albumin |
| C- | Carboxy |
| ° C | Degree Celcius |
| CAM | Cell adhesion molecule |
| cDNA | Complimentary deoxyribonucleic acid |
| CD2AP | CD2 adaptor protein |
| CDK | Cyclin dependant kinase |
| CDK-I | Cyclin dependant kinase inhibitor |
| Clo | Cloche mutant (zebrafish) |
| cM | Centimorgan |
| CMV | Cytomegalovirus |
| CNF | Finnish type congenital nephrotic syndrome |
| CNS | Congenital nephrotic syndrome |
| dATP | Deoxyadenosine triphosphate |
| dCTP | Deoxycytosine triphosphate |
| DCT | Distal convoluted tubule |
| DEPC | Diethyl pyrocarbonate |
| $ddH_2O$ | Distilled, deionised water |

| | |
|---|---|
| DDS | Deny Drash syndrome |
| DMS | Diffuse mesangial sclerosis |
| DNA | Deoxyribonucleic acid |
| dsDNA | Double-stranded deoxyribonucleic acid |
| ddNTP | Dideoxynucleoside triphosphate |
| DTT | Dithiothreitol |
| E | Embryonic day |
| EA | Efferent arteriole |
| Edr | Embryonal carcinoma differentiation regulated |
| EDTA | Ethylenediaminetetraacetic acid |
| EGFR | Epidermal growth factor receptor |
| EMSA | Electromobility shift assay |
| EONS | Early onset nephrotic syndrome |
| ERG-1 | Early growth response gene |
| FGF | Fibroblast growth factor |
| Flm | Floating head mutant (zebrafish) |
| FN III | Fibronectin III |
| FS | Frasier syndrome |
| FSGS | Focal segemental sclerosis |
| g | Gram |
| *g* | Acceleration due to gravity |
| GBM | Glomerular basement membrane |
| GFB | Glomerular filtration barrier |
| GNDF | Glial-cell-line-derived neurotrophic factor |
| GPI | Glycosylphosphatidyl inositol -anchor |
| GST | Glutathione-S-transferase |
| HA | Haemaglutinin |
| H and E | Haematoxylin and eosin |
| IG | Immunoglobulin |
| IGF-2 | Insulin like growth factor 2 |
| IPTG | Isopropyl- β-D-thiogalactopyranoside |
| k | Kilo |
| kB | Kilobase |
| kda | Kilodalton |
| L | Litre |
| Li | Lithium |

| | |
|---|---|
| M | micro |
| m | Milli-/or/ meter |
| M | Molar |
| MAPK | Mitogen activated protein kinase |
| M/MC | Mesangial cell |
| MCNS | Minimal change nephrotic syndrome |
| Min | Minute |
| MIS | Mullerian inhibitory substance |
| mmHg | millimeters mercury |
| MPGN | Mesangioproliferative glomerulonephritis |
| mRNA | Messenger ribonucleic acid |
| MW | Molecular weight |
| n | Nano- |
| N- | Amino |
| nm | Nanometer |
| NF1 | Nuclear factor 1 |
| NK | Not known |
| NMR | Nuclear magnetic resonance |
| *NPHS1* | Nephrotic syndrome 1 gene |
| *NPHS2* | Nephrotic syndrome 2 gene |
| NSB | Nuclear storage buffer |
| nt | Nucleotide |
| OD | Optical density |
| ORF | Open reading frame |
| p | Pico |
| P | podocyte |
| PBH | prohibitin homologue domain |
| PBS | Phosphate buffered saline |
| PCR | Polymerase chain reaction |
| PCT | Proximal convoluted tubule |
| PDGF-A | Platelet derived growth factor A |
| PEG | Polyethylene glycol |
| PKA | Protein kinase A |
| PKC | Protein kinase C |
| PMSF | Phenylmethylsulphonyl fluoride |
| PT | Proximal tubule |

| | |
|---|---|
| psi | Pounds per square inch |
| PAN | Purine aminglycoside |
| PID | Proliferation Ion Death |
| RNA | Ribonucleic acid |
| RNAase | Ribonuclease |
| rpm | Revolution per minute |
| RT-PCR | Reverse transcriptase PCR |
| SDS | Sodium dodecyl sulphate |
| SDS-PAGE | SDS-polyacrylamide gel electrophoresis |
| SF-1 | Steroidogenic factor 1 |
| SLE | Systemic lupus erythematosus |
| SORB | Sorbitol |
| SPFH | Stomatin Prohibitin Flottilin Hflk/c |
| SRN1 | Steriod resistant nephrotic syndrome 1 |
| SRY | Sex-determining region Y |
| SSCP | Single stranded conformational polymorphism |
| TA | Transcriptional activator |
| TAE | Tris-acetate/EDTA |
| TBE | Tris-borate/EDTA |
| TBS | Tris-buffered saline |
| TE | Tris/EDTA |
| TEMED | N,n,n',n'-tetramethylethylenediamine |
| Tm | Melting temperature |
| TM | Transmembrane domain |
| TR | Transcriptional regulator |
| Tris | Tris(hydroxymethyl) amino-methane |
| UAS | Upstream activation sequence |
| UTR | Untranslated region |
| UV | Ultraviolet light |
| V | Volt |
| VEGF | Vascular endothelial growth factor |
| WAGR | Wilms' tumour aniridia genitourinary malformation syndrome |
| wt | Wild type |
| WT | Wilms' tumour |
| WT1 | Wilms' tumour gene |
| X-gal | 5-bromo-4-chloro-3-indolyl-D-galactoside |

# CHAPTER 1: INTRODUCTION

## 1.1 Kidney Structure and Function

The two kidneys are anatomically complex organs located in the retroperitoneal space and composed of a large number of specialised cells arranged in a highly organised three-dimensional pattern. The length and weight of each kidney ranges from approximately 6 cm and 24g in the full term newborn to 11-12 cm in length and about 115 to 170g in the adult (Tisher and Madsen, 1991). The structural and functional unit of the kidney is the nephron, and each kidney contains approximately one million of these. Nephrons are composed of a renal corpuscle consisting of a glomerulus, Bowman's capsule and the juxtaglomerular apparatus leading into a long tube made of a single layer of epithelial cells segmented into distinct parts, a proximal tubule, Loop of Henle, distal tubule and collecting duct. Each area has a typical cellular appearance and specific functional characteristics.

Macroscopically, the kidney consists of an outer fibrous capsule and the renal parenchyma, which predominantely consists of tightly packed nephrons and can be divided into two distinct regions: an outer cortex, and central medulla (Figures 1.1 and 1.2). The cortex contains glomeruli, much of the proximal tubules and some of the distal portions whereas the medulla consists of parallel arrays of the loops of Henle and the collecting ducts. The medulla is arranged into cone shaped regions called pyramids, which extend into the renal pelvis (Briggs *et al*, 1998). The process of urine formation begins at the glomerular capillary tuft, where an ultra-filtrate of plasma is formed. The filtered fluid collects in Bowman's capsule and enters the renal tubule where it is successively modified by exposure to a sequence of specialised tubular epithelial segments with differing transport functions. Most of the glomerular filtrate is absorbed, with some additional substances secreted. The proximal convoluted tubule is located entirely within the renal cortex and absorbs approximately two-thirds of the glomerular filtrate. Remaining fluid enters the Loop of Henle which dips in a hairpin configuration into the medulla, is processed further, and returns to the cortex passing close to its

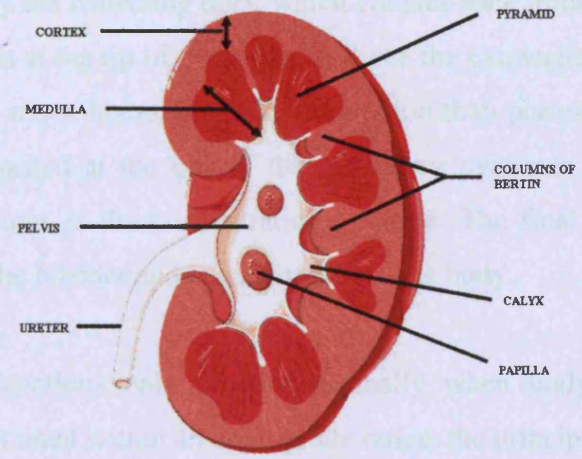


**Figure 1.1 Gross morphology of the kidney** ***(adapted with permission from http://www.kumc.edu/instruction/ medicine/pathology/ed/ch_16/c16_skid_xsect.html)***

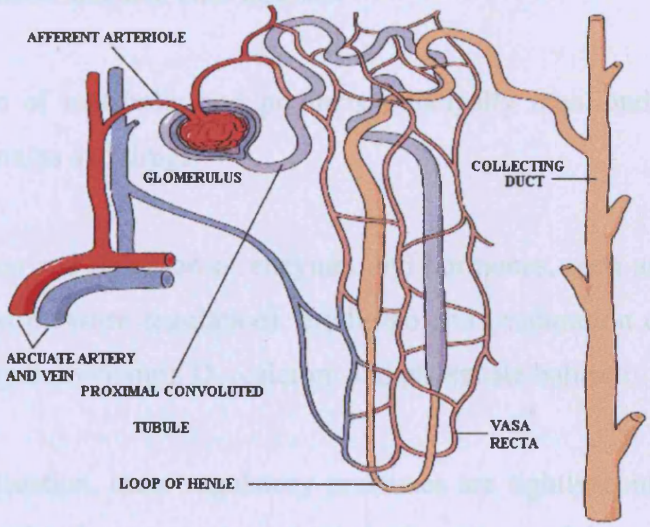


**Figure 1.2 Schematic representation of the nephron** ***(adapted with permission from http://www.Kumc.edu/instruction/medicine/pathology/ed/ch_16/c16_skid_xsect.html)***

parent glomerulus at the juxta-glomerular apparatus. It then enters the distal convoluted tubule and finally the collecting duct, which courses back through the medulla to empty at the renal pelvis at the tip of the medulla. Since the extracellular fluid in this region of the kidney has a much higher solute concentration than plasma, with the highest solute concentration reached at the tips of the medullary pyramids, the primary function of medullary structures is the concentration of urine. The final product enters the renal pelvis and then the bladder and is excreted from the body.

Since cellular functions only proceed normally when body fluid composition and volume are maintained within an appropriate range, the principle function of the kidneys is to correct the variations in these that occur as a consequence of food intake, metabolism, environmental factors and exercise. Consequently, the main functions of the kidneys can be categorised as follows:

1) Maintenance of body composition; i.e. volume, osmolarity, electrolyte concentration and acid base balance.

2) Excretion of metabolic end products principally urea, and foreign substances such as toxins and drugs.

3) Production and secretion of enzymes and hormones, such as renin (salt balance and blood pressure regulation), erythropoietin (maturation of erythrocytes) and 1,25 di-hydroxyvitamin $D_3$ (calcium and phosphate balance).

In the normal situation, these regulatory processes are tightly controlled to the extent that the body fluid volume and concentration of most ions do not deviate to any great extent from normal set points. In disease states, however, this regulation is disturbed resulting in persistent deviations in fluid volumes or ionic concentrations and cellular malfunction.

## 1.2 Renal Blood Supply

The blood supply to each kidney comes through a single renal artery arising from the descending aorta. This enters the kidney at the renal hilum and carries about one-fifth of the cardiac output, representing the highest tissue-specific flow of all larger organs in the body (approximately 350 ml/min/100g tissue). The renal artery branches into the arcuate arteries, and then into interlobular arteries. The afferent arterioles supplying glomeruli in turn branch off the interlobular vessels (Tisher and Madsen 1991). The renal circulation is unusual in that it breaks into separate glomerular and the peri-tubular capillary beds arranged in series so that all the renal blood flow passes through both. Approximately 25% of the plasma arriving at the glomerulus becomes glomerular filtrate, whereas blood cells, most proteins and about 75% of the fluid and small solutes stay in the capillary and leave the glomerulus via the efferent arteriole into the peri-tubular network. The high concentration of protein and red blood cells in the post-glomerular blood results in a high oncotic pressure within the peri-tubular capillaries, facilitating return of the tubular reabsorbate to the circulation (Kanwar *et al* 1991). The peritubular capillaries coalesce to form venules and eventually leave the kidney as the renal vein.

## 1.3 The Glomerulus

The normal glomerulus is the primary ultrafiltration unit of the kidney and consists of a capillary tuft supported on a basement membrane lined by highly specialised epithelial cells called podocytes on the urine-space aspect. These form an array of lace-like foot processes over the outer layer of the capillaries. To facilitate glomerular filtration, the hydrostatic pressure within this glomerular capillary bed is considerably higher than normal, ranging between 40 to 50 mmHg as opposed to between 5 and 10 mmHg. A Bowman's capsule forms an outer epithelial layer around the glomerulus and acts as a pouch to capture the filtrate and direct it to the proximal tubule (Tisher and Madsen 1991). The glomerulus is also associated with specialised cells known as mesangial cells, and which have both structural and regulatory functions. These glomerular structures are represented in Figures 1.3 to 1.5.

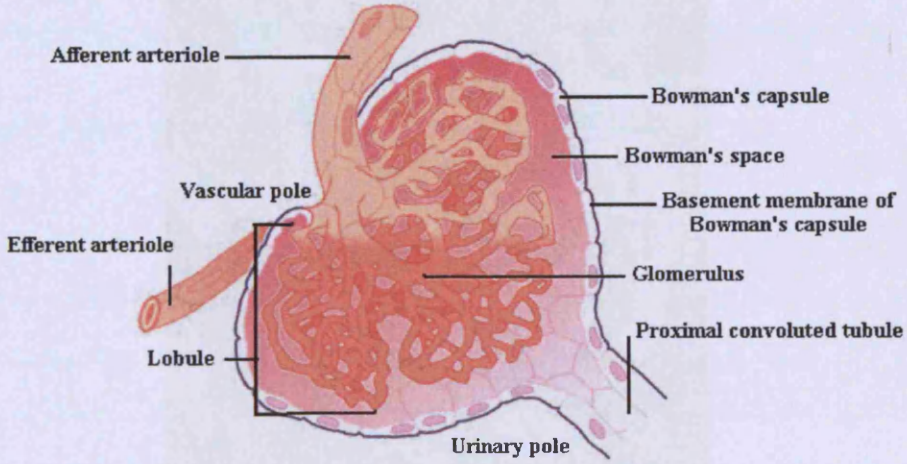


**Figure 1.3 Schematic representation of the glomerulus** ***(adapted from http://www.utmck.edu/surgery/KidneyTransplant2.asp)***

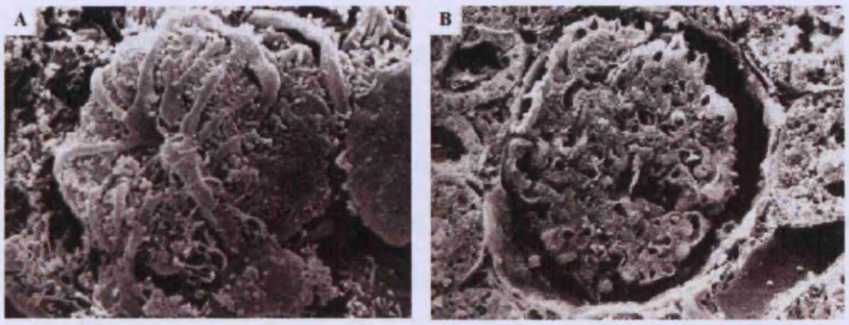


**Figure 1.4 Scanning electron micrograph of the normal glomerulus. A) Complete glomerulus with afferent arteriole. B) Freeze fractured renal glomerulus surrounded by renal tubules.** ***(reproduced with permission from http://www.sghms.ac.uk/ em/galleries/0_gallery_main/gall_frameset.html)***

**Figure 1.5 Normal renal glomerulus (H and E stain) viewed under light microscopy to show distribution of cellular components.**

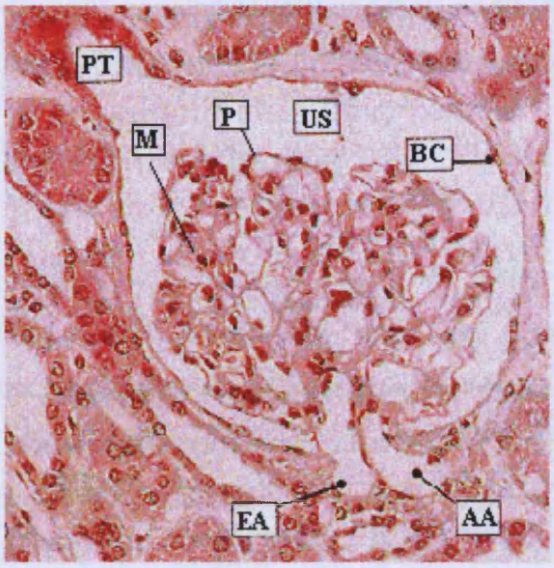


**Key: AA**- afferent arteriole , **EA**- efferent arteriole, **BC**- Bowman's capsule; **US** – urinary space; **PT** - first part of the proximal tubule; **P** – podocytes; **M** – mesangial cells.

Glomerular mesangial cells have multiple physiological roles in maintaining structure and function of the glomerular capillary ultrafiltration apparatus, and are thus able to affect glomerular hydrostatic pressure, ultrafiltration surface area and the glomerular filtration rate. This predominantly occurs through the provision of structural stability to the glomerular filtration barrier, synthesis of the extracellular matrix and secretion of a wide variety of hormones and growth factors that coordinate the activities of a variety of target cells such as podocytes and invading macrophages within the glomerulus. Mesangial cell processes attach to glomerular capillaries and complete the partial covering of the capillary by the basement membrane. The direct contact between some endothelial cells and the mesangial extracellular matrix equalises the hydrostatic pressure between the capillary and mesangium, allowing it to play a key role in regulating glomerular volume and countering the glomerular microaneurysms that result from increased capillary pressure (Blantz *et al*, 1993; Kriz *et al*, 1996). In addition, mesangial cells also form loops that regulate blood flow to the capillaries that they

surround (Inkyo-Hayasaka *et al* 1996) and extraglomerular mesangial cells provide structural support to the glomerular tuft (*reviewed in* Kriz *et al*, 1996). Although their morphology is very similar to vascular smooth muscle cells and marker expression supports a common origin for mesangial cells and the smooth muscle cells of glomerular afferent and efferent arterioles (Lindahl *et al*, 1998), their lineage remains unknown.

## 1.4 The Glomerular Filtration Barrier

Filtration of blood within the glomerular capillaries takes place at the glomerular filtration barrier (GFB). This consists of three key components: a fenestrated endothelium, an extracellular glomerular basement membrane (GBM) and glomerular visceral epithelial cells or podocytes, with distal foot processes and interposed slit diaphragms which bridge the filtration slits between adjacent podocyte foot processes (Figures 1.6 and 1.7). The flow of glomerular filtrate from the capillary lumen to the urinary space follows a strictly extracellular route, passing across the fenestrated endothelium and GBM, across the slit diaphragms and finally through the filtration slit into the urinary space where it enters the proximal tubular lumen. In essence, the GFB is a size and charge selective molecular sieve highly permeable to water, small solutes and ions, but in the normal situation restricting the passage of plasma proteins and other large macromolecules based on their size, three dimensional structure and charge (Seiler *et al*, 1975; Brenner *et al*, 1978; Venkatachalam *et al*, 1978; Kanwar *et al*, 1991). The filtration of macromolecules is generally inversely related to molecular weight. Consequently, substances of increasing size are retained with increasing efficiency and molecules with a molecular weight above 60-70 kDa are normally unable to traverse the barrier. However, ionic charge also affects filtration, so that negatively charged molecules are filtered in smaller amounts in comparison to neutrally charged molecules of comparable size, and the passage of positively charged molecules appears facilitated. Although the exact locations of the filtration functions within the barrier remain a matter of much debate, traditionally the fenestrated endothelium and GBM are thought to be the primary contributors to charge selection, whereas the GBM, podocytes and slit diaphragms appear primarily responsible for size selection. In addition, large plasma proteins appear restricted by the GBM, but the ultimate barrier for smaller proteins is thought to reside in the slit diaphragm (Karnovsky and Ainsworth, 1972; Latta 1970).

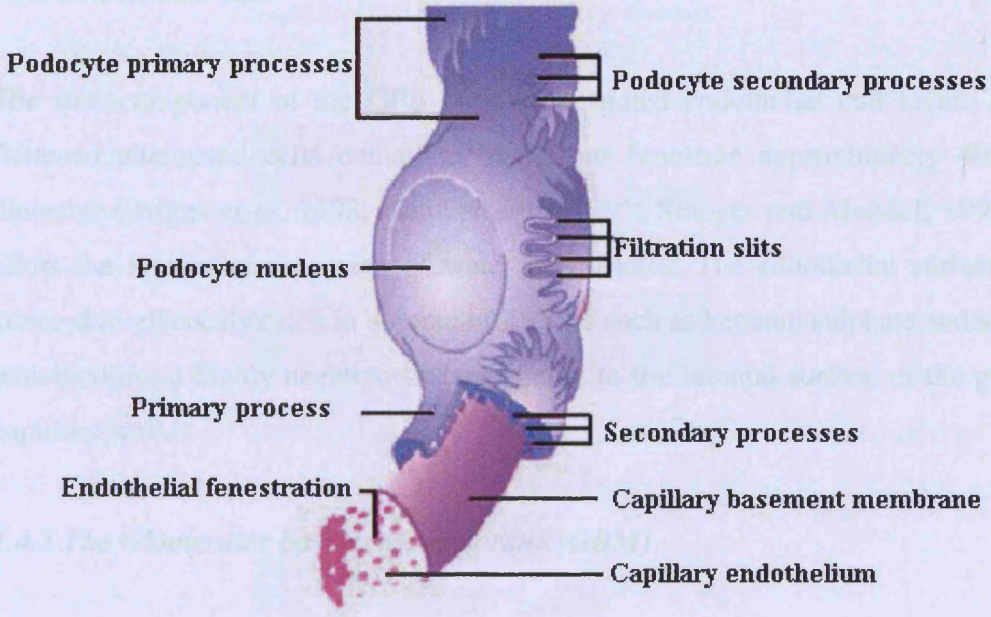


**Figure 1.6 Schematic representation of the glomerular filtration barrier** ***(adapted from http://www.utmck.edu/surgery/Kidney/Transplant2.asp)***


**Figure 1.7 Ultrastructure of the glomerular filtration barrier. A) endothelial cells lining the capillary lumen B) glomerular basement membrane and C) podocyte layer lining the urinary space** ***(Photo courtesy of Professor Risdon)***

### *1.4.1 Endothelial cells*

The first component of the GFB is the fenestrated endothelial cell layer. These are flattened attenuated cells containing numerous fenestrae approximately 40-70nm in diameter (Briggs *et al*, 1998; Kanwar *et al*, 1991; Smoyer and Mundel, 1998), which allow the intercellular passage of water and solutes. The endothelial surface layer is covered in glycocalyx rich in anionic molecules such as heparan sulphate and sialic acid, which confer a highly negative surface charge to the luminal surface of the glomerular capillary wall.

### *1.4.2 The Glomerular basement membrane (GBM)*

The GBM lies directly beneath the endothelial cells and their fenestrae. It is approximately 300nm wide and consists of a central electron-dense layer, the lamina densa, flanked by electron lucent regions, the lamina rara interna and externa (Figure 1.7) and is thought to contain pores 10 nm wide. Structural integrity is conferred by a hetero-polymeric network of type IV collagen, laminin, fibronectin, entactin and heparan sulphate proteoglycans (Maddox *et al*, 1974; Laurie *et al*, 1984). Collagen IV, a triple helical polypeptide is thought to form an interconnected network of fibres within the GBM to which the other matrix components are attached. Laminin, an asymmetrical four-armed structure, is also thought to play an important role in the structural integrity of the GBM and its interactions with the cellular layers of the capillary wall. The sulphated glycoprotein entactin, and fibronectin, a 500 kDa glycoprotein, both bind collagen IV, heparan sulphate proteoglycans and laminin cross-link the GBM components to each other. The predominant GBM proteoglycan is made up of a 400-kDa core protein called perlecan which has four to five heparan sulphate chains bound to one end of the core protein. (Kanwar *et al*, 1980; Kanwar *et al*, 1984) This results in an overall negative charge and contributes further to the anionic charge selectivity of the GFB.

### *1.4.3 Glomerular podocytes*

Glomerular podocytes form the outer component of the GFB, and play a major role in glomerular permselectivity. In common with extra-glomerular mesangial cells, an additional role is the provision of structural support to the glomerular tuft. Podocytes are highly specialised, terminally differentiated cells with a complex cellular organisation. Their function is critically based on complex cytoskeletal machinery which regulates adhesion to the GBM, motility of the foot processes on the GBM, and the function of intervening filtration slits. The cell cycle of podocytes is under tight control, and there is mounting evidence that cell cycle quiescence is required for the apparent terminal differentiation of mature cells. This may be mediated by the CDK inhibitors such as p27 and p57 (Coombs *et al*, 1998; Nagata *et al*, 1998; Nagata *et al*, 1999) and even when they are diseased, it is unusual for podocytes to undergo cell division (Nagata *et al*, 1995; Kriz *et al*, 1996). Exceptions are proliferative glomerulopathies such as HIV nephropathy, associated with decreased levels of CDK inhibitors and where podocytes regain their ability to divide (Barisoni *et al*, 2000, Shankland *et al*, 2000). It is possible that this apparent terminal differentiation of podocytes is a prerequisite for the development of their highly specialised cellular architecture and ability to attach to the GBM, although by the same token this greatly enhances their vulnerability to damage.

Podocytes are organised in a polarized fashion with apical and basolateral membrane domains and consist of three different segments: a cell body, major processes and foot processes. The basolateral domain includes the sole plates of the foot processes, which are completely embedded in the GBM and is separated from the apical domain by a structure known as the slit diaphragm. In general, the cell bodies and major processes are not directly connected to the GBM but hang freely in the urinary space fixed to the underlying capillaries only via attachment of their foot processes to the GBM (Figure 1.8), leaving a sub-cell body space between the cell body and the foot processes. The major processes arise from the cell body and split directly, or after additional branching into the more distal foot processes. These decorate the outer aspect of the GBM, and establish a typical interdigitating pattern with foot processes of neighbouring cells (Figure 1.9). Foot processes originating from a single podocyte are never adjacent to each other along the GBM, but are separated by foot processes from a neighbouring cell.

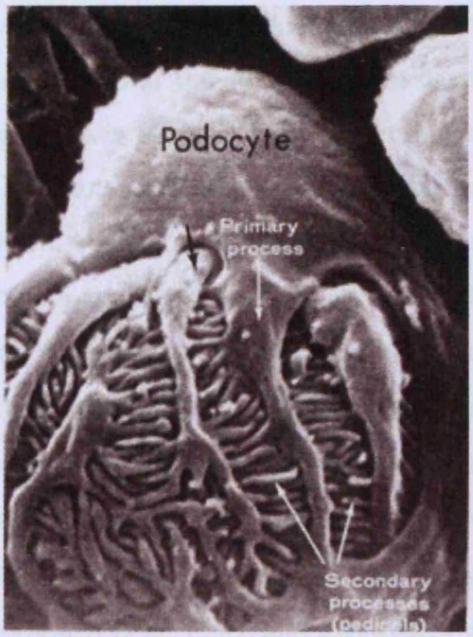


**Figure 1.8. Scanning electron micrograph of a podocyte viewed from the urinary space. The major processes can be seen extending out from the cell body and branching into the more distal foot processes. The resulting spaces between the foot processes are the filtration slits.** ***(Photo reproduced with permission from http://www.nephcure.org/mechanism.html).***

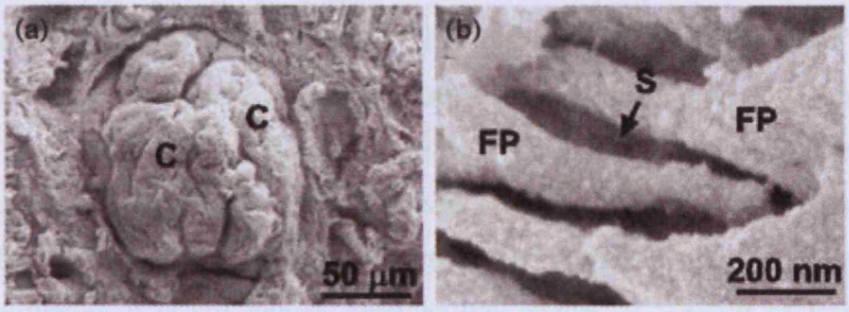


**Figure 1.9 (a) Scanning electron micrograph of a human glomerulus showing the spherical tuft formed by glomerular capillaries (C), visible after removal of the covering Bowman's capsule. (b) On higher magnification of the capillary surface, filtration slits (S) are seen between interdigitating podocyte foot processes (FP).** ***(reproduced with permission, from Tryggvason and Wartiovaara, 2001).***

Segmentation of podocytes into cell body, major foot processes and foot processes can also been seen at the level of the cytoskeleton. The gaps between them form filtration slits bridged by a structure known as the slit diaphragm described in detail in the next section (1.4.4). The intermediate filament proteins vimentin (Holthofer *et al*, 1984; Oosterwijk *et al*, 1990; Bachmann *et al*, 1983; Drenckhahn and Franke, 1988) and desmin (Yaoita *et al*, 1990), typical of mesenchymal cells, are found in the cell body. The major processes contain mainly microtubules of mixed polarity, which appear essential for process formation (Kobayashi *et al*, 2001). In contrast, the foot processes contain an actin-based cytoskeleton, which is composed of actin, myosin-II, α-actinin, talin and vinculin (Drenckhahn and Franke, 1988) which functions as a microfilament based contractile apparatus. This apparatus is anchored to focal contacts at the basal cell membrane (sole plate) of the foot processes via an $\alpha_3\beta_1$- integrin complex (Adler, 1992; Kerjaschki *et al*,1989; Korhonen *et al,* 1990) and a dystrophoglycans complex, (Raats *et al*, 2000; Regele *et al*, 2000) which in turn anchor the entire foot process to the GBM. The actin bundles are also linked to the slit diaphragm by adaptor proteins ZO-1 and catenins (Reiser *et al*, 2000) and CD2AP (Yuan *et al*, 2002). From a structural viewpoint, cell matrix contacts in podocyte foot processes are probably crucially involved in the maintenance of GBM substructure and hence GFB function. In addition, the apical membrane of the foot processes has a negatively charged surface primarily made up of podocalyxin, a CD34 related membrane glycoprotein which contacts the actin cytoskeleton through an interaction with ezrin, a member of the ERM family of actin binding proteins (Orlando *et al*, 2001). Enzymatic modification of podocalyxin causes collapse of normal foot process structure, suggesting it plays an essential role in maintaining this domain and thus GFB integrity (Gelberg *et al*, 1996). Further evidence that podocalyxin contributes to foot process stability comes from the knockout mouse, which has immature glomeruli with flattened embryonic podocytes (Doyonnas *et al*, 2001), although it is not known whether this occurs as a result of loss of negative surface charge, or through disruption of the connection with the actin cytoskeleton. In addition to the structural and charge selective contributions podocytes make to barrier integrity, an ancillary influence on glomerular permselectivity is likely to come from outside–in signalling which regulates the podocyte cytoskeleton and thus podocyte function. However, the mechanisms involved are yet to be identified.

### *1.4.4 The Slit Diaphragm*

Although it is generally acknowledged that the GBM can restrict the passage of large plasma proteins, there is evidence that the ultimate barrier for smaller proteins the size of albumin resides within a structure known as the slit diaphragm (Edwards *et al*, 1999; Rodewald and Karnovsky, 1974). This is located within the filtration slits established by the inter-digitations of the foot processes, and is attached to their sides (Figure 1.10). Aside from its putative function as an isoporous filter contributing to the size limit of the GFB, the slit diaphragm may also reinforce the GFB against the relatively high tensile force resulting from the capillary filtration pressure of about 40mmHg. Alternatively, the slit diaphragm may impede filtrate flow, thus increasing the hydraulic pressure within the inflated GBM and preventing its collapse. Initial investigations into the structural and molecular composition of the slit diaphragm membrane were through ultrastructural studies. The most frequently cited configuration for the slit diaphragm is that of Rodewald and Karnovsky (1974), who describe a central filament orientated in parallel to the podocyte membranes and regularly spaced bridge fibres, alternating from side to side, that connect the central filament to the membranes. This arrangement has been termed the "zipper" structure and the reported dimensions of the openings were 40 x 140 Å, slightly smaller than albumin (Figure 1.11). These dimensions are problematic as they imply a much more size-selective barrier than suggested by functional measurements, although all models are partly hampered by the lack of a satisfactory in vitro model able to incorporate both the charge and size restrictive elements (reviewed in Deen *et al*, 2001). A simpler ladder structure has also been postulated, based on the observations of Hora *et al* (1990), although this remains tentative, as specific dimensions for it have not been made. The slit diaphragm is thought to have a fairly constant width of about 40nm, although a few electron microscopic studies have indicated that the width may vary between 20 and 50 nm (Furunkawa *et al*, 1991; Ohno *et al*, 1992). Moreover, more recent evidence suggests that the slit diaphragm area may increase with increasing intraglomerular pressure, implying it is partially elastic (Kriz *et al*, 1996; Yu *et al*, 1997).

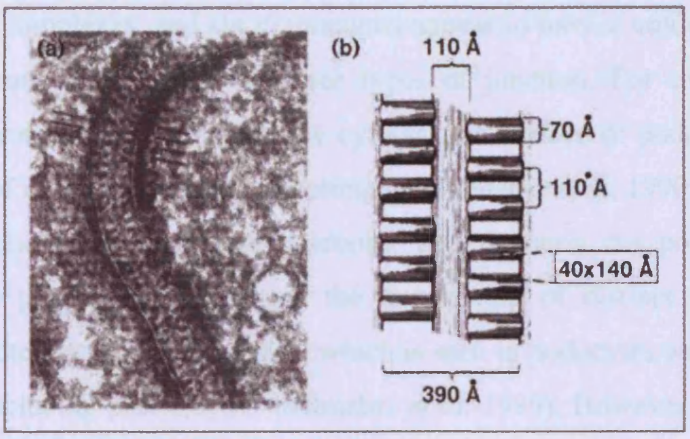


**Figure 1.10 Parallel view of slit diaphragm and structural model (a) Electron micrograph showing a zipper-like pattern in tannic acid-stained and glutaraldehyde-fixed rat glomerulus. (b) Proposed structural model of the isoporous slit diaphragm. Central filament (110 Å) and cross bridges (70 Å) delineate the 40×140 Å pores.** ***(Reproduced with permission, from Tryggvason and Wartiovaara, 2001).***

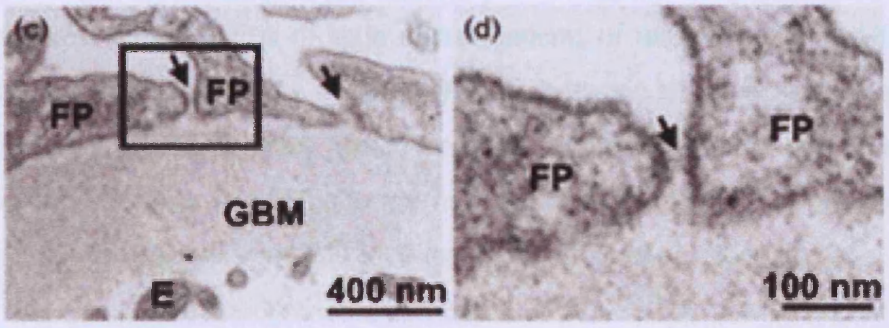


**Figure 1.11 (c) Transmission electron micrograph of the glomerular capillary wall with its three layers: endothelial (E) cells, glomerular basement membrane (GBM), and podocyte foot processes (FP). Arrows indicate filtration slits. (d) Enlargement from (c). Arrow points at the faintly stained slit diaphragm between foot processes (FP).** ***(Reproduced with permission, from Tryggvason and Wartiovaara, 2001).***

Polarised epithelial cells such as podocytes typically possess typical tripartite junctional complexes: tight junctions, actin microfilament-anchoring adherens junctions and intermediate filament adhering desmosomes. It is unclear whether podocytes have true junctional complexes, and slit diaphragms appear to have a unique morphology as they express proteins typical of all three types of junction. For example, ZO-1, a tight junction protein is expressed on the cytoplasmic surface of podocyte foot processes at the point of insertion of the slit diaphragms (Schnabel *et al*, 1990; Kurihara *et al*, 1992). Tight junctions are occluding junctions, and maintain the polarized distribution of membrane proteins by restricting the intermixing of distinct apical and basolateral surface proteins (Gumbiner, 1987), which is seen in podocytes with a number of surface proteins including podocalyxin (Schnabel *et al*, 1989). However, slit diaphragms differ morphologically from tight junctions in that adjacent podocyte plasma membrane surfaces are separated by filtrations slits, rather than lying in apposition. These relatively wide intercellular spaces are a feature more commonly seen in association with desmosomes and adherens junctions. Furthermore, proteins commonly associated with anchoring junctions such as P-cadherin, α-, β-, and γ-catenin (Reiser *et al*, 2000) and FAT, a novel member of the cadherin superfamily (Inoue *et al*, 2001) have been detected at slit diaphragm. Interestingly, ZO-1, initially thought to be specific to tight junctions, has also been detected in adherens junctions (Itoh *et al*, 1993). However, there is no apparent accumulation of actin microfilaments or intermediate sized filaments at the slit diaphragms, indicating a clear difference between slit diaphragms and adherens junctions and desmosomes. Moreover, the down regulation of catenins and desomosomal proteins during podocyte maturation corroborates their unique nature as intracellular junctions (Garrod and Fleming, 1990; Goto *et al*, 1998).

Study of rare inherited glomerular diseases and mouse models generated by gene targeting in embryonic stem cells has characterised other important components of the slit diaphragm, although its exact composition remains unclear. A key constituent of the complex to be identified in this way is the *NPHS1* gene encoding nephrin, a member of the immunoglobulin superfamily. *NPHS1* mutations are associated with severe glomerular protein leak both in human disease (Kestila *et al*, 1998), and in animal models (Putaala *et al*, 2001). Functional interdependence of nephrin on podocin, a protein similar to band-7 group of stomatins and also expressed at the slit diaphragm

(Boute *et al*, 2000; Roselli *et al*, 2002), has recently been suggested through mutational analysis of human glomerular disease, binding assays and signal transduction experiments in transfected cells (Koziell *et al*, 2002; Schwartz *et al*, 2001; Huber *et al*, 2001). A further recently identified slit diaphragm protein is NEPH-1 (Donoviel *et al*, 2001), discovered by gene trapping through retrovirus-mediated mutagenesis. Although the IgG-like domain structure and phenotype in homozygous knockout mice are remarkably similar for nephrin and NEPH-1 (Donoviel *et al*, 2001; Putaala *et al*, 2001), it is not yet clear how NEPH-1 contributes to sit diaphragm patency.

## 1.5 Development of the Nephron and the Glomerular Filtration Barrier

### *1.5.1 General aspects*

The kidney derives from the intermediate mesoderm that forms the nephric ridge. Although three kidneys differentiate in mammalian embryos, only the third or metanephros forms the permanent kidney in the adult. The first is the pronephros, which is the functional kidney in xenopus and zebra fish, but in mammals forms a rudimentary structure that degenerates. The pronephric tubule contributes to the formation of the pronephros, which elongates caudally into the intermediate mesoderm of the second kidney, or mesonephros, to form the Wolffian duct. The mesonephros functions as a primitive filtering organ in the embryo, and consists of nephron tubules and glomeruli connecting with the Wolffian duct, which may act as a signalling centre contributing to the determination of the both meso- and metanephric mesenchyme. The mesonephros regresses and remnants of the ductal systems ultimately contribute to the tubule system of the male and female reproductive tracts, rather than the permanent kidney. The third kidney, or metanephros, develops from an out branch of the Wolffian duct called the ureteric bud. Reciprocal inductive interactions between the ureteric bud epithelium and the surrounding metanephric mesenchyme result in the formation of the collecting duct system and the nephrons of the permanent kidney. Interestingly, the pronephros, mesonephros and metanephros all display similar filtration units with corresponding patterns of gene expression, for example for *Pax-2* and *WT1*, suggesting a degree of conservation within the genetic programme of kidney organogenesis (Carroll and Vize, 1996; Heller and Brandli, 1997).

### *1.5.2 Development of the nephron*

The metanephros starts to develop when the metanephric blastema appears, and the accepted model of nephron formation involves reciprocal inductive signalling between the tips of the ureteric bud to metanephric mesenchyme programmed to renal bias (Saxen, 1987). This signal induces mesenchyme condensation, migration, proliferation and mesenchyme-to-epithelial conversion resulting in the formation of a simple epithelial vesicle as shown schematically in Figure 1.12, which subsequently gives rise to the segmented nephron. The mesenchyme is transformed into a distinct epithelium that forms nephrons whereas the ureteric bud grows and branches, and eventually differentiates into the collecting ducts of the kidney.

Although nephron induction is initiated when the ureteric bud invades the nephrogenic mesenchyme, this process continues throughout most of embryogenesis. The conversion of nephrogenic mesenchyme to nephron epithelium is complex, and is arbitrarily divided into the induction period, when the mesenchyme condenses in response to inductive signals (Saxen, 1987), and the morphogenetic period, when actual epithelialisation takes place. Soon after the formation of the primary condensate the invading ureteric bud divides for the first time, yielding a T-shaped structure. At this stage, two small cell aggregates appear at the lateral side of the tips of the T-bud, and represent the induction of the first nephrons. These pre-tubular aggregates become detectable by three-dimensional confocal microscopy when they consist of only four to six cells and proliferate rapidly (Bard *et al*, 2001), with the first signs of epithelialisation appearing when they reach approximately thirty cells. With maturation, the pretubular aggregates undergo a mesenchymal to epithelial transformation forming a simple epithelial tubule, which then undergoes a complex pattern of differentiation through comma-shape and S-shape stages. This involves elongation, segmentation and convolution and results in the segregation of the simple tubule into different segments of the secretory nephron: glomerulus, proximal and distal tubules. As each nephron matures, a connection is established between the distal tubule and a portion of maturing collecting duct. The

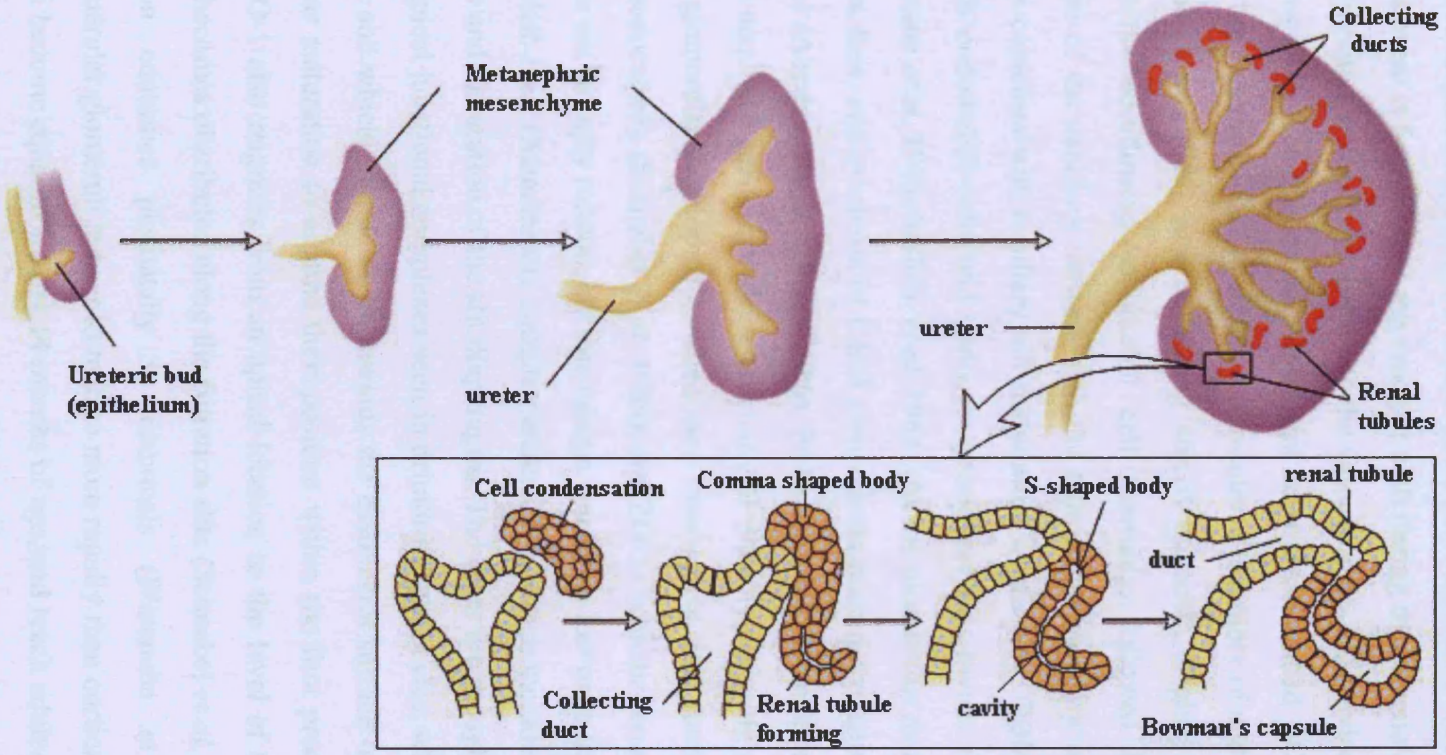


**Figure 1.12. Embryonic development of the kidney. The ureteric-bud epithelium is induced to branch by interactions with the metanephric mesenchyme. A reciprocal induction drives the mesenchyme to form an epithelium that gives rise to the nephron (Modified from Molecular Cell Biology, 4th edition).**

condensed mesenchyme is also thought to generate renal stem cells, which are expressed in the extreme periphery of the nephrogenic zone and provide a constant supply of precursor cells until the generation of additional nephrons ceases (Bard *et al*, 1994). An additional event is formation of the vascular cleft during the comma and S-shaped body stages. This site ultimately develops into the vascular pole and provides an entry point to which progenitor endothelial and mesangial cells are recruited (Abrahamson, 1987), although the exact sequence of events that results in assembly of endothelial, mesangial and podocyte precursors into a filtering unit is unknown. Tightly controlled signals result in the coordinated endothelial cell assembly, followed by formation and maturation of the capillary network into the glomerular capillary tuft. Mesangial cell formation coincides with capillary tuft maturation, whereas the GBM appears to derive from both endothelial cells and podocyte precursors that invade the S-shaped body (Abrahamson *et al*, 1988; Sariola *et al*, 1984). As the glomerulus matures the two GBM precursors fuse, and synthesis of GBM components becomes exclusively mediated by podocytes (Abrahamson and Perry,1986). Podocytes arise from induced mesenchymal cells and acquire a predominantly epithelial cell phenotype during the S-shaped body stage of glomerular development, when they form apical tight junctions and begin to express podocalyxin (Schnabel *et al*, 1989), and ZO-1 (Schnabel *et al*, 1990). Immature podocytes are strongly mitotic, but this mitotic activity is lost once they begin to mature and establish their characteristic complex architecture, which includes formation of foot processes and maturation of the slit diaphragms. The latter are thought to originate from the sub-apical junctional complexes seen in primordial podocytes, which resemble tight junctions and which migrate down towards the basolateral surface of podocytes during glomerular maturation to assume their position within the foot process (Reeves *et al*, 1978). ZO-1 also migrates from an apical location to the level of the slit diaphragm, where it becomes distributed along the filtration slits (Schnabel *et al*, 1990). Glomerular maturation continues postnatally in mammals (Watanabe *et al*, 1996), and juxtaglomerular glomeruli appear to mature more rapidly than cortical ones. In humans, glomeruli become equal in size by 14 months of age, and reach adult size by 3½ years of age, with the glomerular filtration rate reaching adult values by 1 to 2 years of age.

### *1.5.3 Molecular aspects of renal development*

All stages of metanephric kidney development are under complex molecular control, but the molecular mechanisms of nephron patterning remain poorly characterised. Data has been provided by the study of mouse mutant models, but since tubule induction and nephrogenesis is repeated approximately one million times during the formation of the metanephros, the use of conventional knockout models is limited. In addition, since many metanephric genes are also expressed during the development of the pro- and mesonephros, the phenotype seen may represent secondary effects. It is likely that renal development proceeds as a consequence of sequentially activated genes, and that secreted and contact mediated signals are involved. Induced in-growth of the ureteric bud into the mesenchymal metanephric blastema may involve co-operation of genes such as *Pax-2,* (Rothenpieler 1993), *Lim-1* (Barnes *et al*, 1994), *formin* (Maas *et al*, 1994), *Hox* genes (Davies 1996), *Emx2* (Miyamoto *et al*, 1997) and *WT1* (Kreidberg, *et al*, 1993) which are regulated by GNDF and *c-ret* (reviewed in Piscione 1999; Kuure *et al*, 2000; Schedl and Hastie, 2000). Reciprocal inductive signalling is initiated and triggers condensation of the metanephric mesenchyme. Although *WT1* is required for mesenchymal cells to complete this programme, studies in *WT1* -/- embryos suggest that initial differentiation of the mesenchyme appears independent of *WT1* expression and the ureteric bud (Donovan *et al*, 1999). This condensation results in the expression of adhesion molecules such as integrins (Novak *et al*, 1998) and cadherins (Cho *et al*, 1998), which contribute to the assembly of pretubular cell aggregates. This process may be further modulated by proteoglycans, *Eya-1,*( Xu *et al*, 1999), the *Wnt* pathway (Stark *et al*, 1994; Kispert *et al*, 1996) and various *FGF* growth factor signalling genes (Barasch *et al*, 1997; Plisov *et al*, 2001). *BMP* genes may also contribute, in particular *BMP-7*, which appears to control the maturation of mesenchymal, derived epithelial structures (Dudley *et al*, 1999). *Pax-2* and *WT1* appear to form a close regulatory circuit and to initiate the epithelialisation programme, with subsequent recruitment of integrins and laminins to facilitate the polarisation of epithelial cells during tubule formation (Ekblom, 1993). WT1 expression becomes restricted to the proximal part of the S-shaped body, which subsequently differentiates into podocytes, whereas PAX2 becomes restricted to the tubule forming part of the S-shaped body. An emerging framework of other genes such as *Pod-1*, a basic helix-loop-helix transcription factor expressed in

podocytes, also appears to regulate the mesenchymal epithelial switch and expression coincides with the onset of podocyte differentiation (Quaggin *et al*, 1998; Kuure *et al*, 2000). Glomerular endothelial cells are initially dispersed throughout the metanephric mesenchyme, and are then recruited to the clefts of the comma-shaped tubules where they proliferate and assemble in glomerular capillaries. An important mediator of this process appears to be VEGF/flk and Ephrin-B2 signalling between podocytes and endothelia (Neufeld *et al*, 1999; Takahashi *et al*, 2001). Conversely, the recruitment of glomerular mesangial cells appears dependant on PDGF-β (Lindahl *et al*, 1998). A schematic representation of some of the molecular events thought to surround the development of the kidney is made in Figure 1.13 (adapted from Piscione 1999).

Important data on glomerular differentiation and patterning is now also emerging through study of pronephric kidney development in zebrafish (Majumdar 2000; Serluca 2001), and *Xenopus* (reviewed in Brandli, 1999), which provide useful models as gene expression is extensively conserved between pronephric and metanephric kidneys. This has allowed study of the cell lineage of glomerular cells and their contribution to glomerular assembly and has provided important information about podocyte development. For example, studies of the zebrafish floating head mutant (flm) suggest that podocytes play a significant role in directing glomerular differentiation (Majumdar and Drummond, 2000), whereas study of another zebrafish mutant, cloche (clo) where endothelial cell development is blocked at an early stage, suggests that podocytes are able to differentiate in the absence of endothelia or endothelial-derived signals (Majumdar 1999). However, the subsequent appearance of irregular aggregates in the clo GBM, and apparent podocyte foot process effacement implies a role for endothelial cells in the maintenance of the mature pronephric GFB. Interesting new data has also been provided through the study of human congenital disorders resulting in glomerular dysfunction. The recently cloned genes *NPHS1* and *NPHS2*, (Kestila *et al*, 1998; Boute *et al*, 2000) are both required for the formation of slit diaphragms in podocytes and show similar patterns of expression within the developing kidney (Ruotsalainen *et al*, 2000; Roselli *et al*, 2002). Both are expressed within the mesonephros and podocyte progenitors within the S-shaped body. However the exact contribution of these genes to the molecular pathways regulating glomerular development remains unknown.

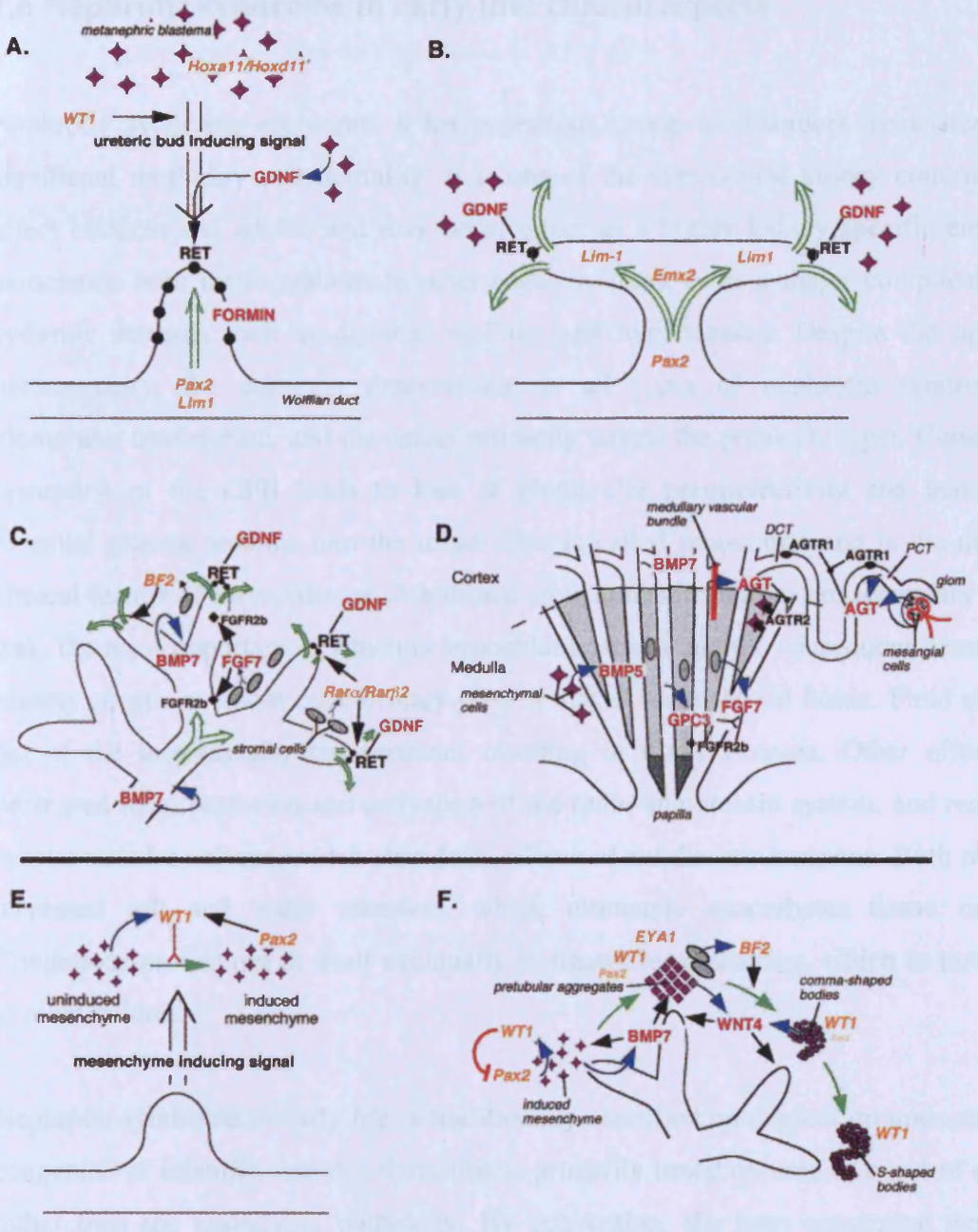


**Figure 1.13 Schematic representation of the putative molecular control of kidney development. A) – D) Branching morphogenesis: A) Ureteric bud outgrowth in response to inductive signals from the metanephric mesenchyme. B) Initiation of ureteric bud branching. C) Iterative branching and growth of the collecting system. D) Corticomedullary patterning. E) to F) Signals controlling the mesenchymal to epithelial switch: E) Initiation F) Mesenchymal – epithelial transformation *(adapted from Piscione 1999)***

## 1.6 Nephrotic syndrome in early life: clinical aspects

Nephrotic syndrome represents a heterogeneous group of disorders associated with significant morbidity and mortality. It is one of the commonest kidney conditions to affect children and adults, and may occur either as a highly kidney specific entity, in association with malformations in other organ systems, or as a major complication of systemic diseases such as diabetes mellitus and hypertension. Despite the apparent heterogeneity, the common denominator in all types of nephrotic syndrome is glomerular dysfunction, and the defect primarily targets the podocyte layer. Consequent disruption of the GFB leads to loss of glomerular permselectivity and leakage of essential plasma proteins into the urine. This is called proteinuria and is the defining clinical feature of the syndrome. Additional clinical manifestations are secondary to this leak, the most important of which is hypoabluminaemia and the consequent decrease in plasma oncotic pressure once urinary protein loss exceeds 2g /24 hours. Fluid diffuses out of the intravascular compartment resulting in tissue oedema. Other effects are decreased renal perfusion and activation of the renin-angiotensin system, and reduction in intravascular volume, which stimulates release of antidiuretic hormone. Both result in increased salt and water retention, which ultimately exacerbates tissue oedema. Continuous proteinuria in itself eventually instigates renal scarring, which in turn leads to renal failure.

Nephrotic syndrome in early life is traditionally classified on clinical grounds as either congenital or infantile, and this definition is primarily based on time of onset of disease rather than the underlying pathology. By convention, the term congenital nephrotic syndrome (CNS) is reserved for those infants presenting in the first three months of life, whereas early onset nephrotic syndrome (EONS) usually presents between 4 and 12 months. Although somewhat arbitrary, these designations do have a use, as the clinical progress of infants with CNS tends to be more severe than nephrotic syndrome occurring at other ages. Further classification is based on clinical presentation, family history, laboratory findings and renal pathology as shown in Table 1.1. Some of the histological features are not pathognomonic, but many are of well-defined diagnostic significance, for example, the immune deposits characteristically associated with secondary causes of CNS such as SLE or syphilis easily recognisable on renal biopsy.

**Table 1.1 Causes of nephrotic syndrome in early life**

**A. Primary Causes of nephrotic syndrome in early life (based on renal pathology)**

***Congenital (CNS, onset 0-3 months of life)***

Finnish type congenital nephrotic syndrome (CNF)

Diffuse mesangial sclerosis (DMS)

Focal segmental glomerulosclerosis (FSGS)

Minimal change (MCNS)

***Early onset (EONS, 4 – 12 months of life)***

Minimal change nephrotic syndrome (MCNS)

Focal segmental glomerulosclerosis (FSGS)

Diffuse mesangial sclerosis (DMS)

Diffuse mesangial proliferative glomerulonephritis (MPGN)

**B. Secondary causes of nephrotic syndrome in early life**

Infectious: syphilis, toxoplasmosis, CMV, rubella, hepatitis, malaria

Toxic: mercury, drug reactions

Systemic lupus erythematosus (SLE)

Haemolytic uraemic syndrome

**C. Specific syndromes involving other organ systems**

Denys Drash syndrome (DDS): intersex, DMS and nephroblastoma

Frasier syndrome (FS): intersex, FSGS and gonadoblastoma

Nephropathy associated with congenital brain malformations e.g. Galloway Mowat

Nail Patella syndrome

Lowe Syndrome

### *1.6.1 Congenital nephrotic syndrome (CNS)*

#### *1.6.1.1 Finnish type congenital nephrotic syndrome (CNF)*

Finnish type congenital nephrotic syndrome (CNF) was first described by Hallman *et al* in 1956, and is the prototypic from of CNS with severe proteinuria beginning *in utero*. CNF is most common in Finland, with an incidence of 1.2 per 8200 live births (Hallman *et al*, 1967), but has also been described in various ethnic groups throughout the world where the incidence is unknown (Habib *et al*, 1971; Sibley *et al* 1985; Hamed *et al*, 2001). Inheritance is autosomal recessive and both sexes are equally involved. Heterozygous individuals are normal. Positional cloning identified *NPHS1* as the causative gene for CNF in Finns (Kestila *et al*, 1998), and subsequently in non-Finns (Lenkkeri *et al*, 1999), as described in further detail in Section 1.7.2 and Chapter 4. CNF becomes manifest during early foetal life, beginning at a gestational age of approximately 15-16 weeks. The initial symptom is foetal proteinuria, which leads to a more than a 10-fold increase of the alpha-fetoprotein (AFP) concentration in the amniotic fluid (Seppala *et al*, 1976; Albright *et al*, 1990). A parallel, but less marked increase in the maternal plasma AFP level may be observed. Most CNF infants are born between 35 and 38 weeks of gestation, have a low birth weight for gestational age and foetal distress is common. The placenta is enlarged, often representing more than 25% of the total birth weight. Distinctive physical features include wide cranial sutures and large open fontanelles due to delayed ossification, small nose, wide-set eyes, low-set ears and umbilical hernia, although these are thought to be a consequence of intrauterine proteinuria rather than associated dysmorphic features. In general, infants feed and grow poorly because of substantial loss of proteins, effects of oedema, and increased incidence of pyloric stenosis and reflux. Flexion deformities of the hips, knees and elbows may be present, and are thought to be secondary to the large placenta. Early diagnosis and aggressive medical and surgical intervention are required for survival.

In most cases of CNF, symptoms appear at birth or during the first week of life. Severe nephrotic syndrome with marked ascites is generally present by 3 months, and classical features are abdominal distension, umbilical hernias and generalised oedema (Norio, 1966; Norio, 1974), as seen in Figure 1.14. This infant also demonstrates mottling of the

skin associated with hypovolaemia, and nephrotic diarrhoea secondary to bowel oedema. Initially, urinary protein losses are always severe and accompanied by profound hypoalbuminaemia and severe hypogammaglobulinaemia, compounded by a concurrent loss of complement factors B and D. Affected infants are highly susceptible to bacterial infections particularly peritonitis and respiratory infections, (Huttunen 1976; Mahan *et al*, 1984, Harris *et al*, 1986; Mathias *et al*, 1989). Thromboembolic complications due to the severity of the nephrotic syndrome are also common (Huttunen 1976; Alexander and Campbell, 1971), as is hyperlipidaemia and hypothyroidism due to urinary losses of lipid and thyroxine-binding proteins (Antikaninen *et al*, 1992; Mattoo *et al*, 1990; McLean *et al*, 1982). Seizures, frequently metabolic in origin, occur in approximately 30% of cases. Haematuria is uncommon, reflecting the lack of inflammation in the glomeruli and blood pressure and renal function are initially normal. Renal ultrasonography shows enlarged, hyperechogenic kidneys without normal corticomedullary differentiation.

Macroscopically, the kidneys are 2-3 times larger than normal, and accelerated glomerular maturation has been suggested (Autio-Harmainen, 1981). The number of glomeruli in CNF kidneys is increased (Tryggvason, 1978), and these are abnormally large and immature, which possibly mirrors defective podocyte development (Haltia *et al*, 1998). Numerous light and electron-microscopic studies of CNF kidneys have been made, and a wide variety of abnormalities detected (Huttunen *et al*, 1980; Autio-Harmainen, 1981; Autio-Harmainen *et al*, 1981; Habib and Bois, 1973; Sibley *et al*, 1985). The salient histological features of CNF are shown in Figures 1.15 and 1.16. Initially there is epithelial cell proliferation with effacement of the foot processes, evident in foetal life. Mesangial cell proliferation may also been seen, with cystic dilatation of the proximal tubules, often filled with colloid-like material. In view of this, CNF has been called "microcystic disease" in the past, but this finding is not specific and only occurs in about 75% of cases. Later there is an increase in mesangial matrix and glomerular sclerosis with tubular atrophy and a slow but progressive accumulation of glomerular basement membrane material, particularly laminin and type IV collagen in the mesangium. Immunoglobulin and complement components are not detectable in the glomeruli, but the consequences of hyperlipidaemia are evident in the renal arteries of early nephrectomy specimens (Antikainen *et al*, 1994).

**Figure 1.14 (A) Infant with CNF showing the typical clinical features of severe congenital nephrotic syndrome such as oedema and abdominal distension.**

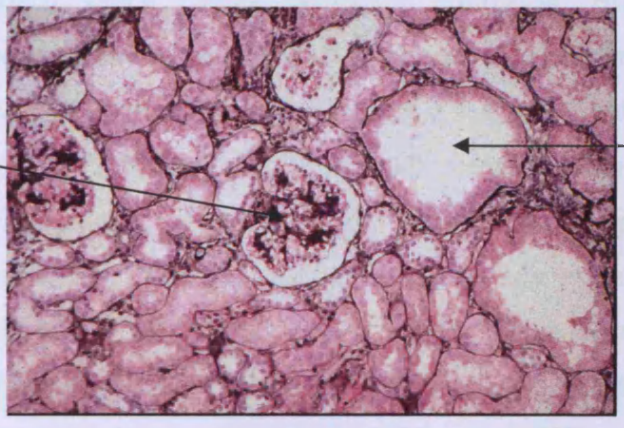


**Figure 1.14 (B) Typical CNF histology under light microscopy (Jones silver stain, x 40)**

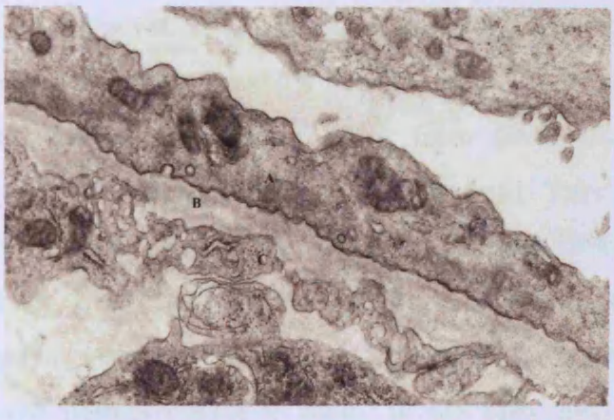


**Figure 1.14 (C) Electron micrograph of CNS showing foot process fusion: A) fused podocytes B) GBM C) hypertrophied fenestrated epithelium**

CNF is usually a progressive disease, and end-stage renal failure occurs between 3 and 8 years of age, although there are rare reports of spontaneous remission (Banton *et al*, 1990; Smith *et al*, 1991; Haws *et al*, 1992). However, this is unusual, and if untreated, the majority of CNF cases have a dismal prognosis and die by the age of 4-5 years. Prolonged survival is now possible through the use of aggressive supportive treatment with albumin infusions, diuretics and anti-proteinuric drugs, followed by dialysis and renal transplantation.

### *1.6.1.2 Diffuse mesangial sclerosis (DMS)*

Diffuse mesangial sclerosis (DMS) is the next most common variety of CNS (Habib *et al*, 1993), and its clinical course can be very similar to that of CNF, including onset of proteinuria *in utero* which causes diagnostic confusion. However, the nephrotic syndrome may be less severe than CNF at presentation, hypertension is more common and progression to end stage renal failure is often extremely rapid and occurs within the first year of life. Infants may be term, and without birth weight or placental abnormalities. Furthermore, in contrast to CNF where the pathology is confined exclusively to the kidney, DMS is also more commonly associated with extra-renal manifestations, especially neurological abnormalities. There does not appear to be any racial or ethnic predisposition, and the male to female incidence is equal. The molecular genetic background is less well defined than for CNF, as DMS represents a heterogeneous group of conditions. Many cases appear sporadic, but some families follow an autosomal recessive pattern of inheritance. Importantly, some cases are associated with *WT1* gene mutations, especially those who go on to develop Denys Drash syndrome (Denys *et al*, 1967; Drash *et al*, 1970), described in detail in section 1.6.3 (i), but the causative genes have not been identified in the majority of cases. Apart from the clinical features that distinguish it from CNF, renal histology shows a characteristically different involvement of the glomeruli. This may not be detectable initially; so renal biopsy to distinguish between CNF and DMS should be performed after 3 months of age. Usual light microscopic findings in the early stages are a fibrillar increase in mesangial matrix, expanding in mesangial areas and with no increase in mesangial cells and normal capillary walls. In the fully developed lesion of DMS (Figure 1.15 a and b), widespread hypertrophy of the podocytes is seen, with thickening

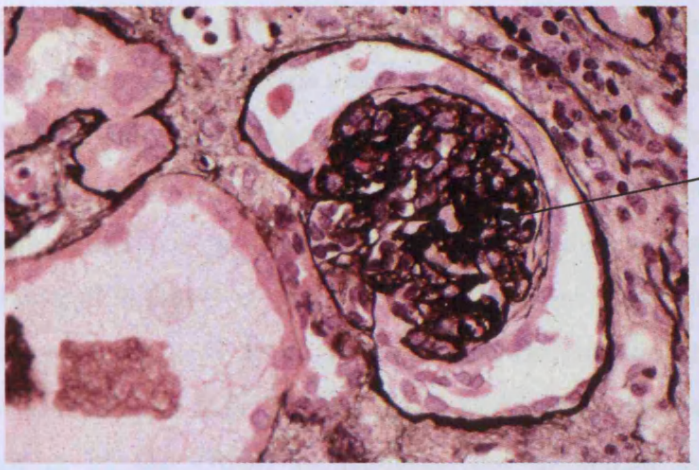


**Figure 1.15 (a) Typical light microscopic features of late DMS (Jones silver stain, x40)**


**Figure 1.15 (b) Electron micrograph if DMS showing markedly increased mesangial matrix without hypercellularity**

of the basement membranes and accumulation of mesangial matrix, which almost obliterates the capillary lumens. In advanced stages, the mesangial sclerosis results in contraction of the capillary tufts and consequent expansion of the urinary space. A layer of hypertrophied and vacuolised podocytes surround the tufts, but crescents are unusual. These various stages may co-exist, and often a corticomedullary gradient is seen with the deepest glomeruli being less affected than the more superficial ones. Tubular dilatation is frequent, especially in the deeper cortex. On electron microscopy, there is typical foot process fusion as seen in CNF, mild hypertrophy of the endothelial cells and segmental splitting of the GBM. In addition, the mesangial cells are markedly hypertrophic and surrounded by abundant mesangial matrix that often contains collagen fibrils. Mesangial deposits of Ig M, C3 and C1q may be present in the mildly affected glomeruli, while deposits of Ig M and C3 outline the periphery of sclerosed glomeruli.

Other laboratory findings mirror those of CNF, although onset of end stage renal failure may occur earlier and proteinuria may be less severe. In common with CNF, DMS is refractory to all treatment and clinical management is focused around supportive therapies such as dialysis and eventual transplantation.

#### *1.6.1.3 Congenital focal segmental glomerulosclerosis (FSGS) and minimal change (MCNS)*

These morphological variants of congenital nephrotic syndrome exist, but are rare. FSGS and MCNS represent a heterogeneous mix of aetiologies, and their clinical features may overlap. Clinical and laboratory features usually mirror CNF, at least initially, but this type of CNS may respond to immunosuppressive therapy. The mode of inheritance is often unclear, although interestingly, the risk of a sibling affected by nephrotic syndrome is often higher in a family where an infant has developed congenital FSGS or MCNS, and some cases do appear to follow an autosomal recessive pattern of inheritance. As in DMS, cases of congenital FSGS in particular may be associated with developmental abnormalities in other systems.

The renal histology seen in FSGS and MCNS mirrors that seen in later life. MCNS is associated with normal light microscopic findings and foot process fusion on electron microscopy. In FSGS, initial histology shows mildly enlarged glomeruli with small

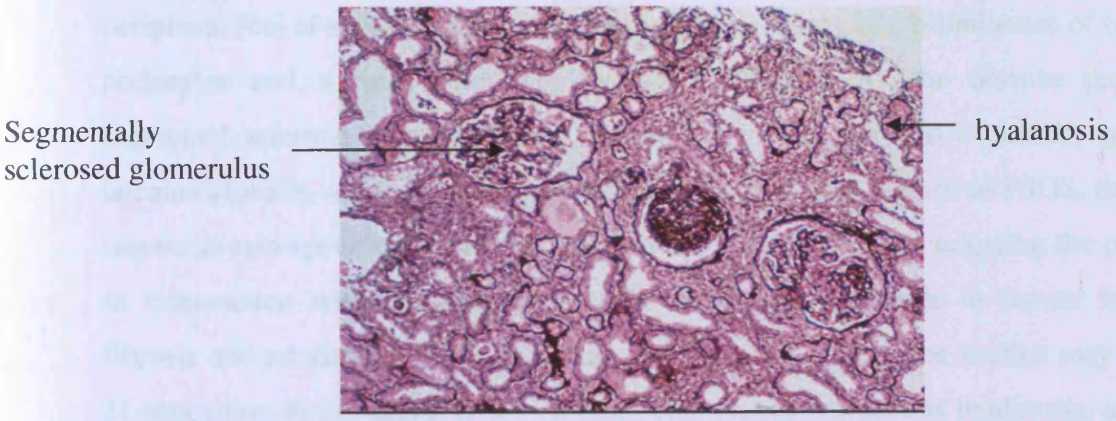


**Figure 1.16 (a) Typical light microscopic features of FSGS (Jones silver stain, x40)**

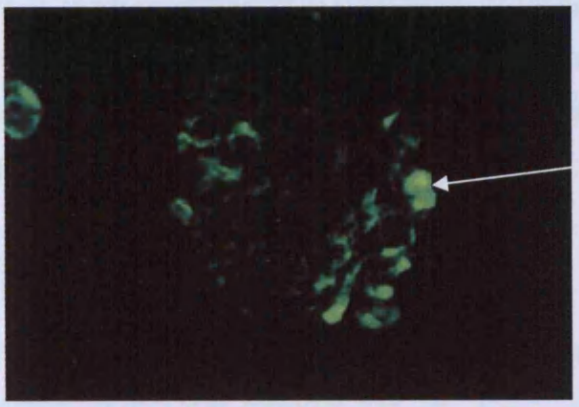


**Figure 1.16 (b) Ig M immunofluorescence in FSGS**

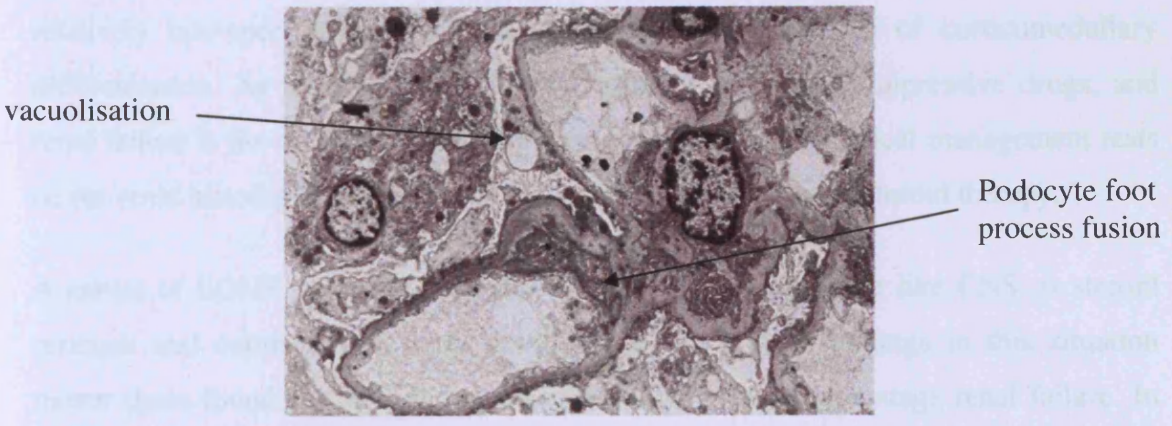


**Figure 1.16 (c) Electron micrograph of FSGS showing podocyte foot process fusion, with early microvillous transformation, occasional vacuolisation and blebbing.**

peripheral foci of segmental sclerosis, intracapillary foam cells, prominence of overlying podocytes and some surrounding interstitial fibrosis. As the disease progresses, segmental sclerotic lesions increase in size and in number and eventually glomeruli become globally sclerosed. Although this is a common late feature of FSGS, this lesion can occur non-specifically, or in relation to any injury processes targeting the podocyte. In conjunction with the changes seen in podocytes, moderate to severe interstitial fibrosis and tubular atrophy also occur, and immunofluorescence studies may show Ig M deposition in mesangial areas. Another common appearance is hyalinosis, a smooth, glassy-appearing material, resulting from the insudation of plasma proteins and this is typical of FSGS.

Clinical management is again predominantly supportive, although cases of MCNS and isolated cases of congenital FSGS may respond to steroids or other immunosuppressive therapy. Those that do not, require the same aggressive supportive therapy as infants with CNF followed by dialysis and transplantation.

### *1.6.2 Early onset nephrotic syndrome (EONS)*

Early onset nephrotic syndrome (EONS) usually presents between 3 and 12 months of age. Infants have normal gestational histories and are larger than those with CNS, as they have benefited from several more months of normal growth and development prior to the onset of symptoms. They generally present with severe oedema and ascites, and exhibit all the usual complications of nephrotic syndrome. Renal ultrasound shows relatively non-specific changes of enlarged kidneys with loss of corticomedullary differentiation. As a general rule, EONS responds to immunosuppressive drugs, and renal failure is the exception. The mainstay of diagnosis and clinical management rests on the renal histology, and if appropriate, subsequent response to steroid therapy.

A subset of EONS cases develops disease that behaves far more like CNS, is steroid resistant and culminates in early renal failure. Laboratory findings in this situation mirror those found in CNS, and cases may even present in end stage renal failure. In common with CNS, a number of morphological variants are represented, namely DMS, FSGS, MCNS, occasionally MPGN, but not CNF. Cases are often sporadic, and many do not have a clear genetic basis, although autosomal recessive inheritance is well

described for familial DMS (Habib and Bois, 1993), familial MCNS (White 1973) and FSGS (Fuschuber *et al*, 1995). Autosomal dominant FSGS loci have also been identified predominantly in adult onset FSGS (Mathis *et al*, 1998; Winn *et al*, 1999), with cloning of *ACTN4* as one of the causative genes (Kaplan *et al* 2000). A well-characterised form of autosomal recessive EONS is familial steroid resistant idiopathic nephrotic syndrome, or SRN1. This has an onset between 3 months and 5 years of age, is resistant to steroid therapy, progresses rapidly to renal failure and does not recur after renal transplantation. Linkage analysis of families with SRN1 initially mapped a locus to chromosome 1q25 – q31 (Fuschuber *et al*, 1995), with subsequent cloning of the gene, *NPHS2* (Boute *et al*, 2000), described in detail in section 1.13.

### *1.6.3 Nephrotic syndrome in early life associated with extra-renal manifestations*

As indicated previously, nephrotic syndrome in early life may be associated with extra renal manifestations, either in isolated organs, for example the association of DMS and ocular abnormalities is especiallly common (Barakat, *et al*, 1982; Zies *et al*, 1996), or as part of a more widespread malformation syndrome. All are rare, but the most common examples are the Denys Drash syndrome (DDS) and Frasier syndrome (FS), both associated with *WT1* gene mutations (Pelletier *et al*, 1991; Barbeaux *et al*, 1997), Galloway Mowat syndrome in which no causative gene has as yet been identified, Nail Patella syndrome, which results from *LMX1B* mutations (Vollrath *et al*, 1998), and Lowe's syndrome, associated with mutations of the *OCRL1* gene (Leahey *et al*, 1993; Nussbaum *et al*, 1997). The *WT1* gene is a presumptive transcription factor, with four C terminal $Cys_2$-$His_2$ zinc fingers mediating sequence specific binding, and an N terminal proline/glutamine rich domain implicated in transcriptional activation (Gessler *et al*, 1990; Call *et al*, 1990). In view of the critical role the *WT1* gene plays throughout the formation of the metanephros, nephrotic syndromes associated with *WT1* gene mutations are thought to be associated with defective glomerular development. In view of this, DDS and FS were considered the most likely to provide insights into the molecular basis of nephrotic syndrome, and were examined in more detail.

### *1.6.3.1 The Denys Drash syndrome (DDS)*

The Denys Drash syndrome (DDS) (Denys , 1967; Drash *et al*, 1970), consists of a triad of intersex, Wilm's tumour and nephrotic syndrome secondary to DMS (Eddy, 1985). Extra-renal manifestations are exceedingly rare, but have also been described: namely ventriculoseptal defect, mental retardation, other cerebral and ocular abnormalities and diaphragmatic hernia (Gertner *et al*, 1980; Jadresic *et al*, 1990; Coze *et al*, 1993; Devriendt *et al*, 1995).

The classic presentation of DDS is within the newborn period as a child with ambiguous genitalia. Although some cases may present with normal male genitalia, the vast majority will appear phenotypically female or have ambiguous genitalia and a normal male karyotype. The relative paucity of cases with a female karyotype may be because of a relative under-diagnosis of the syndrome in females with DMS, but no intersex or Wilm's tumour, which undoubtedly form part of the DDS spectrum. A wide variety of genital abnormalities are seen, and usually the internal gonad present is inappropriate for the external genitalia and the chromosomal sex, resulting in true hermaphroditism (Edidin, 1985). Most cases with a 46XX karyotype appear normal, but may occasionally have streak gonads, whereas most patients with a 46XY karyotype exhibit ambiguous genitalia or male pseudo-hermaphroditism. Thus in phenotypic females with 46 XY, the internal gonads are often dysgenetic, and present as streak ovaries, rudimentary testicular tissue, or a mixture of both (Edidin, 1985; Eddy and Mauer, 1985), with persistence of Wolffian duct structures, or a mixture of both Mullerian and Wolffian duct structures. Gonadoblastomas may occur, and these may be uni- or bilateral (Eddy, 1985; Manivel *et al*, 1987; Pelletier *et al*, 1991).

The renal involvement in DDS is two-fold, the development of a progressive glomerulopathy and Wilm's tumour. The glomerulopathy characteristically manifests as DMS, although an association with FSGS unrelated to hyperfiltration injury has also been documented (Schmitt *et al*, 1995). Onset of nephrotic syndrome is either at birth as a classical CNS with intrauterine onset (Devriendt *et al*, 1995), or in the first few years of life. The presence of nephrotic syndrome is now generally regarded as the key defining feature as DDS, as this can exist in either a complete form, consisting of all

three components of the triad, or in an incomplete form in which the nephropathy is present in association with only one of the other features, either Wilm's tumour or intersex (Manivel *et al*, 1987; Coppes *et al*, 1993; reviewed in Mueller, 1994). The average age of onset of the nephropathy is 1.37 years (range 0-17 years), and progression into renal failure inevitable. Other renal defects have also been described in association with DDS, namely unilateral hydronephrosis (Barakat e*t al*, 1974), duplication of the renal pelves and ureters (Goldman *et al*, 1981), double left kidney, and horseshoe kidney (Gallo and Chemes, 1987), but these are uncommon.

Most but not all DDS patients develop Wilms' tumour, with a median age of presentation in 18 months (range 0.01 – 13 years). Approximately 80% are unilateral and 20% bilateral (Coppes *et al*, 1993; reviewed in Mueller, 1994). This is in contrast to the median age of sporadic Wilms' tumour, which is 44 months, and the incidence of bilateral tumours, which is 8% (Coppes *et al*, 1989, Montgomery *et al*, 1991). The histological features of Wilms' tumour are no different to the sporadic form, but intralobar nephrogenic rests are found in the kidneys of most cases of DDS compared with only 15% of cases with sporadic Wilms' tumour (Beckwith *et al*, 1990). Intralobar nephrogenic rests are thought to arise as a result of disruption of early events in nephrogenesis, and to be precursor lesion of Wilms' tumour (Beckwith *et al*, 1993).

DDS is usually sporadic. However there are reports of a probable affected male and female sib-pair (Stump *et al*, 1954), as well as affected male twins (Carter *et al*, 1980). The majority of DDS cases are now known to be associated with *de novo* constitutional mutations of the *WT1* gene (Pelletier *et al*, 1991), although in isolated cases typical DDS-related mutations have been detected in the phenotypically normal father, raising the possibility of incomplete penetrance (Coppes *et al*, 1992; Nordenskjold *et al*, 1994). The most common mutation is an R394W change in exon 9, which encodes the third zinc finger. This is present in almost half of the cases studied, and DDS mutations tend to cluster within the third zinc finger region (reviewed in Little, 1997). However, *WT1* mutations have also been detected in other regions of the gene, and genotype-phenotype correlation has provided important insights into the molecular pathology of DDS.

### *1.6.3.2 Frasier syndrome (FS)*

Frasier syndrome (FS) was first described in a pair of female monozygotic twins, one of whom presented with abdominal pain and was subsequently found to have a streak gonad and a teratoma, and went on to develop renal failure. Her twin was also found to have streak gonads with a gonadoblastoma *in situ* ( Frasier *et al*, 1964). Both twins had a normal male karyotype. Similar reports followed, and the entity of FS as a separate clinical syndrome to DDS eventually described (Moorthy *et al*, 1987).

The classic definition of FS includes only 46XY individuals with a female phenotype. Clinical presentation is similar to DDS, but with some important differences, as illustrated in Table 1.2. An association with CNS has not been described, and the nephropathy tends to present later in life, typically between 2 and 6 years of age or older. Progression to renal failure tends to be more gradual, and the renal pathology is characterised by FSGS, rather than DMS. There is no recurrence after renal transplantation, and no clear predisposition to Wilms' tumour, although one case of Wilms' tumour in association with FS has been described (Barbosa *et al*, 1999). This is the only description present in the literature, so it remains unclear as to whether this occurred by chance, or whether the features of FS should be redefined. In contrast, the risk for development of gonadal malignancies such as gonadoblastoma is more common than in DDS, and may be the presenting feature. This predisposition is likely to result from the presence of streak gonads and a Y chromosome in the same individual.

Although FS usually results from *de novo* heterozygous germline splicing mutations in intron 9 of the *WT1* gene (Barbaux *et al*, 1997; Kikuchi *et al*, 1998; Klamt *et al*, 1998), there is increasing evidence that mutations may be also detected in 46 XX females with normal genital development and FSGS, and that familial cases may occur (Klamt *et al*, 1998; Demmer *et al*, 1999), possibly following an autosomal dominant form of inheritance. This inherited form of FS is very rare, but does appear to give XY offspring a 50% likelihood of being phenotypic female with FS, and XX offspring a 50% risk of FSGS with normal ovarian development. However, the situation is complex as vertical transmission of a *WT1* splicing mutation characteristically associated with FS, but resulting in classical DDS in the child, has also been reported (Denamur *et al*, 1999).

This supports the hypothesis that FS and DDS form two ends of a spectrum of developmental disorders rather than distinct clinical entities, and that the clinical definition of FS should be broadened to include individuals with a 46XX karyotype. Progression of the FSGS nephropathy to end-stage renal disease in 46 XX cases occurs as expected, but whether there is an increased risk for gonadoblastoma is unknown. This is probably negligible, as when tested, normal ovarian function is present.

**Table 1.21 Comparison of the clinical characteristics of Denys Drash and Frasier syndrome**

| **Clinical features** | **Denys Drash Syndrome** | **Frasier Syndrome** |
|---|---|---|
| **Presentation** | Early presentation: 0-3 years | Later presentation: 10-20 years |
| **Gonadal Development** | Broad spectrum of intersex phenotype | Sex reversal in 46XY individuals.<br><br>Little or no impairment in 46 XX individuals |
| **Renal disease** | DMS | FSGS |
| **Tumour development** | High risk of Wilms' tumour | High risk of gonadoblastoma |

## 1.7 Nephrotic syndrome in early life: molecular aspects

### *1.7.1 Pathobiology of the podocyte during nephrotic syndrome*

The onset of nephrotic syndrome and loss of glomerular permselectivity is closely correlated with profound structural changes within the podocyte layer of the glomerular filtration barrier (Farquhar *et al*, 1957). It is thus likely that the primary cellular target in most types of nephrotic syndrome is the podocyte, which appears to react in a very stereotypic pattern to injurious stimuli irrespective of their nature. The understanding of the importance of podocytes in the pathogenesis of proteinuria is partly based on an increasing body of cell biological and molecular genetic evidence, and partly on anecdotal clinical reports. An example of the latter is the recent observation that the strongest predictor of renal disease progression in PIMA Indians with Type II diabetes and microalbuminuria is the number of podocytes detected per glomerulus; the fewer detected, the more rapid was disease progression (Meyer *et al*, 1999).

Podocytes may be particularly vulnerable to injury because of their relative inability to mount a proliferative response after injury. However, the factors controlling this are poorly understood. There is some evidence that the Cip/Kip family of cyclin-dependant kinase inhibitors (CDK-I), specifically p21, p27 and p57 may play a role (Combs *et al*, 1998, Shankland *et al*, 1999, 2000), but the situation is complex. Whereas the presence of p27 and p57 is associated with persistence of a differentiated and quiescent podocyte, there is now evidence to suggest that p21 expression in podocytes is associated with a pro-proliferative antiquiescent effect. Since p21, p 27 and p57 null mice all have normal glomerular architecture (Kim *et al*, 1999; Ophascharoensuk *et al*, 1998; Hiromura *et al*, 2001), it is probable that the balance of all three members, as well as other as yet uncharacterised factors, determines the ability of a podocyte to proliferate.

Injured podocytes change phenotype and appear to de-differentiate, with loss of podocyte differentiation markers such as Glepp1, WT1, synaptopodin and podocalyxin. Numerous morphological changes are seen, but the most characteristic structural alteration is the retraction and effacement of podocyte foot processes, resulting in the formation of a diffuse sheet of flattened, simple epithelium along the GBM, as seen in

Figures 1.17 and 1.18. Other structural changes include cell swelling, and reoccurrence of occluding junctions, with apical displacement of the slit diaphragms. Eventually the podocyte foot processes detach from the GBM, and this is considered the most severe structural manifestation of nephrotic syndrome (Caulfield *et al*, 1976; Ito *et al*, 1986). Moreover, mathematical models have demonstrated that initial partial detachment may propagate the process (Cho *et al*, 1993). Several studies now demonstrate that the detachment of podocytes from the GBM results in the leakage of protein across the GFB (Kanwar and Rosenzweig, 1982; Whiteside *et al*, 1989; Messina *et al*, 1987; Laurens *et al*, 1995), and nephrotic proteinuria is thought to result directly from this detachment. Subsequent adhesion of cells to the denuded GBM results in scarring and obliteration of the urinary space. Theses changes are irreversible and ultimately lead to glomerulosclerosis and end stage renal failure (Kriz *et al*, 1998).

In addition to the changes in foot process structure during nephrotic syndrome, significant changes also occur in the morphology of the intervening filtration slits and slit diaphragms. Foot process effacement results in narrowing of these structures, the development of tight junctions between the foot processes, and reduction in the total number of filtration slits along the GBM (Kurihara *et al*, 1992). These structural alterations to the GFB may act together to reduce glomerular filtration, which occurs in human nephrotic disease (Myers and Guasch, 1994). Furthermore, animal models of proteinuria resulting from many different types of injury induce similar type of podocyte damage, with concurrent disruption of the intervening slit diaphragms. For example, podocytes are particularly susceptible to oxidative damage, as seen in the puromycin aminoglycoside (PAN) rat, which has been used extensively as a model of podocyte injury. Injection of PAN induces oxidant injury in cells via the xanthine oxidase pathway (Diamond and Karnovsky, 1986), and this can be ameliorated by antioxidants (Ricardo *et al*, 1994). In addition, podocyte injury is the major phenotype in the Mpv-17 antioxidant defective mouse (Weiher *et al*, 1990; Binder *et al*, 1999). Other experimental animal models indicating podocyte damage is key to the pathogensis of nephrotic syndrome are Masugi nephritis resulting from injection of heterologous anti-GBM antibody (Kondo, 1972), Heymann nephritis (Heymann *et al*, 1959; Kerjaschki *et al*, 1996), and more recently transgenic mice, a subject discussed in further detail in section 1.7.3.

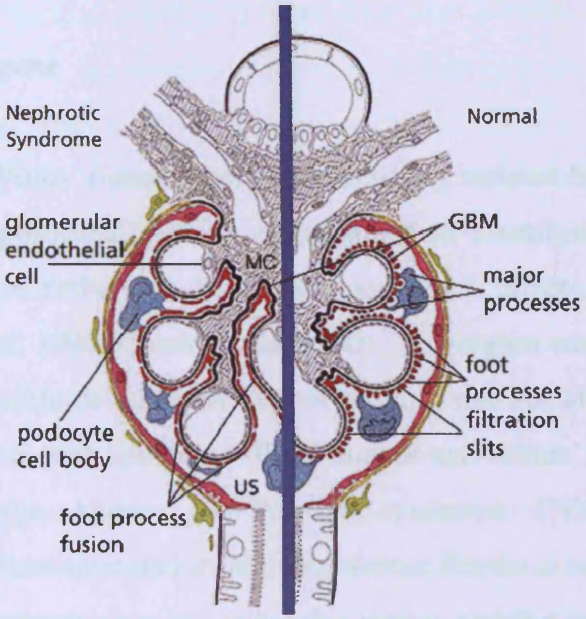


**Figure 1.17 A schematic diagram of the effect of nephrotic syndrome on glomerular components. US=urinary space; MC=mesangial cell.** ***(reproduced with permission from Somlo and Mundel)***

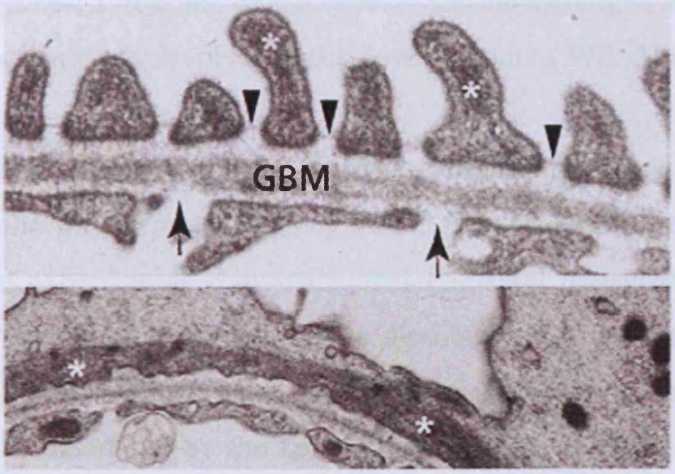


**Figure 1.18 Glomerular ultrastructure in nephrotic syndrome. The normal glomerular filter (top) consisting of a fenestrated endothelium (arrow), the GBM and podocyte foot processes with the interposed slit membrane (arrowheads). Actin filaments are present in normal foot processes (*). In nephrotic syndrome (bottom), the effaced foot process form a continuous band of cytoplasm containing a dense band of actin filaments (*) running parallel to the GBM** ***(reproduced with permission from Somlo and Mundel, 2000)***

### *1.7.2 Genes directly associated with human nephrotic disease*

#### *1.7.2.1 The WT1 gene*

The *WT1* gene (Wilms' tumour gene) was originally isolated from the chromosome 11p as a result of a positional cloning effort aimed at identifying a candidate gene for Wilms' tumour, an embryonic kidney tumour which affects approximately 1:10,000 children (Call *et al*, 1990; Gessler *et al*, 1990). This region was of particular interest as cytogenetically visible deletions of 11p, of varying size but always involving band 13, had been reported in both sporadic Wilms' tumour and Wilms' tumour associated with a complex phenotype known as WAGR syndrome (Wilms' tumour, aniridia, genitourinary malformation and mental retardation; Franke *et al*, 1979). It was presumed that a tumour suppressor gene lay within this region, and that inactivation of both copies would lead to tumourgenesis (Knudson and Strong, 1972). However it is becoming increasingly clear that the *WT1* gene has a number of different roles in health and disease, and that its function is far more complex that simply tumour suppression. The *WT1* gene is homozygously mutated in 5-10% of Wilm's tumours (Little *et al*, 1992; Gessler *et al*, 1994; Little and Wells, 1997), and interestingly, remains the only gene cloned that is definitively involved in the development of Wilms' tumour.

As well as its documented role in the pathogenesis of disease, there is considerable evidence that the *WT1* gene plays a key role in the development of those mesodermally derived tissues experiencing a mesenchymal–epithelial transition during development. This includes the genital ridge, developing mesothelium, kidney, and gonads (Pritchard-Jones *et al*, 1990; Buckler *et al*, 1991). The critical role for WT1 in urogenital development is underlined by the failure of kidney and gonadal development in mice homozygous for a *Wt1* null mutation, which die in mid-gestation from an epicardial defect (Kreidberg *et al*, 1993). As mentioned in section 1.5.3, WT1 is expressed during all stages of renal development, and expression is linked to podocyte differentiation during nephrogenesis. Initial differentiation of the metanephric mesenchyme appears independent of WT1 (Donovan *et al*, 1999), and the gene is only weakly expressed in the uncondensed metanephric blastema (Armstrong *et al*, 1993). However, expression of *WT1* increases dramatically during the mesenchymal to epithelial switch, and is highest

in the proximal part of the S-shaped body, which subsequently flattens to form podocytes. Aside from an essential role in switching of cells between a mesenchymal and epithelial state, a requirement for WT1 is apparent at multiple stages of renal development. Data obtained from genetically modified mice (Kreidberg *et al*, 1993; Moore *et al*, 1999) has provided evidence that WT1 may be required for the inductive signalling that induces outgrowth of ureteric bud from the mesonephros, and that it is involved in either survival or the reception of a survival signal from the ureteric bud, which may involve *BCL2* (Mayo *et al*, 1999). Furthermore, although WT1 does not appear to be required for the first step in nephron formation, its requirement becomes absolute in its maturation (Moore *et al*, 1999; Patek *et al*, 1999). WT1's involvement in nephrogenesis is under complex control, and there is evidence for reciprocal interactions with the *PAX2* gene modulating this process (Ryan *et al*, 1995). A number of other genes have also been implicated such as *PAX 8*, which is able to activate transcription of the *WT1* gene (Dehbi and Pelletier, 1996), *amphiregulin* (Lee *et al*, 1999), *syndecan-1* (Cook *et al*, 1996) and *E-cadherin* (Hosono *et al*, 2000), although their combinatorial role with *WT1* in renal development remains speculative.

The *WT1* gene spans about 50kb at chromosome locus 11p13, and comprises of 10 exons encoding mRNAs of approximately 3kb (Gessler *et al*, 1992). Its protein product contains two domains with apparent functional properties: a C-terminal $C_2H_2$ zinc finger domain involved in DNA binding and an N-terminal proline/glutamine rich transactivation domain. Each zinc finger is coded for by exon 7 to 10 respectively, and in mammals exon 5 and 9 are alternatively spliced, giving rise to four different splice isoforms (Haber *et al*, 1991; Gessler *et al*, 1992). In all other vertebrates tested, exon 5 is not present in the *WT1* gene, so that only two different mRNA transcripts are generated (Kent *et al*, 1995). Inclusion of exon 5 inserts 17 amino acids between the proline and glutamine rich N-terminus and the zinc finger domain. Usage of an alternative splice donor site at the end of exon 9 results in the incorporation of three additional amino acids, lysine, serine and threonine (K,T,S) and this is highly conserved throughout evolution (Kent *et al*, 1995). The mRNA isoform containing both inserts is the most common form in humans and mice, whereas the least common is the transcript lacking both, and the ratio of splice variants is highly conserved in normal foetal kidney and maintained throughout development (Haber *et al*, 1991). Depending on the presence

or absence of the two splice inserts, WT1 proteins have molecular masses of between 52 and 54 kDa (Morris *et al*, 1991). A schematic representation of *WT1* is made in Figure 1.19.

Up to 24 different isoforms may result form the combination of the alternative RNA splicing described above, RNA editing and use of alternative translational start sites, and it is likely that balanced expression of all isoforms is essential for correct gene function. This clearly generates enormous potential for WT1 proteins to fulfil many different functions within the cell. Additional *WT1* mRNA's are also generated through mRNA editing at nucleotide 839, which replaces leucine 280 by proline (Sharma *et al*, 1994), and two alternative translational initiation sites located 204 base pairs upstream of the major ATG site (Breuning and Pelletier, 1994), and one located 127 base pairs downstream (Scharnhorst *et al*, 1999). Translation initiation at the upstream in frame CTG codon results in protein isoforms with molecular masses of 60-62 kDa, whereas internal translation initiation at an in frame ATG127 codon generates smaller WT1 isoforms with apparent molecular masses of 36-38 kDa. This downstream ATG is conserved in all species sequenced so far. A separate mechanism has also recently been suggested which produces N-terminally truncated WT1 proteins (Dechsukhum *et al*, 2000). RT-PCR and Northern blot studies detected the presence of short *WT1* transcripts containing only sequences downstream of exon 5. The presence of sequence deriving from intron 5 at the 5' end suggests activation of a cryptic promoter during tumourgenesis, but further characterisation of these aberrant *WT1* transcripts is required before any putative function can be assigned.

Initial predictions made from the primary structure of the WT1 protein suggested that it was a sequence specific transcriptional regulator. In addition, the zinc finger domain of WT1 was subsequently shown to contain two putative nuclear localisation signals, in zinc finger 1 and between zinc fingers 2 and 3 (Breuning *et al*, 1996). Many groups have performed extensive structure and function analyses, but despite this WT1 function remains poorly characterised. Aside from transcriptional regulation, WT1 may also have RNA binding capability (Caricasole *et al*, 1996), and play a role in modulating RNA metabolism and post-transcriptional regulation through its ability to interact with components of the splicing machinery.

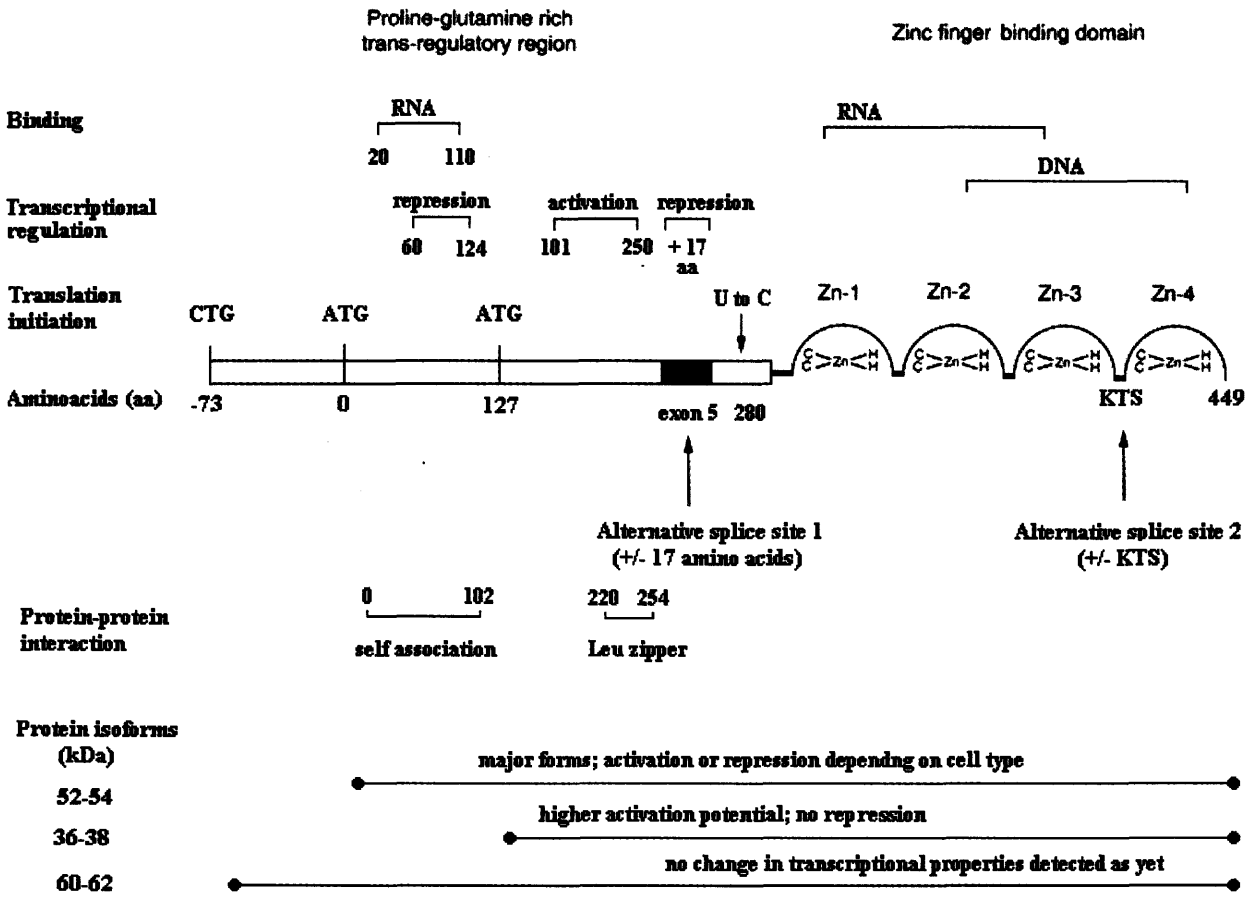


**Figure 1.19 Schematic diagram of the structural features of the WT1 gene and its protein isoforms**

It is becoming increasingly clear that WT1 function is conformation and isoform dependant, and that +KTS and –KTS isoforms serve distinct functions within the nucleus. –KTS isoforms are generally more active in transcriptional regulation and are able to bind DNA well, whereas +KTS isoforms have been shown to co-localise with splicing factors, do not bind DNA and are may have a role in RNA metabolism (Larsson *et al*, 1995; Landomery *et al*, 1999; Englert *et al*, 1995). It is now well established that the WT1 (–KTS) isoform binds DNA via its Kruppel like $C_2H_2$ zinc fingers. Recent NMR relaxation experiments have demonstrated that this ability appears to be directly related to the absence of the KTS insertion between zinc fingers 3 and 4. Insertion of KTS in this position increases the flexibility of the linker between fingers 3 and 4, which prevents zinc finger 4 from binding to its cognate site on the DNA (Laity *et al*, 2000). The WT1 zinc finger domain binds to the characteristic GC-rich *ERG1* DNA-binding element, although with about 40-fold less affinity (Rauscher *et al*, 1990; Drummond *et al*, 1994). Zinc fingers 2-4 are known to have 61% amino acid homology with those of the *early growth response 1* gene (*ERG1*) (Sukhatme *et al*, 1988), although the three zinc fingers of *ERG1* are only encoded for by a single exon, rather than three separate ones. This suggests that *WT1* and *ERG1* do not have a common evolutionary origin. A second potential DNA-binding site for WT1 consists of TCC repeats, mapped by analysis of the WT1 responsive promoters of *PDGF-A* (Wang *et al*, 1993), and *epidermal growth factor receptor EGFR* ((Englert *et al*, 1995). More recently, PCR selection of genomic DNA sequences with high affinity for the WT1 (-KTS) zinc fingers coupled with extensive mutational studies, led to the characterisation of an optimised binding site 5'-GCGTGGGAGT-3' (Nakagama *et al*, 1995). This binding site, called WTE, displays a 20-30 fold higher affinity for WT1 than the ERG1 sequence. This high affinity site has been recently reported to mediate WT1 (-KTS) binding to the promoters of *amphiregulin* (Lee *et al*, 1999) and *Bcl2* (Mayo *et al*, 1999), two genes that appear to be regulated by WT1 in vivo. There is some evidence to suggest that WT1 (+KTS) isoforms also bind DNA, but the precise binding sites and whether this happens *in vivo* remains uncertain (Bickmore *et al*, 1992; Little *et al*, 1996).

WT1 (-KTS) isoforms can both repress and activate transcription, and more than 20 putative downstream targets have been identified (summarised in Lee and Haber, 2001;

Scharnhorst *et al*, 2001). However, WT1 effects can either be repressing or activating depending on the cell type, and the target gene with which it interacts. Moreover, most target genes have been identified in transfection assays and therefore the data should be interpreted with caution as the effects of chromatin and other interacting proteins are usually not assessed. In many cases there is no *in vivo* data to support the *in vitro* observations, although some corroboration of *in vitro* findings has been made for a few putative downstream targets, namely *EGFR* (Englert *et al*, 1995), *PAX2* (Dressler *et al*, 1990), *insulin-like growth factor-2 (IGF-2)* (Drummond *et al*, 1992) which appear repressed by WT1, and more recently, for targets that appear to be activated such as *amphiregulin* (Lee *et al*, 1999) and *podocalyxin* (Palmer *et al*, 2001). Post-translational modification may also play a part in determining DNA binding, although little is known about how these alter DNA-binding and/or transcription-regulating properties. WT1 can be phosphorylated by both PKA and PKC, and phosphorylation inhibited its DNA binding activity (Sakamoto *et al*, 1997; Ye *et al*, 1996). The PKA phosphorylation sites have been mapped to two serine residues in zinc fingers 2 and 3 (Sakamoto *et al*, 1997).

The first clue that WT1 (+KTS) played a non-transcriptional role emerged from its sub-nuclear expression pattern (Larsson *et al*, 1995). Confocal microscopy revealed that this isoform preferentially co-localised with molecules implicated in RNA splicing, resulting in a "speckled" pattern, whereas WT1 (-KTS) appeared to be expressed diffusely through the nucleoplasm. Treatment of cells with RNA-ase after fixation significantly decreased the number of nuclei with this pattern, and WT1 proteins were able to co-immunoprecipitate with proteins of the splicing apparatus. A putative RNA recognition motif in amino acids 11-72 has also been identified (Kennedy *et al*, 1996), but it remains speculative as to whether this can bind RNA. In addition, WT1 has been shown to bind via the zinc finger domain to RNA sequences present in exon 2 of *IGF2* (Caricasole *et al*, 1996), although a biological role for WT1(+KTS) in the post-transcriptional regulation of *IGF2* mRNA has yet to be demonstrated. WT1 (+KTS)-RNA interactions could potentially stabilise or destabilise certain RNA forms, or could be involved in RNA editing or splicing. There is however more convincing evidence that WT1(+KTS) modulates posttranscriptional regulation via protein-protein interactions with components of the splicing machinery. A recent study showed that WT1 (+KTS) directly associates with the constitutive splicing protein U2AF65, and was incorporated

into spliceosomes during an *in vitro* splicing assay (Davies *et al*, 1998). Further evidence that WT1 proteins may bind splicing factors has come from the observation that WT1 proteins co-purify with nuclear poly(A)+ ribo-nucleoprotein (Landomery *et al*, 1999). This complex, purified by oligo(DT) chromatography, also contains amongst others, the U2AF65 protein and p116, an essential splicing factor.

However, WT1 isoforms are likely to participate in more general protein binding than just components of the splicing apparatus, and a number of other protein partners have been identified through yeast two hybrid assay and co-immunoprecipitation experiments (summarised in Table 1.4). Although none of the candidates detected so far has as yet have given direct clues about the role of WT1 in kidney disease, in contrast they have provided important information about the role of WT1 in gonadal development and sex determination. The detection of SF-1 as a WT1 binding partner, and its putative role in the regulation of *Dax-1* (Nachtigal *et al*, 1998; Kim *et al*, 1999), as well as *SRY* (Hossain and Saunders, 2000) have been instrumental in this process.

A summary of the contrasting properties of –KTS and +KTS isoforms is made in table 1.3. This predominantly *in vitro* evidence to date was recently underpinned by the recent generation of specific mouse strains in which either the –KTS or +KTS isoforms were ablated. Reduction of +KTS levels resulted in glomerular disease and complete sex reversal in XY animals, whereas reduction of the –KTS isoform resulted in hypo-dysplastic kidneys and the streak gonads in both XY and XX animals. This provided further important *in vivo* evidence that the + and – KTS splice variants have distinct roles in both renal and gonadal development (Hammes *et al*, 2001).

**Table 1.3 Summary of the properties of (+KTS) and (-KTS) WT1 isoforms**

| Isoform | DNA binding affinity | Activation of transcription | RNA binding affinity | Co-localisation with splicing speckles | SF1 binding | U2AF65 binding | Induction of Bcl2 and cell survival |
|---|---|---|---|---|---|---|---|
| -KTS | +++ | yes | +++ | low | ++ | weak | yes |
| +KTS | + | no | +++ | high | + | strong | no |

**Table 1.4 Protein binding partners of the WT1 protein *(adapted from Scharnhost et al, 2001)***

| Protein | WT1 binding site | Physiological effect | References |
|---|---|---|---|
| WT1 | First 180 amino acids | Homodimerisation; possible perquisite for TR by WT1. Mutant WT1 proteins may inhibit wt WT1 protein function through a dominant negative effect | Englert *et al*, 1995 a,b; Holmes *et al*, 1997; Reddy *et al*, 1995 |
| p53 | Zinc fingers | Stabilisation of p53; increased DNA binding by p53; modulation of TR by WT1 and p53; inhibition of apoptosis by p53 | Maheswaran *et al*, 1993; Zahn *et al*, 1998; Scharnhorst *et al*, 2000 |
| p73 | Zinc fingers | Inhibition of DNA by WT1 (-/-); modulation of TR properties of WT1 and p73 | Scharnhorst *et al*, 2000 |
| p63 | Not determined | ? | Scharnhorst *et al*, 2000 |
| SF-1 | N- terminus | Competition between WT1 (-KTS) and DAX1 for SF-1 binding leads to elevated MIS transcription | Nachtigal *et al*, 1998 |
| Par 4 | Zinc fingers<br><br>+17 amino acids | Inhibits WT1 dependant TA; augments transcriptional repression by WT1; rescues growth suppression effects of WT1<br><br>Stimulates WT1+17 amino acid TA; prevention of UV induced apoptosis | Johnstone *et al*, 1996<br><br>Richard *et al*, 2001 |
| Ciao 1 | N- terminus | Decrease TA by WT1, no effect on TR | Johnstone *et al*, 1998 |
| UBC9 | N- terminus | ? | Wang *et al*, 1996 |
| Hsp70 | N- terminus | Promotes WT1 mediated growth arrest | Maheswaran *et al*, 1998 |
| Splicing complexes (U2-B, UI-70K, coilin | Not determined | Co-localisation of WT1 (+KTS) isoforms with splicing complexes | Larsson *et al*, 1995 |
| U2AF65 | Several: zinc fingers essential | Preferential binding by WT1 (+KTS) isoforms; ?RNA metabolism | Davies *et al*, 1998 |
| WTAP | C-terminus, all forms | Partial co-localisation with splicing factors; ?sex determination | Little *et al*, 2000 |

**Key: TR, transcriptional regulation; TA, transcriptional activation; wt, wild-type; MIS, Mullerian inhibiting substance**

### *1.7.2.2 The NPHS1 gene*

The *NPHS1* gene was positionally cloned through linkage disequilibrium analysis of a Finnish population with the rare form of autosomal recessive congenital nephrotic syndrome known as Finnish Type or CNF (Kestila *et al*, 1998). Initial studies mapped the locus to chromosome 19q13.1 (Kestila *et al*, 1994), and the critical region was subsequently narrowed to 150kb (Manniko *et al*, 1995). Exon prediction programmes and database searches predicted at least ten genes within this region, of which only *NPHS1* was specifically expressed in the kidney on Northern blot analysis (Kestila *et al*, 1998). *In situ* hybridisation revealed the highest expression to be in the periphery of mature and developing glomeruli, the location of podocytes (Figure 1.20), subsequently confirmed by immunofluorescence study (Figure 1.21). The *NPHS1* gene is 26kb long and contains 29 exons, of which one, exon 23, has an unconventional donor site in that a GC replaces the usual conserved GT. The cDNA transcript is 4.3 kb. Sequence analysis of the Finnish CNF families has revealed the presence of two mutations in over 90% of CNF cases suggesting that *NPHS1* was the causative gene. Approximately 78% of Finnish CNF cases carry a two base pair deletion in exon 2 (nt121 (del 2), Fin major), which causes a frameshift resulting in a truncated 90 residue protein, whereas the remainder carry a nonsense mutation in exon 26 (R1190X, Fin minor), which results in a truncated 1109 residue protein. A variety of *NPHS1* mutations have now also been detected in many CNF cases with no demonstrable Finnish ancestry (Lenkkeri *et al*, 1999; Aya *et al*, 2000; Beltcheva *et al*, 2001; Koziell *et al*, 2002), and in contrast to Finnish CNF, these are distributed throughout the whole gene. Mice knockout studies provide further supportive evidence that mutations or absence of *NPHS1* results in a congenital nephrotic syndrome, as mice with a null mutation died from proteinuria and oedema within 24 hours (Putaala H, *et al* 2001). The importance of the *NPHS1* gene in the pathogenesis of other types of nephrotic syndrome is unknown, although there are reports of diminished *NPHS1* expression in human nephrotic syndrome (Furness *et al* 1999, Doublier *et al*, 2001), including diabetic nephropathy (Aaltonen *et al*, 2001) and an apparent causal link between *NPHS1* and some experimental models of nephrotic disease (Topham *et al*, 1999; Luimula *et al*, 2000).

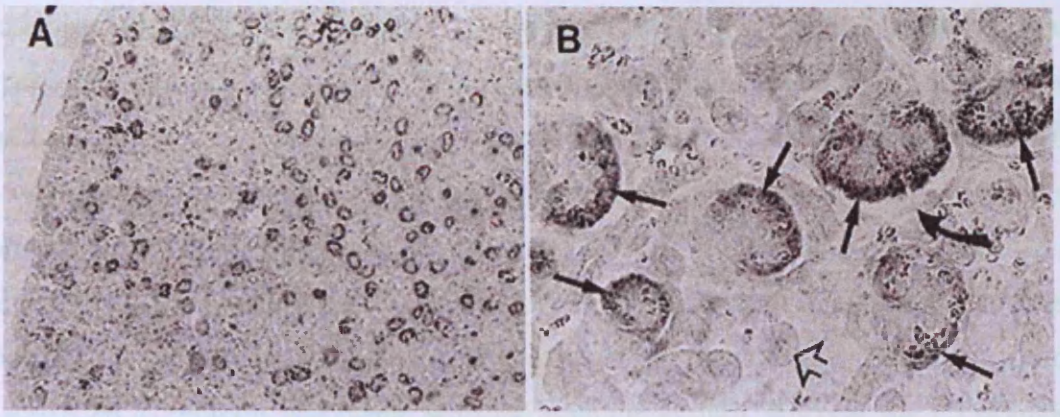


**Figure 1.20 Expression of nephrin mRNA in human embryonic tissue. A) Renal cortex showing exclusively glomerular expression B) Intense expression in the periphery of glomeruli (straight arrows), but none in Bowman's capsule (bent arrow) ot proximal tubules (open arrows)** ***(reproduced with permission from Kestila et al, 1998)***

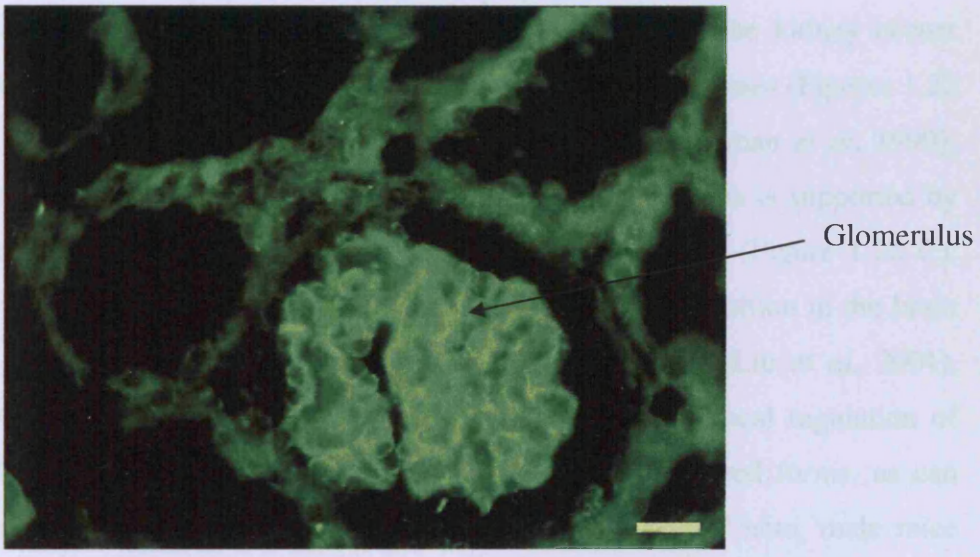


**Figure 1.21 Immunofluorescence staining in human kidney using antibodies against recombinant human nephrin. Immuno-reactivity is present in the glomerulus, but not mesangial or endothelial cells. (Bar = 20 nm)**
***(Photo courtesy of Prof Karl Tryggvason)***

The *NPHS1* gene encodes nephrin, a 1,241 amino acid single pass transmembrane protein predicted to be a type-1 glycoprotein belonging to the immunoglobulin superfamily (Kestila *et al* 1998). This represents a diverse collection of proteins with multiple roles such as mediation of immune response, various aspects of cell surface recognition and cell signalling. Superfamily members contain immunoglobulin (Ig) domains, which typically belong to one of three different subclasses V, C1 and C2 and are one of the commonest motifs found in mammalian proteins (Henikoff *et al*, 1997). The subclass represented to some extent confers protein function, so that the C1 domain is restricted to proteins associated with the immune system, whereas the C2 domain is prevalent among immune receptor related proteins and cell adhesion molecules participating in cell-cell and cell-matrix interactions (Brummendorf *et al*, 1994 and Chothia *et al*, 1997). Examples of this group are the N-CAM group (Cunningham *et al*, 1987), MAG (Fahrig *et al*, 1987), L1 (Moos *et al*, 1988), KIM-1 (Ichimura *et al*, 1998) and gicerin (Tsukamoto *et al*, 1998). C2 modules are also found in proteins participating in various developmental pathways, such as basgrin (Igakura *et al*, 1998), gicerin (Tsukamoto *et al*, 1998) and irregular chiasm C-roughest protein (Ramos *et al*, 1993).

Immunoelectron microscopy has shown the nephrin expression in the kidney occurs almost exclusively in the slit diaphragm region of podocyte foot processes (Figures 1.22 A, B and C) (Ruotsalainen *et al*, 1999; Holthofer *et al*, 1999; Holzman *et al*, 1999), further supporting an integral role in the slit diaphragm function. This is supported by the concurrent detection of nephrin within the slit diaphragm itself (Figure 1.22 C). More recently, nephrin expression was also detected in a restricted fashion in the brain and pancreas (Putaala *et al*, 2000; Putaala *et al,* 2001) and testis (Liu *et al,* 2001), although it remains unclear what role it plays in these locations. Local regulation of nephrin functions may be modulated by usage of alternatively spliced forms, as can occur in the kidney (Ahola *et al*, 1999; Holthoffer *et al*, 1999). Of note, male mice heterozygous for a null mutation of *NPHS1* do not have diminished fertility. Two alternative splice isoforms of nephrin have been detected in humans and rats, the first represents the full-length protein, whilst the second lacks the transmembrane domain and may produce a truncated soluble form of nephrin. However, the role these alternative splice isoforms may play *in vivo* is not known.

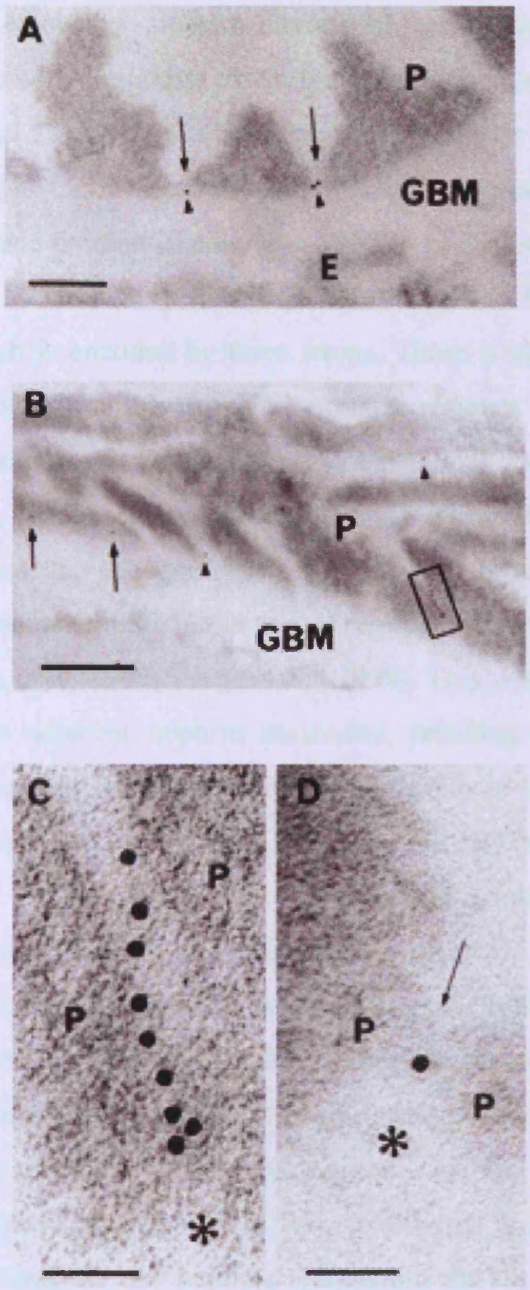


**Figure 1.22 (A,B,C) Immunoelectron microscopic localization of nephrin in human renal glomeruli. Indirect postembedding staining for nephrin by using affinity purified IgG against extracellular region of recombinant human nephrin and 10 nm gold-coupled secondary antibody. (A) The GFB. Gold label (arrowheads) is detected between foot processes of podocytes (P). Endothelium (E) is unlabeled. (Bar = 200 nm). (B) Tangentially sectioned podocyte (P) foot processes: several gold particles in a row (boxed) can be seen. (Bar = 500 nm). (C) Blow-up of boxed area of B. The GBM is marked with asterisk. (Bar = 50 nm). (D) Gold particle between slit diaphragm joining two podocytes (P). (Bar = 50 nm).**
***(photos courtesy of Professor Karl Tryggvason)***

Nephrin has a molecular weight of 150 kDa without post-translational modification and 180 kDa with, as shown on western blotting of transfected COS-7 lysates and human glomerular lysates with antibodies directed against both extra- and intracellular epitopes (Ruotsalainen *et al* 1999). The N terminal is extracellular and consists of a 22-residue signal peptide, eight C2 Ig domains and a fibronectin type III like domain connecting via a transmembrane domain to a cytoplasmic tail rich in serine, threonine and tyrosine residues (Figure 1.23). The Ig motifs are each encoded by two exons, except for Ig domain two, which is encoded by three exons. There is also a putative spacer domain between Ig modules six and seven. Two cysteine residues are present in each of the Ig repeats and are thought to form disulphide bridges. Four additional cysteines are located in Ig domain one, the spacer, the fibronectin motif and in the transmembrane domain. It has been postulated that the free cysteine in the first Ig repeat may form a disulphide bond with the cysteine residue in the spacer region of a nephrin molecule in an adjacent cell (Ruotsalainen *et al*, 1999; Tryggvason, 1999). This would lock together the first six Ig repeats of two adjacent nephrin molecules, resulting in a homophilic interaction within the slit diaphragm (Figure 1.24), comparable to that seen with other Ig cell adhesion molecules, such as N-CAM (Kiselyov *et al* 1997), C-CAM (Öbrink 1997) and L1 (Sonderegger *et al*, 1992). This cross-linking could represent the zipper like isoporous filter structure shown identified by electron microscopy (Rodewald and Karnovsky, 1974), but would result in a relatively inelastic structure. In this situation, the spacer domain and possibly also the fibronectin domain would have to be elastic, allowing the nephrin protein to stretch in response to the changes in filtration pressure that occur *in vivo* (reviewed in Tryggvason *et al*, 1999). However, experimental data confirming this dimerisation either *in vivo* or *in vitro* is lacking, and it is likely that additional components are also required to assemble the slit diaphragm.

Recent evidence indicates that nephrin may be a component of lipid rafts, dynamic assemblies within cell membranes enriched with glycosphingolipids, cholesterol, GPI-anchored proteins and signalling molecules such as Src kinases. Lipid rafts are known to participate in a variety of cellular processes such as cellular trafficking, signal transduction and cell adhesion, and that kinases and phosphatases may be required to regulate the assembly of the complex, and to facilitate the integration of newly synthesised proteins (Simons *et al*, 1997; Brown *et al*, 1998; Simons *et al*, 2000).

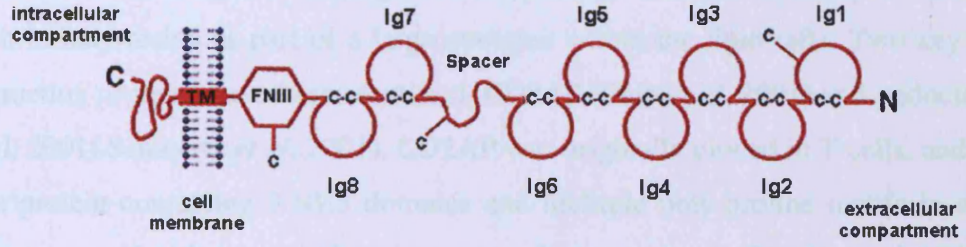


**Figure 1.23 Schematic representation of the domain structure of nephrin. The Ig repeats are shown by incomplete circles (Ig 1 - 8) connected by disulfide bridges (C-C). The locations of free cysteine residues are indicated by a ---*C*. FNIII represent the fibronectin motif and TM the transmembrane domain *(adapted from Rutosalainen et al, 1999)***

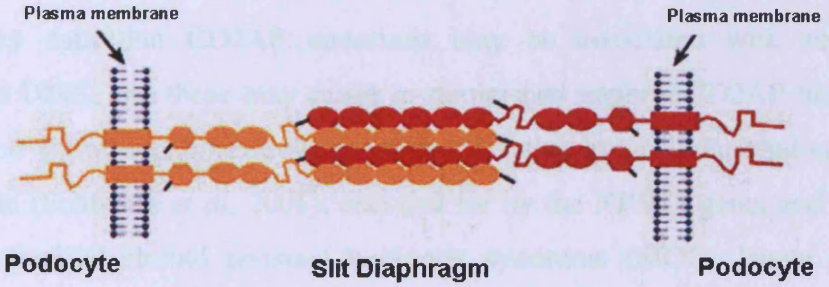


**Figure 1.24 Hypothetical model of nephrin assembly to form the isoporous filter of the podocyte slit diaphragm. Cysteine residues and two potential disulfide bridges cross-link the four nephrin molecules (black lines). The remaining single free cysteine in the fibronectin domain may react with another nephrin molecule, or another unknown molecule within the slit diaphragm *(reproduced with permission from Rutosalainen et al, 1999)***

There is preliminary data that podocyte lipid rafts may participate in nephrin phosphorylation and thus organisation of the slit diaphragm (Simons *et al*, 2001). Interestingly, these appear to contain a specific 9-O-acetylated GD3 ganglioside, and intravenous injection of a monoclonal antibody to this ganglioside into rats resulted in flattening of podocyte foot processes. However, the rats did not develop proteinuria, which makes the apparent changes in morphology difficult to interpret. In addition, nephrin may reside as part of a large complex within the lipid rafts. Two key putative interacting proteins have been identified, CD2AP (Shih *et al*, 2001) and podocin (Huber *et al*, 2001; Schwartz *et al*, 2001). CD2AP was originally cloned in T cells, and is an 80 kDa protein containing 3 SH3 domains and multiple poly-proline motifs in a tandem array, suggesting that it may function as an adapter molecule (Dustin *et al*, 1998). Mice with a null mutation for CD2AP have immune abnormalities, but surprisingly die at 6-7 weeks of nephrotic syndrome and renal failure, with histology reminiscent of human DMS (Shih *et al,* 1999). Immunofluorescence studies indicate that CD2AP is expressed in podocytes, proximal tubule, distal tubule and collecting duct of the kidney as well as being widely expressed in both mouse and human tissues, and that nephrin and CD2AP co-localise in both murine and human podocytes (Li *et al,* 2000). Dominant negative experiments have suggested a role for CD2AP in cytoskeletal rearrangement and CD2 clustering upon antigen receptor engagement (Dustin *et al,* 1998). CD2AP may play an analogous role in podocytes, anchoring nephrin to the cytoskeleton. Currently there is no direct link between CD2AP mutations and human nephrotic disease, except for preliminary data that CD2AP mutations may be associated with some cases of congenital DMS, and these may result in diminished nephrin-CD2AP binding (Green, Koziell and Shaw, unpublished observations). Another intracellular binding partner may be podocin (Schwartz *et al*, 2001), encoded for by the *NPHS2* gene, and the causative gene for familial steroid resistant nephrotic syndrome (SRN1, Boute *et al*, 2000). Podocin appears to also bind CD2AP, suggesting that all three proteins may be associated in a complex within lipid rafts at the slit diaphragm (Schwartz *et al*, 2001).

There is speculation that as well as playing a major role in the function of the mature slit diaphragm, nephrin participates in its development during nephrogenesis (Ruotsalainen *et al*, 2000). Nephrin is first detected in late S-shaped bodies, and expression is maximal adjacent to the vascular cleft. In the normal situation, maturing glomeruli all become

strongly positive for nephrin, especially during the capillary loop stage before the appearance of either foot processes or slit diaphragms. Nephrin co-localises with ZO-1, although their patterns of expression do not completely overlap. Interestingly, nephrin expression in foetal kidneys with Fin major/Fin minor genotype is absent, whereas that of ZO-1 and P-cadherin is normal. Here, early podocyte junctional complexes appear to form normally, but slit diaphragms subsequently fail to develop, which indicates that although there is no absolute requirement for nephrin in early junctional complex formation, it is indispensable for the development of slit diaphragms. Of note, this failure of slit diaphragm development is also seen in nephrin null mice (Putaala *et al*, 2001). These observations further underpin nephrin's crucial role in slit diaphragm function and in glomerular permselectivity.

### *1.7.2.3 The NPHS2 gene*

Positional cloning recently identified a third gene associated with nephrotic syndrome in early life, *NPHS2* (Boute *et al*, 2000). Initial linkage analysis of families with autosomal recessive steroid-resistant nephrotic syndrome (SRN1; onset between three months and five years) mapped the causative gene to a 12cM region on chromosome 1q25 to q31 (Fuchshuber *et al*, 1995). SRN1 is characterised by FSGS renal histology, variable mesangial cell proliferation and presence of immuno-reactants. Patients do not respond to steroid treatment and end stage renal failure is rapid following the onset of proteinuria. The locus was subsequently fine mapped to a 2.5cM region within this area, and the *NPHS2* gene identified (Boute *et al*, 2000). *NPHS2* encodes a transcript approximately 2kb in length, with a 1,149 base pair open reading frame and 635 base pair 3' UTR containing an atypical polyadenylation signal. Northern blot analysis detected strong *NPHS2* expression in adult and foetal kidney, but not in other tissues, and *in situ* hybridisation studies specifically localised expression to the podocyte layer of the glomerulus. Although homozygous mutations of the *NPHS2* gene were detected in most of the of SRN1 cases tested, only the paternal mutation was detected in four individuals.

*NPHS2* encodes a 49kDa integral membrane protein called podocin with sequence homology to the band-7 stomatin family. Database searches indicate strong homology

with human stomatin (47% identity, 67% similarity) and *Caenorhabditis elegans* MEC2 (44% identity, 67% similarity). Human stomatin (Band 7.2b) is a 31 kDa erythrocyte integral membrane protein, initially isolated from erythrocyte plasma membranes, and subsequently found to have more widespread expression (Stewart *et al*, 1992). Stomatins are thought to belong to a novel protein superfamily, bound by similar primary and secondary predicted protein structures and hydropathy profiles. This superfamily is named PID (proliferation, ion, and death), because it contains prohibitins, involved in proliferation and cell cycle control, stomatins which are involved in ion channel regulation, and the plant defence-related genes, which are involved in cell death (Nadimpalli *et al*, 2000). Members of this family expressed in eukaryotic cells have been implicated in the control of ion channel permeability and cytoskeletal organisation (Stewart *et al*, 1993), mechanoreception (Huang *et al*, 1995), tumour suppression (McClung *et al*, 1989), and lipid domain organization (Salzer, 2001).

The podocin protein is 383 amino acids long, and the band-7 stomatin signature is located between amino acids 238 and 266 (Figure 1.25). It consists of a cytoplasmic N-terminal domain, a short transmembrane domain (amino acids 105-121) and a cytoplasmic C-terminal domain, which results in a hairpin structure that probably loops through the cell membrane. The C-terminal tail also contains a characteristic SPFH (stomatin, prohibitin, flotilin, Hflk/c) or PHB (prohibitin homolgue) domain (Pfam entry: Band_7, accession number:PF1145), predicted to lie close to the membrane-associated region (http://smart.embl-heidelberg.de/), but other than the band-7 signature, the remaining sequence shows no homology with any known proteins. So far, little is known about the functions of podocin within the podocyte, although there is evidence that this group of proteins from independently organised high order homo-oligomers, resulting in a wide spread structure, which as well as serving as a stabilising molecule, interacts with other podocyte proteins and function as a linker between the plasma membrane and the cytoskeleton. There is increasing evidence that stomatin-like proteins form core components of membrane associated proteolytic complexes (reviewed in Tavernarakis *et al*, 1999), and of lipid rafts (Salzer and Prohaska, 2001). Podocin expression is confined to glomerular podocytes in the mature kidney, and clusters at the basolateral cellular surface of the foot process, on either side of the slit diaphragm (Figure 1.26).

**Figure 1.25 Schematic representation of podocin, showing predicted intra-cellular structure**

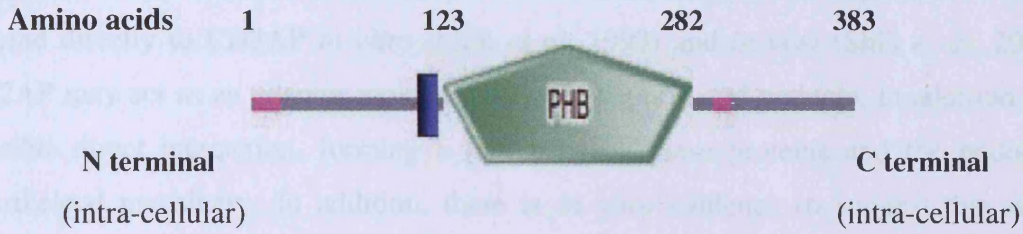


**Key: Transmembrane segments as predicted by the *TMHMM2* program (▬), segments of low compositional complexity, determined by the *SEG* program (▬). PHB represents PHB domain, located within the stomatin signature (not shown).**

**Figure 1.26 Localization of podocin in the glomerular capillary wall of normal mice (immunogold labelling); magnification: a–b, x24,000; c–d, x40,000 *(reproduced with permission from Roselli et al, 2001)***

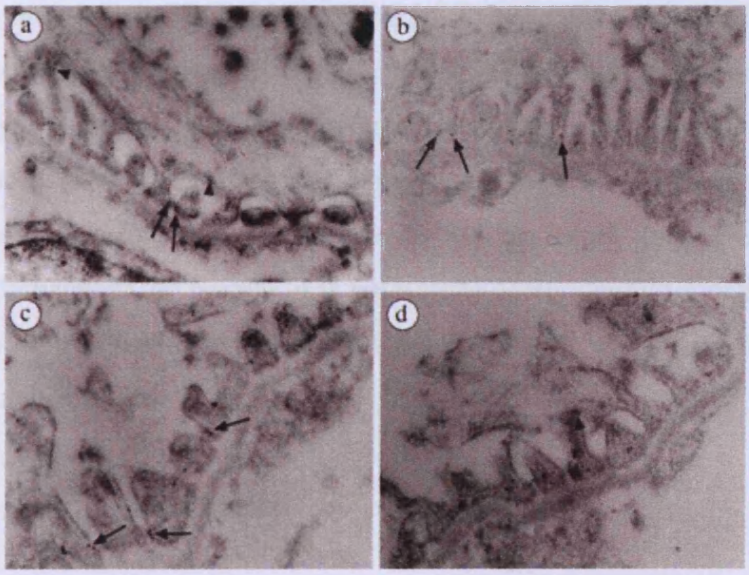


**N-terminal (a and c) or C-terminal (b and d) antibodies. With both antibodies, podocin is seen at the base of podocyte foot processes, along the GBM, on either part of the slit diaphragm (arrow), predominantly at the inner face of the plasma membrane**

Recent data suggests that, like nephrin, podocin is also associated with lipid rafts, and may form a complex with nephrin and CD2AP within these structures (Schwartz *et al*, 2001). Whether this is direct or indirect is not known, but GST pull down assays have predicted a direct interaction between the C-terminal portion of podocin, and with both CD2AP and nephrin (Huber *et al*, 2001; Schwartz *et al*, 2001). Since nephrin is also able to bind directly to CD2AP *in vitro* (Shih *et al*, 1999) and *in vivo* (Shih *et al*, 2001), CD2AP may act as an adaptor molecule between nephrin and podocin, in addition to a possible direct interaction, forming a link between these proteins and the podocyte cytoskeletal machinery. In addition, there is *in vitro* evidence to suggest that when present in a complex with nephrin, podocin synergistically contributes to the activation of the mitogen-activated protein kinase (MAPK) pathway by nephrin, although this study did not detect binding to CD2AP (Huber *et al*, 2001).

Podocin has a very similar expression pattern to nephrin during renal development (Roselli *et al*, 2002). The *NPHS2* transcript was first detected in the mesonephros, specifically in mesonephric podocyte precursors (Roselli *et al*, 2002). *NPHS2* was subsequently detected in the metanephros in podocyte precursors in the lower limb of the S-shaped body, but not in future parietal cells. Expression persisted throughout glomerular differentiation and in mature glomeruli. During this and the early capillary loop stage, podocin is distributed at the basal pole and along the lateral surface of immature podocytes that have not yet developed foot processes. Podocin expression increases with glomerular maturation, and persists at a high level at the basal pole of mature podocytes. Interestingly, using specific antibodies raised against either the N- and C- terminal domains of the protein, it is possible to detect their co-localisation at the cytoplasmic face of the plasma membrane, which is in agreement with the proposed hairpin – like structure (Figure 1.26).

#### 1.7.2.4 *The α-Actinin 4 gene* (ACTN4)

Genotype analysis of two different families mapped an FSGS locus to chromosome 19q13, and subsequent mutation screening revealed that the causative gene was *ACTN4* (Kaplan *et al*, 2000). *ACTN4* encodes for α-Actinin 4, an actin-filament crosslinking protein, with widespread expression (Honda *et al*, 1998) and belonging to a family of

homologous proteins highly conserved among species. α-Actinin 4 is expressed in the kidney, and in podocytes is located predominantly within the foot process (Kuihara H *et al* 1995). Competitive co-sedimentation experiments performed using labelled and unlabeled F-actin along with mutated (K228E, T232I or S235P) and wild type full length α-Actinin 4 suggest that the mutated form has a higher affinity for F-actin (Kaplan *et al*, 2000). This suggests that an intact sub-membranous actin cytoskeleton play a crucial role in maintaining the podocyte architecture. This is supported by recent unpublished reports on an *ACTN4* mouse knock out, which suggest that the renal phenotype is similar to that seen in other mouse models of nephrotic syndrome such as in *NPHS1* and *NEPH-1*. However, this data still requires confirmation.

### *1.7.3 Mouse models of nephrotic syndrome*

A number of transgenic models of nephrotic syndrome are now available, however the major limitation of this approach is that many glomerular genes are expressed during all three stages of mammalian development, which complicates the interpretation of the eventual phenotype seen. However, a number of clues for the molecular basis of glomerular permselectivity have come from studies of mouse models of nephrotic syndrome. Null mutations of *CD2AP* (Shih *et al*, 1999), *s-laminin/laminin beta 2* (Noakes *et al*, 1995), *Mpv17* (Binder *et al*, 1999) *Glepp-1* (Wharram *et al*, 2000), *NEPH1* (Donoviel *et al*, 2001), *podocalyxin* (Doyonnas *et al* 2001), and over expression of *Pax2* (Dressler *et al,* 1994), all result in glomerular damage in mouse models, and indicate which genes may play an important role in podocyte homeostasis. In many cases, null mice develop either typical effacement of podocyte foot processes, or normal foot processes and slit diaphragms simply fail to form. Various abnormalities may be seen on histological examination of the kidneys including FSGS, DMS and interestingly over-expression of *Pax2* in transgenic mice, results in a histology reminiscent of CNF (Dressler *et al*, 1994). However, in the majority of cases, mutations within these genes have as yet not been detected in humans, and the relevance to human nephrotic disease remains speculative.

## 1.8 Rationale for study

Proteinuria, the hallmark of nephrotic syndrome, occurs as a consequence of the loss of normal permselective properties of the glomerular filtration barrier. Although the consequences of this phenomenon are well studied, the actual pathophysiological mechanisms involved are poorly resolved and as a result, many scientific studies of nephrotic syndrome are confusing. Traditionally, childhood nephrotic syndrome has been attributed to various mechanisms, such as immune derangement (Neuhaus *et al*, 1995 a,b), loss of negative charge/charge neutralisation in the GFB (Taylor, 1997), or aberrant proteoglycan composition of the glomerular basement membrane (van den Heuvel *et al*, 1995), with little understanding of how these cause the protein leak. However, it is becoming increasingly recognised that although the aetiology of nephrotic syndrome may vary, the primary target for cellular injury is the glomerular podocyte, and many nephrotic syndromes presenting in early life are inherited disorders, with a genetic basis.

The aim was to explore the genetic basis of congenital and early onset nephrotic syndrome by examining the roles of three renal glomerular genes *WT1*, *NPHS1* and *NPHS2* in the pathogenesis of glomerular protein leak. Although these diseases are rare, many are both inherited and kidney specific. Consequently, elucidation of the underlying genetic defects might be expected to contribute significantly to current knowledge about the role of the different regions and protein components of the GFB, and thus the molecular basis of glomerular filtration.

# CHAPTER 2: Materials and Methods

## 2.1 Materials

### *2.1.1 Reagents*

All reagents used were of AnalaR grade and obtained from either British Drug Houses (BDH) or Sigma Aldrich, except as indicated below. Glassware, solutions and media were autoclaved at 15psi, 121°C for 20 minutes as required. Water was purified using a MilliRo 15 Water Purification System (Millipore SA), further purified were necessary using a Milli-Q Reagent Grade Water Ultrafiltration System (Millipore), and sterilised by autoclaving.

Buffer Saturated Phenol was from Life Technology. Proteinase K Solution was from Boehringer Mannheim/Qiagen. Tris-buffered phenol and NaOH pellets were from Fisons Scientific Equipment. Sequagel and Protogel polyacrylamide gel products and buffers were obtained from National Diagnostics. Agarose and TEMED (N,N,N',N'-tetramethylethylenediamine) were obtained from Gibco-BRL Life technologies and NuSeive GTG low melting point agarose from FMC Bioproducts. Acrylamide solution 40% w/v, (29:1 acrylamide:N,N@-methylene bisacrylamide), Protogel acrylamide solution 30% acrylamide, 0.8% bisacrylamide (37.5:1 acrylamide:N,N@-methylene bisacrylamide) and urea were from Bio-Rad Laboratories. Amberlite resin (50mg/ml) was from Perkin Elmer. Alconox detergent was from Alconox Inc. Bacto-agar, bactotryptone, agar, nitrogen base without amino acids and yeast extract were from Difco laboratories. Absolute alcohol was from Hayman Ltd. Ultrapure dNTP's, NAP5 Sephadex columns, and poly(dI-dC).poly(dI-dC) were supplied by Pharmacia Biotech.

### *2.1.2 Materials*

In addition to standard laboratory items, use was made of the following special items. X-OMAT AR and BioMax-MR autoradiography film (Kodak) was used for $^{32}P$ and $^{35}S$ applications. For chemiluminescent methods XB-200 Blue Sensitive, High definition X-

ray film (X-ograph Imaging Systems) was used. Slides and slide boxes were from BDH laboratory supplies and cover slips from Chance Pepper Ltd. ART aerosol resistant barrier tips were obtained from Molecular Bioproducts. Miniflex 0.2mm flat tips were from Sorenson BioScience, Inc. Glassware was obtained from Pyrex® (USA) and Schott Duran (Germany). Plastic ware was sourced from Becton Dickson Lab ware or Bibby Sterilin Ltd. 0.2ml PCR tubes from ABgene®. Sterile loops, cryotubes and filter sterilisation units were acquired from Nunc Nalgene®. Hybond N+ and Hybond C nylon membranes were from Amersham International PLC. Microsample™ plates and NAP5 Sephadex G-25 columns were obtained from Pharmacia. DNA electrophoresed on agarose gels was visualised through ethidium bromide fluorescence detected at 300nm on a Chromato-vue transilluminator. Gels were photographed on a Polaroid Direct Screen Instant camera using Polaroid Film (Polaroid Corporation), or on a Herolab digital camera (Molekulare Trenntechnik) printed onto thermal paper (Mitsubishi Electric Corporation). PCR amplification and cycle sequencing reactions were performed on a GeneAmp PCR System 2400 (Perkin Elmer Applied Biosystems) or RoboCycler gradient 96 (Stratagene). DNA sequence analysis and microsatellite repeat analysis were performed on an ABI PRISM™ 377 DNA Sequencer (Perkin Elmer Applied Biosystems).

### *2.1.3 Commercial Kits*

Sequenase™ Version 2 DNA sequencing kits and Thermo Sequenase dye terminator cycle sequencing pre-mix kits were purchased from Amersham International. pCR-Script™ Amp SK(+) Cloning Kits were from Stratagene. QIAmp Blood kits, QIAquick PCR purification Kits, QIAquick Gel extraction kits and QIAprep Spin Miniprep and Maxiprep kits were from Qiagen Ltd.

### *2.1.4 Enzymes*

Restriction endonucleases were obtained from Gibco-BRL Life Technologies. Biopro™ DNA polymerase was from Bioline. Cloned *Pfu* DNA polymerase was from Stratagene. All enzymes were used with the appropriate 10x buffers supplied by the manufacturers.

### *2.1.5 Radioisotopes*

[$\alpha$-$^{32}$P] dCTP and [$\gamma$-$^{32}$P] dATP (3000 Ci/mmol was from ICN Biomedicals Inc. [$\alpha$-$^{35}$ S] dATP (>600 Ci/mmol) was from Amersham.

### *2.1.6 Nucleotide Size Markers*

50 bp and 1 kb DNA ladders were purchased from Gibco-BRL Life technologies, and the GENESCAN-350™ TAMRA internal lane standard from Perkin Elmer.

### *2.1.7 Immunoglobulins*

The anti-HA tag and anti-WT (F6) mouse monoclonal IgG (200μg/ml) antibody used was made commercially by Santa Cruz. Anti-nephrin antibodies were kindly donated by Professor Karl Tryggvason, Karolinska Institute, Stockholm.

### *2.1.8 Vectors, cDNA Clones and Libraries*

pCR-Script™ Amp SK(+) vector was purchased from Stratagene. Rc/CMV-WT1 +/- KTS cDNA, and GAL4-WT1 +/- KTS fusions in pAS1 and pACTII vectors were kindly donated by Professor Nick Hastie (MRC unit, Edinburgh), and the pVP16 mouse E 9.5 and 10.5 day cDNA library by Stan Holleberg (Vollum Institute).

### *2.1.9 Bacterial Strains*

HB101: Δ(*gpt*-p10A)62, *leu*B6, *thi*-1, *lac*Y1, *hsd*$S_B$20, *rec*A, *rps*L20(str+), ara14, *Gal*k2, *xyl*-5, *mtl*-1, *sup*E44, mcr$B_B$

Epicurian Coli® XL1-Blue MRF' Kan supercompetent cells were supplied with the pCR-Script™ Amp SK(+) Cloning Kit (Stratagene) and used according to the manufacturer's instructions.

### *2.1.10 Yeast Strains*

Y190 MATa, *gal*4, *gal*80, *his*3-200, *trp*1-902, *ade*2-101, *ura*3-52, *leu*2-3, -112 +URA:GAL(UAS) → HIS3, *cyh*$^r$.

This was kindly provided by Stephen Elledge (Baylor College of Medicine, Houston, Texas).

### *2.1.11 Oligonucleotides*

All oligonucleotide primers were synthesised to order by Genosys Biotechnologies Inc. Primers used for general PCR and sequencing of clones during this project are listed in Tables 2.1 to 2.5. Exon 1-10 *WT1* gene oligonucleotide primer pairs used were those published by Baird *et al* (1992). *NPHS1* micro-satellite repeats were amplified using oligonucleotide primer pairs published by Mannikko *et al* 1995. The forward primer of each pair was labelled with a fluorescent dye. *NPHS1* primers (Lenkkeri *et al* 1999) were a kind gift from Professor Karl Tryggvason, Karolinska Institute, Stockholm. *NPHS2* exon amplification was performed using primers published by Boute *et al* (2000). All primers were designed using flanking sequence between 30-50 base pairs upstream and downstream of exons to be amplified, to include exon-intron boundaries. Melting temperature (Tm) was estimated as follows:-

For oligonucleotides < 25 bp:

$$Tm = 2 (A + T) + 4(G + C)$$

For oligonucleotides > 25 bp:

$$Tm = 69.3 + (0.41 \times GC \text{ content as a } \%) - (650/\text{length of primer})$$

## Table 2.1 General primers for PCR

| Primer name | Sequence 5'→ 3' | Annealing temperature (°C) | Uses |
|---|---|---|---|
| T7 | taatacgactcactataggg | 48 | General PCR and sequencing of clones in pCR-Script™ SK(+) |
| T3 | aattaaccctcactaaaggg | 48 | |
| pAS-1 | tcatcggaagagagtag | 50 | Sequencing of Gal4 binding and activation domain fusions |
| pACTII | ataccactacaatggatg | 52 | |
| VP16F | gagtttgcgcagatgttt | 52 | Amplification and sequencing of VP16 library inserts |
| VP16R | gttgtaaaacgacggccagt | 60 | |

## Table 2.2 Primers used for PCR amplification and sequencing of the *WT1* gene

| Exons | 5' Primer (Sequence 5'→ 3') | 3' Primer (Sequence 5'→ 3') | Product size (bp) | Annealing temperature (°C) |
|---|---|---|---|---|
| 1 | ccagcgctgaacgtctccag | taggggcgctccccggccta | 526 | 67 |
| 2 | accgctgacactgtgcttctctccg | agaggaggatagcacggaag | 215 | 64 |
| 3 | ggcagcactcgctcagctgtcttcg | ggtcccaaggacccagacgcagagc | 180 | 70 |
| 4 | gtggttatgtgttctaactctagat | ataagttactgtggaaaggcaatgg | 158 | 60 |
| 5 | gctccattccccactccccacctct | ttgctttgccatctccgcattgtcc | 120 | 60 |
| 6 | cactgaccctttttcccttc | ggccggtaagtaggaagaggc | 189 | 61 |
| 7 | gacctacgtgaatgttcacatg | ctcttgaaccatgtttgcccaagac | 255 | 60 |
| 8 | ccagtatcatttcaaatagatatgtg | agggaacacagctgccagcaatgag | 167 | 58 |
| 9 | tagggccgaggctagaccttctctg | atccctctcatcacaatttcattcc | 204 | 60 |
| 10 | gcaagtgtctctgactggcaattgt | tgcctgggacactgaacggtccccg | 190 | 60 |
| DDS1 | gcgaaagttctcccggtcc | - | | 60 |
| Fras 1 | ccagctcaaaagacaccaaag | - | | 60 |
| Fras2 | - | tttctgacaacttggccacc | | 60 |

**Table 2.3 Primers used for PCR amplification and sequencing of the *NPHS1* gene**

| Exons | 5' Primer (Sequence 5'→ 3') | 3' Primer (Sequence 5'→ 3') | Product Size (bp) | Annealing temperature (°C) |
|---|---|---|---|---|
| 5' UTR | gctgactctgccagtgcctg | cagggccatcacaggtcccc | 643 | 60 |
| 1–2 | gagaaagccagacagacgcag | agcttccgctggtggct | 491 | 60 |
| 3–4 | agccaccagcggaagct | ctcccttcccactccagagg | 530 | 60 |
| 5 | cagaatctatcttgcggggag | catggggaaaattaggggtcaag | 187 | 60 |
| 6–7 | tctccctgactccccaaatttc | ctcaggactggctcccagac | 544 | 60 |
| 8–9 | gacagtggggtctgggagccagtcctgag | gagtcatgccctcagcccc | 623 | 60 |
| 10–11 | cacgatggataggggtgctg | cctggtccttcccccacatt | 465 | 60 |
| 12–13 | aacccagtgggcagggtagggg | gacatgcgtggaggggggcga | 668 | 60 |
| 14 | cctagtgcctctccagcc | gagtagtttagggtcaagaagg | 288 | 60 |
| 15–16 | cctgatctccaatctgtccttg | ccacaatgggcaaggttccttg | 484 | 60 |
| 17 | cacccagacctgtctgggcc | gtccccactcccaaggaactc | 257 | 60 |
| 18–19 | gaggctacagaagggacaatttg | gctggaggtccagacctggg | 561 | 60 |
| 20 | ggatggatgcatagatgattcc | caatcagggatgtgggaatg | 297 | 60 |
| 21–22 | cctggacagaatcttctggaatt | cctacacatcctctgaggaatac | 487 | 60 |
| 23 | gaggctgagaaatatttaaagcttat | gagaccaggaggttccattct | 188 | 60 |
| 24–26 | ctcggggagacccacccc | cctgatgctaacggcagggc | 611 | 60 |
| 27–28 | tgcccttccgggcacagtgg | tacaagcaataggaggtaggc | 438 | 60 |
| 29 | cagatcttcaatgaagacctaca | gagacagaatctcgctctg | 747 | 60 |

**Table 2.4 Primers used for PCR amplification of the *NPHS2* gene**

| Exons | 5' Primer (Sequence 5'→ 3') | 3' Primer (Sequence 5'→ 3') | Product Size (bp) | Annealing temperature (°C) |
|---|---|---|---|---|
| 1 | gcagcgactccacagggact | tcagtgggtctcgtggggat | 410 | 60 |
| 2 | aggcagtgaatacagtgaag | ggcctcaggaaattaccta | 195 | 55 |
| 3 | ttctgggagtgatttgaaag | tgaagaaattggcaagtcag | 175 | 56 |
| 4 | aaggtgaaacccaaacagc | cggtaggtagaccatggaaa | 210 | 55 |
| 5 | cataggaaaggagcccaaga | tttcagcatattggccatta | 295 | 56 |
| 6 | ctcccactgacatctga | aatttaaaatgaaaccagaa | 156 | 50 |
| 7 | ctaaatcatggctgcacacc | cttcctaaagggcagtctgg | 176 | 60 |
| 8 | ggtgaagccttcagggaatg | ttctatggcaggccccttta | 395 | 60 |

**Table 2.5 Chromosome 19q13.1 microsatellite repeats**

| Locus | Sequence 5'→ 3' | Hetero-zygosity | Number of alleles | Size of Alleles (bp) | Annealing temperature (°C) | Primer Labelling dye and display colour |
|---|---|---|---|---|---|---|
| D19S608F<br>D19S608R | gcagactgcttgagctca<br>cgtgcccagctaaccagg | .89 | 10 | 112-140 | 56 | 5'TET (green) |
| D19S609F<br>D19S609R | gtcgactgaggcttacaga<br>gtcgactgcaggcttacaga | .35 | 4 | 114-120 | 54 | 5'FAM (blue) |
| D19S610F<br>D19S610R | ctctctccaaggactcgg<br>gtggatctatctgccaatctc | .75 | 10 | 204-220 | 54 | 5'TET (green) |

## 2.2 Solutions, Buffers and Media

### *2.2.1 DNA related solutions*

#### *2.2.1.1 Genomic DNA extraction*

| | |
|---|---|
| Nuclei Lysis Buffer | 100mM Na Cl, 100mM Tris pH7.8, 10mM EDTA |
| DNA extraction solution | 100mM Tris-HCl, 4mM EDTA (pH 8.0) |
| 1X TE | 10mM Tris-HCl, 1 mM EDTA, pH 7 |

#### *2.2.1.2 Solutions for DNA preparation*

| | |
|---|---|
| Solution I | 50mM glucose, 25mM Tris-HCl, 10mM EDTA (pH 8.0) |
| Solution II | 0.2M NaOH, 0.1% w/v SDS |
| Solution III | 3M KAc , adjusted with glacial acetic acid to pH 5.2 |
| QBT | 750Mm NaCl, 50mM MOPS (pH 8.0), 15% ethanol, 0.15% Triton X |
| QC | 1M NaCl, 50mM MOPS (pH7.0), 15% ethanol |
| QF | 1.25mM NaCl, 50mM Tris-HCl (pH 8.5), 15% ethanol |

#### *2.2.1.3 DNA Electrophoresis buffers*

| | |
|---|---|
| X1 TAE buffer | 40mM Tris-Acetate, 1mM EDTA pH 7.0 |
| X1 TBE buffer | 89mM Tris-borate, 1mM EDTA pH 8.3 |

#### *2.2.1.4 DNA Gel loading buffers*

| | |
|---|---|
| Orange G | 0.25% w/v orange G, 20% w/v Ficoll 400, 100mM EDTA |
| Bromophenol Blue | 0.25% w/v bromophenol blue, 0.25% w/v xylene cyanol, 15% w/v Ficoll 400 |
| Formamide buffer | 95% formamide, 20mM EDTA, 0.05% bromophenol blue, 0.05% xylene cyanol FF |
| Amplification dilution Solution (ADS) | 0.1% SDS 10mM EDTA |

### *2.2.1.5 RNA extraction solution*

| | |
|---|---|
| RNA digestion buffer | 10mM Tris (pH8.0), 100mM NaCl, 25mM EDTA, 0.5% SDS and 100μg/ml of Proteinase K. |

### *2.2.1.6 Restriction Enzyme Buffers*

The buffers used in restriction enzyme digest were enzyme specific and supplied at 10x concentration by Gibco BRL. All were stored at -20°C.

| | |
|---|---|
| 1x BRL restriction buffer | 50mM Tris HCl (pH8.0), 10mM $MgCl_2$, 0 - 100mM NaCl, 0 - 100mM KCl |

### *2.2.1.7 Taq PCR Buffer*

*Taq* PCR buffer was supplied by Bioline at 10X concentration and stored at -20°C.

| | |
|---|---|
| 10x Taq buffer | 670mM Tris HCl, pH 8.8, 160 mM $(NH_4)_2SO_4$<br>1% Tween 20 |

### *2.2.1.8 Pfu PCR buffer*

*Pfu* PCR buffer was supplied by Stratagene at 10X concentration and stored at –20°C.

| | |
|---|---|
| 10x *Pfu* PCR buffer | 200mM Tris-HCl pH 8.8, 20mM Mg $SO_4$,100mM KCl, 100 mM $(NH_4)_2SO_4$,1% Triton X-100 ,1 mg/ml nuclease-free BSA |

### *2.2.2 Protein related solutions*

### *2.2.2.1 General buffers*

| | |
|---|---|
| 10X TBS | 0.5M Tris-HCl (pH 8.0), 1.5M NaCl |
| 10X PBS | 137mM NaCl, 1.5mM $KH_2PO_4$, 8mM $Na_2HPO_4$, 2mM KCl |

### *2.2.2.2 Protease inhibitors*

The following protease inhibitors were added immediately prior to use to solutions used in the majority of protein techniques.

| Protease Inhibitor | Specificity | Stock Solution | Final Concentration |
|---|---|---|---|
| PMSF | Serine and cysteines proteases | 0.1M in isopropanol | 1mM |
| Aprotinin | Serine proteases | 10mg/ml in $H_2O$ | 1μg/ml |
| Leupeptin | Serine and cysteines proteases | 1mg/ml in $H_2O$ | 1μg/ml |
| Pepstatin | Aspartate proteases | 1mg/ml in ethanol | 1μg/ml |
| Trypsin Inhibitor | Trypsin | 1mg/ml in $H_2O$ | 10μg/ml |
| EDTA | Metalloproteases | 0.5M in $H_2O$ | 0.5-1mM |

### *2.2.2.3 Protein gel buffers*

| | |
|---|---|
| 4X SDS resolving gel buffer | 0.15M Tris base, 0.4% SDS |
| 4X SDS stacking gel buffer | 0.05M Tris base, 0.4% SDS |
| 10X Tris-glycine/SDS electrophoresis buffer | 0.25M Tris base, 2M glycine, 1% SDS |
| 2X Laemmli loading buffer | 250mM Tris-Cl (pH6.8), 4% SDS, 25% glycerol, 0.1% bromophenol blue, 5% β mercaptoethanol (added fresh). |
| Protein transfer buffer | 0.5X Tris-glycine/SDS electrophoresis buffer, 20% methanol |
| Bradford buffer (estimation of protein concentration) | 100mls 85% phosphoric acid + 100mg Coomassie Brilliant Blue G-250 dissolved in 50ml 95% ethanol, made up to 1L with $ddH_20$. |

### *2.2.2.4 Hybond-C membrane blocking and wash buffers*

| | |
|---|---|
| TBS-T | 1X TBS, 0.05% Tween-20 |
| Blocking buffer | 1X TBS, 5% non-fat milk, 0.05% Tween-20 |
| Wash buffer | 1X TBS, 0.5% Tween-20 |

### *2.2.3 Yeast Analysis*

### *2.2.3.1 Yeast media*

| | |
|---|---|
| YPD | 20g/l Bacto-peptone, 10g/l yeast extract, 2% glucose |
| YPAD | YPD + 0.002% adenine |
| Minimal media | 6.7g/l yeast nitrogen base (without amino acids), 2% glucose, 0.002% adenine, 0.0002% uracil, 0.0003% lysine (+ 25-50ml 1M 3-Aminotriazole as necessary) |
| 10X dropout solution (- L, - W, - H) | 300M g/l isoleucine, 1500mg/l valine, 200mg/l arginine-HCl, 300mg lysine-HCl, 200mg/l methionine, 500mg/l phenylalanine, 2000mg/l threonine, 300mg/l tyrosine, 300mg/l adenine, 200mg/l uracil |
| Added according to selection criteria: | 0.003% leucine, 0.002% histidine, 0.002% tryptophan |
| Plates: | Appropriate medium containing 20g/l agar |

### *2.2.3.2 Yeast manipulation solutions*

| | |
|---|---|
| 10X LiAc | 1M LiAc |
| 10X TE | 100mM Tris-HCl (pH8.0), 10mM EDTA |
| LiAc/TE | 100mM LiAc, 10mM Tris-HCl (pH8.0), 1mM EDTA |
| Li/SORB | 0.1M LiAc, 10mM Tris-HCl (pH8.0), 1mM EDTA, 1M Sorbitol |

| | |
|---|---|
| LiAc/TE/PEG | 0.1M LiAc, 10mM Tris-HCl (pH8.0), 1mM EDTA, 40% polyethylene glycol (PEG) |
| Yeast lysis buffer | 10mM Tris-HCl (pH8.0), 2% Triton X-100, 1% SDS, 100mM NaCl, 1mM EDTA |
| Z-buffer | 60mM $Na_2HPO_4.7H_20$, 40mM $NaHPO_4.H_2O$, 10mM KCl, 1mM $MgSO4.7H_2O$, adjusted to pH 7.0 |
| Cracking Buffer | 125 mM Tris-HCl (pH 6.8), 8M urea, 4% SDS, 10% glycerol, 0.05% bromophenol blue + "fresh" β – mercaptoethanol (50 µl per ml) |

### *2.2.4 Bacterial Analysis*

#### *2.2.4.1 Media*

| | |
|---|---|
| L-Broth (LB) | 10g/l Bacto-tryptone, 5g/l yeast extract, 5g/l NaCl |
| SOB broth | 20g/l Bacto-tryptone, 5g/l yeast extract, 0.5g/l NaCl |
| SOC broth | 9.6ml SOB broth, with 100µl 1M $MgCl_2$, 100µl $MgSO_4$ and 200µl 20% w/v glucose solution added immediately prior to use. |
| Minimal medium (1 litre) | 200ml 5XM9 salts, 100ml dropout solution, 5ml 40% glucose, 1ml 1M $MgSO_4$, 4ml 10mg/ml proline, 1ml 1M thiamine, 2ml 1% histidine, 2ml 1% tryptophan, 1.5ml ampicillin |
| 5X M9 salts | 30g $Na_2HPO_4.7H_20$, 15g $NH_2PO_4$, 5g $NH_4Cl$, 2.5g NaCl, 15mg $CaCl_2$ (optional) |
| Plates | Appropriate medium containing 20g agar |

*2.2.4.2 Antibiotics*

| | |
|---|---|
| Ampicillin | 50mg/ml, filter sterilised stored at 20°C as 1000X stocks |

*2.2.4.3 Colour selection*

| | |
|---|---|
| X-gal (1000X) | 25mg/ml in dimethyl formamide |
| IPTG (1000X) | 25 mg/ml, filter sterilised |

***2.2.5 Solutions used in the preparation of cytoplasmic and nuclear extracts***

| | |
|---|---|
| Buffer A | 10 mM Hepes (pH7.6), 85 mM KCl, 5.5% sucrose, 0.5 mM spermidine, 0.5 mM DTT, 0.5 mM EDTA + protease inhibitors |
| Buffer B | Buffer A + 0.8% NP-40 |
| Buffer C | Buffer A minus EDTA |
| NSB | 20 mM Hepes (pH 7.9), 140 mM NaCl, 40 % glycerol, 0.5 mM DTT, 0.5 mM EDTA + protease inhibitors |
| HSU buffer | 2M NaCl, 8M urea in TE |
| Hypotonic Buffer | 10 mM Hepes (pH 7.6), 10 mM KCl, 1.5 mM $MgCl_2$, 0.5 mM DTT, 0.2 mM EDTA, 0.5 mM EGTA, + protease inhibitors |

***2.2.6 Solutions used for electrophoretic mobility shift assay (EMSA)***

| | |
|---|---|
| BBO binding Buffer | 25mM HEPES pH 7.4, 10% glycerol (v/v), 75mM NaCl, 0.25mM EDTA, 1mM $MgCl_2$, 1mM DTT, 0.1% NP-40 |
| T4 DNA polymerase buffer (PNK buffer) | 50mM NaCl, 10mM Tris-HCl, 10mM $MgCl_2$, 1mM DTT (pH7.9) |

## 2.3 METHODS

### *2.3.1 Isolation and purification of DNA and RNA*

#### *2.3.1.1 Preparation of DNA from human venous blood*

Two methods were used. For routine isolation and purification of genomic DNA from whole venous blood, the QIAmp Blood and Tissue kit (Qiagen Ltd) was used in accordance with the manufacturer's instructions. This was suitable for DNA preparation from both fresh and frozen blood, including samples treated with citrate, heparin or EDTA and yielded pure DNA, at a concentration of 30-60 ng/μl which could be used directly as a template for PCR reactions. Since only 200 μl of blood was required, sufficient quantities of DNA could be obtained from small-volume blood samples, such as those taken from infants and young children.

If larger quantities were required, standard phenol chloroform extraction was used. 5-10 mls of blood was subjected to detergent lysis with 0.1 % NP40 and 0.1% SDS, followed by incubation with Proteinase K (100μg/ml) and lysis buffer overnight at 37°C. The sample was subsequently phenol/chloroform extracted and the DNA precipitated with 0.3M sodium acetate and 2 ½ times the sample volume of ice-cold 100% ethanol. DNA was re-suspended in x1 TE (pH 8.0) and quantified as described above.

#### *2.3.1.2 Extraction of DNA from paraffin sections*

Again two methods were employed. For larger sections, the QIAmp Blood and Tissue kit (Qiagen Ltd) was used according to the manufacturer's instructions. However, if only small sections were available, a modified phenol/chloroform extraction protocol was followed. Paraffin was dissolved using xylene, followed by a 100% ethanol wash. DNA extracted by incubation with Proteinase K (12.5mg/ml) in DNA extraction buffer (100mM Tris-HCl and 4mM EDTA (pH8.0)) at 37°C overnight. The samples were then phenol/chloroform extracted, and the DNA precipitated with 0.3M sodium acetate (pH

8.0) and x3 sample volume of 100% ethanol at -70°C. The DNA was subsequently pelleted and resuspended 25-100µl x1 TE to a concentration of 50-100ng/µl.

### *2.3.1.3 Extraction of RNA from paraffin sections*

A method originally described by O'Driscoll *et al* (1996) was followed. Ten 5µm sections were deparaffinised using xylene and 100% ethanol. These were then air-dried, suspended in 200µl of RNA digestion buffer (section 2.2.1.4) and digested for 16 hours at 50°C. Total RNA was then extracted using phenol/chloroform extraction and precipitated with 100% ethanol, followed by a 70% ethanol wash. The pellet was suspended in 100µl of DEPC water prior to use in RT-PCR.

### *2.3.1.4 Plasmid minipreps*

Initially, a standard alkaline lysis plasmid miniprep technique was used as described in Sambrook *et al* (1989). 5-10mls of an overnight bacterial culture was centrifuged at 12,000 rpm for 5 minutes. The supernatant was poured off and this procedure repeated three times. The final supernatant was removed and the cell pellet was resuspended in 100µl of solution I. 200µl of solution II was then added, the suspension inverted several times and kept on ice for 10 minutes. After addition of 150µl of solution III, the sample was again inverted and kept on ice for a further 10 minutes. The sample was then spun at 4°C for 10 minutes to remove cellular debris. After a 1:1 phenol chloroform extraction, the DNA was precipitated by addition of x2 volumes of 100% ethanol and left on ice for 20 minutes. The DNA was pelleted by centrifugation at 4°C for 20 minutes, washed in 70% ethanol and resuspended in 50µl of x1 TE containing 10µg/ml RNase A.

Later in this project, preparation of plasmid DNA was carried out using QIAprep Spin minipreps (Qiagen Ltd), in accordance to the manufacturer's instructions. In this system, alkaline lysis of bacterial cells in followed by adsorption of DNA onto a silica-gel membrane, thus eliminating the need for phenol/chloroform extraction. The DNA is eluted in Tris pH 8.0 and can be used directly in subsequent applications.

### *2.3.1.5 Plasmid Maxipreps*

Large-scale DNA preps were performed according to the Qiagen handbook, using the Qiagen-100 or 500 tips. 200ml bacterial cultures were harvested for 5 minutes at 3000rpm, and the cell pellet resuspended in 10ml Solution I containing RNase A (50μg/ml). 10 mls of Solution II was added, the sample mixed by inversion and left on ice for 20 minutes. The lysed cells were centrifuged at 4°C at 12,000rpm for 20 minutes to remove cell debris. During this time, a Qiagen-500 tip was equilibrated with 10 mls QBT buffer under gravity flow. The cleared lysate was then added to the pre-equilibrated column. Due to the salt and pH conditions of the lysate, the DNA will selectively bind to the resin, while the degraded RNA and cellular proteins can be removed by two washes using buffer QC. DNA was eluted from the tip by addition of 15mls of buffer QF, and then precipitated using 0.7 x volume of isopropanol. The DNA was pelleted by centrifugation at 12,000 rpm for 25 minutes at 4°C. After a 70% ethanol wash, the pellet was dried and resuspended in 200μl 10mM Tris pH8.0.

For long-term storage, 20 % glycerol stocks were made by combining 400μl overnight culture with 600μl 50% glycerol in a cryotube, followed by storage at -70°C. When a fresh supply of plasmid DNA was required, 10μl of stock was removed for inoculation into LB broth, followed by overnight culture.

### *2.3.2 Analysis of DNA and RNA*

#### *2.3.2.1 Quantification of nucleic acid concentration*

Nucleic acid concentration was determined by measuring the absorbance of the solution at 260 nm as quantified by a UV spectrophotometer. A value of $A_{260} = 1$, correlates to a concentration of ~ 50μg/ml for a solution of double stranded DNA, and 40μg/ml of RNA. The $A_{260:280}$ ratio was also determined to ensure that the sample was relatively free of proteins. If this is the case, this should have a value of 1.8 for a pure DNA solution. For dilutions, DNA concentration was calculated using the following equation:

$$\text{OD} \times \frac{\text{dilution} \times 50}{1000} = \text{concentration in } \mu g/\mu l$$

### *2.3.3 PCR Amplification of DNA*

#### *2.3.3.1 General PCR*

DNA was amplified using some modifications to the standard conditions as described by Saiki *et al* (1985,1988). Reactions were carried out in 1x PCR buffer (enzyme dependant), 25 mM each dNTP's, between 100-250 ng each primer and 1 unit polymerase. Between 60-90 ng DNA was used as template. For routine amplification, Biopro™ *Taq* polymerase (Bioline) was used. Amplification reactions contained 1x $NH_4$ PCR buffer (Bioline), 1.5 mM $MgCl_2$, 0.25 mM dNTP's,100-250 ng each primer, and 1U of *Taq* polymerase in a 25µl reaction. If proof reading or the production of blunt ended products for blunt ended ligation was required, *Pfu* polymerase was used. This produces blunt ended products and has a 12-fold lower error rate than *Taq* polymerase. Amplification reactions contained 1x *Pfu* buffer (Stratagene), 25 mM dNTP's, 100-200 ng each primer and 0.6-1.2 units of *Pfu* polymerase in a final volume of 25-50 µl. For GC rich areas, co-solvents such as 10% DMSO and 0.4M betane were used in addition to the standard PCR mix. PCR of DNA extracted from paraffin sections was often problematic due to carry-over of polymerase inhibitors. However, this was overcome by the use of *Pfu* polymerase and addition of 10% bovine serum albumin to the PCR reaction. The primer pairs used were described in section 2.1.11 and in Tables 2.1, 2.2, 2.3, 2.4 and 2.5. Standard precautions were taken to avoid PCR contamination, such as use of autoclaved MilliQ water and aerosol resistant ART tips. A negative control, consisting of a reaction mix with no template DNA, was included in most experiments to check for overt contamination. PCR was generally performed on either a Hybaid Omnigene, Perkin Elmer Geneamp PCR system 2000 or a Stratagene Robocycler gradient 96. The following programmes were used:

*Hybaid/Geneamp:*

| | |
|---|---|
| 1 cycle | Denaturation: 94-96 °C, 2 minutes |
| 30-40 cycles | Denaturation: 94-96 °C, 30 seconds<br>Annealing: specific annealing temperature calculated for primers ($T_m$ – 5°C), 30 seconds<br>Extension: 72°C, 30 seconds |
| 1 cycle | Final extension 72°C 5 minutes |

*Robocycler:*

| | |
|---|---|
| 1 cycle | Denaturation: 94-96 °C, 2 minutes |
| 30-40 cycles | Denaturation: 94-96 °C, 30 seconds<br>Annealing: specific annealing temperature calculated for primers ($T_m$ – 5°C), 1 minute 30 seconds<br>Extension: 72°C, 1 minute 10 seconds |
| 1 cycle | Final extension 72°C 5 minutes |

### *2.3.3.2 Colony PCR*

The general PCR method described above was followed. Template DNA was prepared by suspension of a bacterial colony in 30µl of LB. 5µl of the suspension was aliquoted into a screw cap tube and boiled for 5 minutes. 2 - 4 µl of this was then added to the PCR reaction.

### *2.3.3.3 SSCP PCR*

A similar protocol was followed, using either *Taq* or *Pfu* polymerase. However, only 0.2mM dCTP was initially added to accommodate the addition of 10µCi/µl CTP labelled with $^{32}P$ as a final step, yet maintain a concentration of dNTP's at 25 mM in the final PCR mix. 5µl of the amplified PCR product was then diluted 1:8 in ADS, and 3µl of the diluted mix used for polyacrylamide gel electrophoresis, unless the PCR product was generated using DNA extracted from paraffin sections, in which case neat product was loaded.

### *2.4.3.4 RT-PCR*

First strand cDNA synthesis was performed by mixing the following components on ice in the following order:- 7µl 5x reverse transcriptase buffer, 3.5µl DTT (0.1M), 2µl 20mM dNTP's, 1µl RNA-ase inhibitor, 1000pM random primer and 1-2 µl RNA. The final volume was made up to 33µl with DEPC $H_2O$ and the samples heated at 65°C for 10 minutes. These were placed on ice and 2µl of reverse transcriptase added, followed

by incubation at 42°C for 90 minutes. Samples were stored at -20°C prior to second strand synthesis by PCR.

### *2.3.4 Agarose gel electrophoresis*

PCR and digested PCR products larger than 100bp, were routinely separated by horizontal gel electrophoresis on 1-2% agarose minigels (0.5 – 1g agarose/100mls TAE buffer, 2.5µl 10mg/ml ethidium bromide). Samples were loaded in one-fifth to one-third volume of Orange G loading buffer, and a 1kb ladder routinely used as a molecular size standard. Gels were run in x1 TAE buffer containing 5 µl 10mg/ml ethidium bromide per 100mls at 100V, until the orange G dye had reached the desired position. This was in turn dependant on the size of the fragments and the resolution required. DNA was then visualised by ethidium bromide fluorescence under UV light. To separate fragments <100bp, 4% NuSieve GTG agarose was used for gels with a 50bp size marker as standard for sizing DNA fragments; electrophoresis performed as described above, whereas 1 – 1.5% low melting point agarose was used in preparative gels for the purification of DNA fragments.

### *2.3.5 Purification of PCR products*

PCR products were purified by one of two methods in order to obtain pure, concentrated DNA, which could be used in subsequent manipulations. For restriction enzyme digest and subcloning, PCR products were generally purified using the QIAquick PCR Purification Kit (Qiagen Ltd), according to the manufacturer's instructions which removed unwanted components such as template DNA, excess primers, unincorporated nucleotides, salts, DNA polymerase and co-solvents if these were used in the reaction. To remove non-specific PCR products amplified during the PCR reaction, PCR products were electrophoresed on a 1-1.5% low melting point agarose gel, and then gel extracted using a QIAquick Gel extraction kit (Qiagen Ltd). The band of interest was excised after visualisation by ethidium bromide fluorescence under UV light. The DNA was then extracted and purified according to the manufacturer's instructions and eluted in between 30-50µl of elution buffer (Tris pH 8.0).

### *2.3.6 Restriction Enzyme digest of DNA*

DNA was digested according to the manufacturer's guidelines using the appropriate reaction buffer for any given enzyme. Digestion of non-genomic DNA was performed for 1.5 to 2 hours at the recommended temperature, which in the majority of cases was 37°C. PCR products were digested in 10µl, and plasmids in 20-50µl..

### *2.3.7 Subcloning of DNA*

#### *2.3.7.1 Subcloning into pCR-Script™ Amp SK(+)*

This kit is manufactured by Stratagene and was in routine use for cloning of PCR products prior to sequencing, as it allows rapid and efficient cloning of blunt ended products with a low false positive rate, as blue/white colour selection is employed to pick colonies likely to contain inserts. The pCR-Script™ Amp SK(+) cloning vector is derived from pBluescript II SK(+) phagemid, comes pre-digested with *Srf*I, and contains an ampicillin resistance gene for antibiotic selection. Ligation reactions were carried according to the manufacturer's instructions, using the appropriate quantity of purified PCR product (usually 50-150ng to give an insert: vector molar ratio of 40:1 to 100:1) diluted in water and 1µl T4 ligase, and performed in the presence 1µl of *Srf*I to digest any residual empty vector and increase ligation efficiency. The ligation reaction was then transformed into 200µl of Epicurian Coli XL1-Blue MRF' Kan supercompetent cells supplied with the kit by heat shock, and the cells recovered in pre-warmed SOC medium by incubation for 1 hour at 37°C. The transformation reactions were then spread on LB- agar (LBA) plates containing X-Gal (1 ml of 25mg/ml in dimethyl formamide/litre of LBA), IPTG (25mg/ml (filter sterilised)/litre LBA) and 1ml of ampicillin (50mg/ml), and incubated overnight at 37°C. Plates were then incubated at 4°C for 1 hour to enhance the blue colour of negative colonies, and facilitate colour selection. Pure white colonies expected to contain insert only were selected for further analysis.

### *2.3.7.2 General ligation of DNA into vectors*

Vector and inserts were digested with the appropriate enzyme and checked on an agarose gel. Vector and insert DNA was gel extracted using a QIAquick Gel extraction kit (QIAGEN Ltd) according to the manufacturer's instructions. Ligation reactions were generally carried out in 20µl volumes containing 1x ligation buffer, 25 ng vector, 10-100ng insert DNA and 1U T4 ligase and incubated at 16°C overnight.

### *2.3.7.3 Transformation of bacteria with plasmid DNA*

#### *2.3.7.3.1 Preparation of chemically competent bacterial cells*

A single, fresh colony of cells was used to inoculate a 5 ml LB culture, and grown overnight. 1 ml of this culture was used to inoculate 400mls of LB and this was grown at 37°C until $A_{600}$ was in the range of 0.37 – 0.38. The culture was then aliquoted into 8 x 50ml pre-chilled Falcons and left on ice for 10 minutes. The cells were spun at 3000g and 4°C for 5 minutes, and the pellet resuspended in 10 mls ice-cold $CaCl_2$ solution. After spinning again, each pellet was resuspended in 10 mls ice-cold $CaCl_2$ solution and left on ice for 30 minutes. The cells were re-spun and the final pellets resuspended in 1.5mls cold $CaCl_2$ solution. 100µl aliquots were made and stored at -70°

#### *2.3.7.3.2 Chemical heat shock*

The method originally described by Dagert and Ehrlich (1974) was followed. 1-2µl of reaction mix was added to 100µl of chemically competent cells in an Eppendorf and incubated on ice for 30 minutes. The cells were transformed by heat shock at 42°C for 45 seconds and then chilled on ice for a further 2 minutes. The cells were then diluted in 500µl of SOC and placed in a 37°C orbital shaker for 1 hour. The transformed cells were then plated out on LB agar containing the appropriate antibiotic.

*2.3.7.3.3 Preparation of electro-competent bacterial cells*

5 mls overnight LB culture was inoculated with a single fresh colony of cells. 1 ml of the culture was then used to inoculate 500mls LB, and grown until the $A_{600}$ was in the range of 0.45-0.55. The culture was then placed on ice for 20 minutes and then harvested at 4°C, 3000rpm for 5 minutes and the pellet resuspended in 500mls of 10% glycerol and left on ice for 20 minutes. After another spin, the pellet was resuspended in 50mls 10% glycerol, and left for a further 20 minutes on ice. The suspension was then spun, the supernatant removed and the pellet resuspended in 400µl of 10% glycerol for every 100mls of starting culture. Cells were stored in 40µl aliquots at -70°C.

*2.3.8 SSCP Analysis*

*2.3.8.1 Preparation of PCR Samples.*

3µl of PCR product diluted 1:8 in APS or neat PCR product if generated by PCR using paraffin sections (previously described in section 2.3.3.3) was added to an equal volume of formamide buffer. Samples were then denatured for 5 minutes at 94°C and subsequently quick chilled on ice, ready for immediate loading onto an SSCP polyacrylamide gel.

*2.3.8.2 SSCP Polyacrylamide gel electrophoresis.*

Glass plates for use with Hybaid vertical electrophoresis tanks were cleaned with detergent and then wiped with 70% and 100% ethanol. The smaller of the two plates was siliconised by coating with dimethyldichlorosilane solution. Plates were sandwiched together separated by 0.4mm spacers and clamped along the edges. Acrylamide gels were prepared at 6% and 10% acrylamide concentrations as shown in Table 2.6 below, with 5% and 10% glycerol respectively and polymerised using 10% ammonium persulphate (APS) and TEMED. The gel mix was poured between the plates using a 50 ml syringe, a sharks tooth or square tooth comb inserted, and the gel allowed to polymerise for 1-2 hours. The gel was run either at 4°C or room temperature at 30-50V

for between 10-16 hours, until the cyanol marker reached the bottom of gel. The plates were then prised apart, the gel transferred onto 3mm Whatman chromatography paper, covered in cling film and dried on a gel dryer (Rapidry) at 80°C for 90 minutes. Gels were exposed overnight on Kodak X-Omat or Biomax paper at -70°C.

**Table 2.4 SSCP gel mixes**

| | **10% Acrylamide 10% Glycerol (60mls)** | **6% Acrylamide 5% Glycerol (60mls)** |
|---|---|---|
| **10X TBE** | 6 mls | 6 mls |
| **50% glycerol** | 12 mls | 6 mls |
| **Acrylamide (Protogel)** | 20 mls | 12 mls |
| **MilliRo $H_2O$** | 21.6 mls | 35.5 mls |
| **10% APS** | 50 µl | 50 µl |
| **TEMED** | 400 µl | 400 µl |

### *2.3.9 DNA Sequencing*

Manual sequencing was performed until the department purchased an ABI Prism 377 Automated DNA sequencer (Perkin Elmer). Subsequent to this, all sequencing was carried out using this technique and some manual sequencing was repeated to improve result quality.

#### *2.3.9.1 Preparation of double stranded template by alkali denaturation*

20µl of template was denatured by adding 20µl of 0.4M NaOH + 10mM Na EDTA and incubating the sample at 37°C for 30 minutes. The DNA was then precipitated using 0.3M Na Acetate (pH 5.5) and 2-4x the volume of 100% ethanol for 15 minutes on dry ice. The pellet was washed briefly using 70% ethanol and kept in pellet form until use.

The recovered pellet was resuspended in 7µl of autoclaved MilliQ water immediately prior to use in the sequencing reaction.

### *2.3.9.2 Manual Sequencing*

All sequencing reactions were performed using a Sequenase™ Version 2.0 DNA Sequencing kit and run in 0.5ml Eppendorf tubes. Annealing reactions were set up by adding 2µl 5x Sequenase Reaction Buffer and 1µl (0.5-1.0 pM) of each primer to 7µl denatured template. The reactions were heated at 65°C in a beaker for 2 minutes and then allowed to cool slowly to <35°C over a period of about 20 minutes. The tubes were centrifuged briefly and samples chilled on ice. While the reactions were cooling, 2.5µl of each termination mix (dideoxy-G,A,T and C) were aliquoted into wells in a Microsample™ plate, which was kept covered at room temperature for use later. A labelling reaction mix consisting of 1µl DMSO, 1µl 0.1M DTT, 2µl diluted Labelling mix (1:5), 0.5µl $^{35}$S dATP and 2µl of diluted Sequenase (1:8 dilution in enzyme dilution buffer) was added to the ice-cold annealed DNA mixture, and this was incubated on slush (4°C) for 5 minutes. Finally, 3.5µl of each reaction mix was added to the termination mix (G,A,T and C) pre-warmed to 37°C with careful mixing and the termination reactions incubated at 37°C for 5 minutes. To stop the termination reactions, 4µl of stop solution was then added sequentially to each. Samples could be kept at -20°C until gel electrophoresis.

### *2.3.9.3 Polyacrylamide gel electrophoresis of sequencing reactions*

Sequencing plates were cleaned with detergent and wiped with 70% and 100% ethanol. The smaller plate was siliconised with dimethyldichlorosilane solution. Plates were sandwiched together separated by 0.4mm spacers and clamped along the edges. Denaturing gels were poured generally consisting of 6% acrylamide and 7M urea and made according to the manufacturer's instructions. For 60 ml gels, 40mls of Sequagel diluent, 14.4mls Sequagel concentrate, 6 mls 10x TBE, 500µl of 10% APS and 30µl of TEMED were mixed and poured between the plates using a 50ml syringe. A sharks tooth comb was placed inverted along the top of the gel and then replaced with teeth into

the gel, once this had set. Sequencing reactions were denatured for 2 minutes by placing the Microsample™ plate on a boil block for two minutes and then onto ice . 3µl of each sequencing reaction was loaded onto the gel and samples electrophoresed at 70V for 2-4 hours depending on the required length of run. Plates were then prised apart and the gel lifted off onto a sheet of 3MM Whatman chromatography paper, covered in cling film and dried for 90 minutes at 80°C on a Rapidry gel dryer. The gel was exposed to Kodak Biomax film at room temperature for 1 - 4 days.

### *2.3.9.4 Automated Sequencing*

Sequencing reactions were performed using a Thermo Sequenase™ dye terminator cycle sequencing pre-mix kit (Amersham International). This system relies on the same principles as the chain termination methods described above, but employs ddNTP's labelled with fluorescent dyes instead of radiolabelled ddNTP's. Also the four ddNTP's are labelled with different dyes, and since these can be distinguished on an automated sequencer, all four sequencing reactions can be set up in one tube and electrophoresed in the same gel lane. In addition, multiple rounds of template denaturation, primer annealing and DNA extension are carried resulting in a larger amount of product and hence a stronger signal. This approach is made possible by the use of a thermostable DNA polymerase, Thermosequenase™, which can withstand the repeated thermal denaturation at the beginning of each sequencing cycle.

Approximately 50-100ng of PCR product or 1µg of plasmid DNA was used for reactions. 1µl of a 1:2 dilution of the primer originally used to generate the PCR product (typically 50-100ng) or 5µM of plasmid primer (T7 or T3, as shown in Table 2.1) was added to the DNA and the mixture made up to 6µl with autoclaved MilliQ water. 4µl of sequencing reagent pre-mix was added as a final step and the samples cycle sequenced using the following cycle sequencing protocol:

Initial denaturation step at 94°C 2 minutes
Followed by,

| | | |
|---|---|---|
| 25 cycles of denaturation | (94°C) | 30 seconds |
| | annealing (50°C) | 30 seconds |
| | extension (60°C) | 3 minutes 30 seconds |

Unincorporated dNTP's were removed from the completed sequencing reactions by ethanol precipitation. 3.5µl of 7.5mM ammonium acetate was added to a 1.5ml Eppendorf tube, followed by the cycle sequencing sample. 100µl of 100% ice cold ethanol was then added to each tube and samples precipitated for 20 minutes at –70°C, followed by centrifugation at 12,000 rpm at 4°C to pellet the sample. The supernatant was poured off and pellets washed in 250µl of 70% ethanol. Samples were then vacuum dried in a vacuum centrifuge for 5 minutes and stored at – 20 °C until further use.

For electrophoresis on the ABI PRISM™ 377 DNA Sequencer, 4.5% acrylamide gels were prepared. A pair of 42.4 x 25.5 cm sequencing plates (36cm well-to-read distance) were soaked for 30 minutes in 0.1M NaOH as necessary. They were then cleaned thoroughly with Alconox detergent, washed first with tap water, rinsed comprehensively with MilliRo water and allowed to dry upright before being clamped into position in a clean gel cassette, separated by 0.2mm spacers. 16.3mls of MilliQ water and 3.4 mls of acrylamide stock solution was added to 10.8g of urea and 0.2g of Amberlite deionising resin. This was mixed by stirring for 30 minutes before removing the resin by filter sterilisation. 3 mls of filtered x10 TBE was also added to yield a 30 ml gel mix. The polymerisation reaction was catalysed using 150µl of freshly made 10% APS and 21µl of TEMED and poured using a 20 ml syringe between the plates. A sharks tooth comb was inserted flat side to the top of the gel, and clamped into place with a Perspex clamp. The gel was left to set for 1 ½ to 2 hours, after which the comb was removed, cleaned and reinserted with the teeth just penetrating the top of the gel. The gel cassette was clamped into a vertical position in the electrophoresis chamber of the automated sequencer. The upper and lower buffer chambers were filled with x1 TBE and samples electrophoresed and analysed on the ABI PRISM™ 377 sequencer according to the manufacturer's instructions using Sequencing Data Collection and Analysis software, run on a Apple Power Macintosh 7100 computer. The gel was pre-heated to 51°C by running for 20 – 30 minutes at 1,000V. Samples were resuspended in 4µl of formamide

loading dye supplied with the sequencing kit and then denatured at 94°C for 4 minutes. The samples were then placed on ice and 2µl loaded immediately in alternate lanes of the gel. The gel was run for 5 minutes before loading the remainder in the empty alternate gel lanes. This procedure was followed to maximise the clarity of reading of each lane during gel analysis. Samples were electrophoresed for either 7 hours at 1,200V or 3.5 hours and 2,400V and a gel temperature of 51°C.

Direct sequencing was the method of choice for mutation screening, and electropherograms interpreted on the basis of substitution and changes in peak heights. However, if a mutation was detected, but the actual change could not be accurately interpreted, verification was through sequencing of single stranded subcloned products which provided an accurate method of delineating the actual sequence change.

### *2.3.10 General sequence analysis.*

Computer programmes used for general sequence analysis and database searching were accessed at the Human Genome Mapping Project (HGMP) web site (www.hgmp.mrc.ac.uk). The Basic Local Alignment Tool (BLAST; Altschul *et al* 1990) was used to compare sequences with Genbank (Benson *et al* 1993), EMBLE (Emmert *et al* 1994) and SWISS-PROT protein database (Emmert *et al* 1994).

### *2.3.11 Microsatellite Repeat Analysis*

Microsatellite repeats were amplified by PCR as described previously, using primers listed in Table 2.5. The forward primers were labelled with 5' FAM (blue) and 5' TET (green) respectively. 5µl of PCR product was first checked on a 2% agarose gel, and the remaining sample diluted either 1:5 or 1:10 in sterile purified water, depending on the quantity of product obtained.

1µl of diluted PCR product was added to 4µl of a loading mix made up of blue dextran (50mg/ml)/EDTA (25mM): deionised formamide: GENESCAN-350™ TAMRA internal lane standard in a 1:3:1 ratio. This dye-labelled internal dye standard (displayed

as red) allowed accurate sizing of DNA fragments in the 35-350 bp range. Samples were denatured at 95°C for 5 minutes and then held on ice before 2μl was loaded onto an acrylamide gel prepared exactly as described for automated sequencing. The gel was preheated to 48°C by pre-running at 1,000V for 20-30 minutes, and the samples electrophoresed for 2 hours at 3,000V and a gel temperature of 48°C on an ABI PRISM™ 377 DNA Automated Sequencer according to the manufacturer's instructions using ABI PRISM™ GeneScan™ Analysis software.

### *2.3.12 Detection of glomerular WT1 and nephrin protein expression*

Slides were provided by Professor Risdon, Professor of Histopathology, Great Ormond Street Hospital NHS Trust. These were first de-waxed by two histaclear washes, followed by progressive washes in diminishing concentrations of ethanol as follows: 100%, 95%, 75%, 50% and 30%. The slides were rinsed in purified water, and then washed in PBS for 1-2 minutes. 4% peroxide was applied, followed by another PBS wash. Citric Acid (pH 6.0) was then applied and the slides micro-waved at high heat for 10 minutes. They were then cooled and after a further PBS wash, the slides blocked for half an hour with 10% calf fetal serum. WT1 (Santa Cruz) or nephrin (gift from Karl Tryggvason) primary antibodies were then applied in a 1:80 dilution and the slides left for 1 hour in a 37°C incubator. The secondary antibody labelled with biotin was then applied in a 1:100 dilution for half an hour and finally the tertiary antibody (streptavadin and peroxidase) was applied in a 1:100 dilution in TBS. DAB was then applied briefly, the slides washed and stained with methyl green. The slides were washed with water and 100% butanol, dried and mounted.

### *2.3.13 Yeast Analysis*

#### *2.3.13.1 Genotyping of yeast strainY190*

Yeast strain Y190 (MATa gal4 gal180 his3trp1-190 ade2-101 ura3-52 leu2-3,-122 + URA3::GAL→ lacZ, Lys::GAL→HIS3 cyh$^r$) was used for yeast two hybrid analysis. This was first grown on appropriate selective minimal media with sequential omission of His, Trp, Ade, Ura, and Leu to ensure that the yeast genotype was correct. Once this

had been established, a yeast glycerol stock was made, stored at -70°C and the yeast could be used for transformation experiments after initial propagation on YAPD complete medium.

### *2.3.13.2 Preparation of yeast competent cells for transformation*

A colony was used to inoculate 200mls of minimal medium + His, Trp, Ade, Ura, and Leu and grown overnight at 30°C. This was then used to inoculate 500 mls YAPD to an OD of 0.2 – 0.25 and grown to until 0.5 to 0.8. The culture was spun for 5 minutes at 3.500 rpm, washed with 100 mls of MilliQ water and re-spun for 5 minutes. The pellet was resuspended in 50mls LiSORB warmed to 30 - 50°C, and spun at 3.500 rpm, followed by re-suspension in 15 mls pre-warmed LiSORB + 75µl 2M DTT and lyticase (1000U). This was spun at 2000 rpm for 5 minutes, washed in a further 15mls LiSORB and respun at 2000 rpm for 5 minutes. The final pellet was resuspended in 1 ml of LiSORB, and either used directly or 75µl DMSO added and the suspension aliquoted prior to storage at -70°C. Stored cells were thawed rapidly for 1 minute at 30°C prior to use.

### *2.3.13.3 Transformation of pAS1-WT1 + or - KTS into the Y190 strain*

0.1µg pAS1 plasmid + or – *WT1* KTS Gal 4 fusion protein DNA was added to 100 µl of Y190 competent cells. 300µl of 0.1M LiAcetate 0.1M TE and 40% PEG was also added and the mixture incubated for 30 minutes at 30°C. 70µl of DMSO was added and the DNA transformed into the yeast cells by heat shock at 42°C. Cells were spun for 10 seconds and resuspended in 500µl of MilliQ water prior to plating on minimal medium + Trp.

### *2.3.13.4 Yeast protein extraction to check expression of bait protein*

Six colonies were picked and re-streaked on minimal medium –Trp. Once these had grown, a generous scoop was taken to inoculate 20 mls of minimal medium –Trp, and the sample vortexed. The culture was grown overnight at 30°C, an OD estimated and a

further 5 mls of minimal medium –Trp inoculated to an OD of 0.2. This was grown at 30°C top an OD of between 0.3 and 1.1.5 mls of this culture was pulse spun for 10 seconds, the pellet resuspended in 75µl of cracking buffer and the suspension vortexed for 30 seconds. This was then subjected to two freeze cycles of 1 minute in liquid nitrogen, followed by 2 minutes at -70°C with a fifteen second vortex at each step. The sample was boiled at 100°C for 10 minutes, vortexed and 20 µl subjected to SDS-PAGE electrophoresis.

### *2.3.13.5 Yeast Cell preparation for library screening*

A colony transformed with GAL4-*WT1* was used to inoculate 100mls of minimal medium -Trp, for pAS1 bait plasmid selection, and this was grown overnight at 30°C to saturation. The following day, the culture was used to inoculate 500mls of YAPD such that within 2 generations (3-4 hours), the $OD_{600}$ had reached between 0.5 – 0.8. Cells were then harvested at 5000rpm for 5 minutes, washed with 100 mls YPD and resuspended in 50 mls LiSORB, followed by 30minute incubation at 30°C. The cells were then spun down again, resuspended in 625 µl of LiSORB and chilled on ice until further use.

### *2.3.13.6 Small scale library transformation*

The carrier DNA mix was prepared by adding 800µl of LiTE or LiSORB to 200µl cooled to room temperature, boiled sheared salmon sperm DNA(20mg/ml). 1-2µg of library DNA was combined with 50µl of the carrier mix, and 40µl of prepared yeast cells added. Carrier mix alone was used for a negative control. The 40µl of cells + carrier/library DNA mix was then incubated for 30 minutes at 30°C, followed by heat shock at 42°C for 7 minutes. The cells were recovered by washing 2-3X with X1 TE, then resuspended in 200µl of x1TE and plated on the appropriate selective media.

### *2.3.13.7 Large scale library transformation*

A carrier DNA mix was prepared using 800µl LiTE or LiSORB to 200µl of cooled to room temperature, boiled sheared salmon sperm (20mg/ml). 40µg library DNA was combined with the carrier mix and 625µl of freshly prepared yeast competent cells and incubated at 30°C for 30 minutes. Carrier mix and cells alone were used as a negative control. 900µl of LiTEPEG solution was then added for every 100µl of cell-DNA mix (usually 18 mls LiTEPEG solution added to 2 mls mix), and the mixture incubated for a further 30 minutes at 30°C. Cells were heat shocked at 42°C for 7 minutes and 5µl inoculated onto minimal medium -Trp Leu plates to test transformation efficiency. The remaining cells were recovered by adding 100 mls liquid minimal medium-His-Trp-Leu and shaking for 1-3 hours at 30°C. Cells were then harvested and resuspended in 15 mls of liquid minimal medium-His-Trp-Leu. 300µl of cells were then plated on selective media + 50mM 3AT and incubated at 30°C for approximately 5 days.

### *2.3.13.8 X-Gal colony filter assay*

Colonies that grew after 3 to 5 days were then tested for β-galactosidase activity using the X-Gal colony filter assay. β-galactosidase assay buffer was prepared by adding 137µl of β-mercaptoethanol and 1.25 ml X-Gal (40mg/ml in DMSO) to 50mls Z-buffer. A circle of 3MM paper was placed in a 150mm petri dish and 6 mls of assay buffer added, ensuring that the paper soaked up the buffer uniformly. Colonies were lifted onto Hybond $N^+$ nylon filters ensuring that the filter and plates were orientated with respect to each other. The filters were then immersed in liquid nitrogen for 30 seconds and allowed to thaw. These were then placed colony side up into the petri dishes containing assay buffer, and the filters incubated at 30°C for a maximum of 5-6 hours, or un til a blue coloration appeared. Blue colonies were taken for further study.

### *2.3.13.9 Recovery of activation domain plasmid DNA from yeast.*

A single transformant colony was used to inoculate 5 mls of selection medium and grown overnight at 30°C. 1.5 mls of the culture was then spun at 12,000rpm for 5

seconds to pellet the cells. The supernatant was discarded, and the pellet resuspended in 200µl yeast lysis solution. 200µl of phenol chloroform mix (1:1) and 0.3g of acid-washed beads were added and the mixture vortexed vigorously for 2 minutes. This was then spun for 5 minutes at 12,000rpm at room temperature, and the supernatant transferred to a clean Eppendorf. The DNA was ethanol precipitated and resuspended in 20µl X1TE. The DNA was then transformed into HB101 cells by electroporation and plated onto M9 minimal medium selecting for leucine.

#### *2.3.13.10 Analysis of positives*

Once the yeast DNA had been transformed into HB101 bacterial cells, these were grown overnight and colonies picked and cultured overnight in LB ampicillin liquid medium. Plasmid DNA was extracted using the alkaline lysis miniprep technique and checked for inserts by Not I restriction enzyme digest. Inserts were then sequenced using VP16 primers and analysed using database analysis programmes accessed through the Human Genome Mapping Project (HGMP) at www.hgmp.mrc.ac.uk.

### *2.3.14 Electromobility Shift Assay (EMSA)*

#### *2.3.14.1 Preparation of nuclear extracts by detergent cell lysis*

Renal tissue was homogenised in Buffer A containing protease inhibitors using a Dounce homogeniser. An equal volume of Buffer B containing protease inhibitors was added, the solutions mixed, and incubated on ice for 5 minutes. Nuclei were then pelleted by centrifugation at 2000g for 5 minutes at 4 C, whereas the supernatant containing the cytoplasmic fraction was aliquoted and stored at -70°C. The pellet was resuspended in 0.5 mls Buffer A containing protease inhibitors and layered onto 5 mls of 0.8M sucrose (in Buffer A). This was spun for a further 10 minutes at 4000g at 4 C to sediment the nuclei, which were then washed once in Buffer C containing protease inhibitors. Nuclei were either used immediately or resuspended in NSB for storage at -70 C.

### *2.3.14.2 Estimation of nuclear concentration.*

Cell lysis was verified by light microscopy, using 0.4% Trypan Blue as a stain. Intact cells exclude this dye, but upon lysis nuclei stain blue. Nuclear concentration was estimated from the $OD_{260}$ of an aliquot lysed in HSU buffer. A 10 µl aliquot of nuclei was resuspended in 0.5 ml HSU buffer, boiled at 100°C for 5 minutes, and an $OD_{260}$ taken. Each mammalian nucleus is estimated to contain approximately 6pg of DNA, and the OD260 corresponds to approx. 70% genomic DNA, 30% nuclear RNA.

### *2.3.14.3 Nuclear extracts.*

Nuclei were prepared in Hypotonic Buffer and purified through a 0.8 M sucrose cushion as follows. First, nuclei were resuspended in Hypotonic Buffer at $5x10^7$ nuclei/ml and an equal volume of 2x extraction buffer (0.6M KCl and 1% NP-40 in Hypotonic Buffer containing protease inhibitors) added. This was extracted at 4 C for 1-2 hours on a rotating wheel, followed by centrifugation at 25,000g for 15 minutes to sediment nuclear debris. The supernatant was removed, aliquoted and snap-frozen for storage at -70°C.

### *2.3.14.4 Preparation of $^{32}P$ labelled probes*

#### *2.3.14.4.1. Probe labelling*

Single stranded palindromic oligonucleotides corresponding to the region of interest within the *NPHS1* promoter, namely 5'cccaacacttggggaggccaaggtgggagg 3' and the antisense equivalent were chemically synthesised by Genosys UK Ltd. The oligonucleotides were annealed in 100µl of 100mM NaCl by boiling in a beaker for 5 minutes, and then allowing the mix to cool slowly to room temperature. 100-150ng (1-2µl) of the annealed oligonucleotides was 5'-end labelled using 1-2µl T4 polynucleotide kinase (T4 PNK) in 2µl of PNK buffer (1x) and 2-3µl of [$\gamma$-$^{32}$P] ATP in a total reaction volume of 20µl and incubating the mixture at 37°C for 1 ½ - 2 hours. T4 PNK enzyme activity was then inactivated by adding 480µl of x1 TE, giving a total volume of 500µl.

*2.3.14.4.2 Removal of unincorporated $\gamma^{32}$ P- dATP and probe elution.*

NAP5 Sephadex G-25 columns were used. These were washed 2-3 times with x1 TE to equilibrate (1-2mls) and then the 500µl probe sample was applied to filter matrix in column discarding eluent. Finally the probe was eluted in 1ml x1 TE into 1.5ml Eppendorf. The aim was to have at least 50% incorporation, which was measured by cpm/dpm of 1-2µl pre-filtration sample (500µl) compared to a 2-4µl post-filtration sample.

*2.3.14.4.3 Binding Reaction*

Once the gel was undergoing pre-electrophoresis (as described in the next section), binding reactions were performed so that samples could be loaded immediately. Reactions were performed in 20µl volumes and contained labelled probe, competitor DNA and protein sample in the relevant buffer. 1µg poly (dI-dC) (1mg/ml), 1-3µg of nuclear protein extract, 5 µl 4x BBO buffer, 1µl 10 µg/ml BSA (binding stabiliser) and 1µl 1mM PMSF/protease cocktail were mixed together and made up to 17µl with MilliQ $H_2O$.This was incubated at room temperature for 20 minutes and then 3µl $\gamma$-$^{32}$ P –dATP probe was added, followed by a further incubation for 30 minutes at room temperature or on ice. 2µl sample loading buffer (150mM Tris (pH7.6), 20% glycerol, 0.25% bromophenol blue was added and samples chilled on ice before loading.

*2.3.14.4.4 EMSA Gel Electrophoresis*

Plates were thoroughly cleaned with detergent, dried and wiped with 70% ethanol. These were sandwiched together using 1.0mm spacers, clamps applied at equal tension and the clamped plates placed into a Pharmacia Biotech gel cassette. A 5% non-denaturing polyacrylamide gel mix consisting of 6ml polyacrylamide (40% 49:1 acrylamide/bis-acrylamide), 1.25ml 10x TBE (x0.25 TBE) and 42mls MilliQ water was made using 300µl 10% APS and 100µl TEMED for polymerisation, and poured between the plates. Once set, the gel was put at 4°C to cool, generally overnight. 2L of 0.25x TBE was made up and also cooled to 4°C. The gel was pre-run in a Pharmacia

Biotech gel tank in x0.25 TBE for 60-90mins at 150V at 4°C, and then the samples loaded and electrophoresed at 180V for 2.8 hours, also at 4°C. The gel was then dried at 80°C for 1 hour on a Rapidry gel dryer and exposed on Kodak MXB Xograph film at -70°C overnight.

## 2.4 Patient selection and control material

The patients studied in this project were drawn primarily from the specialised tertiary referral nephrotic syndrome clinic and the Nephrology ward at Great Ormond Street Hospital NHS Trust. In addition, patients were acquired through collaborations with other Paediatric Nephrology units, Paediatric Endocrinology units, and Clinical Genetics departments in the UK, following calls for patients made during interim presentations of the work at the Royal College of Paediatrics and Child Health annual conference, the Renal Association, British Society for Human Genetics and British Association for Paediatric Nephrology. Patients were also obtained from overseas through further data presentations at European Society of Paediatric Nephrology, International Society of Paediatric Nephrology, European Society of Paediatric Endocrinology and the American Society of Nephrology through direct liaison with local clinical teams. The largest cohort of patients studied from outside the UK was from the island of Malta, through collaboration with Dr Victor Grech, Senior Registrar at St Luke's Hospital, Guardamangia, Malta. Almost all of the Maltese patients were assessed as inpatients at Great Ormond Street Hospital, by virtue of a special arrangement between the Maltese and British governments for their clinical care.

The majority of patients studied had non-syndromic nephrotic disease confined to the kidney. However two types of syndromic disease were also studied, namely Denys Drash and Frasier syndromes associated with intersex and Wilms' tumour and gonadoblastoma respectively. Again, these patients predominantly originated from the Paediatric Nephrology and Endocrinology units at Great Ormond Street Hospital NHS Trust and Drs Detlef Blockhause in Boston, USA and Dr Mariana Arcena in Santiago, Chile.

Control DNA samples were also obtained from consenting individuals, with thirty English and Asian normal controls and twenty Maltese normal controls studied in total. For *NPHS1* mutation analysis, there was further access to a database of 50 controls originating from the United States, Scandinavia and Europe, characterised by Professor Karl Tryggvason's teams at the University of Oulu, Oulu, Finland and the Karolinska Institute, Stockholm, Sweden.

Patients were examined either at Great Ormond Street Hospital NHS Trust or by the referring specialist clinician. A diagnosis of congenital nephrotic syndrome was made on the basis of the presence of proteinuria at birth or nephrotic syndrome appearing within the first three months of life. The additional feature of large placenta was present in many cases, indicative of significant proteinuria in utero. Early onset nephrotic syndrome was defined as a nephrotic syndrome appearing after 3 months, but before 2 years of age. Clinical diagnosis was confirmed by a family history if present and in addition, a renal biopsy performed after three months of age. Further sub-classification was based on renal histological appearance, examined in the majority of cases by Professor Risdon, Professor of Histopathology at Great Ormond Street Hospital NHS Trust. Histology determined by the referring centre, was also reviewed if possible at Great Ormond Street Hospital NHS Trust. Patients were identified as having renal histology compatible with congenital/early onset CNF, FSGS, or DMS as defined previously, and wherever possible, the histology was confirmed in at least two centres.

If stored blood or DNA was not already available for laboratory analysis, referring clinicians were asked to obtain samples of venous blood from consenting individuals, and these were forwarded for DNA extraction. Karyotyping was performed at the referring hospital as necessary. In accordance with the guidelines laid down by Great Ormond Street Hospital NHS Trust and Institute of Child Health Research Ethics committee, the laboratory findings of this study whether positive or negative were fed back to the referring clinician, who was then able to inform the patients, their GP's and other clinicians involved in the patients care. Identification of a causative mutation in the proband, allowed the referring clinician to offer mutation screening to the other members of the family, followed by the appropriate genetic counselling if this was accepted.

# CHAPTER 3: Molecular analysis of the *WT1* gene in nephropathic phenotypes associated with Denys Drash and Frasier syndrome

## 3.1 Background

As outlined in Chapter 1, disruption of the glomerular filtration barrier is characterised by leakage of plasma proteins into the urine, resulting in nephrotic syndrome. Presentation during childhood is typically as a congenital nephrotic syndrome (0 to 3 months), an early onset nephrotic syndrome (4 to 36 months), or later in childhood. Although Finnish type congenital nephrotic syndrome is the most common type of hereditary nephrotic syndrome seen in early life, less common aetiologies such as diffuse mesangial sclerosis (DMS) and focal segmental glomerulosclerosis (FSGS) also form a significant component of the overall pathology. These may occur together with developmental abnormalities in other organ systems, and importantly form the defining features of Denys Drash syndrome (DDS), a triad of DMS, intersex and Wilms' tumour (Denys *et al*, 1967; Drash *et al*, 1970), and Frasier syndrome (FS), characterised by FSGS, intersex and gonadoblastoma (Frasier *et al*, 1967; Moorthy *et al*, 1987). However, the characteristic nephropathies connected with these syndromes occur more commonly as disorders confined to the kidney, and although the association of constitutional heterozygous *WT1* gene mutations with the majority of cases of DDS (e.g. Pelletier *et al*, 1991; Baird *et al*, 1992) is well described, it was unknown whether mutations also affected this wider population. The initial aim was therefore to identify whether *WT1* gene mutations are also responsible with DDS/FS nephropathic phenotypes occurring in isolation. Glomerular WT1 protein expression was examined in affected individuals, in conjunction with screening for *WT1* mutations (Section 3.2). Secondly, although preliminary investigation did not detect *WT1* gene mutations in FS (Poulat *et al*, 1993), it was noted that only exonic regions and a very small number of cases had been screened. In view of this, four new cases of FS were assessed for the presence of *WT1* mutations (Section 3.3), and functional analysis subsequently performed to establish the effect of the abnormalities detected on + and – KTS protein isoforms (Section 3.4). Finally, yeast two hybrid analysis was used to determine

downstream protein binding partners of both + and – KTS WT1 isoforms, in order to identify novel renal genes contributing to the pathogenesis of glomerular disease (Section 3.5). Results are discussed in Section 3.6.

## 3.2 WT1 gene mutations are an infrequent cause of isolated DMS and FSGS

### *3.2.1 Patient selection*

A total of twenty-nine cases of congenital and early onset nephrotic syndrome were studied. A diagnosis of DMS or FSGS was established on the basis of the clinical history, and confirmed by renal biopsy and/or by post-mortem renal histology. Patient details are summarised in Table 3.1 and 3.2. Twenty-six cases had documented karyotype analysis, and any coincident abnormalities of the internal gonads were determined by pelvic ultrasound, or by laparotomy. The majority of surviving patients with isolated DMS were followed up with yearly renal ultrasounds to exclude Wilms' tumour formation. Other congenital malformations were investigated by clinical examination and the appropriate investigations. None of the patients with psychomotor abnormalities fitted any particular syndrome.

Twenty-two of the cases studied had a renal histology of DMS, unaccompanied by the extra-renal features of DDS or FS. Twelve had a diagnosis of congenital nephrotic syndrome, and the remainder early onset nephrotic syndrome, with onset of disease ranging from between six and eighteen months. Of note, case 14 had an equivocal report for karyotype, and thus a possible intersex state. However, by the time of study, case 14 had died and the karyotype analysis could not be repeated. Three cases of DDS (cases 20, 21 and 22; Table 3.1) were also analysed. Case 22 represented a novel diagnosis of DDS, whereas characteristic R394W *WT1* missense mutations had already been detected in cases 20 and 21 (Baird *et al*, 1992), and these were used as positive controls. Seven cases of isolated FSGS, again unaccompanied by features of DDS or FS were also screened for *WT1* gene mutations.

### *3.2.2. WT1 protein expression is normal in cases of DMS, FSGS and DDS*

Glomerular WT1 protein expression was examined in selected cases of DMS and congenital/ early onset FSGS, occurring in the absence of other features of DDS or FS. Renal biopsy specimens from cases of benign haematuria were used as normal controls. Immunoperoxidase staining was performed using a WT1 monoclonal antibody (Santa Cruz) raised against the C-terminal portion of the WT1 protein. No abnormalities of expression were detected in the glomeruli of cases of isolated DMS, FSGS, or in the two cases of DDS with pre-determined R394W mutations (Figure 3.1). This indicated that if *WT1* gene mutations were present, these did not appear to result in abnormalities of WT1 protein expression. This suggested that either missense mutations, or mutations that did not result in either truncated or unstable proteins might be responsible.

### *3.2.3 WT1 gene mutations are not present in isolated DMS and FSGS*

The two most common DDS mutations are located in exon 9 (1180 C→T R394W 60%, 1186 G→A D396N 15%), and abolish an *Rsr* II site in zinc finger 3 (Little *et al* 1993). This was used as an initial screen to exclude cases of DDS that might have been missed through incomplete clinical criteria. As expected, heterozygous loss of the site was observed in cases 20 and 21, as well as case 22, whose clinical phenotype was compatible with DDS. Cases 1 to 19, and 23 to 29, showed normal restriction enzyme digest, virtually excluding a diagnosis of DDS. A representative agarose gel is shown in Figure 3.2. Single stranded conformational polymorphism (SSCP) was then used to screen *WT1* exons 1 to 10 and intron/exon boundaries for mutations, performed at 4°C under two different non-denaturing polyacrylamide gel concentrations (6 % and 10%). In addition, *WT1* exons 5, 8 and 9 were directly sequenced in all affected individuals.

Any sequence changes were first detected as an aberrant band on SSCP analysis. However, since this was unable to indicate whether the change represented a silent polymorphism or a change likely to affect gene function, any samples demonstrating changes detected on SSCP were examined further by sequencing. The only sequence changes detected were in case 14, who demonstrated a novel C→T polymorphism in codon 178 (exon 4) conserving a threonine, and in case 16 and three of the parents

screened, who all carried a previously described polymorphism, an A→G transition in codon 301 (exon 7) conserving an arginine (Groves *et al* 1992). This base change destroys an *Afl* III restriction enzyme recognition site, which allowed additional confirmation by *Afl* III restriction enzyme digest. Aside from these two polymorphisms, DDS cases 20 and 21 showed expected 1180 C→T mutations (R394W) in exon 9, as previously reported by Baird *et al*, 1992a. The same mutation was also detected in case 22, a case of congenital DMS, with a 46XY karyotype and hypospadias, but no Wilms' tumour. Since case 22 died of septicaemia at the age of four months, these clinical features were compatible with a diagnosis of DDS despite the lack of Wilms' tumour at presentation.

Direct sequencing provided corroborative evidence that *WT1* gene mutations were absent in the 19 patients with isolated DMS, and 7 patients with isolated FSGS as had been suggested by SSCP analysis and confirmed the polymorphisms detected. These findings provided the first evidence for the genetic heterogeneity of nephropathic phenotypes associated with Denys Drash and Frasier syndromes (Koziell *et al*, 1998). Results are tabulated in Tables 3.1 and 3.2, and representative results for the R394W missense mutation detected in cases 20, 21 and 22 are shown in Figure 3.3.

**Figure 3.1 (a) Representative picture of immuno-peroxidase staining for normal WT1 protein expression in isolated DMS.**

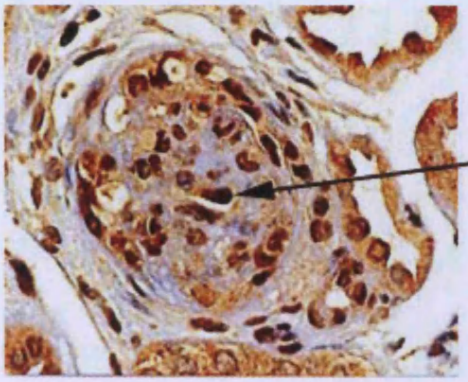

**Brown immunoperoxidase staining of podocyte nucleus to show nuclear expression of the WT1 protein**

**(b) Control glomerulus showing normal distribution of WT1 protein expression.**

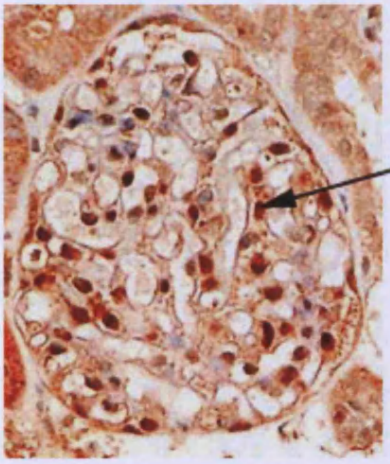

**Brown immunoperoxidase staining of podocyte nucleus to show nuclear expression of the WT1 protein**

**Figure 3.2. Representative *Rsr* II restriction enzyme digest analysed on a 2% agarose gel . The only sample to demonstrate heterozygous loss is sample 20, with DDS and a R394W mutation (demarcated by *).**

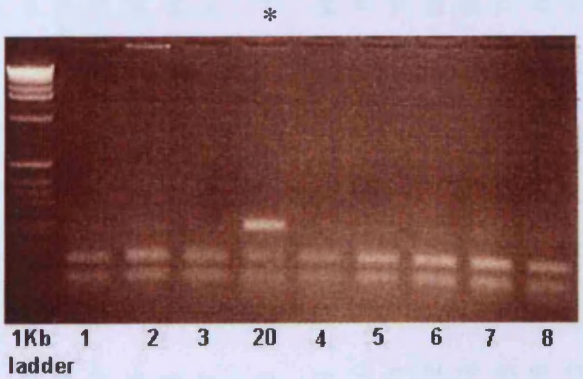

**Table 3.1 Clinical details and results of *WT1* mutation analysis of cases with a renal histology compatible with DMS (n=22)**

| Case | Karyotype | Nephropathy | | | | Syndromal tumour | Genital status int/ext | Other renal or extra-renal | Family history | WT1 gene mutation | age at last follow-up |
|---|---|---|---|---|---|---|---|---|---|---|---|
| | | onset of proteinuria | ESRF/ Dialysis | nephrec -tomy | transplant | | | | | | |
| 1 | 46 XX | day 1 | yes | no | yes | no | F | psychomotor | yes | no:exons 1-10 | 10 years |
| 2 | 46 XX | day 1 | yes | yes R, L | yes | no | F | no | no | no:exons 1-10 | 4 |
| 3 | 46 XX | day 1 | yes | yes R, L | no | no | F | no | yes | no:exons 1-10 | 8 |
| 4 | 46 XY | day 1 | yes | no | no | no | M | no | no | no:exons 1-10 | died 3 1/2 |
| 5 | 46 XY | >1 year | yes | yes R, L | yes | no | M | no | no | no:exons 1-10 | 13 |
| 6 | 46 XY | >1 year | yes | yes R,L | yes | no | M | no | no | no:exons 1-10 | 11 1/2 |
| 7 | 46 XY | >1 year | no | no | no | no | M | no | no | no:exons 1-10 | 3 |
| 8 | 46 XX | day 1 | no | no | no | no | F | psychomotor, hypothyroid pulmonary | no | no:exons 1-10 | died: 7 months |
| 9 | 46 XY | 6 months | yes | no | yes | no | M | stenosis | no | no:exons 1-10 | 14 1/2 |
| 10 | 46 XX | >1 year | no | no | no | no | F | psychomotor | no | no:exons 1-10 | died 3 1/2 |
| 11 | 46 XY | 18 months | yes | no | no | no | M | no | no | no:exons 1-10 | 5 1/2 |
| 12 | 46 XX | day 1 | yes | no | no | no | F | psychomotor | ? yes | no: exons 2 -10 | died: 2 months |
| 13 | NK | day1 | yes | no | no | no | F | no | yes | no: exons 2 -10 | died: 7 months |
| 14 | 46 XY | day1 | no | no | no | no | F | no | no | exon 4 polym | died: 3 months |
| 15 | 46 XX | day1 | no | no | no | no | F | psychomotor | no | no: exons 2 -10 | died:10 months |
| 16 | 46 XY | day 1 | no | no | no | no | M | no | no | AflIII polym | died: 2 months |
| 17 | NK | day 1 | no | no | no | no | NK | no | no | no: exons 2 -10 | died: 10 weeks |
| 18 | NK | day 1 | no | no | no | no | NK | no | no | no: exons 2 -10 | died: 8 months |
| 19 | 46 XX | 1 year | yes | no | no | no | F | L dysplastic kidney | no | no: exons 5,8,9 | 2 1/2 |
| 20 | 46 XY | >2 years | yes | yes R, L | yes | Wilms' | F | no | no | exon9: 1180C→T R394W | 13 |
| 21 | 46 XY | 1 year | yes | yes R,L | yes | Wilms' | ambiguous | no | no | exon9: 1180C→T R394W | 11 1/2 |
| 22 | 46 XY | day 1 | yes | no | no | no | hypospadias | no | no | exon9: 1180C→T R394W | died: 3 months |

**Table 3.2 Clinical details and results of *WT1* mutation analysis of cases with a renal histology compatible with FSGS (n=7)**

| Case | Karyotype | Nephropathy | | | | Syndromal tumour | Genital status int/ext | Other renal or extra-renal | Family history | WT1 gene mutation (exons 1-10) | age at last follow-up |
|---|---|---|---|---|---|---|---|---|---|---|---|
| | | onset of proteinuria | ESRF/ dialysis | nephrec-tomy | transplant | | | | | | |
| 23 | 46 XX | 4 months | | no | no | - | F | no | no | no | 12 |
| 24 | 46 XX | > 1year | ? | ? | ? | - | F | no | yes | no | died |
| 25 | 46 XY | > 1year | ? | ? | ? | - | M | no | yes | no | died |
| 26 | 46 XX | Day 1 | no | no | no | - | F | no | yes | no | 8 |
| 27 | 46 XY | 18 months | yes | no | yes | - | M | no | yes | no | 14 |
| 28 | 46 XY | > 1year | yes | ? | yes | - | M | no | no | no | 15 |
| 29 | 46 XX | 1 year | yes | yes R,L | no | - | F | spondyloepiphyseal dysplasia | no | no | died |

**KEY:** NK: not known; R: right; L:left; F: female; M:male

**Figure 3.3 (A to D). The typical 1180 C→T (R394W) mutation detected in >60% of DDS cases, used as a positive control for this study and detected as a novel event in case 22.**

**(A) *WT1* exon 9 1180 C→T missense mutation 5' to 3'**

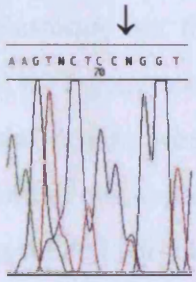

**(B) *WT1* exon 9 normal control**

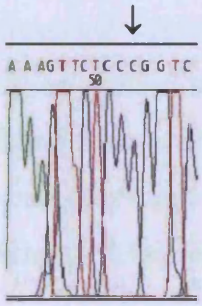

**(C) *WT1* exon 9 1180 C→T missense mutation 5' to 3'**

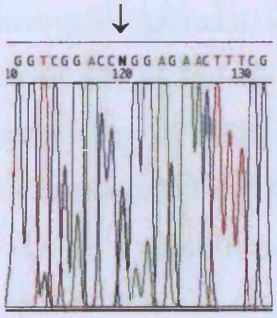

**(D) *WT1* exon 9 normal control**

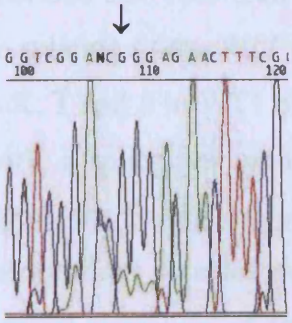

## 3.3 *WT1* gene mutations are responsible for Frasier Syndrome (FS)

In common with DDS, FS is also characterised by intersex and renal disease, although the associated nephrotic syndrome typically results from FSGS rather than DMS. Patients may develop gonadoblastoma, but there is no true predisposition to Wilms' tumour. Since mutations of the *WT1* gene were not initially detected in this condition (Poulat *et al*, 1993), its molecular origins were thought to differ from DDS. However, since there were a number of limitations to this particular study, four new cases of FS: DG, CC, SS and CO were re-examined for mutations of the *WT1* gene. Clinical details are given in Table 3.3. All were phenotypically normal girls, but with a 46XY karyotype and characteristic features of FSGS nephropathy. DG and CC presented with gonadoblastoma, whereas SS presented with nephrotic syndrome and delayed puberty, and CO with nephrotic syndrome, short stature and delayed puberty. Nephrotic syndrome developed between 3 and 8 years of age in all four cases, with a mean age of onset of 5 years. DG and CO had developed renal failure and had been transplanted. None of the cases had Wilms' tumour. The clinical features are described in Table 3.3.

The focus for mutation screening was the region of the mutation "hot spot" for DDS. Intronic PCR primers amplifying exon 9 of the *WT1* gene together with the intron/exon boundaries were designed 34 base pairs upstream, and 77 base pairs downstream of the exon 9 coding region. This ensured any mutations within these boundary areas would be reliably detected. Direct sequencing of PCR products on an ABI 377 detected mutations in all four FS cases examined, but not in parents or siblings. Three carried identical heterozygous 1228+5 (G $\rightarrow$ A) substitutions, and one case a 1228+4 (C $\rightarrow$ T) substitution within the exon 9 splice donor site (Table 3.3; Figures 3.4 A to D), which indicated a consistent association between intronic mutations within the splice donor site of exon 9 of the *WT1* gene, and FS. This area lies within the second and highly conserved region of alternative splicing of the *WT1* gene, which results in inclusion or exclusion of three amino acids K, T and S in WT1 protein isoforms. Sequence analysis of exon 9 using Neural Network, a splice site prediction programme identified these two splice donor sites (http://www.fruitfly.org/seq_tools/splice.html). Subsequent introduction of the two base substitutions detected in the cases of FS, and reanalysis of the two sites resulted in a marked reduction of the score of the second splice site

(Figure 3.5). This finding suggested that the effect of these mutations might be to severely impair the use of the second alternative splice donor site, and thus alter the ratio of WT1 protein isoforms produced.

## 3.4 Intronic *WT1* gene mutations in Frasier Syndrome result in defective alternative splicing of *WT1*, and reversal of the normal +/- KTS isoform ratio

Since the predicted effect of the two heterozygous *WT1* gene mutations detected in FS was to severely impair alternative splicing at the second splice donor site in exon 9, the most likely outcome was an alteration of the normal +/- KTS protein isoform ratio, suggesting that aberrant splicing might underlie the pathogenesis of FS. Alternative splicing of the *WT1* gene normally results in four different zinc finger protein isoforms with either inclusion or exclusion of exon 5 encoding 17 amino acids and/or three amino acids, K T S (Lys, Thr, Ser) between the third and fourth zinc fingers, generating four splice isoforms. In general –KTS isoforms bind DNA well, and are thought to participate in transcriptional regulation, whereas +KTS isoforms do not bind DNA and may modulate RNA metabolism (Larsson *et al*, 1995; Ladomery *et al*, 1999; Englert *et al*, 1995). The insertion of KTS between zinc fingers 3 and 4 is thought to increase the flexibility of the linker, preventing DNA binding (Laity *et al*, 2000). The usual ratio of + and – KTS protein isoforms detected is approximately 2:1 in all tissues tested (Klamt *et al*, 1998), and in view of the different physical properties conferred to the protein isoforms, their interplay is clearly critical for correct gene function.

Archival gonadoblastoma tissue was available from case DG, which allowed the analysis of *in vivo* expression of WT1 protein isoforms in FS. RT-PCR was performed with exon specific primers to quantify the protein isoform ratio in DG, one specimen of normal kidney and one specimen of Wilms' tumour. Experiments performed in parallel detected a range of 1.5 to 2.8 for the +/- KTS isoform ratio in archival Wilms' tumours not associated with *WT1* gene mutations (Klamt *et al*, 1998).

**Table 3.3 Clinical characteristics of the four FS cases screened in this study (n=4)**

| case | karyotype | nephropathy | | | | | gonadal | syndromal | family | WT1 |
|---|---|---|---|---|---|---|---|---|---|---|
| | | onset of protienuria (years) | histology | ESRF/ dialysis | nephrec-tomy | transplant | development | tumour | history | mutation |
| DG | 46 XY | 5 | FSGS | yes | no | yes | gonadal dysgenesis rudimentary uterus | gonadobalstoma | no | +5 G to A |
| CC | 46 XY | 6 | FSGS | yes | no | no | gonadal dysgenesis | gonadobalstoma | no | +4 C to T |
| SS | 46 XY | 8 | FSGS | yes | no | no | gonadal dysgenesis delayed puberty | no | no | +5 G to A |
| CO | 46 XY | 4 | FSGS | yes | no | yes | gonadal dysgenesis delayed puberty | no | no | +5 G to A |

**Figure 3.4 (A) Electropherogram to show the *WT1* 1228+5 (G → A) splice site mutation detected in FS**

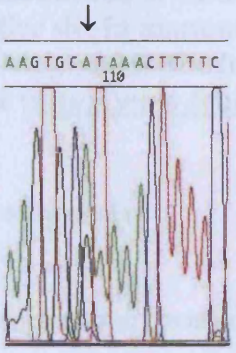


**(B) Electropherogram of normal control**

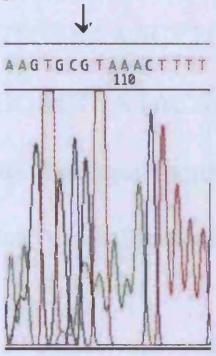


**(C) ) Electropherogram to show the *WT1* 1228+4 (C → T) splice site mutation detected in FS**

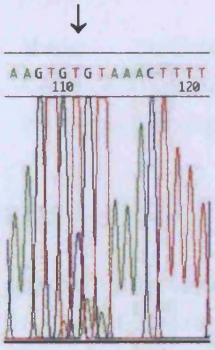


**(D) Electropherogram of normal control**

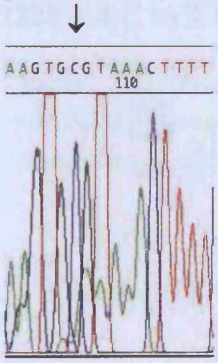

**Figure 3.5 Splice site prediction by Neural network. This is able to indicate the potential effect of a base substitution or other putative mutation within the consensus sequence of a splice site in mammals. The results given are for the two different base substitutions detected in the four cases of FS within the *WT1* exon 9 alternative splice donor site (http://www.fruitfly.org/seq_tools/splice.html).**

**Exon 9 wild type sequence analysed:**

5'gtgcagaatcagtgattcttgttgggcctgggggactggggaaatctaaggtgaggcagatgcagacattgcaggcatggcaggaaat

gctgggctcctccagctgccggaagtcagccttgtgggcctcactgtgcccacattggttagggccgaggctaaccttctctgtccattt

AGGTGTGAAACCATTCCAGTGTAAAACTTGTCAGCGAAAGTTCTCCCGGTCCGACC

ACCTGAAGACCCACACCAGGACTCATACAG gt AAAACAA gt g t g t aaa

tttcttcacatttatttttcattatttttttaaactattgtggaatgaaattgtgatgagagggattggaaaagactagtgtaaagttctaaggtttaga

ctcagttgagagaaggaatagtgcgtggctatctttaaataataaataataacattttaaagaaggggagggtggaaatacagagaaggag

aagatggaaagatgctgactg 3'

**Donor site predictions for wild type exon 9 :**

| Start | End | Score | Exon | Intron |
|---|---|---|---|---|
| 262 | 276 | 0.94 | CATACAG | gtaaaaca |
| 271 | 285 | 0.76 | AAAACAA | gtgcgtaa |

**Donor site predictions with 1228 + 5 G to A substitution:**

| Start | End | Score | Exon | Intron |
|---|---|---|---|---|
| 262 | 276 | 0.94 | CATACAG | gtaaaaca |
| 271 | 285 | 0.00 | AAAACAA | gtgctaa |

**Donor site predictions with 1228 + 4 C to T substitution:**

| Start | End | Score | Exon | Intron |
|---|---|---|---|---|
| 262 | 276 | 0.94 | CATACAG | gtaaaaca |
| 271 | 285 | 0.55 | AAAACAA | gtggtaa |

To quantitate WT1 splice isoforms, a second round of hemi–nested PCR was performed using DDS1 and FRAS2 primers (Chapter 2, Table 2.2), and [$^{32}$P] dCTP radio-labelled products separated (Figure 3.7). Only tissue from case DG was available at the time. Quantification of band intensity performed using a Phospho-imager (Molecular Dynamics) revealed that, in contrast to normal kidney and Wilms' tumour, there was an apparent reversal of the normal +/- KTS isoform ratio *in vivo*. The experiment was repeated twice, and this reversal from approximately 2:1 to approximately 1:2 was present on each occasion (Figure 3.6). These findings supported the results of computer predictions that *WT1* gene mutations in FS lead to abnormal splicing at the second splice donor site in exon 9, disrupting the normal ratio of + to - KTS WT1 isoforms present, which resulted in an FS phenotype. These findings provided one of the first pieces of experimental evidence that the different WT1 protein isoforms have different functions, and that renal and gonadal development may be especially sensitive to imbalance or relative under-representation of the WT1 +KTS isoform. These results were subsequently supported by the detection of WT1 mutations in a larger series of FS cases (Klamt *et al*, 1998), and provided key evidence for a critical role for the *WT1* gene in ensuring correct differentiation of the indifferent gonad and renal tract.

**Figure 3.6 RT-PCR analysis of WT1 in Wilms tumour, normal kidney and archival gonadoblastoma tissue from case DG.**

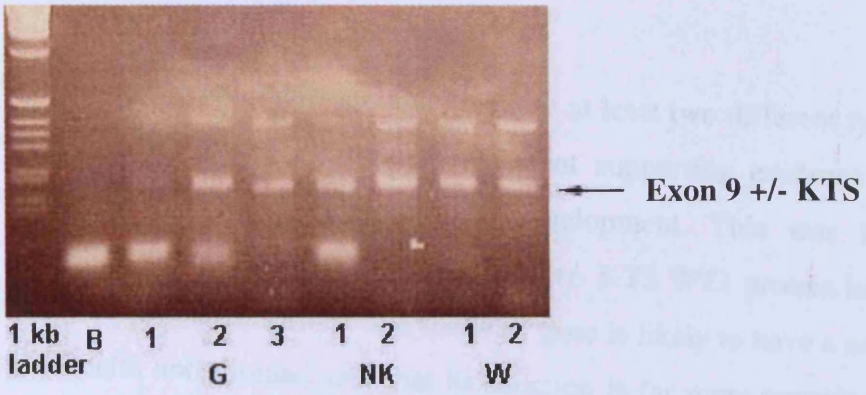


(KEY: G = gonadoblastoma; NK = normal kidney; W = Wilms' tumour)

**Figure 3.7 RT-PCR analysis of +/- KTS isoforms in FS. Lanes A and B demonstrate the normal pattern seen in tissues of approximately 2 : 1+ KTS : – KTS, whereas lanes C and D the reversal seen in FS.**

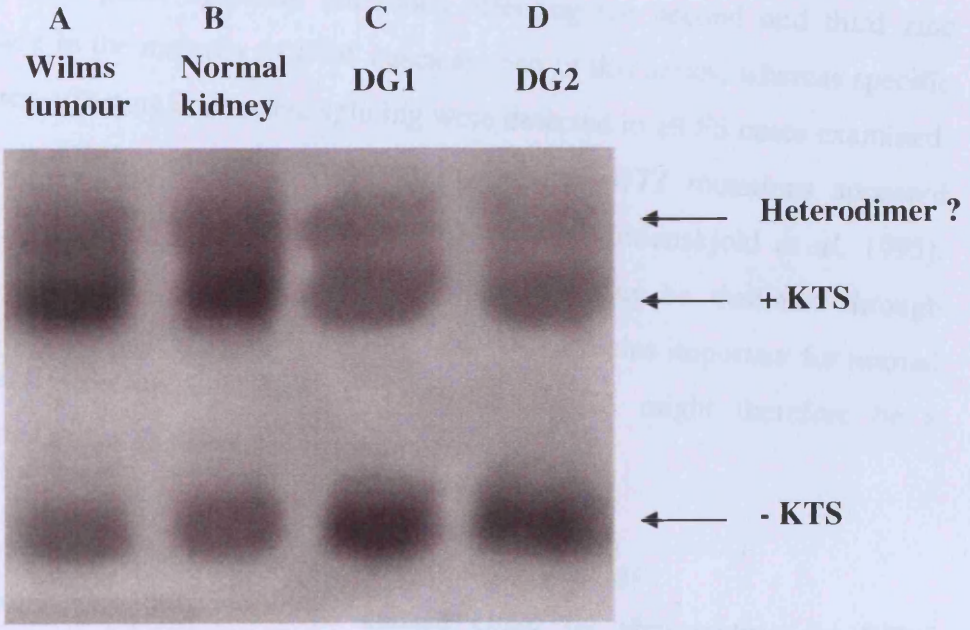


| Ratio of band intensity of +/- KTS isoforms as measured on phospho- imager | 2.3 | 2.4 | 0.57 | 0.56 |
|---|---|---|---|---|

## 3.5 Yeast two hybrid analysis of murine + and – KTS WT1 protein isoforms

### *3.5.1 Rationale for yeast two hybrid analysis*

The discovery that *WT1* gene mutations are able to cause at least two different types of glomerular damage in DDS and FS provided important supporting evidence for a critical role for the *WT1* gene in genitourinary development. This was further underpinned by the detection of a reversal of the normal +/- KTS WT1 protein isoform ratio in FS. These initial results confirmed that the *WT1* gene is likely to have a number of different roles in health and disease, and that its function is far more complex than simply tumour suppression. However, unanswered questions remained regarding the exact role WT1 plays in podocyte maintenance and the integrity of the glomerular filter, and how abnormalities might contribute to nephrotic disease. Accumulating evidence supported a regulatory role for WT1 in kidney development, but little was known about what its targets may be or which cascades may be affected by its abnormal function.

The conclusion that could be drawn from sections 3.2 to 3.4 was that *WT1* gene mutations form a key feature of DDS and FS. Although mutations may occur throughout the *WT1* gene, missense mutations affecting the second and third zinc fingers are present in the majority of DDS cases as seen in this series, whereas specific intron 9 mutations affecting alternative splicing were detected in all FS cases examined. In contrast, when DMS and FSGS occurred in isolation *WT1* mutations appeared unusual, which is in common with pure intersex states (Nordenskjold *et al*, 1995). These findings suggested that some effects of mutations may be mediated through altered regulation of genes and/or altered interaction with proteins important for normal renal and gonadal development. Isolated DMS and FSGS might therefore be a consequence of mutations in genes downstream of *WT1*.

The following hypothesis was tested on the basis of these findings:
Inappropriate protein-protein interactions caused either by abnormalities in WT1 proteins, or their isoform ratio results in malformed renal glomeruli, abnormal gonadal development and oncogenesis.

### *3.5.2 The yeast two hybrid system*

Yeast two hybrid analysis was used to establish potential target proteins *in vivo,* concentrating primarily on those that may result in abnormal glomerular development. This technique was first proposed by Fields and Song (1989), and utilises the yeast genetic machinery to detect protein-protein interactions *in vivo*. The protocol is based on the essentially modular properties of many transcription factors, and the fact that they have two distinct domains: one able to bind to specific DNA sequences upstream of target genes, and the other to activate transcription of the target gene in question (Keegan *et al*, 1986). Transcription factors may be split into these two separate functional domains, which when expressed separately, are unable to independently activate transcription. In the two hybrid approach, these domains are used to generate hybrid proteins, which are then tested for potential protein-protein interaction through their ability to activate specific reporter genes. The majority of yeast two hybrid systems are based on either the yeast GAL4 transcription factor, or the prokaryotic LexA transcription factor found in *E. coli*. In addition, exchange of DNA binding domains and activation domains between these transcription factors can occur without compromising function.

The bait protein is first fused to a DNA binding domain, forming a fusion cDNA, which is then transferred to a yeast strain. This expresses the protein as a fusion, and can be transformed with a library of cDNA's fused to a corresponding activation domain. If no interaction occurs between the bait and library proteins, the domains remain apart. If interaction does occur, they come into apposition and reconstitute the transcription factor. This specifically activates reporter genes, allowing detection of the interaction by growth in selective media and/or colorimetric assay (Figure 3.8). Once isolated, potential interactors can be sequenced, and the appropriate databases interrogated allowing correct identification of interacting proteins. Any novel proteins detected can be assessed for the presence of motifs indicative of their putative function.

**Figure 3.8. The yeast two hybrid system**

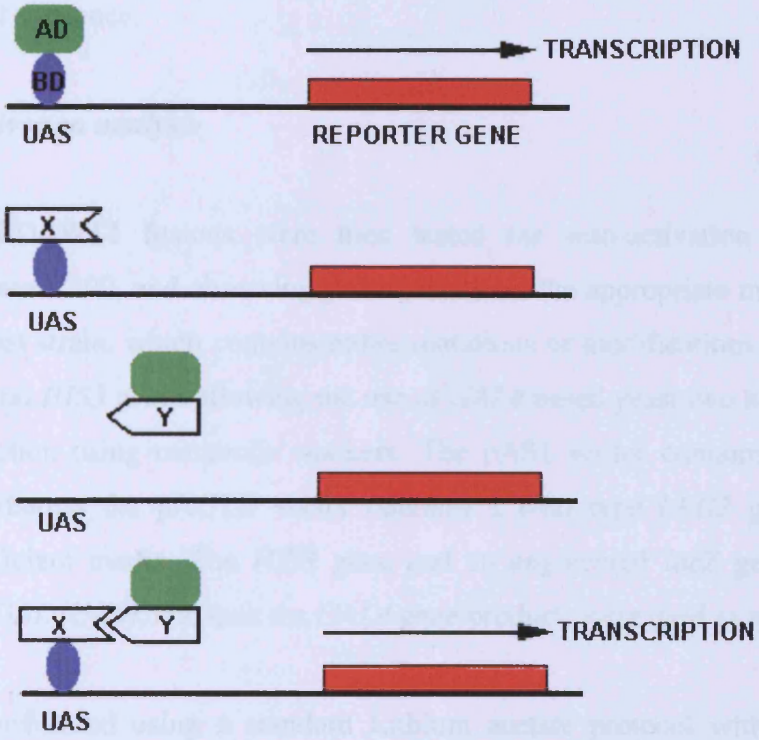


**KEY**

**AD = activation domain**

**BD = binding domain**

**UAS = upstream activation sequence**

**X = bait protein fused to binding domain**

**Y = prey protein with cDNA library fused to activation domain**

### *3.5.3 Subcloning of full-length murine WT1 constructs*

-KTS WT1 isoforms were subcloned in as a BamHI fragment, whereas + KTS isoforms as a SmaI/BamHI fragment in pAS1 and pACTII respectively to form in frame GAL4 DNA binding domain (BD) and GAL4 activation domain (AD) full-length murine WT1 fusion proteins (Figures 3.9 and 3.10). The presence of inserts was confirmed prior to transformation into yeast by *Sma*I and *BamH*I digest (Figure 3.11). All constructs were sequenced to confirm in-frame subcloning of the *WT1* cDNA, and absence of mutations within the *WT1* sequence.

### *3.5.4 Auto-activation analysis*

GAL4-DNA BD WT1 fusions were then tested for auto-activation potential by transforming into Y190, and observing yeast growth on the appropriate media. Y190 is a modified yeast strain, which contains either mutations or modifications of the *GAL4*, *LEU2*, *TRP1* and *HIS3* genes allowing the use of *GAL4* based yeast two hybrid vectors, and their selection using metabolic markers. The pAS1 vector contains a wild type *TRP1* gene, whereas the pACTII vector contains a wild type *LEU2* gene allowing growth on deficient media. The *HIS3* gene and an engineered *lacZ* gene under the control of the *GAL (UAS)*, and thus the *GAL4* gene product, were used as reporters.

Y190 was transformed using a standard Lithium acetate protocol with both empty pAS1, and with - and + KTS WT1 fusion proteins in pASI. Transformations were plated on minimal medium containing –Trp selection alone, -Trp, -His selection, and –Trp, -His together with either 25 and 50 mM 3-amino triazole (3-AT). Growth was observed on the –Trp plate as expected, which selected for bait plasmid alone. Some minimal growth was observed on –Trp, -His selection, suggesting either leakage of the His reporter, or a mild degree of autoactivation. This was completely abolished by the addition of 25 and 50 mM 3-AT, a structural analogue of histidine able to act as a competitive inhibitor of histidine synthesis, thus reducing the level of histidine within the cell to a minimum.

**Figure 3.9 GAL4 DNA-BD - full length murine +/- WT1 isoforms in frame fusions in pAS2 generated using *Sma*I and/or *BamH*I (red arrows)**

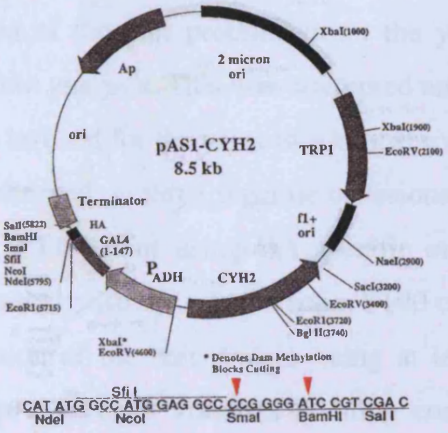


**Figure 3.10 GAL4 DNA-AD - full length murine +/- WT1 isoforms in frame fusions in pACTII generated using *Sma*I and/or *BamH*I (red arrows)**

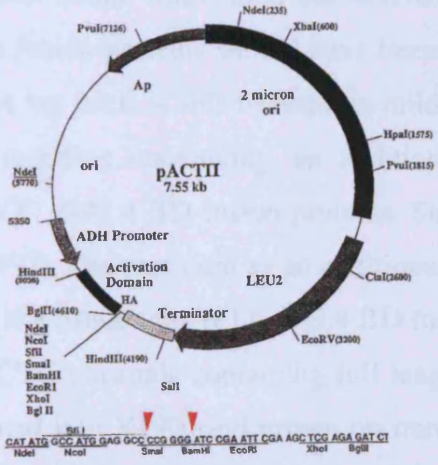


**Figure 3.11. *SmaI/BamH*I and *BamH*I digest of WT1 Gal4 fusion proteins in pAS2 and pACT2 analysed on a 1% agarose gel**

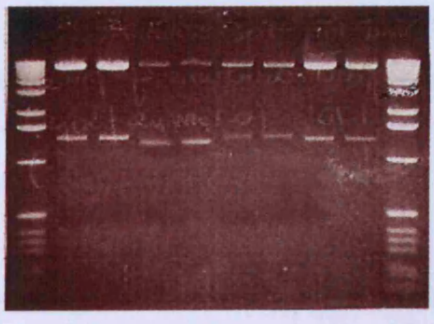

**1kb ladder** **+/+** **-/-** **+/+** **-/-**

### 3.5.5 Confirmation of WT1 fusion protein expression within Y190

By convention, expression of the bait protein within the yeast is confirmed prior to library screening by Western analysis. This was attempted unsuccessfully for the WT1 -/+ KTS fusion proteins to be used for the yeast two hybrid screen. Western blot analysis of eighteen colonies transformed on three separate occasions (in batches of six) did not demonstrate presence of WT1, either using HA specific or WT1 specific antibodies. This was however not unusual with the pAS1 vector/Y190 combination, and may have resulted from the expression of the bait protein being at levels too low for antibody detection. Although the pAS1 vector contains a strong constitutive full length ADH promoter to drive the expression of chimeric proteins, expression may be repressed as much as 10-fold by ethanol accumulation in the medium (Denis *et al*, 1983). This occurs if the yeast is allowed to grow beyond logarithmic growth, a situation difficult to manage with the Y190 yeast strain. Since mild autoactivation was observed for both isoforms, by definition the fusion proteins should have been expressed, however it was observed that the pAS1 HA tag itself is able to result in mild autoactivation of the yeast reporter. In view of the resulting uncertainty, an additional test was undertaken to confirm presence of the WT1 GAL4 BD fusion proteins. Since WT1 is known to self-associate (Holmes *et al*, 1997), this was used as an additional test of protein expression. pAS1 plasmids containing the full length WT1 GAL4 BD fusion proteins to be used for library screening, and pACTII plasmids containing full length WT1 GAL4 AD fusion proteins were co-transformed into Y190, and grown on minimal medium selecting for both plasmids (-Trp, -Leu) and reporter activation (-His and +25 mM 3-AT). Good growth was observed on selective media, suggesting that a protein-protein interaction between the BD and AD fusion proteins had occurred, enabling activation of the His reporter gene. This was considered sufficient proof that the WT1 GAL4 BD fusion proteins were being expressed within the yeast, despite negative Western analysis.

### *3.5.6 Yeast two hybrid interaction assays*

pAS1 - and + KTS WT1 constructs were used as baits to perform two separate library screens. In order to maximise transformation efficiency, bait and library plasmid were transformed into Y190 sequentially, with initial selection being for tryptophan alone. In

view of the results of the autoactivation analysis, 25 mM 3-AT was used, as the addition of excessive 3-AT may compromise the detection of weak, but real interactions. Screens were performed using a mouse embryo library (E 9 1/2 and 10/2) cloned into the *Not*I site yeast two hybrid vector pVP16 (Figure 3.12). Murine homologues of WT1 are expressed at this stage of development, so theoretically, prospective interaction candidates should be similarly expressed. The library had been generated by random hexamer-primed cDNA synthesis of E9.5/10.5 CD1 embryo polyA+ RNA, followed by size selection with a preference for insert sizes in the range of 350-700 nucleotides (Hollenberg *et al*, 1995). The rationale for short cDNAs was to minimise bias towards C-terminal sequences, separate protein interaction domains from inhibitory regions contained within the full length polypeptide, to reduce the toxicity sometimes seen with full-length foreign proteins expressed in the yeast, and to facilitate more rapid analysis by sequencing. However, the disadvantage of small inserts is that more clones must be screened, large domains may be missed and shorter protein fragments may have interaction specificities irrelevant to the parental native protein, thus increasing the frequency of false positives. A theoretical library of two million independent clones was screened, and since pVP16 has a wild type *leucine* gene, this was used as the metabolic selection marker for AD plasmid selection.

**Figure 3.12 Map of the pVP16 vector used for subcloning of the E9.5/10.5 cDNA library used for yeast two hybrid screening. The red arrow indicates the cloning site.**

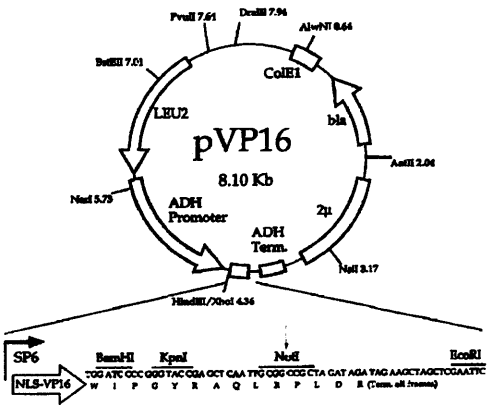


Transformation efficiency was assessed by plating a 1:10,000 dilution of the library transformation on –Trp, –Leu and +His plates. Good transformation efficiencies of approximately 3.7 x $10^6$ cotransformants/μg of DNA for the +KTS isoform, and 2.9 x

$10^6$ cotransformants/μg for the –KTS isoform were obtained for each of the two screens performed. Interacting clones were initially selected for by growth on minimal medium –Trp, –Leu, –His + 25 mM 3AT. A total of fourteen colonies were picked for the +KTS isoform and six for the –KTS isoform. Of these, six +KTS colonies and four –KTS isoforms also resulted in activation of the *lacZ* reporter gene on β-Gal assay. These were recovered into HB101, followed by analysis of insert size by *Not*I digest (Figure 3.13). Inserts were subsequently PCR amplified using vector specific flanking primers, and sequenced. BLAST analysis of the sequences of captured clones is shown in Figure 3.14, and the results summarised in Table 3.4. Of note, the first library screen produced a better result for the –KTS isoform (despite comparable transformation efficiencies), with four colonies resulting in activation of both reporters as opposed to one, whereas the second screen produced a better result for the + KTS isoform, with six colonies activating both reporters as opposed to none in the first screen. None of the interactors were detected in both screens.

**Figure 3.13 *Not*I digests of clones selected through *His* and *lacZ* reporter gene activation analysed on a 1.5% agarose gel. The numbers represent each clone; enzyme digest was performed in triplicate**

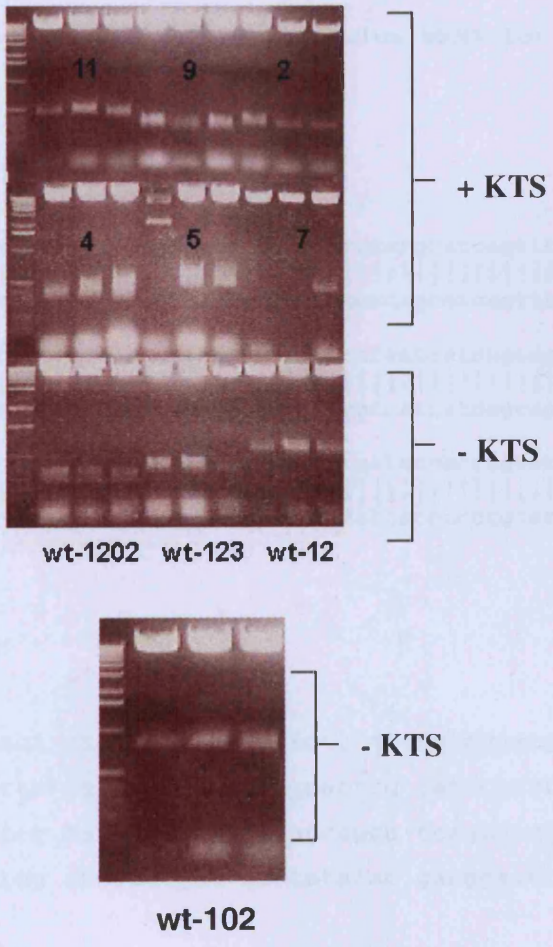

**Figure 3. 14 Results of BLAST searches of the sequences of putative interactors identified through yeast two hybrid screening of a E 9.5/10.5 day VP16 whole mouse embryo library, using murine WT1 + and – KTS GAL4 fusions**

## A) Results of BLAST searches of yeast two hybrid screen with +KTS isoform (http://www.ncbi.nlm.nih.gov/blast)

### (i) Edr protein (AJ006464)

Three of six clones (Clones 2, 9 and 11) were identified as EDR protein (AJ006464). EDR protein has two putative ORF's, but no protein translations are present as yet in databases. Consequently, protein database searches were inconclusive.

### Clone 2 nucleotide sequence:

```
1   cgcatgtcca tccgtatatg catcagcatc tgcatcagca tctgcatcag tttctgcatc
61  cagatccgca tcagtatccg catccggatc cgcattatca tcatcatcag caggcggata
121 tgcagcacca actgcagcag tatctatatc agtatttgta ttaccacctg tatccggtt
```

### BLAST search of clone 2 nucleotide sequence detected Edr protein.

```
>gi|16945321|emb|AJ006464.1|MMAJ6464 Mus musculus mRNA for Edr protein
          Length = 5166; CD's 433..3358
 Score =  355 bits (179), Expect = 9e-96
 Identities = 179/179 (100%)
 Strand = Plus / Plus


Query: 1    cgcatgtccatccgtatatgcatcagcatctgcatcagcatctgcatcagtttctgcatc 60
            ||||||||||||||||||||||||||||||||||||||||||||||||||||||||||||
Sbjct: 1943 cgcatgtccatccgtatatgcatcagcatctgcatcagcatctgcatcagtttctgcatc 2002

Query: 61   cagatccgcatcagtatccgcatccggatccgcattatcatcatcatcagcaggcggata 120
            ||||||||||||||||||||||||||||||||||||||||||||||||||||||||||||
Sbjct: 2003 cagatccgcatcagtatccgcatccggatccgcattatcatcatcatcagcaggcggata 2062

Query: 121  tgcagcaccaactgcagcagtatctatatcagtatttgtattaccacctgtatccggtt 179
            |||||||||||||||||||||||||||||||||||||||||||||||||||||||||||
Sbjct: 2063 tgcagcaccaactgcagcagtatctatatcagtatttgtattaccacctgtatccggtt 2121
```

### Clone 9 nucleotide sequence:

```
1   cagctccatt gtcctcaact ctgattactg ccgacttcgc tgccggatgc ccgcacagat
61  accttctaac ttactgttta cagtgccaca accgaatttg catccgtatc tacttcatca
121 tgtgcatccg catgtcatcg catatgcatc agcatctgca tcagcatctc gatcagttct
181 gcatcagatc gatagtatcg atcgatcgat atatatatac gacggaattc
```

**BLAST search of clone 9 nucleotide sequence detected Edr protein.**

```
>gi|16945321|emb|AJ006464.1|MMAJ6464 Mus musculus mRNA for Edr protein
          Length = 5166; CD's 433..3358.

 Score =  226 bits (114), Expect = 7e-57
 Identities = 164/178 (92%), Gaps = 2/178 (1%)
 Strand = Plus / Plus


Query: 3    gctccattgtcctcaactctgattactgccgacttcgctgccggatgcccgcacagatac 62
            |||||||||||| ||||||||||||||||||||||  ||||||||||   ||||||||||
Sbjct: 1817 gctccattgtcttcaactctgattactgccgactctgctgccggatgtttgcacagatac 1876

Query: 63   cttctaacttactgtttacagtgccacaaccgaatttgcatccgtatctacttcatcatg 122
            |||||||||||||||||||| |||||||||| || ||||||||||||||||||||||
Sbjct: 1877 cttctaacttactgtttacagcgccacaaccgagttcgcatccgtatctacttcatcatg 1936

Query: 123  tgcatccgcatgt-cat-cgcatatgcatcagcatctgcatcagcatctcgatcagtt 178
            |||||||||||||| ||| || ||||||||||||||||||||||||  |||||||
Sbjct: 1937 tgcatccgcatgtccatccgtatatgcatcagcatctgcatcagcatctgcatcagtt 1994
```

**Clone 11 nucleotide sequence:**

```
1    cacgcatgtc catccgcata tgcatcagca tctgcatcag catctgcatc agtttctgca
61   tccagatccg atcagtatcc gcatccggat ccgcattatc atcatcatca gcaggcggat
121  atgcagcacc aactgcagca gtatctatat cagtatttga ttaccatctg tatcggttat
181  gcacaccatg tctagatcag catgagactc tcgatgagta tctcgactat agtatctcga
241  ctagtatctg  catcagttct  gcataca
```

**BLAST search of clone 11 nucleotide sequence detected Edr protein.**

```
>gi|16945321|emb|AJ006464.1|MMAJ6464 Mus musculus mRNA for Edr protein
          Length = 5166;CD's 433..3358

 Score =  303 bits (153), Expect = 4e-80
 Identities = 180/185 (97%), Gaps = 3/185 (1%)
 Strand = Plus / Plus

Query: 3    cgcatgtccatccgcatatgcatcagcatctgcatcagcatctgcatcagtttctgcatc 62
            |||||||||||||| ||||||||||||||||||||||||||||||||||||||||||||
Sbjct: 1943 cgcatgtccatccgtatatgcatcagcatctgcatcagcatctgcatcagtttctgcatc 2002

Query: 63   cagatccg-atcagtatccgcatccggatccgcattatcatcatcatcagcaggcggata 121
            |||||||| ||||||||||||||||||||||||||||||||||||||||||||||||||
Sbjct: 2003 cagatccgcatcagtatccgcatccggatccgcattatcatcatcatcagcaggcggata 2062

Query: 122  tgcagcaccaactgcagcagtatctatatcagtatttg-attaccatctgtat-cggtta 179
            |||||||||||||||||||||||||||||||||||| ||||||| |||||| ||||||
Sbjct: 2063 tgcagcaccaactgcagcagtatctatatcagtatttgtattaccacctgtatccggtta 212

Query: 180  tgcac 184
            |||||
Sbjct: 2123 tgcac 2127
```

BLAST searching of protein databases: various uncharacterised ORF's detected; for example, clone 2:-

```
>gi|220578|dbj|BAA00447.1| (D00570) open reading frame (251 AA) [Mus
musculus]Length = 250

 Score = 32.5 bits (69), Expect = 0.073
 Identities = 20/54 (37%), Positives = 28/54 (51%), Gaps = 23/54 (42%)

Query: 7   CISI---CISICISF-CIQIRISIRIRIRIIIIISRRICSTNCSSIYISI--CI 54
           C+SI   C+SIC+S+ C+ I +SI I               C S+Y+SI  CI
Sbjct: 115 CLSIMSVCLSICLSYVCLSIYLSI-I---------------CLSVYLSIYLCI 151
```

**Sequence alignment of clones 2, 9 and 11 using CLUSTAL W (1.81)**

```
clone_11      ------------------CACGCATGTCCATCCGCATATGCATCAG-CATCTGCATCAGC
clone_2       ----------------------GCATGTCCATCCGTATATGCATCAG-CATCTGCATCAGC
clone_9       CAGCTCCATTGTCCTCAACTCTGATTACTGCCGACTTCGCTGCCGGATGCCCGCACAGAT
                                 **  *   *    *      * *    * ***

clone_11      ATCTGCATCAGTTTCTGCATCCAGATCCG-ATCAGTATCCGCATCCGGATCCGCATTATC
clone_2       ATCTGCATCAGTTTCTGCATCCAGATCCGCATCAGTATCCGCATCCGGATCCGCATTATC
clone_9       ACCTTC-TAACTTACTGTTTACAGTGCCACAACCGAATTTGCATCCGTATCTACTTCATC
              * ** * * * ** ***  * ***  **  * * * **  ******* ***  * * ***

clone_11      ATCATCATCAGCAGG----CGGATATGCAGCACCAACTGCAGCAGTATCTATATCAGTAT
clone_2       ATCATCATCAGCAGG----CGGATATGCAGCACCAACTGCAGCAGTATCTATATCAGTAT
clone_9       ATGTGCATCCGCATGTCATCGCATATGCATCAGCATCTGCATCAGCATCTCGATCAGT-T
              **   **** *** *    ** ******* ** ** ***** *** ****  ****** *

clone_11      TTG-ATTA--CCATCTGTATC-GGTTATGCACACCATGTCTAGATCAGCATGAGACTCTC
clone_2       TTGTATTA--CCACCTGTATCCGGTT----------------------------------
clone_9       CTGCATCAGATCGATAGTATC-GATCGATCGATATATATATACGACGGAATTC-------
               ** ** *   *    ***** * *

clone_11      GATGAGTATCTCGACTATAGTATCTCGACTAGTATCTGCATCAGTTCTGCATACA
clone_2       ------------------------------------------------------
clone_9       ------------------------------------------------------
```

**Consensus key**

```
* - single, fully conserved residue
  - no consensus
```

Alignment of clones 2, 9 and 11 suggested that a series of overlapping sequences had been identified. The occasional lack of match between clone 9, and clones 2 and 11 reflects sequence quality. Alignment of clones would normally have been made using predicted protein sequences, but this was not possible in view of the lack of a reliable protein translation for the *Edr* gene in the databases.

### (ii) Angiomotin (AF461135)

One of six clones detected (clone 4) = Angiomotin (AF461135)

### Clone 4 nucleotide sequence:

```
1   cacctgctac tgtttctcca actgctccac tgctactgct gctgttgctg cagctactac
61  tgctgctatc actgctgctg ctgctgctgc cactactgct attcaggccg ctcagctact
121 tcggctccgg ttccatctca gcttcgattc cggctcagca acggctcagg cttctgctcg
181 atcgactcag catcaactcagtcgactgac tctagtcagt cctc
```

### BLAST search of clone 4 nucleotide sequence detected angiomotin (AF461135):

```
>gi|18479136|gb|AF461135.1| Mus musculus angiomotin mRNA, complete cds
          Length = 2837; CD's 107..2782
 Score =  280 bits (141), Expect = 5e-73
 Identities = 175/181 (96%), Gaps = 4/181 (2%)
 Strand = Plus / Plus


Query: 3    cctgctactgtttctccaactgct-ccactgctactgctgctgttgctgcagctactact 61
            ||||||||||||||||||||||| ||||||||||||||||||||||||||||||||||
Sbjct: 2339 cctgctactgtttctccaactgctgccactgctactgctgctgttgctgcagctactact 2398

Query: 62   gctgctatcactgctgctgctgctgctgccactactgctattcaggccgct-cagctact 120
            |||||||||||||||||||||||||||||||||||||||||||||||  ||| ||||||||
Sbjct: 2399 gctgctatcactgctgctgctgctgctgccactactgctattcaggttgctccagctact 2458

Query: 121  tcggctccggttccatct-cagcttcgattccggct-cagcaacggctcaggcttctgct 178
            |||||||||||||||||| |||||||||||||||| ||||||||||||||||||||||||
Sbjct: 2459 tcggctccggttccatctccagcttcgattccggctccagcaacggctcaggcttctgct 2518

Query: 179  c 179
            |
Sbjct: 2519 c 2519
```

### Clone 4 Protein sequence:

```
TCYCFSNCSTATAAVAAATTAAITAAAAAATTAIQAAQLLRLRFHLSFDSGSATAQASARSTQHQLSRLTL
VSP
```

### BLAST search with clone 4 protein sequence:

```
>gi|18479137|gb|AAL73436.1|AF461135_1 (AF461135) angiomotin [Mus
musculus] Length = 891
 Score = 77.8 bits (176), Expect = 2e-15
 Identities = 37/67 (55%), Positives = 39/67 (57%), Gaps = 24/67 (35%)

Query: 10  TATAAVAAATTAAITAAAAAATTAIQAAQLLRLRFHLSFDSGS-----------ATAQA 57
           TATAAVAAATTAAITAAAAAATTAIQ A           + S           ATAQA
Sbjct: 754 TATAAVAAATTAAITAAAAAATTAIQVAP----------ATSAPVPSPASIPAPATAQA 802

Query: 58  SARS-TQ 63
           SA + TQ
Sbjct: 803 SAPTPTQ 809
```

### (iii) False positives: clones 5 and 7

Two of the six clones detected were false positives, as database searching with the nucleotide sequence revealed prey sequences in the opposite orientation, and protein database searching was unable to isolate a significant match.

### Clone 5 nucleotide sequence:

```
1     cagccagggg ccaagtgtca cttgctgctg ctgctgctgc tgctgctgct gctgctgctg
61    ctgctgcttt gctgctgctg ttgttgctgc gctgctgcg agataataaa agttcgattc
121   tggttcaaag aggccccatc tgctgttgct gaagctgcag ctgttgttgc tggtgcagct
181   gctcgctcga agtgcatgcg tcgtgttgtt gctgctgct
```

### BLAST search of clone 5 nucleotide sequence detected:

```
>gi|6754167|ref|NM_010408.1| Mus musculus hyperpolarization-activated,
cyclic nucleotide-gated K+ 1 (Hcn1), mRNA Length = 3305
 Score =  111 bits (56), Expect = 3e-22
 Identities = 66/68 (97%), Gaps = 1/68 (1%)
 Strand = Plus / Minus

Query: 23   tgctgctgctgctgctgctgctgctgctgctgctgctgct-ttgctgctgctgt 81
            ||||||||||||||||||||||||||||||||||||||||  ||||||||||||
Sbjct: 2328 tgctgctgctgctgctgctgctgctgctgctgctgctgctgctgctgctgctgt 2269

Query: 82   tgttgctg 89
            ||||||||
Sbjct: 2268 tgttgctg 2261
```

### Clone 7 nucleotide sequence:

```
1    caccgcattc tggcgttgct gttgctgctg ctgctgttgc tgctgttgtt gttgctgctg
61   ctgctgctgt tgttgctgct gctgctgctg ctgctgcagg gactaggygg yacggcccac
121  ggtatctcgc aaactagtac gsggaaaaag tgtcgcaca gcgtgtgaac tgctggaggc
181  tggtagcaga gaaatatata attatcatat c
```

### BLAST search of clone 7 nucleotide sequence detected:

```
>gi|16716566|ref|NM_053242.1| Mus musculus forkhead box P2 (Foxp2),
 mRNA Length = 2145

Score =  120 bits (60), Expect = 5e-25
 Identities = 77/82 (93%), Gaps = 3/82 (3%)
 Strand = Plus / Minus

Query: 15  gttgctgttgctgctgctg---ctgttgctgctgttgttgttgctgctgctgctgctgtt 71
            ||||||||||||||||||   ||| |||||||||| ||||||||||||||||||||||
Sbjct: 571 gttgctgttgctgctgctgttgctgctgctgttgctgttgctgctgctgctgctgtt 512

Query: 72  gttgctgctgctgctgctgctg 93
            |||||||||||||||||||||
Sbjct: 511 gttgctgctgctgctgctgctg 490
```

Protein BLAST searches with clone 5 and 7 protein sequence did not detect any significant matches within the databases.

## B) Results of BLAST searches of yeast two hybrid screen with -KTS isoform (http://www.ncbi.nlm.nih.gov/blast)

### (i) AICARFT/IMPCHASE: GENE "ATIC"

One of four clones was identified as 5-aminoimidazole-4-carboxamide ribonucleotide formyltransferase/IMP cyclohydrolase, the AICARFT/IMPCHASE or "ATIC" gene.

### Clone WT1 – 12 nucleotide sequence:

```
1   atatgcaaga gcgaagagga cgtgataggat gtcttcattt ggtgattttg ttggcattg
61  tctgacgatt tgtgatatcc caagtggcaaa aattatctcc agagaagtgt cgg
```

### BLAST search of clone WT1 - 12 nucleotide sequence detected the AICARFT/ IMPCH-ase or ATIC gene:

```
>gi|12848589|dbj|AK012074.1|AK012074 Mus musculus 10 days embryo whole
body cDNA, RIKEN full-length enriched library, clone:2610509C24: 5-
aminoimidazole-4-carboxamide ribonucleotide formyltransferase/IMP
cyclohydrolase, full insert sequence (Length = 2547; (CDS 1..1713)

 Score =  131 bits (66), Expect = 1e-28
 Identities = 106/114 (92%), Gaps = 4/114 (3%)
 Strand = Plus / Plus


Query: 1    atatgcaagagcgaagaggacgtgataggatgtcttcatttggtgattttgttggcattg 60
             ||||||||||||| |||||||  ||||||||||||||||||||||||||||| ||||||
Sbjct: 943  atatgcaagagc-aagaggagctgataggatgtcttcatttggtgattttgtt-gcattg 1000


Query: 61   tctgacgatttgtgatatcccaagtggcaaaaattatctccagagaagtgtcgg 114
             |||||| ||||||||| |||||| | ||||||||||||||||||||||||||
Sbjct: 1001 tctgac-atttgtgatgtcccaact-gcaaaaattatctccagagaagtgtcgg 1052
```

### Clone WT1 – 12 protein sequence:

```
MQERRGRDRMSSFGDFVGIVRFVISQVAKIISREVS
```

### Protein BLAST search:

```
>gi|18553514|ref|XP_055257.3| (XM_055257) 5-aminoimidazole-4-
carboxamide ribonucleotide formyltransferase/IMP cyclohydrolase [Homo
sapiens]Length = 511

 Score = 57.5 bits (128), Expect = 1e-08
 Identities = 23/38 (60%), Positives = 24/38 (62%), Gaps = 11/38 (28%)
```

```
Query: 5   RGRDRMSSFGDFVGIV*RFVISQV-----AKIISREVS 37
           RG DRMSSFGDFV       +S V     AKIISREVS
Sbjct: 306 RGADRMSSFGDFV------ALSDVCDVPTAKIISREVS 337
```

### (ii)Unknown proteins.

Three of the four clones were compatible with as yet uncharacterised proteins.

### Clone WT-123 nucleotide sequence:

```
1   atgataaatg agaattgtgt gtccctggcc gaagttccag gctcctcagc
51  tgggggggct gggcaagagt tgtacccctt tcttggaaag gggactaccc
101 gagagaaatg aacacagggt tcaccgggtt t
```

### BLAST search with nucleotide sequence:

```
>gi|7262713|gb|AC007844.32| Mus musculus chromosome 6 clone ct7-541122
 strain 129/Sv ES cell line CJ7, complete sequence. Length = 152316
 Score = 36.2 bits (18), Expect = 0.39
 Identities = 21/22 (95%)
 Strand = Plus / Plus

Query: 58    gctgggcaagagttgtacccct 79
              |||||||||||||||| ||||
Sbjct: 61274 gctgggcaagagttgtatccct 61295
```

Protein BLAST database searching: no significant matches.

### Clone WT 1202 nucleotide sequence:

```
1   tagcatcgta tgagaccatg tctagaaatg acatatgttt cttacgtcaa
51  tggtccgatg gtccagaagc ccatggcacc catgcgctcc acgccgagaa
101 ccaatgcgct ccatggtctg gcccatgcgc tcaatactgg aggccatgtg
151 gtcaagccta gtgggcccat gcgctcgatg ctggagccca tgcgctcaac
201 tgagcccatg cggtccatga ccaggcccat gcgctca
```

### BLAST search with nucleotide sequence:

```
>gi|13543180|gb|BC005758.1|BC005758 Mus musculus, clone IMAGE:3601067,
 mRNA, partial cds Length = 1439

 Score =  293 bits (148), Expect = 4e-77
 Identities = 162/164 (98%), Gaps = 2/164 (1%)
 Strand = Plus / Minus
```

```
Query: 75  ggcacccatgcgctccacgccgagaaccaatgcgctccatggtctggcccatgcgctcaa 134
           |||||||||||||||||||| ||||||||||||||||||||||||||||||||||||
Sbjct: 433 ggcacccatgcgctccacgcc-agaaccaatgcgctccatggtctggcccatgcgctcaa 375


Query: 135 tactggaggccatgtggtcaag-cctagtgggcccatgcgctcgatgctggagcccatgc 193
           |||||||||||||||||||| ||||||||||||||||||||||||||||||||||||
Sbjct: 374 tactggaggccatgtggtcaaggcctagtgggcccatgcgctcgatgctggagcccatgc 315


Query: 194 gctcaactgagcccatgcggtccatgaccaggcccatgcgctca 237
           |||||||||||||||||||||||||||||||||||||||||||
Sbjct: 314 gctcaactgagcccatgcggtccatgaccaggcccatgcgctca 271
```

**Clone WT1 – 1202 protein sequence:**

ASYETMSRNDICFLRQWSDGPEAHGTHALHAENQCAPWSGPCAQYWRPCGQA

Protein BLAST database searching: no significant matches.

**Clone WT - 102 nucleotide sequence:**

**BLAST search with nucleotide sequence:**

```
>gi|17028440|gb|BC017539.1|BC017539 Mus musculus, Similar to RIKEN cDNA
2610023M21 gene, clone IMAGE:4511155, mRNA (Length = 2440)

 Score = 145 bits (73), Expect = 2e-32
 Identities = 80/81 (98%), Gaps = 1/81 (1%)
 Strand = Plus / Minus


Query: 161  ggcacccatgcgctccacgccgagaaccaatgcgctccatggtctggcccatgcgctcaa 220
           |||||||||||||||||||| ||||||||||||||||||||||||||||||||||||
Sbjct: 1353 ggcacccatgcgctccacgcc-agaaccaatgcgctccatggtctggcccatgcgctcaa 1295


Query: 221  tactggaggccatgtggtcaa 241
           ||||||||||||||||||||
Sbjct: 1294 tactggaggccatgtggtcaa 1274
```

**Clone WT 102 protein sequence:**

HRMRPCLEMTYVCTSMVRWSRSPWHPCAPRREPMRSMVWPMRSILEAMWS

Protein BLAST database searching: no significant matches.

**Table 3.4 Summary of yeast two hybrid analysis using – and + KTS WT1 GAL4 fusion proteins**

| Details of library screens | + KTS | -KTS |
|---|---|---|
| Transformation efficiency | 3.6 - 3.7 x $10^6$ | 2.5 - 2.9 x $10^6$ |
| Number of histidine positives | 14 | 6 |
| Number of histidine and lacZ positives | 6 | 4 |
| Number of known interactors | 4: colonies 2,9,11 = Edr protein; colony 4 = angiomotin | 1: colony WT1 – 12 = aicarft/impch-ase |
| Number of unknown interactors | - | 3 |
| Number of likely false positives (including colonies failing to activate LacZ reporter) | 10 | 2 |

### *3.5.7 Confirmatory yeast analysis*

Once positive clones had been identified, the WT1 bait plasmids and captured clones were retransformed into Y190 to establish that the interactions were reproducible. The GAL4 BD WT1 fusions were also transformed against empty pVP16 vector, to confirm that the interaction was not a result of spurious binding to the library vector. Interactions between +KTS WT1 and both Edr protein and angiomotin were found to be reproducible, as was the interaction between –KTS WT1 and 5-aminoimidazole-4-carboxamide ribonucleotide formyltransferase/IMP cyclohydrolase (ATIC). Interaction between the WT1 bait proteins and empty pVP16 vector were not detected.

### *3.5.8 Further analysis of positives*

Further confirmation by biochemical methods of the WT1 protein-protein interactions detected in the yeast was not performed. The poorly characterised nature of the clones detected, and the lack of an obvious relevance to the pathogenesis of renal disease meant that these experiments would fall outside the overall remit of the project.

## 3.6 Discussion

### *3.6.1 The nephropathic phenotypes associated with DDS and FS are genetically heterogeneous*

Although more than sixty germline *WT1* gene mutations (both familial and *de novo*) have now been described in DDS, these were found to be absent in all cases of isolated DMS and FSGS examined during this study. The infrequent occurrence of *WT1* mutations in isolated FSGS was subsequently confirmed in a study of 37 children with non-familial primary steroid-resistant nephrotic syndrome (Denamur *et al*, 2000). In contrast, three groups reported a minority of cases with isolated DMS and *WT1* gene mutations. Jeanpierre *et al* (1998b) detected mutations in exons 8 and 9 of the *WT1* gene in 4 out of 10 patients with DMS, but no other features of DDS. Three of these four patients were female. One mutation was a novel 1147 T to C (F383L) in exon 9. Two others, 1186 G to A (D396N) in exon 9 and 1129 C to T (H377Y) in exon 8, had been previously detected in DDS. The fourth, an intron 9 (+4 C to T) mutation, is more commonly associated with FS (Barbaux *et al,* 1997, Klamt *et al,* 1998, Kikuchi *et al,* 1998), a condition not generally associated with either Wilms' tumour or gonadal abnormalities in cases with a 46 XX karyotype. In addition, all cases in which mutations were detected underwent nephrectomy in early life. Since nephropathy may precede onset of Wilms tumour by a number of years, and cases of DDS with a normal 46XX karyotype are also not generally associated with abnormal genitalia, this may have resulted in an incomplete diagnosis of DDS. Schumacher *et al* (1998) also studied a broad spectrum of patients with early onset nephrotic syndrome for *WT1* gene mutations. Two of four patients with isolated DMS had *WT1* mutations, one a novel 1135 G to T (G379C) mutation exon 8, and the other the 1180 C to T (R394W) mutation characteristically associated with DDS. Both patients were female, and additionally had bilateral nephrectomies by the age of two years. More recently, Ito *et al* (2001) detected *WT1* mutations in two of seven cases with isolated DMS. One case was male, with DMS and an R312Q mutation in exon 7, but no documented genital abnormalities or Wilms' tumour and again, early nephrectomy. The other case had a 46XX in association with nephropathy and an intronic +4 C to T mutation, with a phenotype compatible with a diagnosis of FS.

Despite the observed differences in the outcome of each mutation screen, all confirmed the genetic heterogeneity of DMS and FSGS despite the uniform appearance in renal histology seen. These studies also illustrate the inherent difficulty in differentiating these relatively similar phenotypes on the basis of clinical criteria. Although a small subset of cases of isolated DMS are likely to arise as a result of *WT1* gene mutations, the results presented here suggest that when a larger, more generalised population of cases with isolated DMS is examined, *WT1* gene mutations are infrequent. The occasional detection of mutations in isolated DMS lends support to the existence of a subgroup of incomplete DDS where nephropathy may be the only defining feature, and indicates that the remit of this disease should be broadened to include these cases. This phenomenon appears more common in females with isolated DMS, which affirms the less critical role of WT1 in female gonadal development suggested by other experimental data (Nachtigal *et al*, 1998; Hammes *et al*, 2001), and correlates with the observation that individuals with a 46XX karyotype and the related syndrome, FS, do not have any obvious gonadal abnormalities (Klamt *et al*, 1998; Demmer *et al*, 1999). Although karyotype analysis remains the most important first line investigation, the presence of characteristic *WT1* gene mutations may indicate an increased Wilms' tumour risk. *WT1* mutation analysis of exons 7 to 9 should therefore be considered in selected individuals, particularly 46 XX individuals who may not demonstrate any other diagnostic clues for an underlying diagnosis of DDS. In addition, there is evidence that WT1 mutations in DDS may be hereditary (Coppes *et al*, 1992; Denamur *et al*, 1999), which underscores the importance of *WT1* analysis in this group.

In view of the phenotypic overlap with DDS, the lack of *WT1* mutations in isolated DMS and FSGS was disappointing. Subsequent linkage studies of two Turkish families with autosomal recessive DMS excluded the *WT1* gene locus (Ozen S, personal communication), and the association of familial FSGS with at least three other genes (e.g.Winn *et al*, 1999; Boute *et al*, 2000; Kaplan *et al*, 2000) has provided further evidence for the genetic heterogeneity of these conditions. It had been hoped that as in DDS (Jeanpierre *et al*, 1998a), genotype-phenotype correlation would provide some indication of the role that WT1 plays in the pathogenesis of nephrotic syndrome. The minority of cases of DMS in whom *WT1* gene mutations were present is likely to represent a subset of DDS, although whether this group has an increased Wilms' tumour

risk cannot be quantified. Factors that determine which aspects of the DDS phenotype are expressed may be related to the genetic background of an individual, or coincidental abnormalities in related genes, possibly resulting in genetic epistasis.

In DDS, the mutations characteristically leave the WT1 protein intact, but result in the disruption or inactivation of DNA binding its zinc fingers (Little *et al*, 1995). Nearly half of all cases have missense mutations affecting a crucial arginine residue in zinc finger 3 (Arg394) and, collectively, missense mutations in zinc fingers 2 and 3 (encoded for by exons 8 and 9) account for more than 80% of DDS mutations. (Coppes *et al*, 1994). It is now recognised that these mutations affect amino acids crucial for the stability of DNA binding of the zinc fingers (Little *et al*, 1995; Borel *et al*, 1996), and may also change its ability to bind RNA. As these mutations were only detected in one allele of the *WT1* gene, it was initially thought that DDS mutations act in a dominant manner. However in some DDS cases, WT1 mutations located either within or upstream of the zinc finger region result in truncated non-functional proteins. In this situation, a more likely mechanism is that these mutant proteins behave in a dominant-negative fashion, and interfere with the function of the wild type protein produced from the remaining allele (Little *et al*, 1993; Reddy *et al*, 1995; Little, 1997). Effective WT1 concentrations in cells are probably reduced to below 50% because the WT1 proteins tend to dimerise, resulting in abundant non-functional homodimers and heterodimers of mutant WT1 protein (Moffett *et al*, 1995). Further support for a dominant negative effect comes from gene-targeting experiments. Heterozygosity for a targeted murine *WT1* allele, *WT1*(tmT396), which truncated the third zinc finger at codon 396, induced mesangial sclerosis characteristic of DDS in adult heterozygous and chimeric mice. Male genital defects also were evident, and there was a single case of Wilms tumour in which the transcript of the non targeted allele showed an exon 9 skipping event, implying a causal link between WT1 dysfunction and Wilms' tumorigenesis in mice (Patek *et al*, 1999). Interestingly, expression from the mutant allele accounted for only 5% of the total amount of WT1 protein, suggesting that even small amounts of mutant protein can have devastating effects on urogenital development.

To date, all *WT1* gene mutations detected in cases of isolated DMS overlap with those characteristically associated with the complete form of DDS, making genotype-

phenotype correlation of little value. It is likely that a large proportion of isolated DMS and FSGS cases result from abnormalities of other glomerular genes, possibly either upstream or downstream of *WT1*, and thus able to partially mimic the effects of *WT1* mutations seen in DDS. These remain unidentified, although there is some preliminary evidence that expression of Pax2, a transcription factor regulated by WT1 *in vitro*, (Ryan *et al*, 1995) is abnormal in some cases of DDS and isolated DMS (Yang *et al*, 1999). In addition, it is tempting to speculate that mutations may be present in a recently identified downstream target of WT1, podocalyxin (Palmer *et al*, 2001). Podocalyxin is a major structural membrane protein in podocytes, and strongly implicated in the maintenance of the slit diaphrgam as null mice exhibit profound defects in kidney development and die within 24 hours of birth from renal failure (Doyonnas *et al*, 2001). Although podocytes are present in the glomeruli of the *podocalyxin* (-/-) mice, they fail to form foot processes and slit diaphragms. Binding of WT1 to conserved elements within the *podocalyxin* gene promoter results in potent transcriptional activation, and the expression pattern of podocalyxin in the developing kidney mirrors that of WT1 itself, providing further evidence for a potential interactive role for these genes, perhaps in the specific activation of a glomerular differentiation program in renal precursors. Other candidates are a novel adaptor protein CD2AP, originally cloned in T cells, where it orchestrates receptor patterning and cytoskeletal polarity in T-cell contacts (Dustin *et al*, 1998). CD2AP also plays a role in glomerular filtration, as CD2AP null mice develop a congenital nephrotic syndrome consistent with DMS (Shih *et al*, 1999), and in addition, CD2AP interacts with the key slit diaphragm protein nephrin, linking it to the actin cytoskeleton (Shih *et al*, 2001; Yuan at al, 2002). Recent screening of cases of isolated DMS for CD2AP mutations has detected two base changes within the interaction domain between CD2AP and nephrin, which appear to diminish the ability of CD2AP's to bind nephrin, a key player in slit diaphragm function (Gopa G, Koziell A, unpublished data). Although these changes have not been detected in normal controls, their significance still requires verification.

### *3.6.2 Defective alternative splicing of* WT1 *leads to a reversal in the normal +/- KTS isoform ratio and causes Frasier syndrome*

The detection of specific *WT1* mutations in all four cases of FS provided clear evidence that this condition is caused by heterozygous mutations of the second alternative splice

donor site in exon 9. Although two different mutations were detected in this series, the phenotypic consequences were indistinguishable. Twenty additional FS cases with intronic *WT1* mutations are now present in the literature (Barbaux *et al*, 1997; Kikuchi *et al*, 1998; Klamt *et al*, 1998; Okuhara *et al*, 1999; Demmer *et al* 1999; Buzi *et al*, 2001), and if mutation data for all twenty-four cases is merged, there is a striking bias in their distribution. Twenty-two cases have either a + 4 C to T or a +5 G to A substitution, whereas the remaining two have mutations at +2 and +6 respectively (Kikuchi *et al*, 1998). The mutation hot spot observed in the majority of FS cases may result from the 5-methylcytosine at the +4/+5 CpG di-nucleotide being especially susceptible to deamination. An association between *WT1* exon 9 mutations and FS has also been described (Kohsaka *et al*, 1999), although on closer examination the clinical phenotype and genotype are more suggestive of a diagnosis of incomplete DDS, than FS.

**Figure 3.15 Location of *WT1* gene mutations in FS**

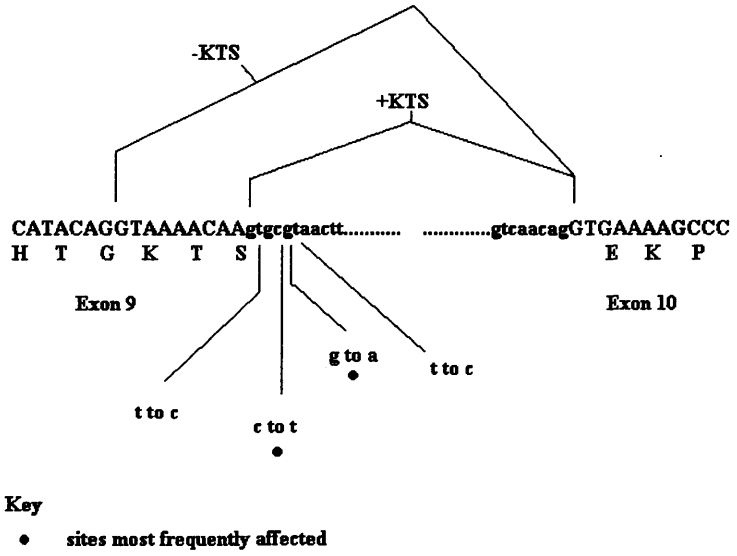


The presence of alternative splice site mutations in FS highlights the importance of a precisely balanced expression of WT1 isoforms for correct function, and suggested that the + and – KTS splice variants are likely to play distinct biological roles within the kidney and gonad. The +5 G to A mutation detected in many cases had previously been shown to abolish alternative splicing in transient transfections using minigene constructs (Bruening *et al*, 1992). Although these experiments have not been repeated for other FS

splice site mutations, computer prediction programmes suggest a similar disruption of alternative splicing through loss of the second alternative splice site (Figure 3.5). Importantly, the analysis of gonadoblastoma tissue from case DG confirmed the *in vitro* and *in silico* findings by demonstrating an altered +/- KTS isoform ratio *in vivo*. Patients with FS therefore have one normal copy of WT1 and one that can only produce the KTS negative isoform. This allele loss leads to cells that cannot produce the + KTS isoform of WT1, but still have large amounts of the - KTS isoform, resulting in a relative deficiency of the usually more abundant + KTS isoform. The WT1 proteins produced are theoretically otherwise normal with normal binding abilities, which appears to have a significant impact on the predisposition to Wilms' tumour, not normally associated with FS despite the existence of one case report (Barbosa *et al*, 1999). Of note three patients reported with diffuse mesangial sclerosis and *WT1* intron 9 mutations usually associated with FS, also did not develop Wilms' tumour (Barbosa *et al*, 1999). This suggests that disruption of the isoform ratio is insufficient for tumour production, which is supported by *in vitro* observations that the tumorigenicity of the G401 Wilms' tumour cell line in nude mice can be suppressed by both + and - KTS isoforms to the same extent (McMaster *et al*, 1995).

Understanding of the molecular mechanisms underlying FS and DDS nephropathy were recently advanced by the generation of specific mouse strains in which either the –KTS or +KTS isoforms were specifically removed (Hammes *et al*, 2001), and these confirm that these splice variants are likely to have distinct functions during sex determination and nephron formation. Heterozygous mice with a reduction of +KTS levels developed glomerulosclerosis within the first three months of life, and a female phenotype regardless of karyotype, thus representing a murine model of FS. The kidney phenotype was perhaps more pronounced than in humans, in that most of the glomeruli showed DMS rather than FSGS, reminiscent of the histology more commonly associated with DDS. Of note, DMS nephropathy has been described in association with the intron 9 mutations characteristically detected in FS (Denamur *et al*, 1999; Ito *et al*, 2001). The finding of DMS in +KTS deficient mice strengthens the hypothesis that the DDS phenotype in man is caused by a reduction of functional WT1 due to dominant negative mutations, and underlines the importance of the +KTS isoform in podocyte homeostasis. In contrast, mice with a reduction of the –KTS isoform had hypo-dysplastic kidneys and

streak gonads in both XY and XX animals. This reduction in the size of the kidneys and gonads may have resulted from an increase in renal and gonadal apoptosis, indicating that –KTS variants are critical for the survival of embryonic tissue. In addition, an almost complete absence of synaptopodin and α-integrin expression suggests that –KTS isoforms are required for an early differentiation step of the presumptive podocyte layer into the visceral epithelium.

FS mutations also have a significant impact on gonadogenesis in individuals with a 46 XY karyotype, but it remains unclear how these exert their effects at a molecular level as *in vitro* and *in vivo* data conflict. Initial work by Nachtigal *et al* (1998) suggested that steroidogenic factor 1 (SF1) participates in sexual development by regulating expression of the polypeptide hormone Mullerian inhibiting substance (MIS). In the normal situation, (-KTS) WT1 isoforms associate and synergise with *SF1* to promote expression of the gene encoding MIS, whereas *DAX1*, a gene thought to direct ovarian development, antagonises this synergy. In contrast, if *WT1* mutations characteristically seen in DDS are introduced, the resultant WT1 protein and SF1 fail to associate and synergise, functional opposition of the *DAX1* gene no longer occurs, and testis development fails. Thus, the severity of the genital phenotype is dependent on the degree to which WT1/SF1 binding is disrupted. Because different mutations might be expected to have different effects on the synergistic action of the protein cascade, this might explain why such a wide variety of genital phenotypes are seen in patients with DDS and a 46 XY karyotype. Interestingly, because an intact *WT1* gene is not an absolute requisite for female gonadal development, individuals with DDS or FS and a 46 XX karyotype usually have no gonadal abnormality. However, WT1 -KTS isoforms are also able to activate the *Dax1* promoter, at least *in vitro* (Kim *et al*, 1999), so the situation is complex. A further *in vitro* target for WT1 appears to be *SRY*, an important component of the male sexual differentiation pathway. Again, these experiments suggested that *SRY* activation was only achieved by -KTS variants (Shimamura *et al*, 1997; Hossain 2001). In contrast, data from the *in vivo* experiments in + and – KTS knockout mice shows the opposite. Here, absence of +KTS variants lead to reduction of SRY expression levels and absence of Sox 9 and MIS activation, whereas -KTS isoforms did not appear to regulate SRY, and were instead required for the survival of the gonadal primordium

(Hammes *et al*, 2001). In keeping with human FS, the effects of mutations were only seen in XY mice, as XX animals had normal female gonads.

The clinical overlap between FS and DDS, and the association of both conditions with mutations of the *WT1* gene opened up a debate as to whether these form part of a spectrum, or different disorders caused by mutations of the same gene. Although historically, specific clinical characteristics apply to FS and DDS, genetic analysis has produced an increasingly complex picture. Mutations commonly associated with DDS have not been reported in FS patients. However, there are now three reports of the two most common intronic splicing mutations associated with FS, +4 C to T and +5 G to A, occurring in patients with DMS and a phenotype compatible with DDS, although not associated with Wilms' tumour. Two had +4 C to T substitutions (Jeanpierre *et al*, 1998b; Denamur *et al*, 1999) and one a +5 G to A substitution (Jeanpierre *et al*, 1998b). Furthermore, 46XX individuals with FS and intronic *WT1* mutations do not have gonadal abnormalities (Klamt *et al*, 1999; Demmer *et al*, 1999), and there is increasing evidence that mutations may occasionally be transmitted to offspring, which may develop DDS. For example, vertical transmission of the +5 G to A *WT1* mutation was reported from a mother with a normal 46XX karyotype, normal renal function and FSGS, to her phenotypically female child who subsequently developed nephrotic syndrome (Denamur *et al*, 1999). On further investigation, the child had a 46 XY karyotype and DMS, features suggestive of DDS. Quantification of WT1 +KTS/-KTS isoforms by semi-quantitative RT-PCR showed reversal of the ratio in both the index case and her mother, as reported in FS. There was no clear explanation for the difference in observed phenotype, as neither mosaicism in the index case's mother, nor additional *WT1* mutations in the index case were detected. As mentioned previously, phenotype may depend on the genetic background of the individual, for example, polymorphisms in *WT1* target genes, which might result in different activation levels by *WT1* mutants, subtly altering the effects of mutations. These findings clearly identify a subset of cases sharing the clinical and genetic characteristics of both disorders, where the pathogenetic mechanisms and the projected clinical course are not clear cut, and although characteristic mutations suggestive of FS or DDS may be present, strict classification on the basis of clinical and genetic criteria is likely to be misleading. These findings provide further evidence that DDS and FS form two ends of an overlapping spectrum,

and the nephropathy seen in both can result from disruption of the normally precisely balanced expression of WT1 isoforms.

### *3.6.3 Yeast two hybrid analysis*

In view of the differing functions + and – KTS isoforms are likely to play *in vivo*, an approach to try and establish their roles in renal and gonadal development was to determine which protein-protein interactions each isoform might participate in. Alteration of protein-protein interactions is known to contribute to many diseases, and the detection of *WT1* mutations resulting in an altered protein isoform ratio suggested that disrupted protein binding might also contribute to disease pathogenesis within the FS/DDS spectrum.

Protein-protein interactions are intrinsic to virtually every cellular process, and their analysis is often able to provide important information about gene function. A number of tools are available, such as biochemical approaches, which in general involve physical methods such as protein affinity chromatography, affinity blotting, co-immunoprecipitation and cross-linking. Alternatively, protein probing using a labelled protein to screen an expression library is another well recognised technique. However, since all combinations of protein-protein interaction are assayed, including those that might never occur *in vivo*, the possibility of identifying artifactual partners is a major disadvantage. A second drawback derives from the use of a bacterial host, where not all post-translational modifications, such as phosphorylation, needed for the interaction might occur. A more recent technique known as the "two hybrid" or "interaction trap", enables the identification of interacting partners *in vivo* using yeast genetic machinery. As mentioned previously, the two hybrid technique exploits the modular properties of GAL4 and other transcription factors, and that the DNA binding domain of GAL4 is unable to activate transcription unless associated with an activation domain. This use of the different functional modules of a transcription factor to study protein-protein interactions was first proposed by Fields and Song (1989), using SNF1 fused to the binding domain and SNF4 fused to the activation domain of GAL4. Expression of both chimeras and subsequent interaction of SNF1 and SNF4 was required for reconstitution of the transcription factor, and thus induction of reporter gene expression. These intial

experiments confirmed that a transcriptional read-out could be used to study interactions between proteins not involved in the transcription process.

The yeast two hybrid has some clear advantages over classical biochemical and genetic approaches. Firstly, it embodies an *in vivo* technique using the yeast host as a live test tube, which is able to mimic more closely the cellular processes seen in higher eukaryotes than most *in vitro* approaches or techniques based on bacterial expression. An important feature is the minimal requirements to initiate a screen. In effect, only the cDNA is needed, in contrast to the large quantities of purified proteins or good quality antibodies often needed in other approaches. Since the genetic reporter strategy results in significant amplification, weak and transient interactions are more readily detected, although there is clearly a trade-off between the detection of weak interactions and the number of false positives encountered when performing a screening procedure. An additional feature of yeast two hybrid screening is that the identification of an interacting protein is concurrent with the cloning of the corresponding gene. This may give important functional information about the bait protein, such that this technique has been instrumental in the resolution of the molecular details of many signalling cascades (Tapon *et al*, 1998; Geijsen *et al*, 1999; Georgakopoulos *et al*, 2001).

There are, however, a number of drawbacks. Since the read-out of the yeast two hybrid makes use of a transcription event, one of the most crucial initial experiments is to establish whether the protein of interest is able to initiate transcription independently, resulting in autoactivation. This is often circumventable by the use of deletion constructs with the autoactivation domains removed, or by manipulation of the sensitivity of the reporters by the use of metabolic antagonists such as 3-aminotriazole, an inhibitor of histidine synthesis. Fortunately neither of the WT1 constructs used for yeast two hybrid assay demonstrated any appreciable autoactivation, and were therefore suitable for use in this system. An obvious criticism is also the use of artificially made fusion proteins, which might change the conformation of the bait and/or prey with a consequent change in protein function. The possibility of identifying artifactual partners as a result is a typical disadvantage, although an empirical way of excluding this is reciprocal transfer of the proteins i.e. switching around from DNA binding domain fusions to activating domain fusions, which should not affect the protein-protein

interaction. In addition, some interactions depend on post translational modifications that do not occur in the yeast. Finally, all library screens require as good as possible representation of cDNA's, and ideally, over a million independent clones should be screened.

Both Gal4 DNA binding domain – murine +KTS and –KTS WT1 fusion proteins were used independently as bait for yeast two hybrid screening of a E9.5/10.5 day mouse embryo cDNA library. Full length proteins were used to maximise the chance of the constructs adopting the correct protein conformation within the yeast cells. Previous experience with the combination of a pAS binding domain vector, pVP16 embryo library and the Y190 yeast strain suggested an average of 20 to 30 positive clones might be expected. This meant that despite good transformation efficiencies, a greatly sub-optimal result was obtained as after dual selection for both the histidine and *lacZ* reporters, only 6 positive clones were detected after two screens for the +KTS isoform, and 4 positive clones for the –KTS isoform. Since the pVP16 library screened was of good quality and other screens had indicated that it was representative, it is unlikely that an insufficient number of clones were screened. The pAS1 vector contains a full length ADH promoter and is able, at least theoretically, to induce strong expression of a hybrid protein. However, this did not appear to be the case in these experiments as neither the + or -KTS isoforms could be detected on Western blot. This was a recurring problem with these particular constructs (Rachel Davies, MRC Unit Edinburgh, personal communication), and meant that even though expression was sufficient to allow self association of the WT1 proteins, weaker protein-protein interactions may not have been able to occur. Full length WT1 proteins were used, and there remains a possibility that using shorter constructs may have improved the result, despite the additional risk of misconformation. In addition, the yeast strain used plays a key role. Y190 only has two reporters and a reputation for false positives, as it is not as sensitive or specific as newer strains e.g. PJ69. These have tightly controlled multiple reporters, which makes them more sensitive, but at the same time less prone to false positives. It is unlikely that WT1 was toxic to the yeast, as self-association could be clearly demonstrated.

Two yeast two hybrid screens were performed and these identified two putative interactors for the +KTS isoform, and one for the –KTS isoform. All interactors initially

represented unknown clones, which were gradually characterised with the improvements made in the databases resulting from the ongoing Human Genome Mapping project (http://www.ornl.gov/hgmis).

Three of the six protein-protein interactions detected for the +KTS isoform were with the predicted novel Edr (embryonal carcinoma differentiation regulated) protein (Shigemoto *et al*, 2001). The *Edr* gene is a novel developmentally regulated gene, originally identified through differential screening of an embryonal carcinoma cDNA library. It is present in whole mouse embryo RNA at all stages between E9.5 and E16.5 days gestation. Further analysis detected *Edr* in most foetal tissues including kidney, but in adult tissue low levels are only detected in brain and testis. Two overlapping open reading frames were identified, one encoding a 320 amino acid polypeptide containing a putative zinc finger binding domain of the CCHC subclass, whereas the second reading frame encoded a 631 amino acid polypeptide containing a consensus motif for an aspartyl protease catalytic site. Both motifs are also characteristic features of retroviral genes, and subsequent experiments showed that *Edr* is also likely to participate in ribosomal frameshifting, a mechanism that enables protein translation to occur from overlapping reading frames. This generally occurs in viral genomes, but is very rare amongst prokaryotic and eukaryotic cellular genes. *Edr* is the first mammalian gene to be identified that is capable of programmed translational recoding, which undoubtedly forms an important mechanism for regulating gene expression.

The putative detection of a protein-protein interaction between +KTS WT1 and Edr protein is of interest, in view of the possible role for +KTS isoforms in the regulation of RNA metabolism. All three clones appeared to be overlapping, lending support to the validity of the interaction, at least in yeast. Sequence quality was however relatively poor. At the time, the best way of plasmid rescue was considered transformation into HB101 bacteria, as these bacteria are unable to grow on a leucine deficient medium, forming additional selection for the activation domain plasmid. However, DNA prepared from HB101 bacteria can be difficult to sequence, and since sequence quality was relatively poor, this accounted for the surprising lack of a 100% match between the captured clones. This interaction remains speculative as no further confirmatory tests

were undertaken due the poorly characterised nature of Edr protein, a lack of an obvious link with renal disease, and the time constraints of the project.

One of the six clones detected using the +KTS isoform encoded an in frame fragment of angiomotin (Troyanovsky *et al*, 1902). This is a novel angiostatin-binding protein, which may regulate endothelial cell migration and tube formation. Angiomotin is expressed on Northern blot in most tissues examined, including the kidney. However it is unlikely to represent a true positive, as intracellular localisation studies indicate that it co-localises with F-actin and is therefore cytoplasmic, whereas WT1 is nuclear. This limits the biological significance of the interaction, which might have occured in the relatively artificial context of a library screen, but in reality the sub-cellular localisation of these two interactors means that they never meet *in vivo*. The remaining two clones were also false positives, as both nucleotide sequences were in the opposite orientation and thus encoded nonsense proteins.

Yeast two hybrid analysis using the –KTS isoform was even less successful. Only one potential interactor was detected, aminoimidazole carboxamide ribonucleotide transformylase/inosine monophosphate cyclohydrolase (ATIC), a bifunctional enzyme catalysing the last two steps in the *de novo* purine biosynthetic nucleotide pathway (Rayl *et al*, 1996). In view of the role of WT1 in oncogenesis, this may have represented a biologically significant positive. Since only one clone was detected, and there was no apparent link to human nephrotic disease, further confirmatory experiments were not undertaken.

Subsequently, a number of groups have now been successful in identifying WT1 protein binding partners using the yeast two hybrid, although none give particular clues about renal development or podocyte function. Of particular significance, are SF1, which provided further insight into the role of WT1 protein in sex determination (Nachtigal *et al*, 1998), and WTAP (Little *et al*, 2000), a nuclear protein, which like WT1 localizes throughout the nucleoplasm as well as in speckles and partially co-localizes with splicing factors. In addition, the detection of protein-protein interaction with U2AF65, a constitutive splicing protein (Davies *et al*, 1998), provided further evidence for a role in RNA metabolism. However, the main *sine qua non* of protein-protein interaction analysis is the differentiation between informative biological interactions, and non-

significant or false interactions, i.e. those unable to occur in nature due to expression at different times or in different locations. Of the interactions detected using the + and – KTS isoforms of WT1, the best candidate for true biological significance was Edr protein. However, a degree of pragmatism must be adopted when assessing the validity of yeast two hybrid results, and the evidence that Edr protein was a true interactor was insufficient to justify further follow-up.

Yeast two hybrid analysis of the WT1 isoforms could easily have been improved on, but unfortunately time constraint did not allow experiments to be optimised. Repeating the screens using improved yeast strains, more refined reporter systems and a kidney cDNA library may have resulted in a more successful outcome. A number of alternative binding domain vectors are now available, which result in better expression of the bait protein within the yeast allowing the detection of weaker, though potentially significant interactions. Another strategy might have been to screen using constructs deleted for the DNA binding domain, which might minimise false positives. However, since all areas of the WT1 protein have been implicated in protein-protein interactions, this could have potentially resulted in false negative results. In addition there is a significant risk of the bait protein adopting an incorrect conformation thus opening up spurious sites and closing biologically significant ones. Multiple reporter yeast strains may well have made a difference in the number of positive clones detected. Since each reporter gene is under the control of a different promoter, sensitivity can be increased without increasing the number of false positives. However, this was not a viable option, so the project moved on to two other genes with critical roles in glomerular filtration, *NPHS1* encoding nephrin and *NPHS2* encoding podocin. Results of *NPHS1* and *NPHS2* analysis are described in Chapter 4.

# CHAPTER 4: Molecular analysis of the *NPHS1* and *NPHS2* genes in congenital and early onset nephrotic syndrome

## 4.1 Background

Finnish type congenital nephrotic syndrome (CNF) is the most common congenital nephrotic syndrome. However, in early life, isolated nephrotic syndromes associated with FSGS and DMS as the renal histology also form a significant component of the overall pathology. CNF is characteristically a disease confined to the kidney, and diagnosis is based on time of onset, clinical features at time of presentation and renal histology. The same diagnostic criteria apply to FSGS and DMS, although in some cases these types of nephrotic syndromes may be associated with extra-renal manifestations, as described in Chapter 3. Inheritance of nephrotic syndromes in early life purely affecting the kidney is usually considered to be autosomal recessive, although apparently sporadic cases without a clear family history are also common.

The molecular basis underlying the loss of glomerular permselectivity seen in nephrotic syndrome characterised by CNF, FSGS or DMS renal histology was investigated. A mutational analysis strategy was adopted to analyse the involvement of two novel renal glomerular genes, *NPHS1* and *NPHS2*. These two genes were chosen for study as both are exclusively expressed within the podocyte layer of the renal glomerulus, and initial data had established a link with human disease. Mutations of the *NPHS1* gene had been detected in CNF cases of Finnish origin (Kestila *et al,* 1998), whereas *NPHS2* gene mutations were detected in a form of autosomal recessive familial FSGS (SRN1), with an onset between 3 months and five years (Boute *et al*, 2000). The initial focus was to test the hypothesis that *NPHS1* gene mutations were also responsible for cases of CNF without Finnish ancestry (section 4.2 and 4.3). Outside Finland, CNF generally follows a similar clinical course, although anecdotal reports of milder phenotypes including spontaneous resolution of proteinuria have been documented (e.g. Haws *et al* 1992), originally thought to be suggestive of genetic heterogeneity. An extension of the initial hypothesis was to determine whether *NPHS1* mutations also caused these milder phenotypes. In addition, other types of congenital nephrotic syndrome, namely those

characterised by FSGS renal histology, and selected cases of DMS, in which *WT1* gene mutations had not been detected were also analysed (section 4.4 and section 4.5). The results led to further experiments to test whether *NPHS2* gene mutations were present in cases of CNF without *NPHS1* gene mutations, and whether they contributed to the variable severity of clinical phenotype occasionally seen in CNF (section 4.6). The role of *NPHS2* mutations in a possible phenotypic switch from CNF to congenital FSGS was explored, and the extent of the overlap between *NPHS1* and *NPHS2* mutations in CNF examined (section 4.7). Five cases with early onset FSGS compatible with SRN1, and two cases of early onset DMS were also screened for *NPHS2* mutations (section 4.8). Finally, electromobility shift assays were performed to explore the significance of the promoter mutation detected in two non-Finnish CNF patients (section 4.9). The *NPHS1* and *NPHS2* mutations detected during this study were mapped to establish whether mutations targeted specific areas of each gene, thereby providing an indication of areas of particular functional importance. In addition, genotype-phenotype correlations were made to confirm whether a functional interrelationship between *NPHS1* and *NPHS2* was present. The results are discussed in section 4.9.

## 4.2 Patient selection and control material

Fifty-four affected individuals with congenital and early onset nephrotic syndrome were studied in total. Selection of cases for the study was based on clinical presentation, family history, laboratory findings and renal pathology. Causes of secondary nephrotic syndrome such as pre-natal infection were excluded, and only cases with pure renal involvement studied. Patients originated from the United Kingdom, Malta, Turkey, Middle East, Pakistan, Bangladesh, India and South Africa. Forty-one cases had CNF, although mutational analysis was only possible in thirty-seven, four congenital FSGS, five early onset FSGS compatible with a diagnosis of SRN1, two congenital DMS and two early onset DMS. The clinical details of each case entered into the study are listed in Appendix I. In order to maximise the ethnic diversity of the control group, fifty European and North American, sixty-one Asian and twenty-two Maltese were examined. The study had ethical approval from the Institute of Child Health Research Ethics committee (number 99MM05) and informed consent was obtained in all cases. Diagnosis of congenital nephrotic syndrome required a clinical history of prematurity, placental weight >25% of infant birth weight, and onset of proteinuria/ nephrotic syndrome between birth and three months of age. By definition, cases of CNF had normal renal function and were normotensive at presentation. Cases of congenital FSGS followed a similar pattern to CNF, but the two cases of congenital DMS both presented with hypertension and renal compromise within the neonatal period in conjunction with a severe nephrotic syndrome. Diagnosis of early onset nephrotic syndrome was made if onset was between three and thirty-six months of age. Cases had a mean onset of 18 months and the presence of characteristic features on renal biopsy was used to refine the diagnosis to FSGS or DMS. The salient clinical features used for diagnosis are listed in Table 4.1, and all cases studied were characterised on the basis of these criteria.

Although it is generally considered that nephrotic syndrome in early life follows an autosomal recessive pattern of inheritance, many of the cases studied were sporadic, with only one individual affected per family. Thirteen of the forty-one CNF cases had a positive family history of an affected a sibling or first-degree relative. Consanguinity between parents was identified in nineteen cases, five of which also had a positive family history. Two of the four cases of congenital FSGS and both cases of congenital

DMS studied had affected siblings. Within the early onset group, three of the five cases with SRN1-like disease and none of the DMS patients had a family history.

The majority of the cases studied developed a severe nephrotic syndrome with progression to end stage renal failure within five years, irrespective of whether presentation was at birth or subsequently. However nine CNF patients originating from Malta, India, Bangladesh, South Africa and the United Kingdom did not follow a typical course and went on to develop an unexpectedly mild phenotype. Initial presentation was identical to those patients who subsequently developed severe CNF, and cases were indistinguishable on clinical and histological grounds until 2-3 years of age. At this point, resolution of proteinuria rather than progression into chronic renal failure was seen. Proteinuria partially resolved in five cases (1, 26, 91, 92 and 94; clinical details listed in Appendix I) with preservation of renal function, and four cases (15, 90, 91 and 96) went into spontaneous remission. This was also not consistently associated with any particular treatment, for example the majority of cases that went on to develop severe CNF disease received anti-proteinuric agents, whereas cases 90 and 92 with mild CNF did not. This suggested that the lack of progression of nephrotic disease was not simply related to differing treatment strategies. The mild phenotype was not observed in conjunction with congenital FSGS or early onset FSGS or DMS, where all cases developed severe nephrotic syndrome.

Clinical findings were confirmed by renal biopsy or post-mortem analysis in fifty of the fifty-four patients studied, and a histopathological diagnosis set based on accepted criteria for the diagnosis of CNF, FSGS and DMS as listed in Table 4.2. Biopsies of patients with a diagnosis of congenital FSGS were independently examined at two centres. These showed early focal segmental changes in 50% of the glomeruli in three cases, and an initial histological appearance of minimal change at five months in one case, which developed into FSGS by the second biopsy at 18 months. Renal histology was not examined in four cases, however all originated from Malta, and two had a family history of CNF in a sibling or first cousin.

**Table 4.1 Diagnostic criteria used to ascertain cases**

**Congenital nephrotic syndrome**

**Clinical features**

**(i) Prenatal**

- Elevated α-fetoprotein (AFP) during pregnancy
- Prematurity
- Low birth weight
- Placental weight > 25% of infant birth weight
- Onset between birth and three months of age

**(ii) Features at presentation**

- Proteinuria at birth
- Oedema/nephrotic syndrome at birth
- Male: female ratio 1:1
- Autosomal recessive inheritance or sporadic

**(iii) Clinical features distinguishing between CNF, FSGS and DMS**

- CNF cases: generally normal renal function and normo-tension
- DMS cases: renal insufficiency and hypertension +/- abnormalities in extra-renal systems. AFP not uniformly elevated and generally normal placental size
- Congenital FSGS: features resemble CNF or DMS

**Early Onset Nephrotic Syndrome**

- Onset of nephrotic syndrome between 6 and 36 months
- Normal gestational history
- occasional response to steroid therapy

**Table 4.2 Histological Criteria used to establish underlying renal pathology**

**CNF**

**Early Features**

- glomeruli normal +/- mesangial hypercellularity
- proximal tubular dilatation

**Late Features**

- enlarged sclerotic glomeruli with marked microcystic dilation of the tubules
- tubular atrophy and interstitial fibrosis

**FSGS**

- presence of areas of both focal and segmental glomerular sclerosis
- focal and segmental tuft collapse
- +/- segmental hyalinosis, +/-glomerular deposits of IgM/C3

**DMS**

**Early Features**

- increased mesangial matrix, no mesangial hypercellularity
- extensive tubular dilatation

**Late Features**

- most glomeruli with condensed sclerotic tufts +/- collar epithelial cells
- dilated Bowman's capsule and tubules

## 4.3 The *NPHS1* gene is a suitable candidate for non-Finnish CNF

Haplotype analysis of Finnish and non-Finnish CNF families (Manniko *et al*, 1995, Fuchshuber *et al*, 1996; Manniko *et al*, 1996; Manniko *et al*, 1997) suggested Finnish and many non-Finnish CNF patients shared the same disease locus. Subsequent detection of *NPHS1* gene mutations in the majority of Finnish cases of CNF (Kestila *et al*, 1998) implied that mutations might also be responsible for non-Finnish CNF. However, linkage analysis in the majority of non-Finnish CNF cases is not feasible, as many cases lack clear autosomal recessive inheritance. Furthermore, the CNF phenotype within the non-Finnish population is more variable, both in severity of clinical presentation and histological appearance. In view of these discrepancies, the first question to answer prior to embarking on mutation screening was whether *NPHS1* was an appropriate candidate gene for the cases of non-Finnish CNF to be studied.

To test this, a partial haplotype analysis was performed on selected families using the three polymorphic markers D19S608, D19S609 and D19S610, originally developed to fine map the critical region of *NPHS1* gene (Mannikko *et al*, 1995, Olsen *et al*, 1996). The *NPHS1* gene lies immediately distal to D19S609, and overlaps marker D19S610 as shown in Figure 4.1. D19S608 is located approximately 100kb proximal to D19S610. A particular emphasis was placed on D19S608 and D19S610. D19S610 was thought likely to be intragenic, and also showed the most significant linkage disequilibrium, with an allelic association of 84% at least within the Finnish population (Manniko *et al*, 1995). Two major haplotype classes were present in Finnish CNF, both sharing allele 6 of D19S610, although this was subsequently linked to both Fin major and Fin minor mutations rather than a single mutation (Kestila *et al*, 1998). However, subsequent haplotype analysis of non-Finnish CNF observed the strongest linkage disequilibrium to be with D19S608 in the population tested (Mannikko *et al,* 1996). Four main haplotype classes were present, and in many cases the alleles found were the same as in Finnish CNF families. This suggested that *NPHS1* was also the causative gene in non-Finnish CNF. In view of the clinical variability of non-Finnish CNF, allelic association was first tested in as many of the non-Finnish CNF families selected for study as possible. A premise was set that the presence of allelic association would corroborate a link between *NPHS1* and non-Finnish CNF, substantiating mutational screening in these cases.

**Figure 4.1 Location of polymorphic markers used to establish allelic association with the NPHS1 locus on chromosome 19q13.1.**

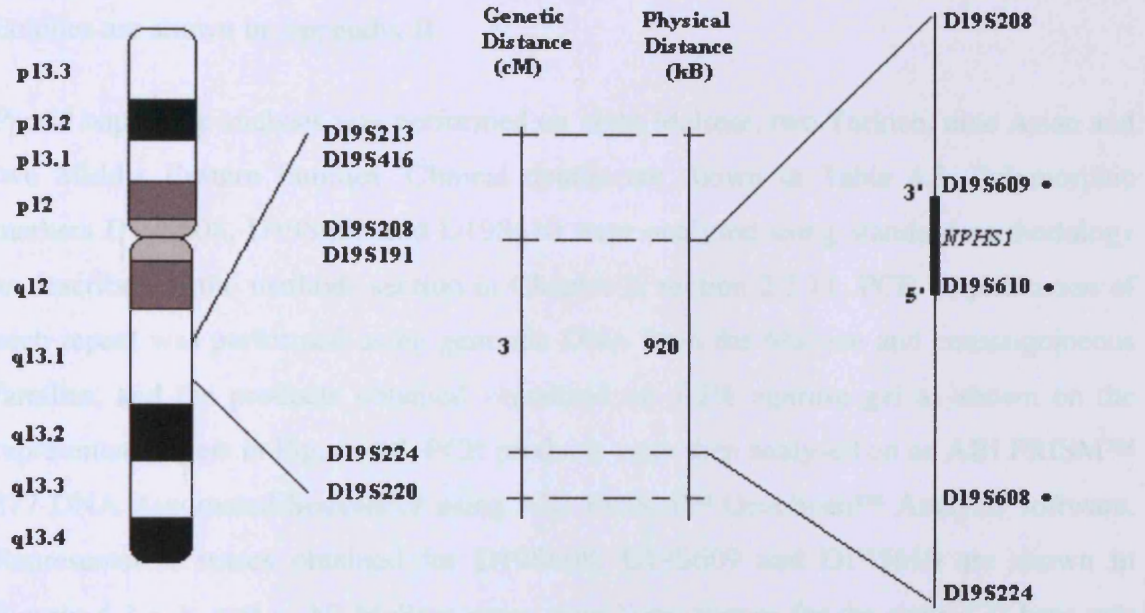


**Key**

- polymorphic markers used to ascertain likelihood that *NPHS1* was a candidate gene for non-Finnish CNF

***Partial haplotype analysis of selected CNF families.*** The two groups considered likely to be informative were families originating from Malta and those with demonstrable consanguinity. The Maltese are known to represent a genetically homogeneous population, and the incidence of congenital nephrotic syndrome is surprisingly high. The carrier frequency was found to be 1 in 20 normal Maltese controls. Consanguineous families originated from the Indian sub-continent, the Middle East and Turkey. None of the Maltese or Asian families examined had demonstrable Finnish ancestry. Affected individuals had a clinical diagnosis of CNF, confirmed by histological diagnosis on renal biopsy or post-mortem in the majority of cases. Seven had a family history of CNF in a sibling or first-degree relative. The family trees for the Maltese and consanguineous families are shown in Appendix II.

Partial haplotype analysis was performed on eight Maltese, two Turkish, nine Asian and two Middle Eastern families. Clinical details are shown in Table 4.3. Polymorphic markers D19S608, D19S609 and D19S610 were analysed using standard methodology as described in the methods section in Chapter 2, section 2.3.11. PCR amplification of each repeat was performed using genomic DNA from the Maltese and consanguineous families, and the products obtained visualised on a 2% agarose gel as shown on the representative gels in Figure 4.2. PCR products were then analysed on an ABI PRISM™ 377 DNA Automated Sequencer using ABI PRISM™ GeneScan™ Analysis software. Representative traces obtained for D19S608, D19S609 and D19S610 are shown in Figures 4.3 a, b, and c. All Maltese cases were homozygous for the same 122 base pair allele for marker D19S608, 118 base pair allele for marker D19S609, and 216 base pair allele for marker D19S610 suggestive of linkage disequilibrium for the *NPHS1* gene. All parents tested were heterozygous, sharing one 216 base pair allele in combination with 210, 212 and 220 in approximately equal incidence. The majority of consanguineous families were also homozygous for different alleles of D19S608, D19S609 and D19S610. Marker D19S610 was considered particularily valuable, as it was intragenic and located at the 5' end of the *NPHS1* gene. The results for this marker are shown in Table 4.3, in conjunction with the clinical details of the cases tested.

**Figure 4.2 Representative gels to demonstrate PCR products for polymorphic markers DS19608, DS19S609 and D19S610**

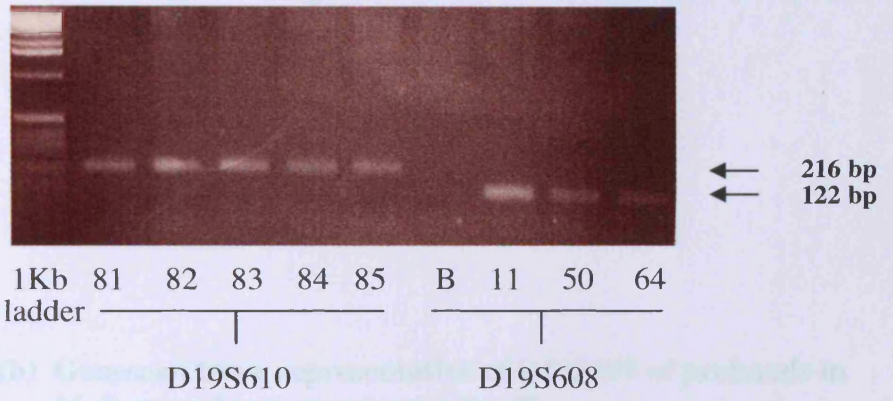


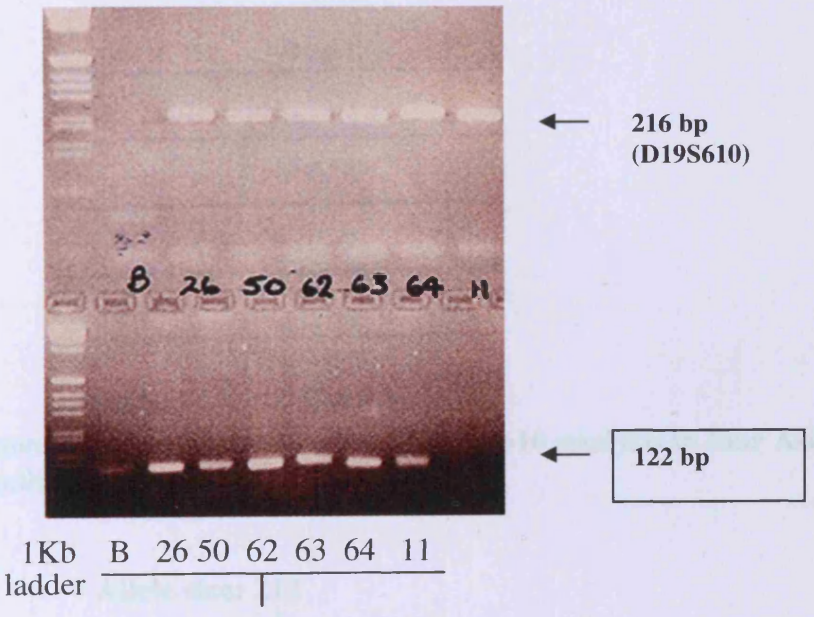

**Figure 4.3 (a) Genescan trace representative of D19S608 analysis of probands in Maltese and consanguineous families**

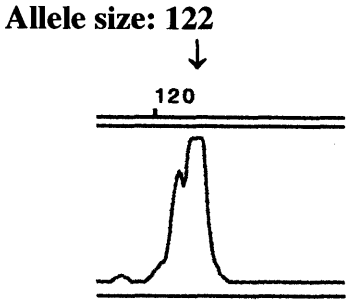


**Figure 4.3 (b) Genescan trace representative of D19S609 of probands in Maltese and consanguineous families**

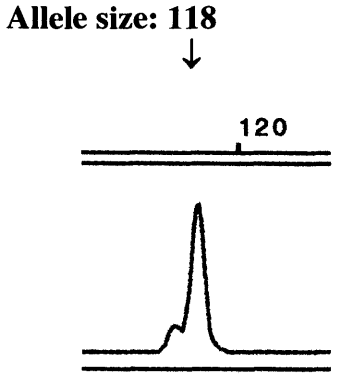


**Figure 4.3 (c) Genescan trace representative of D19S610 analysis in four Asian families.**

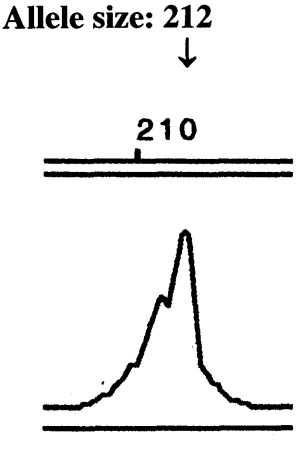

**Figure 4.3 (d) Representative trace of D19S610 analysis of Maltese families: traces showing partial haplotype analysis of case 91 and parents**

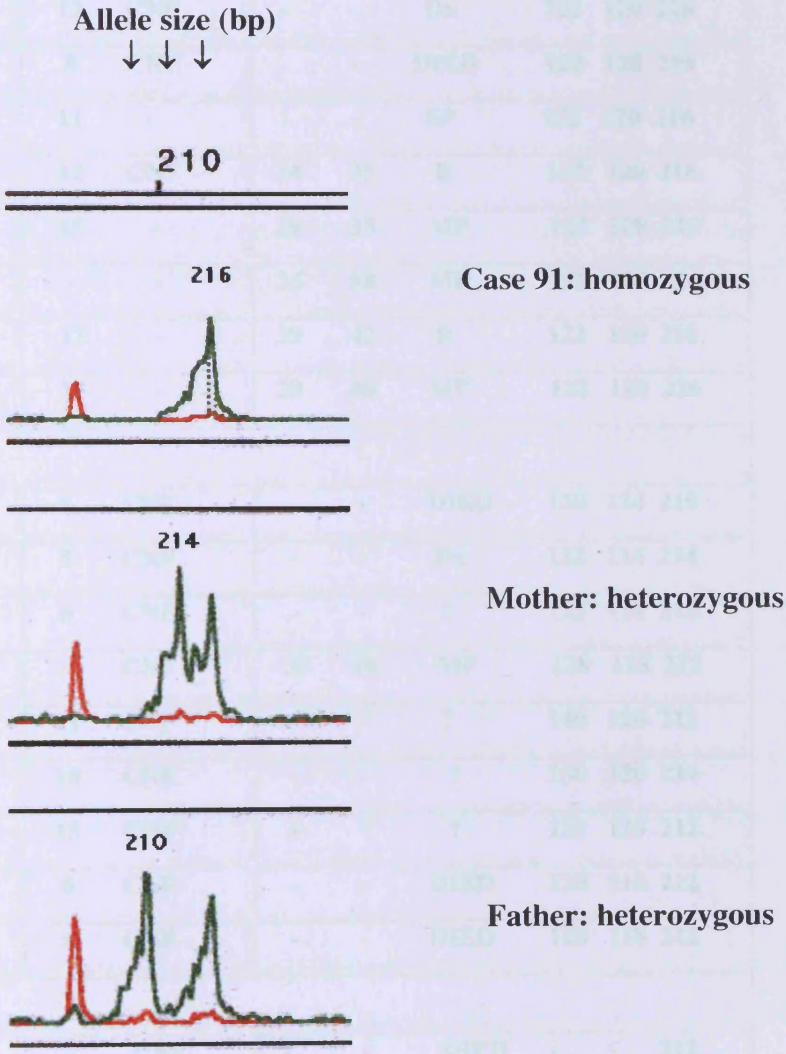

**Table 4.3 Clinical details and partial haplotype analysis of Maltese and consanguineous families tested for allelic association with markers D19S608, D19S609 and D19S610**

| Case | Sex | Family History | Features at presentation | | Clinical status and Haplotype | | | | | |
|---|---|---|---|---|---|---|---|---|---|---|
| | | | | | Alb | Creat | Outcome | Allele size (bp) | | |
| | | ? | Alb | Histo | | | | 608 | 609 | 610 |
| *A) Maltese families* | | | | | | | | | | |
| 81 | M | no | 11 | CNF | - | - | Tx | 122 | 120 | 216 |
| 82 | F | yes:83 | 13 | CNF | - | - | Dx | 122 | 120 | 216 |
| 83 | M | yes:82 | 8 | CNF | - | - | DIED | 122 | 120 | 216 |
| 84 | M | no | 11 | - | - | - | SP | 122 | 120 | 216 |
| 90 | F | no | 12 | CNF | 34 | 35 | R | 122 | 120 | 216 |
| 91 | F | no | 15 | - | 29 | 35 | MP | 122 | 120 | 216 |
| 92 | F | yes | - | - | 34 | 50 | MP | 122 | 120 | 216 |
| 93 | F | no | 13 | - | 39 | 42 | R | 122 | 120 | 216 |
| 94 | M | yes | 13 | - | 29 | 40 | MP | 122 | 120 | 216 |
| *B) Asian families* | | | | | | | | | | |
| 7 | F | no | 6 | CNF | - | - | DIED | 120 | 114 | 210 |
| 10 | M | no | 5 | CNF | - | - | Dx | 122 | 114 | 214 |
| 20 | M | no | 8 | CNF | - | - | ? | 122 | 114 | 218 |
| 26 | F | yes | 4 | CNF | 35 | 40 | MP | 128 | 118 | 212 |
| 62 | F | no | 11 | CNF | - | - | ? | 140 | 120 | 212 |
| 63 | F | no | 10 | CNF | - | - | ? | 130 | 120 | 214 |
| 64 | M | no | 15 | CNF | - | - | ? | 128 | 118 | 212 |
| 80 | M | no | 6 | CNF | - | - | DIED | 128 | 118 | 212 |
| 85 | M | no | 8 | CNF | - | - | DIED | 128 | 118 | 212 |
| *C) Turkish families* | | | | | | | | | | |
| 8 | F | no | - | CNF | - | - | DIED | - | - | 212 |
| 15 | M | no | - | CNF | - | - | Dx | - | - | 210/214 |
| *D) Middle East* | | | | | | | | | | |
| 11 | M | yes | 6 | CNF | - | - | DIED | - | - | 218 |
| 50 | M | yes | 7 | CNF | - | - | Tx | - | - | 212 |

**Key** Alb = albumin concentration (mg/dL); Creat = plasma creatinine (μM/L); Histo. = histology; SP = severe proteinuria; MP = mild proteinuria; Tx = transplant; Dx = dialysis ? = outcome unknown

Partial haplotype analysis for both the intragenic marker D19S610, and markers D19S608 and D19S609 located within the critical region for *NPHS1* consistently demonstrated allelic association in the non-Finnish CNF cases analysed (Table 4.3). These results were suggestive of linkage to the *NPHS1* region on chromosome 19q13.1 for the majority of the non-Finnish CNF families tested. Furthermore, the results indicated a likely founder effect in the Maltese CNF population, making it probable that these cases would carry the same *NPHS1* mutation. On this basis, it was concluded that *NPHS1* was an appropriate candidate gene for non-Finnish CNF in these families, and mutational analysis of affected individuals was appropriate.

## 4.4 Mutations of the *NPHS1* gene are present in the majority of non-Finnish CNF cases, including those with unusually mild phenotypes

Mutational analysis of the *NPHS1* gene was undertaken to identify whether mutations of the *NPHS1* gene were present in a population of non-Finnish individuals with CNF. Although milder phenotypes have been documented, the majority of non-Finnish CNF cases emulate the classically severe clinical phenotype seen in Finland, and renal histology typically represents the mesangial hypercellularity and microcystic dilatation of the proximal renal tubules seen in Finnish cases. Thirty-seven cases of CNF underwent mutational analysis, of which twenty-eight had classically severe, and nine atypically mild disease. The mild and severe groups were clinically indistinguishable for the first two to three years of life.

*NPHS1* exons 1-29, adjacent introns and the promoter region were analysed by PCR amplification and sequencing of DNA from affected individuals. Any mutations detected were confirmed by restriction enzyme digest, parental analysis and absence in normal controls. Twenty-one different mutations were detected throughout the *NPHS1* gene in 29 of 37 CNF cases analysed. All occurred in a homozygous or compound heterozygous manner and affected exons 4, 6, 7, 9, 10, 11, 14, 17, 18, 23, 24, 26, 27, intronic splicing regions and the promoter, and all parents available for analysis were carriers. Isolated heterozygous mutations were not found in association with a CNF phenotype. This indicated that *NPHS1* mutations were responsible for the majority of

CNF cases with no demonstrable Finnish ancestry. The same homozygous exon 27 nonsense mutation (R1160X, Figure 4.4.19) was detected in all thirteen cases originating from Malta, confirming the founder effect suggested by partial haplotype analysis in section 4.3. R1160X was also detected in CNF cases of Asian origin, but the association with different alleles suggested a different founder in this population. Only parental DNA was available for mutation screening from Maltese CNF cases 86, 87, 88 and 89 (Table 4.5). However, the detection of heterozygous R1160X mutations in both parents in conjunction with a typical clinical history and a positive family history in all four provided strong evidence that homozygous R1160X mutations were also responsible for their disease. Importantly, the R1160X mutation was associated with mild CNF in six of the twelve cases analysed, five of which were female. This was seen in both the Maltese and Asian populations, which suggested that the discrepant phenotype seen was influenced by gender but not ethnic origin. The clinical details of each case with an R1160X mutation are also given in Table 4.5. Heterozygous R1160X changes were associated with a normal phenotype, and were present in all Maltese parents, the phenotypically normal sister of case 81, and in 1 of 44 Maltese control chromosomes. Of note, R1160X was the only *NPHS1* mutation to be associated with mild disease, and all other *NPHS1* mutations resulted in a consistently severe CNF phenotype, regardless of location or predicted effect on the protein. An nt 2335-1 (G→A) exon 18 splicing mutation was the commonest mutation in patients of English origin (Figures 4.4.14 A, B, C and D). We also document the first occurrence of Fin minor (R1109X) (Figure 4.18) outside Finland, in a Turkish patient with no demonstrable Finnish ancestry. Nine mutations remain novel (denoted by an * in Table 4.4), whereas the remainder have now also been reported by other groups (Lenkkeri, *et al*, 1999; Aya *et al*, 2000; Beltcheva *et al*, 2001). The mutations detected in non-Finnish CNF are listed in Table 4.4 and representative sequencing analysis traces for each mutation shown in Figure 4.4. *NPHS1* mutations were not detected in eight CNF cases, five of which had severe and three of which had atypically mild nephrotic disease. Table 4.6 illustrates the common polymorphisms detected in patients and normal controls, and Table 4.7, those mutations altering restriction enzyme sites.

**Table 4.4** ***NPHS1*** **mutations in non-Finnish CNF patients (excluding R1160X)**

| Case | Origin | Exon | Nucleotide Change | Effect on coding sequence | Effect on protein | Mutation status |
|---|---|---|---|---|---|---|
| ***Frameshift Mutations*** | | | | | | |
| 5 | England | 6 | nt 650 (delAG) | frameshift | truncation | comp het |
| 50 | Middle East | 10* | nt1291(insA) | frameshift | truncation | hom |
| 4 | England | 24 | nt3250(insG) | frameshift | truncation | comp het |
| ***Non-frameshift mutations and insertions*** | | | | | | |
| 6 | Middle East | 4 | nt514(del ACC) | del Thr 172 | del Thr | hom |
| 7 | Pakistan | 6 | nt603(delCACC C CGG (ins TT) | Tyr205, Pro206 Arg207→Ile205 | del TPR, ins I | hom |
| ***Nonsense Mutations*** | | | | | | |
| 8 | Turkey | 26 | nt3325(C→T) | R1109X | truncation (Fin minor) | hom |
| Splicing mutations | | | | | | |
| 73 | England | 14* | nt1905(C→T) | alternative splice donor site? | aberrant splicing | comp het |
| 25 | England | 18 | nt2335-1(G→A) | exon 18-1(G→A) | splicing | comp het |
| 32 | England | 18 | nt2335-1(G→A) | exon 18-1(G→A) | splicing | comp het |
| 47 | England | 18 | nt2335-1(G→A) | exon 18-1(G→A) | splicing | comp het |
| 65 | England | 18 | nt2335-1(G→A) | exon 18-1(G→A) | splicing | hom |
| 2 | England | 23* | nt2335-1(A→T) | exon 23 donor | splicing | comp het |
| 4 | England | 27 | nt3482(G→T) | exon 27 donor | splicing | comp het |
| 5 | England | 27 | nt3482(G→T) | exon 27 donor | splicing | comp het |
| ***Missense mutations*** | | | | | | |
| 9 | England/ India. | 7* | nt791(C→G) | P264R | Arg268→Pro | comp het |
| 47 | England | 7 | nt808(G→T) | G270C | Gly270→Cys | comp het |
| 10 | India | 9 | nt1099(C→T) | R367C | Arg367→Cys | hom |
| 9 | England/ India | 11* | nt1337(T→A) | I446N | Ile446 →Asn | comp het |
| 11 | Middle East | 11 14 | nt 1379(G→A) | R460Q | Arg460→Glu | hom |
| 25 | England | 14* | nt1868(G→T) | C623F | Cys623→Phe | comp het |
| 20 | India | 17 | nt1927(T→C) | L643P | Leu643→Pro | hom |
| 2 | England | 18 | nt2227(C→T) | R743C | Arg743→Cys | comp het |
| 62 | India | | nt2404(C→T) | R802W | Arg802→Trp | hom |
| ***Promoter mutations*** | | | | | | |
| 32 | England | P* | nt-340(G→C) from ATG | - | - | comp het |
| 73 | England | P* | nt-340(G→C) from ATG | - | - | comp het |

**KEY: del = deletion; ins = insertion; hom = homozygote; comp het = compound heterozygote; nt = nucleotide; * = novel mutation**

**Table 4.5 Clinical details of patients with homozygous R1160X (nt 3478 C→T) *NPHS1* mutations**

| Case | Origin | Sex | Family History ? | Features at presentation Alb | Renal histology | Clinical status/outcome at time of study |
|---|---|---|---|---|---|---|
| ***A) Maltese and Asian families: severe phenotype (n=6)*** | | | | | | |
| 80 | India | M | no | 6 | CNF | died aged 6 months, diagnosis confirmed on postmortem |
| 81 | Malta | M | no | 11 | CNF | renal transplant aged 18 months, 12 yeasr alive and well |
| 82 | Malta | F | yes:83 | 13 | CNF | dialysis aged 4 years, failed transplant |
| 83 | Malta | M | yes:82 | 8 | CNF | died post transplant aged 6 months |
| 84 | Malta | M | no | 11 | - | severe nephrotic syndrome at 15 months |
| 85 | India | M | no | 8 | CNF | died aged 1 month, diagnosis confirmed on postmortem |
| ***B) Maltese and Asian families mild phenotype (n=6)*** | | | | | | |
| 90 | Malta | F | no | 12 | CNF | aged 11 years; alb 34, creat 35; R; Nt |
| 91 | Malta | F | no | 15 | - | aged 5 years; alb 29, creat 35; MP; Nt |
| 92 | Malta | F | yes:86 | - | - | aged 19 years; alb 34, creat 50; MP; Nt |
| 93 | Malta | F | no | 13 | - | aged 5 years; alb 39, creat 42; R; Nt |
| 94 | Malta | M | yes | 13 | - | aged 8 years; alb 29, creat 40; MP; Nt |
| 26 | India | F | yes | 4 | CNF | aged 7 years; alb 35, creat 40; MP; Nt |
| ***C) Patients with a clinical diagnosis of classically severe CNF, mutations status not determined, but both parents heterozygous for R1160X (n=4)*** | | | | | | |
| 86 | Malta | M | yes:92 | - | CNF | died aged 3 months |
| 87 | Malta | M | yes: 88 | - | CNF | died aged 5 years |
| 88 | Malta | M | yes :87 | - | - | died aged 2 months |
| 89 | Malta | M | yes: 94 | - | CNF | died aged 21 months |

**KEY:** alb=albumin; creat=creatinine; MP=mild proteinuria; R=remission; Nt= normotension

**Table 4.6 *NPHS1* polymorphisms detected in patients and controls**

| Nucleotide Change | Exon/intron | Effect on coding sequence |
|---|---|---|
| nt349(g→a) | exon 3 | E117K▪ |
| nt1407(c→t) | exon 11 | P440P |
| del caa –30 nt 1933 | intron 14 | intronic deletion▪ |
| nt 2289 (c→t) | exon 17 | V763V |
| nt3230(a→g) | exon 24 | N1077S▪ |
| nt3403 +36 (c→t) | intron 24 | intronic base change |
| nt3404+89(c→t) | intron 24 | intronic base change |
| nt3315(g→a) | exon 26 | S1106S |

Key: ▪ = very common in all ethnic groups examined

**Table 4.7 Restriction enzyme sites altered by *NPHS1* mutations in CNF**

| Mutation | Altered restriction enzyme site (- removal; + addition) |
|---|---|
| nt603 del CACCCC ins (TT) | - Nci I, Sac I |
| nt514 (del ACC) | - BseM II |
| nt2335-1 (A → T) | - Pfl MI |
| nt3482(G→T) | - Mae III, Bsa JI, Tsp 451 |
| nt791(C→G) | - Tse I |
| nt808(G→T) | - Dde I |
| nt 3478 (C→T) | - Ava I |
| nt340(G→C) | + Sty I |

**Figure 4.4 Representative ABI sequence analysis traces of *NPHS1* mutations in non-Finnish CNF**

**Figure 4.4.1 A) *NPHS1* Promoter G → C missense mutation 5' to 3'**

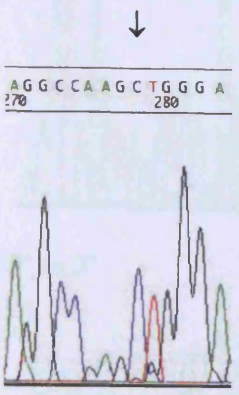


**C) Normal control 5' to 3'**

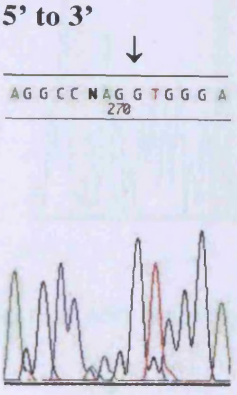


**Figure 4.4.2 A) *NPHS1* exon 4 nt 514 (del ACC, Thr 172) homozygous mutation 3' to 5'**

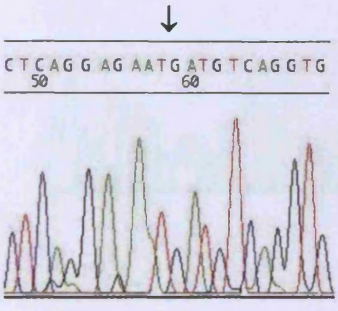


**C) Normal control 3' to 5'**

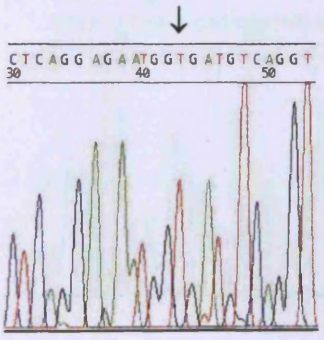

**Figure 4.4.3 A) *NPHS1* exon 6 nt 603 homozygous del CACCCGG(ins TT) 5' to 3'**

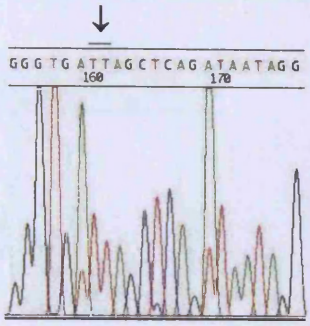


**C) Normal control 5' to 3'**

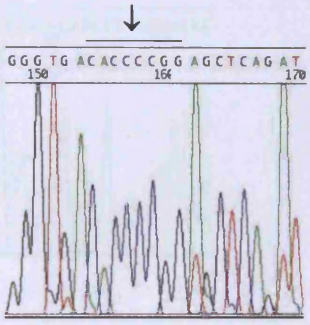


**Figure 4.4.4 A) *NPHS1* exon 6 nt 650 heterozygous del AG 5' to 3'**

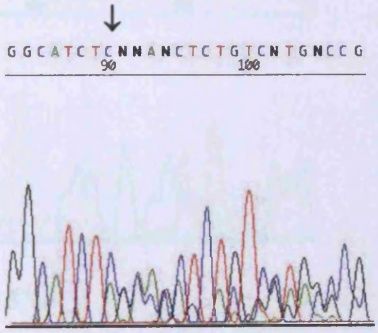


**B) Normal control 5' to 3**

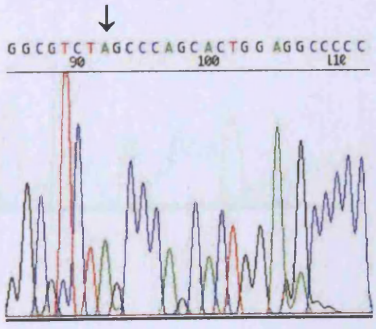

**Figure 4.4.5 A) *NPHS1* exon 7 nt 791(C→G) P264R heterozygous mutation 3'to 5'**

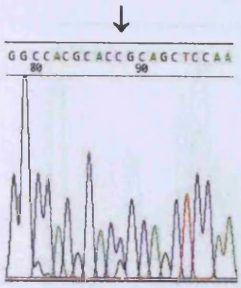


**B) Normal control 3'to 5'**

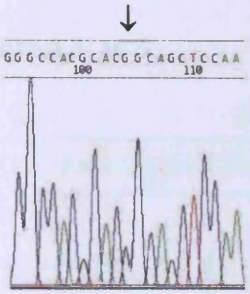


**Figure 4.4.6 A) *NPHS1* exon 7 nt 808 (G→T) G270C heterozygous mutation 5'to 3'**

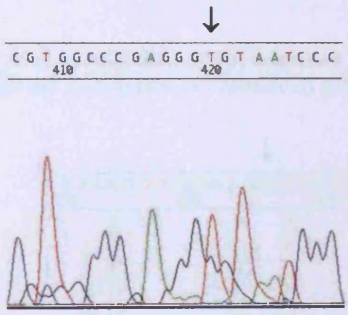


**B) Normal control 5'to 3'**

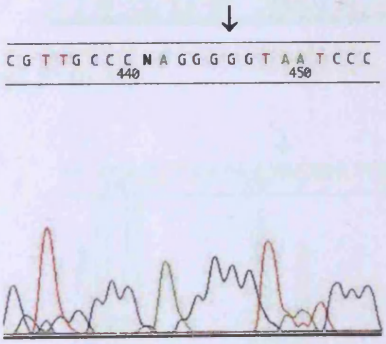

**Figure 4.4.7** **A) *NPHS1* exon 9 nt 1099(C →T) R367C homozygous mutation 3' to 5'**

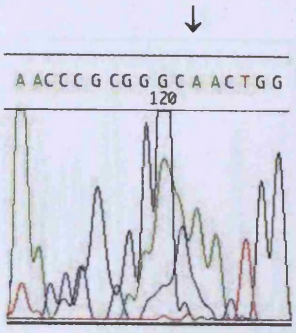


**B) Normal control 3' to 5'**

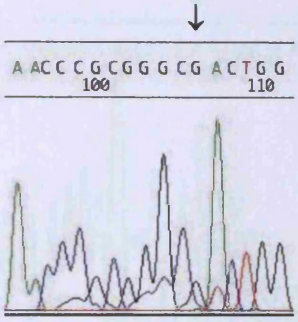


**Figure 4.4.8 A) *NPHS1* exon 10 nt 1291(ins A) homozygous mutation 5' to 3'**

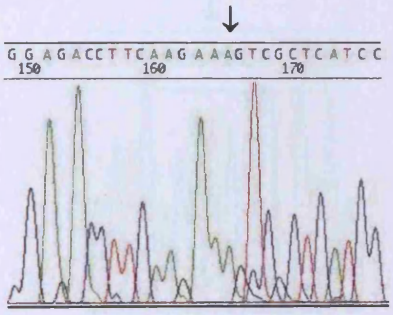


**B) Normal control 5' to 3'**

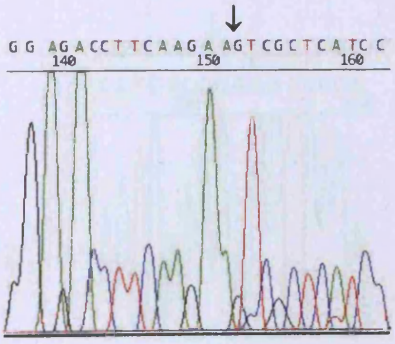

**Figure 4.4.9 A) *NPHS1* exon 11 nt 1379(G →A) I446N heterozygous mutation 3' to 5'**

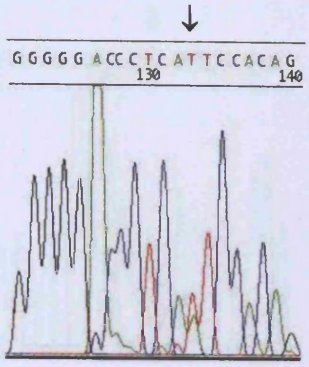


**B) Normal control 3' to 5'**

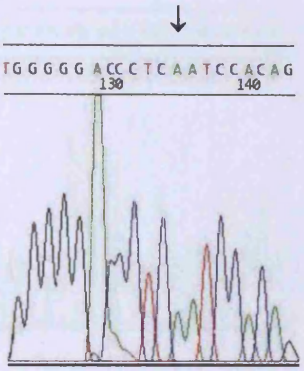


**Figure 4.4.10 A) *NPHS1* exon 11 nt 1337(G →A) R460Q homozygous mutation 3' to 5'**

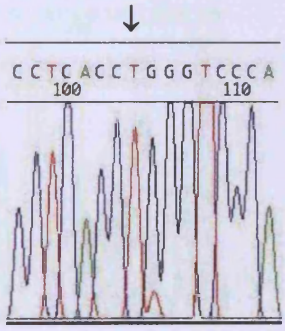


**B) Normal control 3' to 5'**

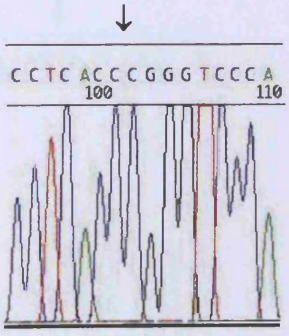

**Figure 4.4.11 A) *NPHS1* exon 14 nt1868 (G→T) C623F heterozygous mutation 5' to 3'**

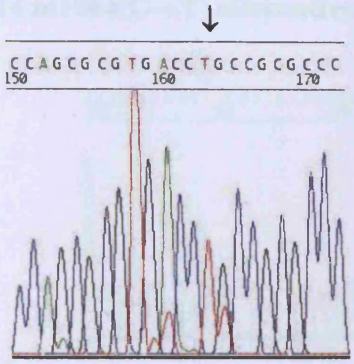


**B) Normal control 5' to 3'**

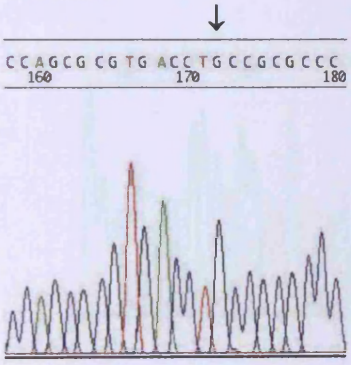


**Figure 4.4.12 A) *NPHS1* exon 14 nt 1928 (T→C) L643P (? Splicing) homozygous mutation 5' to 3'**

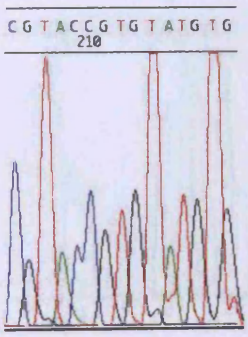


**B) Normal control including +8 bases of splice donor site 5' to 3'.**

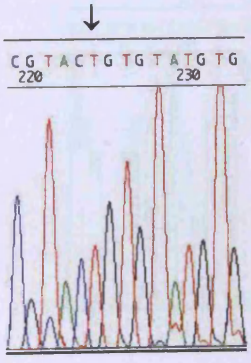

**Figure 4.4.13 A) NPHS1 exon 14 nt1904(C→T) alternative donor splice site mutation 5' to 3'**

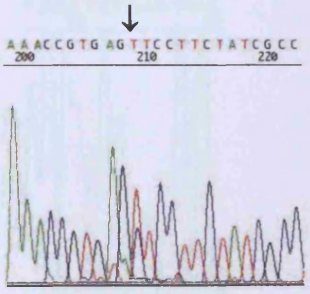


**B) Normal control 5' to 3'**

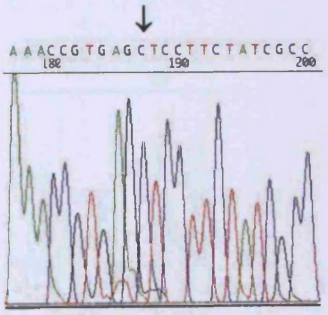


**Figure 4.4.13 A) Exon 17 nt2227(C→T) R743C heterozygous mutation 5' to 3'**

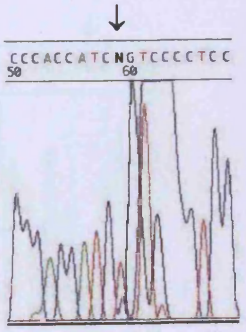


**a. Normal control 5' to 3'**

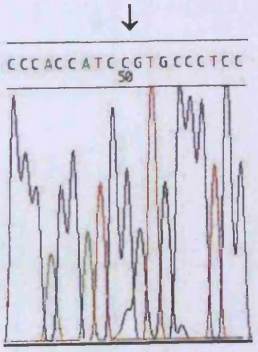

**Figure 4.4.14 A) *NPHS1* exon 18 nt2335-1(G→A) homozygous splicing mutation 5' to 3'**

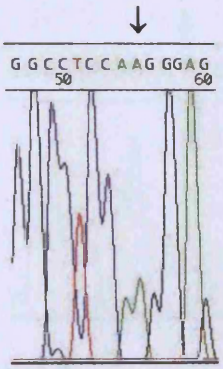


**B) Normal control 5' to 3'**

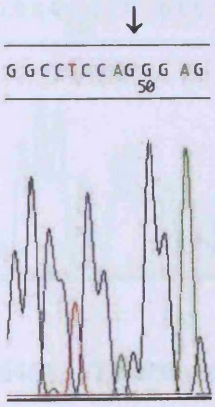


**C) Exon 18 nt2335-1(G→A) heterozygous splicing mutation 5' to 3'**

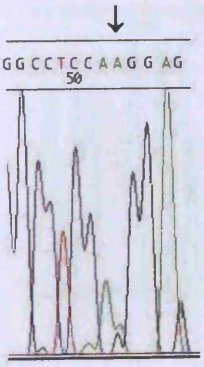


**D) Normal control 5' to 3'**

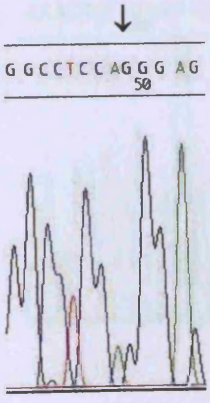

**Figure 4.4.15 A) Exon 18 nt2404(C→T) R802W homozygous mutation 5' to 3'**

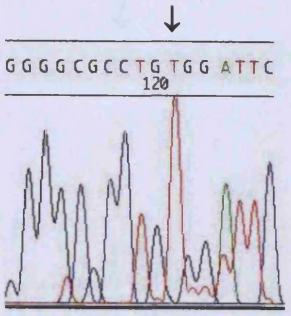


**B) Normal control 5' to 3'**

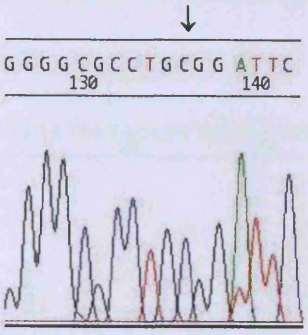


**Figure 4.4.16 A) *NPHS1* exon 23 nt3164(A→T) heterozygous splicing mutation 5' to 3'**

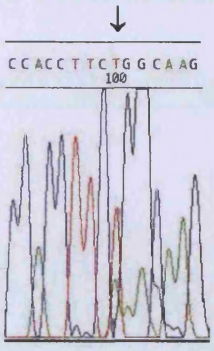


**B) Normal control 5' to 3'**

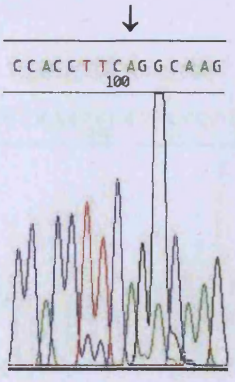

**Figure 4.4.17** **A) NPHS1 exon 24 nt3250 (insG) 5' to 3'**

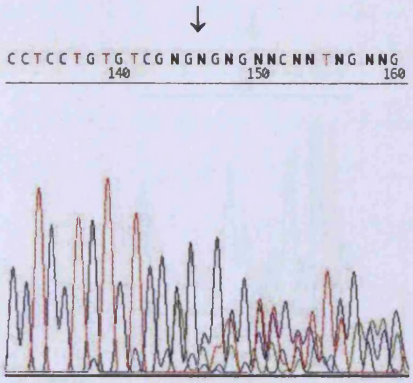


**B) Normal control 5' to 3'**

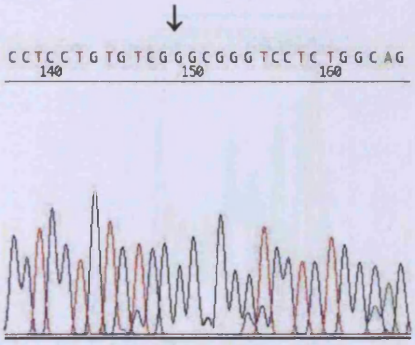


**Figure 4.4.18** **A) *NPHS1* exon 26 nt3325(C→T) R1109X (Fin minor) 3' to 5'**

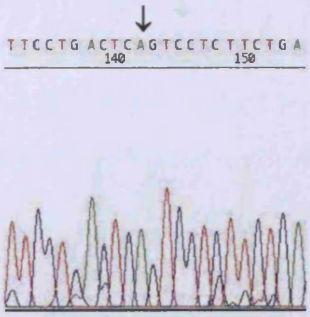


**B) Normal control 3' to 5'**

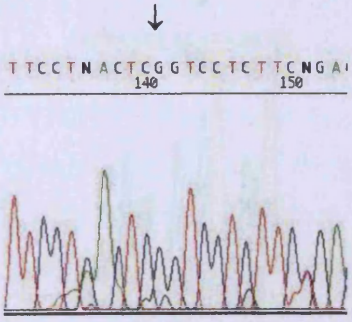

**Figure 4.4.19 A) *NPHS1* exon 27 nt3478(C→T) homozygous R1160X mutation 5' to 3'**

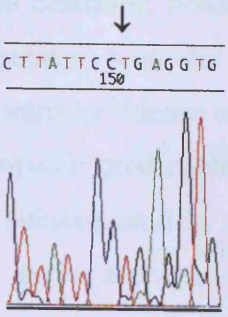


**B) Normal control 5' to 3'**

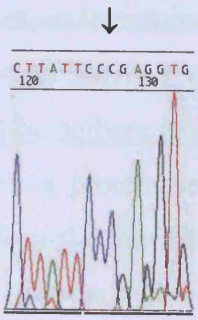


**Figure 4.4.20 A) *NPHS1* exon 27 nt 3482 (G → T) splice donor mutation 5' to 3'**

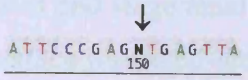


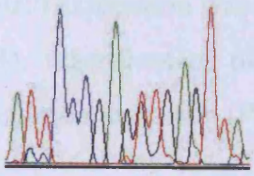

**B) Normal control 5' to 3'**

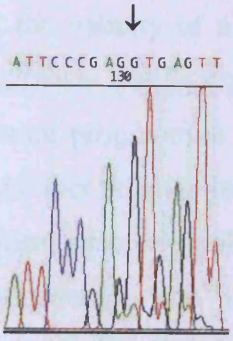

***Bioinformatics.*** Ten of the *NPHS1* mutations detected were predicted to result in frameshifts, non-frameshift insertions and deletions, nonsense and splicing mutations, nine in missense mutations, and one in a putative promoter change. Computer prediction programmes were used to provide corroborative evidence of the predicted effect of these on the translated nephrin protein. Computer predictions are only able to provide hypothetical projections, which must be substantiated by experimental data. However, an indication of the possible effect is given and this may reduce the number of functional assays required to establish the physiological effect of the mutation.

***NPHS1 frameshifts, non-frameshift insertions/deletions and nonsense mutations in CNF.*** The effect of these was assessed using SMART (Simple Modular Architecture Research Tool) analysis (http://smart.embl-heidelberg.de/smart/show_motifs.pl), which estimates the size and domain structure of a protein sequence (Schultz *et al*, 1998, 2000). SMART analysis predicted that three of the four frameshift mutations (cases 4, 5, and 50) would result in truncated proteins, whereas both non-frameshift deletions would produce proteins structurally almost identical to wild type nephrin (Figure 4.5). Nephrin expression was detected in the glomeruli of case 7 (nt 603 (del CACCCCGG, ins TT) *NPHS1* mutation), despite severe changes of end stage renal failure (Figure 4.6 A). Both nonsense mutations were predicted to produce truncated proteins 1109 and 1160 amino acids in length respectively, which retained the transmembrane domain, but had a shortened cytosolic tail. Glomerular nephrin expression was normal in all R1160X cases examined (represented in Figure 4.6 B), regardless of disease severity. In contrast, R1109X resulted in loss of glomerular nephrin expression (Patraaka *et al*, 2000).

***NPHS1 Splicing mutations in CNF.*** These were analysed using a combination of Neural network, which is able to predict the validity of a putative splice acceptor or splice donor site (Ogura *et al*, 1997) (http://www.fruitfly.org/seq_tools/splice.html) and SMART analysis. These computer prediction programmes suggested that the splicing mutations detected during this study would either result in putative splice site activation, which might result in an alteration in isoform ratio or similar mechanism (case 73), or truncated nephrin proteins through read-through into intronic sequence and the generation of premature stop codons (cases 25, 32, 47, 65, 2, 4, and 5). The result of computer predication analysis are shown in Figure 4.7 (A to D).

**Figure 4.5 SMART (http://smart.embl-heidelberg.de/smart/show_motifs.pl) analysis to demonstrate the effects of frameshift and nonsense mutations on translated mutant nephrin protein sequence in comparison to wild type nephrin.**

**(i) Motifs detected in wild type nephrin protein.**

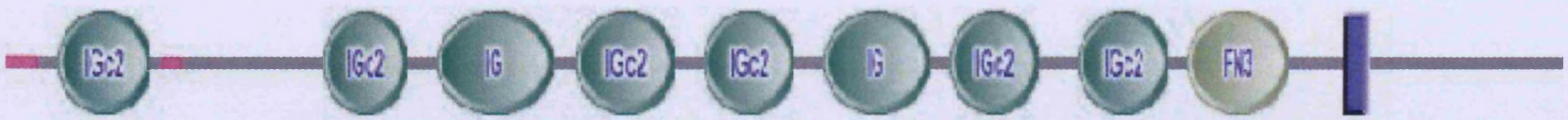


**(ii) Case 7: nt 613 (del T, P, R, ins I) to show domains within the mutant sequence truncated at 1237 residues**

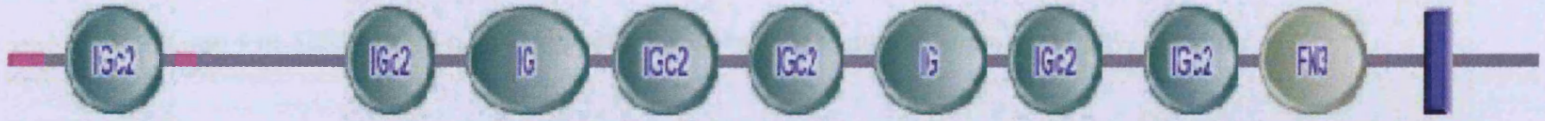


**Key:** Transmembrane segments as predicted by the *TMHMM2* program (▬), coiled coil regions determined by the *Coils2* program (▬) and Segments of low compositional complexity, determined by the *SEG* program (▬). Ig represents immunoglobulin domain, Igc2 C2 type Ig domain and FN3 a fibronectin motif.

(ii) Case 5 : frameshift nt 661(delAG) domain predition within within mutant sequence of 250 residues


(iv) Case 50: truncation nt 1291(insA) domain predition within within mutant sequence of 446 residues


(v) Case 4 nt 3250(insG) ) domain predition within within mutant sequence of 1092 residues

(vi) **Case 8 R1109X: domain predition within mutant sequence truncated at 1109 residues**


(v) **Cases carrying R1160X (nt3478 C→T): domain predition within mutant sequence truncated at 1160 residues.**

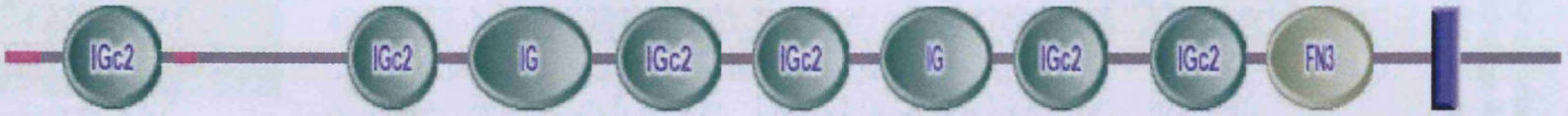

**4.6 (A) Immunoperoxidase staining of nephrin expression associated with homozygous nt 603 (del CACCCCGG ins TT) (X40). Despite end stage disease, nephrin expression is still seen in podocytes (brown pattern). An antibody raised against an unknown intracellular epitope was used.**

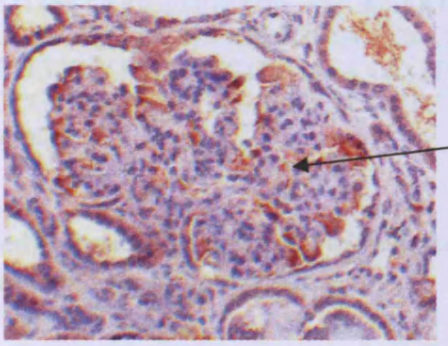


**(B) Nephrin expression associated with R1160X. This is seen in podocytes and follows the linear distribution of the GFB (immunoperoxidase; x40)**

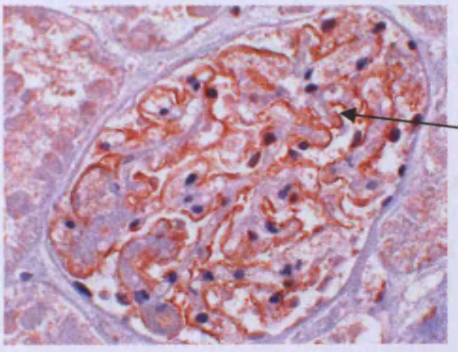


**(C) Normal linear nephrin expression, which follows the GFB (immunoperoxidase; x40)**

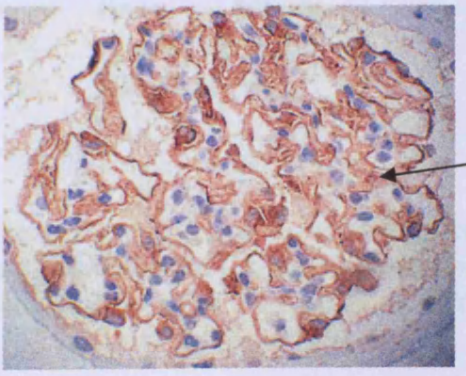

**Figure 4.7 Analysis by Neural network (http://www.fruitfly.org/ seq_tools/ splice.html) to predict effects of *NPHS1* splicing mutations.**

**A. (i) Exon 14 wild type NPHS1 (sequence 1)**

```
1    AGCCCTGGCTTGACCCCGGTTCCACAGGCTGGAGGGCGTGGCCGCCCCAC
51   CCCGGAGAGCCCCATTCAAAGGCTCCGCCGCCGCCAGGAGCGTCCTTCTG
101  CAAGTGTCATCCCGCGATCATGGCCAGCGCGTGACCTGCCGCGCCCACAG
151  CGCCGAGCTCCGCGAAACCGTGAG C TCCTTCTATCGCCTCAACGTACTGT
201  GTatgtgccccggcctgaa
```

**Donor splice site predictions for sequence 1with donor score cut-off 0.10 (exon/intron boundary shown in larger font):**

| Start | End | Score | Exon | Intron |
|---|---|---|---|---|
| 164 | 178 | 0.57 | cgaaacc **gt** | gagctc |
| 195 | 209 | 0.29 | gtactgt **gt** | atgtgc |

**(ii) Exon 14 nt1905(C→T) mutant (sequence 2) at detected in case 73**

```
1    AGCCCTGGCTTGACCCCGGTTCCACAGGCTGGAGGGCGTGGCCGCCCCAC
51   CCCGGAGAGCCCCATTCAAAGGCTCCGCCGCCGCCAGGAGCGTCCTTCTG
101  CAAGTGTCATCCCGCGATCATGGCCAGCGCGTGACCTGCCGCGCCCACAG
151  CGCCGAGCTCCGCGAAACCGTGAG T TCCTTCTATCGCCTCAACGTACTGT
201  GTatgtgccccggcctgaa
```

**Donor splice site predictions for sequence 2 with donor score cut-off 0.10 (exon/intron boundary shown in larger font):**

| Start | End | Score | Exon | Intron |
|---|---|---|---|---|
| 164 | 178 | 0.98 | cgaaacc **gt** | gagctc |
| 195 | 209 | 0.29 | gtactgt **gt** | atgtgc |

If the earlier splice donor site represents a true alternative splice site, the mutation may result in preferential splicing at this location, potentially disrupting the normal isoform ratio with less isoforms containing the extra 9 amino acids SFYRLNVLY normally present.

**B. (i) Exon 18 wild type *NPHS1* (sequence 1)**

1 ggccaattctggactcttgggcctcca **G** GGAGAAGATGAGGAGGACCAGG
51 CCTGGATGACATGGAGAAGATATCCAGGGGACCAACGGGGCGCCTGCGGAT
101 TCACCATGCCAAACTGGCCCAGGCTGGCGCTTACCAGTGCATTGTGGACAAT
151 GGGGTGGCGCCTCCAGCACGACGGCTGCTCCGTCTTGTTGTCAGAT

**Exon 18 mutant *NPHS1* (sequence 2) (Cases 25,32,47,65)**

1 ggccaattctggactcttgggcctcca **A** GGAGAAGATGAGGAGGACCAGG
51 CCTGGATGACATGGAGAAGATATCCAGGGGACCAACGGGGCGCCTGCGGAT
101 TCACCATGCCAAACTGGCCCAGGCTGGCGCTTACCAGTGCATTGTGGACAAT
151 GGGGTGGCGCCTCCAGCACGACGGCTGCTCCGTCTTGTTGTCAGAT

**(ii) Acceptor site predictions for Sequence 1:**

| Start | End | Score | Intron | Exon |
|---|---|---|---|---|
| 8 | 48 | 0.29 | tctggactcttgggcctcc **ag** | GAGAAGATGAGGAGGACCA |

**Acceptor site predictions for Sequence 2**

No site. This removes the exon 18 splice acceptor and a truncated 825 residue protein results on the assumption that read through into intron 17 occurs, with the addition of 141 bases to exon 17 and termination at a premature stop codon:

**Exon 17 → normal termination at E R [redacted]**

1 – TCCCCAAGCCTCTGCCTTCCACCAGAT GCTCCCACCATCCGTGCCCTCCAGGACCCCACT - 60
[redacted] P T I R A L Q D P T
61 - GAGGTGAACGTCGGGGGTTCTGTGGACATAGTCTGCACTGTCGATGCCAATCCCATCCTC - 120
E V N V G G S V D I V C T V D A N P I L
121 - CCGGGCATGTTCAACTGGGAGAGACTGGTGAGGATCCAGCCTTTGGTGAATAGAGGTGGG - 180
P G M F N W E R [redacted] V R I Q P L V N R G G
181 - GTCAAGGGGTTGTGGTTTCTTGACTGTGAGTTCCTTGGGAGTGGGGACCACATACATCTG - 240
V K G L W F L D C E F L G S G D H I H L
241 - TATGACCCTTATAACTATATACTCGCCAGGGCATGCTCCCAGAATGAATAACTGTTGGTG - 300
Y D P Y N Y I L A R A C S Q N E [redacted]

SMART (http://smart.embl-heidelberg.de/smart/show_motifs.pl) analysis to demonstrate the effects of aberrant exon 18 splicing. The mutant protein is truncated.

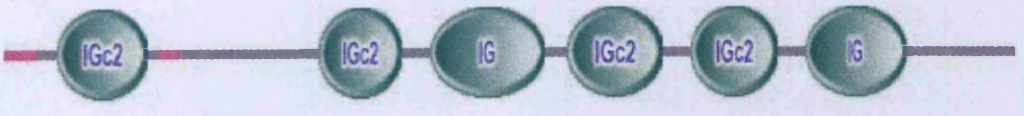

**C. (v) Exon 23 wild type *NPHS1* (sequence 1)**

1 CCACCCCCCAGGTCTCCACCAGCCTTCTGGAGAACCTGAAGACCAGCTGC
51 CCACAGAGCCACCTTCA GGC aagtcctcagtcccctgatccctc

**(vi) Exon 23 splicing mutation nt 3164(A→T) (sequence 2) (case 2)**

1 CCACCCCCCAGGTCTCCACCAGCCTTCTGGAGAACCTGAAGACCAGCTGC
51 CCACAGAGCCACCTTCT GGC aagtcctcagtcccctgatccctc

Splice site prediciton programmes were uninformative, but an assumption was made that this mutation disrupted the splice donor site, resulting in read through into intron 23, as follows:

**Exon 23 → ( normal termination at G)**

```
1 - CCACCCCCCAGGTCTCCACCAGCCTTCTGGAGAACCTGAAGACCAGCTGCCCACAGAGCC - 60
                  L  H  Q  P  S  G  E  P  E  D  Q  L  P  T  E  P
61 - ACCTTCAGGCAAGTCCTCAGTCCCCTGATCCCTCCCGGCTCCCCTGAGAATGGAACCTCC - 120
       P  S  G  K  S  S  V  P  *
```

SMART (http://smart.embl-heidelberg.de/smart/show_motifs.pl) analysis to demonstrate the effects of aberrant exon 23 splicing. The mutant protein is truncated.

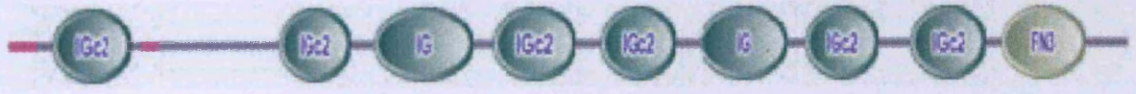

**D. (vii) Exon 27 wild type *NPHS1* sequence (sequence 1).**

```
1    TTGTTTTGCGTGTGGGGAACAGGTCAGCACAACAGAGGCAGAGCCGTATT
51   ACCGCTCCCTGAGGGACTTCAGCCCCCAGCTGCCCCCGACGCAGGAGGAA
101  AGGTGTCTTATTCCCGAG G tgaccatgcttggcctaaaggtt
```

**(viii) Exon 27 nt 3482 (g to t) splicing mutation (sequence 2) (Cases 4 and 5)**

```
1    TTGTTTTGCGTGTGGGGAACAGGTCAGCACAACAGAGGCAGAGCCGTATT
51   ACCGCTCCCTGAGGGACTTCAGCCCCCAGCTGCCCCCGACGCAGGAGGAA
101  AGGTGTCTTATTCCCGAG T tgaccatgcttggcctaaaggtt
```

**Donor site predictions for wild type *NPHS1* sequence (sequence 1):**

| Start | End | Score | Exon | Intron |
|---|---|---|---|---|
| 16 | 30 | 0.91 | ggaacag **gt** | cagcac |
| 110 | 124 | 0.46 | tcccgag **gt** | gaccat |

**Donor site predictions for mutant *NPHS1* sequence (sequence 2):**

| Start | End | Score | Exon | Intron |
|---|---|---|---|---|
| 16 | 30 | 0.91 | ggaacag **gt** | cagcac |
| 110 | 124 | 0.46 | tcccgag **tt** | gaccat |

**Mutation destroys true donor site, and a truncated 1182 residue protein results:**

Exon 27 (normally concludes at R1160) →

```
1   - TGTTTTGCGTGTGGGGAACAGGTCAGCACAACAGAGGCAGAGCCGTATTACCGCTCCCTG - 60
  -                                 V  S  T  T  E  A  E  P  Y  Y  R  S  L
61  - AGGGACTTCAGCCCCCAGCTGCCCCCGACGCAGGAGGAGGTGTCTTATTCCCGAGTTGAG - 120
  - R  D  F  S  P  Q  L  P  P  T  Q  E  E  V  S  Y  S  R  V  E
121 - TTAGGACCATGTCAGGATTCCCTCACTCAGAGGTACCCCCGACGCCTGGACTGGGTGCCT - 180
  - L  G  P  C  Q  D  S  L  T  Q  R  Y  P  R  R  L  D  W  V  P
181-TGA
    *
```

SMART (http://smart.embl-heidelberg.de/smart/show_motifs.pl) analysis to demonstrate the effects of aberrant exon 27 splicing. The mutant protein is truncated.

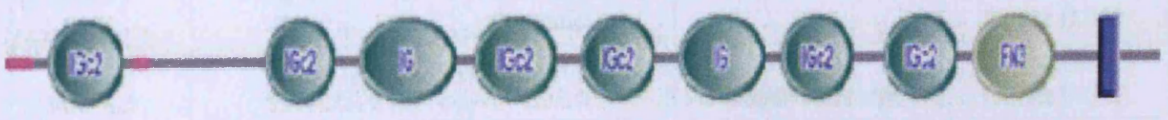

***NPHS1 Missense mutations in CNF.*** The validity of base substitutions is notoriously difficult to interpret, even in the presence of sufficient numbers of controls of the correct ethnic background. Although all missense changes detected within this series resulted in non-conservative amino acid substitutions with the potential to significantly affect protein function, mutational analysis data was supported by the use of a computer prediction by SIFT analysis (http://www.blocks.fhcrc.org/~pauline/SIFT.html) (Ng and Henikoff 2001). This tool uses sequence homology to predict whether a substitution is able to affect protein function, by sorting intolerant from tolerant substitutions based on protein homology and species conservation. Deleterious substitutions score < 0.05, and the median sequence information should be < 3.25 for reasonable accuracy, as this indicates that sequence diversity is adequate for analysis of whether a substitution is deleterious or tolerated. The median sequence information was 3.05 for nephrin indicating significance, with 6 sequences represented at this position during PSI-PHI-BLAST (http://www.ncbi.nlm.nih.gov/BLAST). The results for SIFT analysis of missense mutations detected within this study are shown below in Table 4.8.

**Table 4.8 Predicted effect of *NPHS1* missense mutations on the nephrin protein combined with SIFT analysis**

| Amino acid change | Immuno-globulin (Ig) Domain | Nature of the change | Putative impact on protein | SIFT analysis |
|---|---|---|---|---|
| P264R | Ig-3 | Aromatic to basic | - | Tolerated (score: 0.15) |
| G270C | Ig-3 | Small to SH group | ?novel disulphide bridge | Deleterious (score 0.00) |
| R367C | Ig-4 | Basic to SH group | ?novel disulphide bridge | Deleterious (score 0.05) |
| I446N | Ig-5 | Neutral to basic | - | Deleterious (score 0.00) |
| R460Q | Ig-5 | Basic to acidic | - | Tolerated (score: 0.06) |
| C623F | Ig-6 | SH group to aromatic | ? loss disulphide bridge | Deleterious (score 0.00) |
| L643P | Ig-6 | Neutral to aromatic | - | Deleterious (score 0.01) |
| R743C | Ig-7 | Basic to SH group | ?novel disulphide bridge | Deleterious (score 0.02) |
| R802W | Ig-7 | Basic to aromatic | - | Tolerated (score: 0.07) |

## 4.5 Mutations of the *NPHS1* gene are present in congenital FSGS, but not congenital DMS or early onset FSGS

All four congenital FSGS cases analysed had *NPHS1* mutations. One patient a homozygous nt2335-1 (G→A) exon 18 splicing mutation also identified in connection with CNF (cases 25, 32, 47, 65; Figure 4.4.14), two siblings had heterozygous N188I missense mutations (Figure 4.8.1), also detected in one maternal allele, but absent in 122 Asian, 100 Caucasian and 40 Maltese control chromosomes, and the remaining patient a heterozygous intronic mutation nt1930+11(c→a), predicted to result in activation of a cryptic splice site, detected in one maternal allele but absent in 222 control chromosomes (Figure 4.8.2) These changes were not detected in conjunction with other homozygous or compound heterozygous *NPHS1* mutations. *NPHS1* mutations were not detected in two cases of autosomal recessive congenital DMS or in five cases of early onset FSGS. The results are summarised in as shown in Table 4.10.

## 4.6 Mutations of the *NPHS2* gene are present in cases of CNF lacking *NPHS1* mutations, but not congenital DMS

*NPHS1* mutations were not detected in eight CNF cases (five severe and three atypically mild). However, homozygous *NPHS2* mutations were detected in two of the cases with severe CNF lacking *NPHS1* mutations (Table 4.9 and 4.10). One mutation was a novel homozygous frameshift nt (465/6) ins T in exon 4 (Figure 4.8.5), and the other R138Q, a homozygous missense mutation in exon 3 (Figure 4.8.3, Table 4.9). *NPHS2* mutations were absent in CNF cases with homozygous R1160X mutations, virtually excluding concurrent mutations in *NPHS2* as a cause for the discordant phenotype observed. *NPHS2* mutations were not detected in congenital DMS. Both mutations lay within the PHB domain, which lies within the stomatin signature and is thought to play a crucial role in protein function. Computer predication for the frameshift mutations by SMART analysis (http://smart.embl-heidelberg.de/smart/show_motifs.pl) suggested that this resulted in a truncated protein of 185 amino acid residues (Figure 4.9 iii), and SIFT analysis (http://www.blocks.fhcrc.org/~pauline/SIFT.html) predicted the R138Q substitution to be deleterious with a score of 0.00, (median sequence score 3.21).

## 4.7 Mutations of the *NPHS2* gene are present in congenital FSGS

*NPHS2* mutations were detected in all four cases of congenital FSGS (Table 4.8). One was a novel homozygous nt436delA frameshift in exon 3 (Figure 4.8.4) affecting two siblings, one a heterozygous R229Q missense mutation in exon 5 (Figure 4.8.6) not present in 120 control chromosomes and previously detected as a homozygous event in association with adult onset FSGS (Tsukaguchi *et al*, 2000), and one the homozygous R138Q missense mutation in exon 3, previously described in connection with SRN1 (Figure 4.8.3). All mutations were located within the PHB domain. SMART analysis of the frameshift mutation indicated that this was likely to result in a truncated protein of 179 residues (Figure 4.9 ii). SIFT analysis gave the R229Q mutation a marginal score of 0.06.

To clarify the extent of the *NPHS1/NPHS2* mutation phenotype overlap, cases with pre-determined homozygous and compound heterozygous *NPHS1* mutations and CNF (Table 4.4) were also screened for *NPHS2* mutations. Only two heterozygous R229Q *NPHS2* missense mutations were detected, in cases 25 and 32. Both had heterozygous nt2335-1 (G→A) exon 18 splicing mutations in conjunction with an exon 14 C623F missense mutation (case 25), and a promoter mutation (case 32) in the remaining allele. Of note, *NPHS2* mutations were not identified in case 65, who had the same homozygous nt2335-1 (G→A) exon 18 splicing mutation detected in congenital FSGS (case 49). This may represent a further overlap in the *NPHS1/NPHS2* mutation spectrum. Alternatively, cases 25 and 32 were born at 35 weeks gestation and had renal biopsies in the immediate post-natal period rather than at three months. Features were relatively non-specific, and it may have been too early for FSGS to be apparent.

**Table 4.9 Predicted effects of *NPHS2* missense mutations on podocin combined with SIFT analysis**

| Amino acid change | Location | Nature of the change | Putative impact on protein | SIFT analysis |
|---|---|---|---|---|
| R138Q | PHB domain | Basic to acidic | - | Deleterious (score 0.00) |
| R229Q | PHB domain | Basic to acidic | - | Tolerated (score 0.06) |

**Table 4.10** ***NPHS1*** **and** ***NPHS2*** **mutation phenotype in CNF lacking** ***NPHS1*** **mutations and congenital FSGS (n=6)**

| Case details | | | *NPHS1* mutation | | | | *NPHS2* mutation | | | |
|---|---|---|---|---|---|---|---|---|---|---|
| **Patient** | **Origin** | **Family history?** | **Exon** | **Nucleotide (nt) change** | **Effect on protein** | **Mutation Status** | **Exon** | **Nucleotide (nt) change** | **Effect on protein** | **Mutation Status** |
| ***(A) CNF (n=2)*** | | | | | | | | | | |
| 54 | UK | no | - | - | - | - | 3 | nt 413 (G→A) | R138Q | hom |
| 15 | Turkey | no | - | - | - | - | 4 | nt (465/5) insT | frameshift/ truncation | hom |
| ***(B) Congenital FSGS (n=4)*** | | | | | | | | | | |
| 39 | UK | no | 18 | nt 2335-1 (G→A) | Abnormal splicing | hom | 5 | nt 623 (G→A) | R229Q | het |
| 23,24 | India | Yes; siblings | 5 | nt 563 (A→T) | N188I* | het | 3 | nt (436) del A* | Frameshift/ trunction | hom |
| 49 | UK | no | 14 | Nt 1929+13 (gccccgg→ gcccagg | Cryptic splice site activation? * | het | 3 | nt 413 (G→A) | R138Q | hom |

**KEY: hom = homozygous mutation; het = heterozygous mutation; * = novel mutation**

**Figure 4.8 Representative sequencing traces for *NPHS1* and *NPHS2* mutations associated with congenital FSGS, and *NPHS2* mutations detected in CNF cases lacking *NPHS1* mutations**

**Figure 4.8.1 A) *NPHS1* exon 5 nt563 (A→T) N188I heterozygous splicing mutation 5' to 3'**

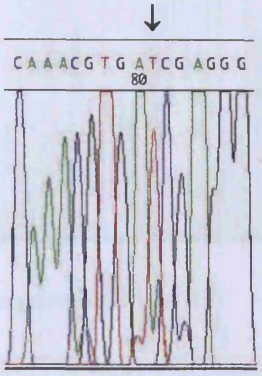


**B) Normal control 5' to 3'**

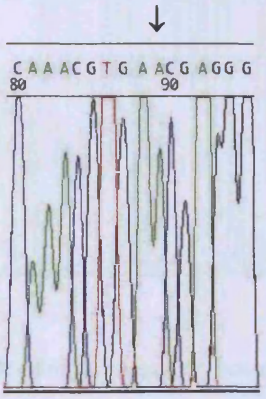


**Figure 4.8.2 A) *NPHS1* intron 14 nt 1929 +13 (G→A) cryptic splicing mutation 5' to 3'**

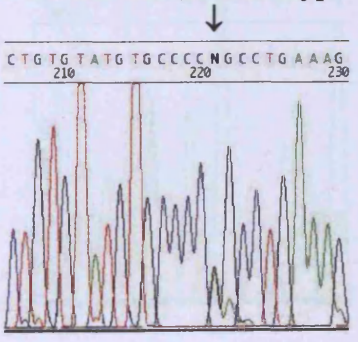


**B) Normal control sequence 5' to 3'**

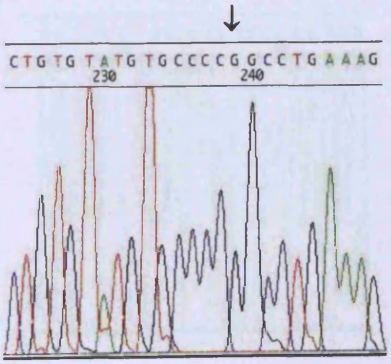

**Figure 4.8.3 A) *NPHS2* exon 3 nt 413 R138Q homozygous mutation 5' to 3'**

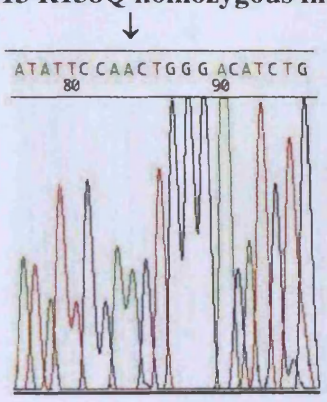


**B) Normal control sequence 5' to 3'**

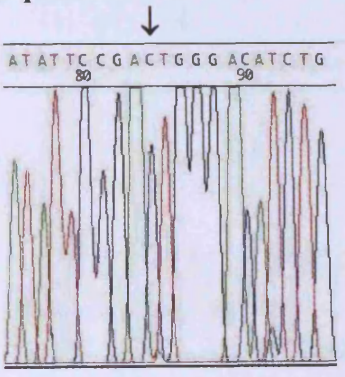


**Figure 4.8.4 A) *NPHS2* exon 3 nt436(del A) homozygous frameshift mutation 5' to 3'**

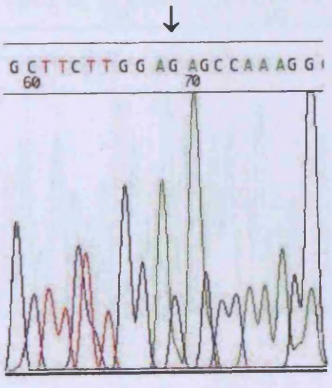


**B) Normal control sequence 5' to 3'**

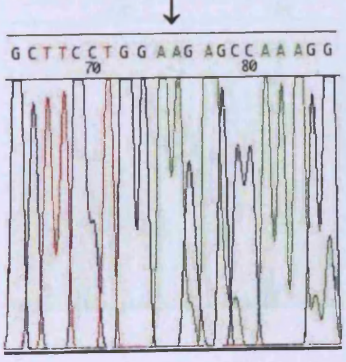

**Figure 4.8.5 A) *NPHS2* exon 4 nt465/6 (ins T) homozygous frameshift mutation 5' to 3'**

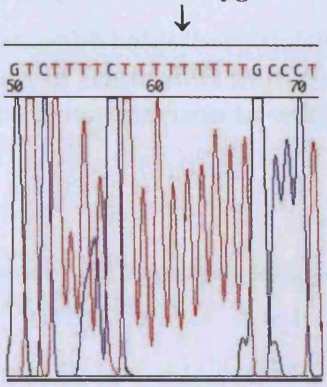


**B) Normal control sequence 5' to 3'**

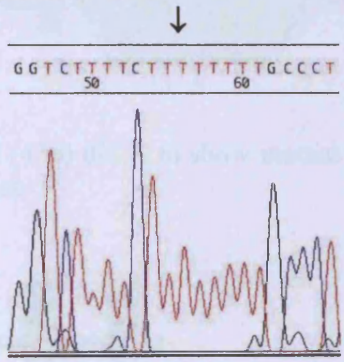


**Figure 4.8.6 A) *NPHS2* exon 5 nt623(G→A) R229Q heterozygous mutation 5' to 3'**

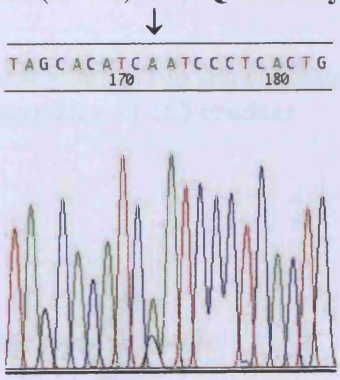


**B) Normal control 5' to 3'**

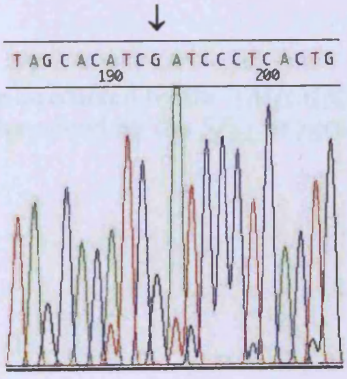

**Figure 4.9 SMART (http://smart.embl-heidelberg.de/smart/show_motifs.pl) analysis to demonstrate the effects of frameshift mutations in *NPHS2* on translated mutant podocin protein sequence in comparison to wild type podocin**

(i) Wild type podocin (383 amino acids) to show location of PHB domain (amino acids 123-282)

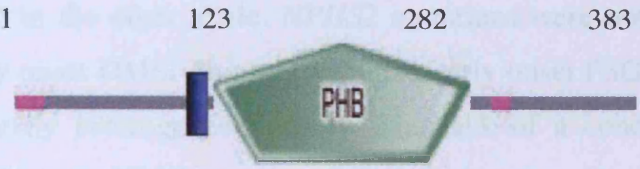


(ii) Frameshift nt (436) del A to show mutant protein with a query sequence of 179 residues

(iii) Frameshift nt(465/6) ins T to show mutant protein with a query sequence of 185 residues

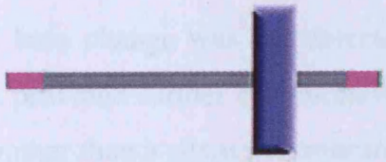

**Key: Transmembrane segments as predicted by the *TMHMM2* program (▬), segments of low compositional complexity, determined by the *SEG* program ( ). PHB represents PHB domain.**

## 4.8 Early onset FSGS is genetically heterogeneous and mutations of the *NPHS2* gene are not present in early onset DMS

Five cases of early onset FSGS were analysed for *NPHS2* mutations. Despite the phenotypic similarity to SRN1, only one mutation was detected, a heterozygous R138Q missense mutation in a patient with autosomal recessive FSGS compatible with SRN1, documented previously (Boute *et al*, 2000), and used as a positive control. Again, no mutation was detected in the other allele. *NPHS2* mutations were not detected in two cases of sporadic early onset DMS. This suggests that early onset FSGS/SRN1 is likely to represent a genetically heterogeneous entity. The lack of a concomitant *NPHS1/ NPHS2* overlap in early onset FSGS suggested hat this phenomenon may be specific to congenital FSGS.

## 4.9 The promoter mutation results in diminished DNA – protein binding on electromobility shift assay

Electromobility shift assay (EMSA) was used to validate the putative G → C promoter mutation detected –340 base pairs of the ATG initiation codon. This change was only detected in two patients, 32 and 73, and was present in combination with exon 18 and exon 14 splicing mutations respectively in the other allele (Table 4.4). The only other change detected in cases 32 and 73 was E117K, a known common polymorphism in exon 3. The G → C base change was not detected in 100 ethnically matched control chromosomes, which provided further corroborative evidence that this may constitute a pathological change rather than a silent polymorphism. No other sequence variants were detected within 1 kb of the putative promoter upstream of the initial ATG.

Although the base change was located two base pairs 3' from a putative NF-1 binding site (see below), it did not itself lie directly within an obvious transcription factor consensus binding sequence. EMSA experiments were performed to determine the effect of the mutation on the ability of this area of the promoter to bind whole mouse kidney nuclear extract. Wild type and mutant thirty base pair oligonucleotides (-362 to –332 from the intial ATG start codon) were generated as described in Chapter 2, section

2.3.14.4. These encompassed the putative mutation and an additional 15 base pairs of promoter sequence both upstream and downstream of this base change. Preliminary results indicated greatly diminished protein-DNA complex formation with the mutant oligonucleotide relative to the wild type, as well as successful competition of the binding by the wild-type but not mutant DNA (Figure 4.11), or an unrelated probe "INS", from the HBLXA-9 promoter, suggesting that the base change resulted in diminished binding of an unknown nuclear protein. This was not due to secondary structure formation, and was reproducible under a variety of experimental conditions (data not shown). These results could be reproduced by whole mouse liver nuclear extract, suggesting that the DNA binding protein was not kidney specific (Figure 4.12). In view of the proximity of the mutation to the NF1 consensus sequence site, further competition experiments were carried out to determine whether the mutation resulted in disruption of NF1 binding. However, it was not possible to compete out protein-DNA binding to the NF1 consensus binding sequence by the wild type *NPHS1* promoter oligonucleotide, or vice versa under a variety of experimental conditions (representative gel shown in Figure 4.13), which virtually excluded NF1 as a candidate transcription factor. These observations provided preliminary data for further investigation of the transcriptional regulation of the *NPHS1* promoter. The following *NPHS1* promoter sequence depits the site of the G to C base change with respect to the intial ATG, as well as the location of the putative NF1 site:

AGAGAGAGAGACAGAGAGAGAGGAAGAGACAGAGACAAAAGGAGAGAGAACGGCTTAGA
CAAGGAGAGAAAGATGGAAAGATAAAGAGACTGGGCGCAGTGGCTCACGCCTGTA

**E BOX** **NF1 site** **C (-340 from ATG; -184 from AG)** ↑

ATCCCAACACTTGGGGAGGCCAAGGTGGGAGGATGGCTTGAAGGAAAGAGTCTG
AGATCAACCTGGCCAACATAGTGAGACCCCGTCTCTAAAAAAAAAAAAAAAGAAAAAAAAA
AGAAAAAAGAAAAAAAAGTTTTTTTAAAGAGACAGAGAAAGAGACTCAGAGATTGAGACT
GAGAGCAAGACAGAGAGAGATACTCACAGGGAAGAGGGGAAGAGGAAAACGAGAAAGGG
AGGAGAGTAACGGAAAGAGATAAAAAAGAAAAGCAGGTGGCAGAGACACACAGAGAGGG
ACCCAGAGAAAGCCAGACAGACGCAGGTGGCTGGCAGCGGGCGCTGTGGGGGTCACAGTAG
GGGGACCTGTGATGGCCCTGGGGACGACGCTCAGGGCTTCTCTCCTGCTCCTGGGGCTGCTG
ACTGAA

Interestingly, an E box binding Helix-loop-helix transcription factors is also located within the near vicinity, although the significance is unknown.

**Figure 4.10 Diminished binding of whole kidney nuclear extract to *NPHS1* mutant promoter sequence in comparison to wild type**

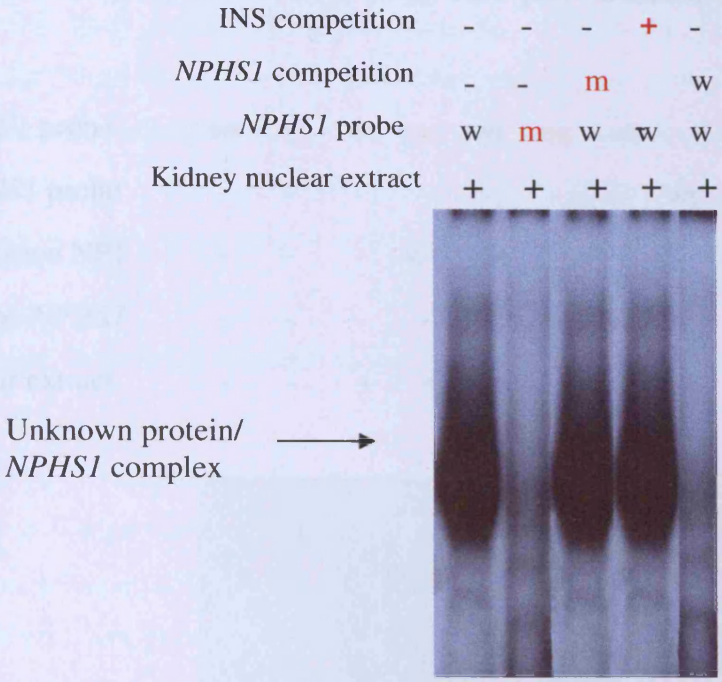


**Figure 4.11 Diminished binding of whole liver nuclear extract to *NPHS1* mutant promoter sequence in comparison to wild type**

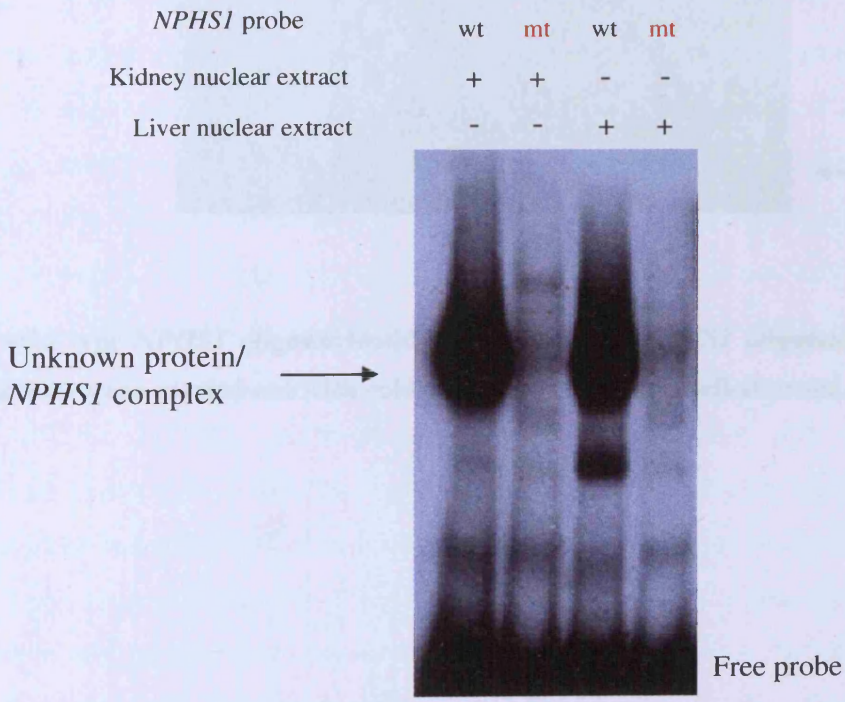


**Key: wt = wild type *NPHS1* oligonucleotide; mt = mutant *NPHS1* oligonucleotide; INS = unrelated probe using sequence from HBLXA-9 promoter**

**Figure 4.12 NF1 transcription factor binding to the *NPHS1* promoter is unlikely to be affected by the –340 (G → C) base pair substitution.**

| | | | | | | | | | |
|---|---|---|---|---|---|---|---|---|---|
| NF1 probe | wt | mt | wt | mt | wt | mt | wt | - | - |
| *NPHS1* probe | - | - | - | - | - | - | - | wt | wt |
| Competition NF1 | - | - | - | wt | wt | - | - | - | wt |
| Competition *NPHS1* | - | - | - | - | - | - | wt | - | - |
| Kidney nuclear extract | - | - | + | + | + | + | + | + | + |

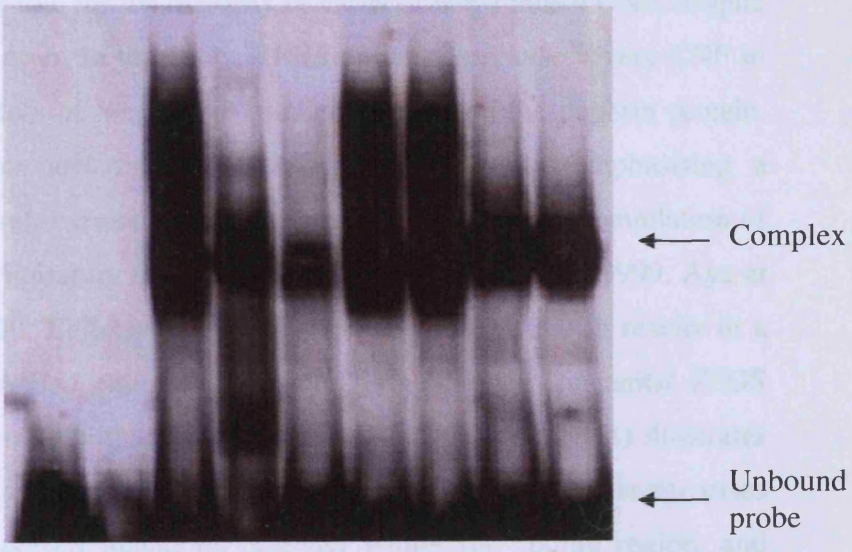


**Key:** **wt = wild type *NPHS1* oligonucleotide; mt = mutant *NPHS1* oligonucleotide. Competition reactions were carried out with cold probe versus radiolabelled probe.**

## 4.9 Discussion

The results of this study confirm the pivotal roles the *NPHS1* and *NPHS2* genes play in renal glomerular filtration and more importantly, provide the first direct evidence of a potential functional relationship between them within the podocyte. A number of key conclusions about the roles of these genes within glomerular filtration and the pathogenesis of nephrotic syndrome in early life are made, as discussed below.

### *4.9.1 Glomerular filtration is critically dependant on normal function of the NPHS1 gene*

*NPHS1* mutations are responsible for the majority of cases of non-Finnish CNF, despite the variability in phenotype seen. In the main, *NPHS1* mutations cause severe CNF in non-Finnish patients, regardless of location or predicted effect on the nephrin protein. Moreover, *NPHS1* mutations are distributed throughout the gene, emphasising a functional requirement for both extracellular and intracellular domains. Compilation of our results with those in the literature (Kestila *et al*, 1998; Lenkkeri *et al*, 1999, Aya *et al*, 2000, Patraaka *et al*, 2000, Beltcheva *et al* 2001, Koziell *et al*, 2002), results in a total of fifty-nine unique *NPHS1* mutations detected in CNF and congenital FSGS patients to date, of which two lie within the promoter region. Figure 4.13(A) illustrates the distribution of mutations detected within this study, and Figure 4.13(B) summarises the distribution of the fifty-seven mutations detected within the coding region, and within donor and acceptor consensus splicing sequences, lying just immediately outside the coding regions. These appear to cluster in immunoglobulin domains two, four and seven, which gives a focus as to where to commence diagnostic tests. To date, approximately 40% of *NPHS1* mutations are nonsense, frameshift and splicing mutations predicted to result in a non-functional truncated nephrin protein, likely to be unstable and therefore not expressed at the cell membrane. Lack of glomerular nephrin expression has been demonstrated for both Fin major (nt 121 del2) and Fin minor (R1109X), which would support this hypothesis (Patraaka *et al*, 2000). A further 5% of mutations are non-frameshift deletions and insertions, resulting in the deletion or insertion of amino acids, but predicted to result in a protein not dissimilar to wild type nephrin. The remainder are missense mutations, which account for just over half of all

**Figure 4.13 (A) Distribution of the unique *NPHS1* mutations within the coding sequence detected in CNF within this series (n=19;Table 4.4) showing locations and gene "hot spots"**

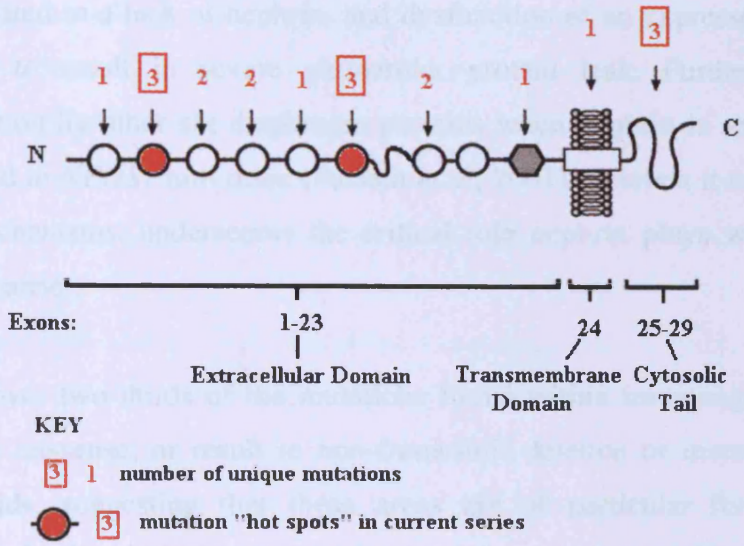


**Figure 4.13 (B) Distribution of all unique *NPHS1* mutations detected within the coding sequence (n=57) to date showing mutation "hot-spots" and location of the mutations detected in congenital FSGS within this study**

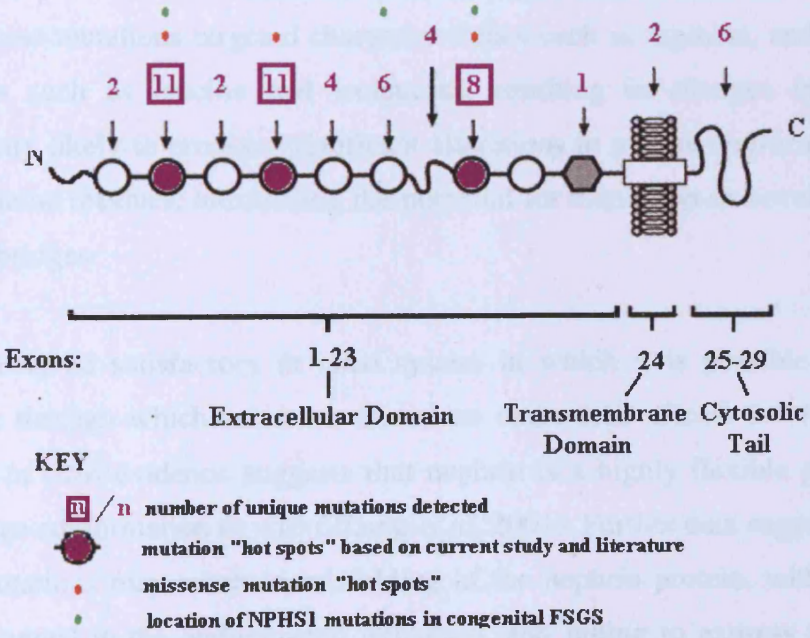

mutations detected and so far, are all located within the extracellular region. Of note, with the exception of one cytosolic nonsense mutation, all *NPHS1* mutations caused a severe CNF phenotype in non-Finnish patients, regardless of location or predicted effect on the nephrin protein. These findings suggest that disease pathogenesis cannot be simply related to a lack of nephrin, and dysfunction of an expressed nephrin protein is also able to result in severe glomerular protein leak. Furthermore, the lack of compensation by other slit diaphragm proteins when nephrin is absent, both in human disease and in *NPHS1* null mice (Putaala *et al*, 2001), or when it malfunctions by more subtle mechanisms, underscores the critical role nephrin plays within the glomerular filtration barrier.

Of note, over two thirds of the mutations found within immunoglobulin domain "hot spots" are missense, or result in non-frameshift deletion or insertion of one or more amino acids, suggesting that these areas are of particular functional importance, potentially for ligand binding or for maintaining the proposed homophilic interaction within nephrin molecules expressed by adjacent podocytes. The missense mutations detected during this study all resulted in non-conservative amino acid substitutions, which were not detected in normal controls. In addition, 81% were also predicted to be deleterious by SIFT analysis (http://www.blocks.fhcrc.org/~pauline/SIFT.html). Many of the missense mutations targeted charged residues such as arginine, and hydrophobic amino acids such as leucine and isoleucine, resulting in changes in charge and hydrophobicity likely to produce significant alterations in protein conformation. Others targeted cysteine residues, introducing the potential for disruption or novel formation of di-sulphide bridges.

As yet there is no satisfactory *in vitro* system in which it is possible to study the mechanisms through which missense mutations exert their effects *in vivo*. However, preliminary *in vitro* evidence suggests that nephrin is a highly flexible protein, easily able to change conformation *in vivo* (Zhang *et al*, 2001). Further data suggests that some missense mutations may result in misfolding of the nephrin protein, with the mutants becoming trapped in the endoplasmic reticulum, and failing to express at the plasma membrane (Liu *et al*, 2001). However, these trafficking experiments are only a guide, as COS-7 cells, which are non-polarised fibroblasts were used for experiments. This is an

entirely different situation to that seen in podocytes, which are polarised epithelial cells. On this basis, the effect of some missense mutations may be similar to that seen with Fin major and Fin minor mutations, and other nonsense and frameshift mutations predicted to create defective, unstable nonsense proteins failing to express. Equally, some mutations do not affect glomerular nephrin expression, so an unexplored area remains location of ligand binding to the extracellular domains, which again might become disrupted by the introduction of a point mutation, or an amino acid change. In addition, these observations provide evidence for a more diverse role for nephrin within the podocyte than simply a structural component of the slit diaphragm, as might be suggested from initial studies of the Finnish CNF population. The cytosolic tail is rich in serine, threonine and tyrosine residues suggesting that nephrin is likely to become phosphorylated and thus participate in signal transduction from the extracellular to the intra cellular compartments. This is supported by preliminary in vitro observations that nephrin is able to activate the MAPK pathway (Huber *et al*, 2001) and that it may form a complex with other key podocyte proteins, for example CD2AP and podocin within lipid rafts ((Schwartz *et al*, 2001, Simmons *et al*, 2001), structures known to play a major role in cellular signalling. An additional disease mechanism for the glomerular protein leak in association with *NPHS1* mutations may therefore be a failure of transduction of key extracellular signals to the podocyte intracellular machinery, resulting in dysfunction of the actin cytoskeleton, foot process effacement and proteinuria.

### *4.9.2 The clinical and genetic heterogeneity of the CNF phenotype*

Mutational analysis of non-Finnish cases of CNF detected a variety of different *NPHS1* mutations located throughout both the extracellular and intracellular regions of the gene. Furthermore, mutations were not detected in all cases, even those with a typical clinical CNF phenotype. This is a different situation to that found in the Finnish population, where mutations have been detected in >98% of cases, the majority being Fin Major. Fin major and Fin minor mutations are very rare in non-Scandinavian populations, suggesting that the wide variety of different mutations detected in non-Finns are likely to be *de novo* events, especially when the ethnic diversity of the test populations is taken into account. Some populations may exhibit a founder effect, such as that detected

within our series in Malta for R1160X, which facilitates the planning of diagnostic tests. Intriguingly, one Turkish CNF patient originating from Anatolia had a homozygous Fin minor mutation (R1109X), hitherto only detected in a small subset of Finnish patients. The apparent ethnic diversity of these populations implied an independent event rather migratory influence, as Fin minor has been not detected in other Turkish patients. However examination of the genetic ancestry of the Finns, and Turks from Anatolia, reveals a significant contribution of Central Asian genes to both groups (Di Benedetto *et al*, 2001), and population admixture between Hungarians, Slavs, Finns, Turks and Iranians (Guglielmino *et al*, 2000) advocating the possibility of a common ancestor.

The majority of *NPHS1* mutations were associated with typically severe CNF disease regardless of mutation type and gene location. However, a specific nonsense mutation located in exon 27, R1160X, resulted in an unexpectedly mild phenotype in approximately 50% of cases, formally expanding the CNF clinical spectrum to include mild disease. There are numerous anecdotal reports in the literature of mild congenital nephrotic syndrome phenotypes, occasionally thought to be the result of a response to anti-proteinuric drugs (Patrakka *et al*, 2000; Guez *et al*, 1998). Interestingly, recent data suggests a link between anti-proteinuric drugs and rescue of the down-regulated *NPHS1* mRNA and diminished glomerular nephrin expression seen as a result of progressive renal injury in rats with Passive Heyman Nephritis through angiotensin II blockade (Benigni *et al*, 2001). However, the use of anti-proteinuric agents is commonplace in the management of congenital nephrotic syndrome in humans (Heaton *et al*, 1999), often slowing the rate of clinical deterioration, but rarely correlating with a favourable long-term outcome. These cannot provide an explanation, as two of the mildly affected CNF cases described in this series did not receive anti-proteinuric drugs during the course of their illness.

The reason for the discordant phenotype remains elusive, and does not appear to be population specific as cases originated from Malta, Bangladesh and Gujerat, India. However, there appears to be a significant gender contribution to disease expression, since the majority of severely affected individuals are male and those mildly affected, female (Table 4.5). This is true both inter- and intra-family; for example patients 86 (male, severely affected) and 92 (female, mildly affected) were siblings, and patient 26

who has mild disease whereas her five brothers died in infancy from severe CNF. In addition, this mutation was originally reported in a female with mild disease (Lenkkeri *et al*, 1999; Guez *et al*, 1998). The apparent influence on phenotype by gender in non X-linked conditions is rare, but has been described with a classic example being autosomal recessive limb-girdle muscular dystrophy (Zatz *et al*, 2000), where strategies such as mutation screening of related genes, investigation of modifier loci in murine models and detection of protein partners have been used to identify modifiers, as yet with no success. A role for oestrogen in the modulation of cellular activity and thus phenotype has also been documented, but remains poorly characterised. There is however, increasing evidence that complex regulatory mechanisms exist by which oestrogen may alter cell function, and that this hormone has important physiological roles beyond those related to gonadal function. Obviously the gender impact can be positive or negative, and may reflect the effects of several gonadal steroids on the varied pathways for inflammation, cell migration or proliferation that mediate different disease models. The potential effect of oestrogens in renal disease has been explored through *in vitro* studies in glomerular mesangial cells. Initial studies showed that oestrogen increases AP-1 transcription factor activity that in turn inhibits type I collagen gene activation (Silbiger *et al*, 1999). Subsequent studies showed that selective inhibition of oestrogen receptor-beta suppresses type I and type IV collagen synthesis, suggesting that this can also mediate the effects of oestrogen on collagen synthesis (Neugarten *et al*, 2000). On this basis, it has been suggested that because accumulation of glomerular extracellular matrix after renal injury is a precursor to the development of glomerular sclerosis and progressive loss of renal function, the ability of estrogens to potentially inhibit fibrogenic cytokine-stimulated collagen IV synthesis may contribute to the anecdotal protective effect of female gender on the progression of renal disease. However, the mechanism of action of oestrogens within the glomerulus is likely to be complex. There is also preliminary data that oestradiol may attenuate glomerulosclerosis by inducing nitric oxide synthesis via an oestrogen receptor-dependent mechanism, and also through its metabolites, 2-hydroxyestradiol and 2-methoxyestradiol, which inhibit glomerular mesangial cell proliferation independent of oestrogen receptors (Xiao *et al*, 2001). It is tempting to speculate that the apparent effect of gender on the progression of nephrotic disease in CNF may be related to an effect of oestrogens on podocyte function. This might occur through a direct effect on oestrogen response elements within the *NPHS1*

promoter, or through receptors on the cell surface. Equally, an indirect effect may be mediated through other transcription factors. Alternatively, differential effects on phenotype may be modulated by separate effects on mesangial or endothelial cells, known to cooperate with podocytes in glomerular filtration barrier function.

At a molecular level, the R1160X mutation results in truncation of the nephrin protein downstream of the last amino acid residue in exon 27. In contrast to Fin minor (exon 26) (Patraaka *et al*, 2000), glomerular nephrin expression appears normal in all patients, regardless of severity in clinical phenotype (Figure 4.6). This suggests that the nephrin protein reaches the cell membrane and remains normally distributed within the cell. These two mutations are only 51 amino acids apart, which perhaps makes the lack of nephrin expression in association with R1109X surprising. Potential explanations are that motifs critical for membrane targeting are preserved in R1160X, but are absent in the R1109X truncation, or that a binding site for a protein required for nephrin trafficking is present in the intervening 51 amino acids. Alternatively, a critical amount of the cytosolic tail may be required for protein stability. The presence of the R1160X mutant protein at the membrane provides further evidence that nephrin dysfunction may occur through the lack of binding of intracellular protein partners, such as adapter molecules, which normally link it to the actin cytoskeleton, or other molecular pathways critical for podocyte function. Evidence presented to date suggests that both podocin (Huber *et al*, 2001) and CD2AP (Shih *et al*, 2001) bind to this region. Of note, other exon 27 mutations, even when situated in the immediate vicinity of R1160X, result in a severe CNF phenotype, but all three cases in which this mutation has been described so far, are male.

Although the variable phenotype associated with the R1160X mutation appeared to be influenced by gender, another possibility remains that this was the result of co-inheritance of a particular allele of an unrelated gene. In view of the key role *NPHS2* also plays in glomerular filtration, a hypothesis that concurrent *NPHS2* mutations were responsible for the variable phenotype seen in association with R1160X was tested. In addition, CNF cases lacking *NPHS1* mutations were also screened for *NPHS2* mutations to determine whether there was a phenotypic overlap. The absence of *NPHS2* mutations in the R1160X group excluded the *NPHS2* gene as a modulator of CNF phenotype, at

least in these individuals. However, two of the five typically severe CNF patients lacking *NPHS1* mutations had homozygous *NPHS2* mutations (Table 4.10). One was a novel frameshift mutation in exon 4, and the other was a missense mutation R138Q, previously been detected in association with SRN1 (Boute *et al*, 2000) and located in a mutation "hot spot" within the predicted location of the PHB domain of the *NPHS2* gene. These findings support the genetic heterogeneity of CNF, which is further endorsed by the lack of mutations in the remaining three patients with typically severe disease. There remains the possibility that mutations were not detected as they lie in intronic regions not screened, or in regulatory regions upstream of the nephrin promoter. Equally, causative mutations may be present in other glomerular genes with clearly demonstrable links to nephrotic disease such as *NEPH1*, which encodes a novel slit diaphragm protein homologous to nephrin (Donoviel *et al*, 2001).

The ability of *NPHS1* and *NPHS2* mutations to result in the same clinical phenotype provided the first evidence of a link between the two genes. However, the argument remains that CNF and SRN1 may represent the same disease, or that the two CNF cases were simply misdiagnosed. The differences between the two disorders are subtle; both exhibit autosomal recessive inheritance, although CNF presents by definition as a congenital nephrotic syndrome, whereas SRN1 presents after three months of age. The histological features in CNF may be non-specific, and focal sclerotic changes can appear, but are a late feature and tend to affect glomeruli in a global rather than a segmental distribution. Global sclerosis is considered to be a non-specific sign of glomerular injury, rather than an indicator of the underlying disease pathogenesis. In SRN1, focal segmental changes are detected early on and the only other histology that has been documented is minimal change, which subsequently develops into the classical appearance of FSGS. The clinical presentation and renal histology of the cases with *NPHS2* mutations was typical of CNF, and it is therefore perhaps more likely that SRN1 and CNF form an overlapping spectrum of disorders. The important conclusion that can be made by the detection of *NPHS2* mutations in CNF is that this condition is genetically heterogeneous, so both *NPHS1* and *NPHS2* genes require screening for diagnostic purposes, and that molecular diagnosis is able to provide a more accurate indication of phenotype than one based on clinical criteria.

### *4.9.3 NPHS1 and NPHS2 mutations are not responsible for congenital or early onset DMS, or all cases of SRN1-like disease*

*NPHS1* and *NPHS2* mutations were not detected in any of the cases of DMS or early onset FSGS compatible with SRN1-like nephrosis analysed, except for one FSGS case known to carry a heterozygous R138Q *NPHS2* mutation. This was perhaps surprising, as *NPHS2* mutations have been reported in apparently sporadic FSGS (Frishberg *et al*, 2002). However, closer examination of the cases screened revealed the same R138X nonsense mutation in the majority of affected individuals, suggestive of a founder effect and autosomal recessive inheritance. This underlines the profound genetic heterogeneity of FSGS, and it is likely that many causative genes will be detected, potentially all able to lead to podocyte damage and the histological appearance of FSGS. Although the number of cases studied was small, the lack *NPHS1* and *NPHS2* gene mutations in DMS make them unlikely candidates for this disease. However, this result needs to be interpreted with caution as in common with FSGS, DMS is a genetically heterogeneous disease.

### *4.9.4 Di-genic inheritance results in congenital FSGS*

Mutational analysis of patients with congenital FSGS was also performed. This is a rare entity, which is traditionally made distinct from CNF on histopathological grounds, and follows a similar albeit more severe clinical course. We detected the co-existence of *NPHS1* and *NPHS2* mutations in all congenital FSGS patients tested (Table 4.10), providing further corroborative evidence for a functional relationship between these two genes. Mutation hits were required in three out four alleles to produce the congenital FSGS phenotype, as parents who were compound heterozygotes for the respective *NPHS1* and *NPHS2* mutations were phenotypically normal. One *NPHS1* mutation was a homozygous exon 18 nt2335-1 (G→A) *NPHS1* splice acceptor mutation previously detected in CNF, and the remaining two *NPHS1* mutations were a novel missense mutation N188I, and a C→ A mutation predicted to introduce a cryptic splice site 11 base pairs downstream of the exon 14 splice donor site, an area already predicted to participate in alternative splicing (http://genome.cbs.dtu.dk/services/NetGene2/). Neither change was detected in control chromosomes or in conjunction with other

*NPHS1* mutations. Although detailed functional studies have not been performed, the N188I mutation could potentially disrupt an N-glycosylation site, a mechanism that has been shown, at least in transfected cells, to play a crucial role in the correct localisation of nephrin to the plasma membrane (Yan *et al*, 2001), whereas the effects of cryptic splice site activation are well described (Krawczak *et al*, 1998; Ars *et al*, 2000; Bruce *et al*, 2001; Pagani *et al*, 2002; reviewed in O'Neill *et al*, 1998,). The C→ A mutation located within intron 14 appears to introduce a splice acceptor site. The predicted result would be inclusion of intronic sequence, possibly with the introduction of a novel exon through the activation of potential cryptic donor splice site sequences within intron 14. However, confirmatory experiments using RT-PCR or hybrid minigene constructs were not possible within the time frame of this project. Cryptic splice site activation has been also described in another immunoglobulin superfamily member, the mouse polymeric immunoglobulin receptor (Bruce *et al*, 1999). Here, the activated cryptic splice sites were located in the junction between two Ig domain boundaries. Exon 14 is predicted to encode the beginning of a putative spacer molecule, lying between the Ig 6 and Ig 7 domains of extracellular nephrin, and could also encompass a protein domain boundary.

The *NPHS1* mutations in congenital FSGS were associated with a heterozygous R229Q *NPHS2* missense mutation, previously detected as a homozygous change in adult onset FSGS (Tsukaguchi *et al*, 2000), a novel homozygous frameshift in *NPHS2* exon 3 and a homozygous R138Q *NPHS2* mutation, previously detected in association with both CNF and SRN1 (Table 4.11). The changes were absent in normal controls, and located within the PBH/SPFH domain, an area likely to be crucial for correct podocin function. Evidence from *C.elegans* suggests that one of the roles of the SPFH domain confers an ability to homo-oligomerise and form core components of membrane associated proteolytic complexes (Tavernakis *et al*, 1999), clearly potentially important functions of podocin. An unanswered question remains the significance of the R229Q mutation, as this has now been detected as a heterozygous change within some series at a frequency of between 1 and 3 % of normal control chromosomes (Antignac, personal communication; Karle *et al*, 2002). In this study, the change was detected at a lesser frequency of 1 in 222 normal chromosomes, or an incidence of approximately in 0.5%. Of note, R229Q has not been detected as a homozygous event in controls to date, and if all published and unpublished data available data is complied, this encompasses a total

of approximately 600 normal chromosomes. As seen in section 4.6, this mutation is tolerated, but only receives a marginal score of 0.06 on SIFT analysis (deleterious scores are <0.05). In addition, it has been detected in SRN1 in conjunction with a heterozygous mutation in the other *NPHS2* allele, with no other apparent *NPHS2* mutation within the same individual (Karle *et al*, 2002). As mentioned previously, a homozygous R229Q has also been found in association with adult onset FSGS, but was not detected in association with apparently sporadic FSGS in Arab-Israeli children (Frishberg *et al*, 2002). However, in the absence of an *in vitro* model able to mimic the effects of missense mutations *in vivo*, it remains difficult to confirm the true pathogenicity experimentally.

These findings provide evidence for a di-genic inheritance of *NPHS1* and *NPHS2* mutations resulting in a tri-allelic hit able to modify disease phenotype from CNF to one of congenital FSGS. This suggests the additional disease allele appears to act as a modifier of disease expression, and could represent a form of genetic epistasis. Di-genic inheritance resulting in three disease alleles may occur in autosomal recessive conditions, such as in the haemoglobinopathies, but generally there is no change in clinical phenotype, or this improves through the activation of compensatory mechanisms (Altay *et al*, 1997; Giordano *et al*, 1998; Kerkhoffs *et al*, 2000). In addition, trans-heterozygous mutations can affect the alleles of two different genes to produce an autosomal dominant phenotype, for example as with the *PKD1* and *PKD2* genes in polycystic kidney disease; (Watnick *et al*, 2000; Pei *et al*, 2001), and for the *RET* proto-oncogene and *neuroturin* in Hirschsprung's disease (Doray *et al*, 1998). However, in congenital FSGS, thought to have autosomal recessive inheritance, a tri-allelic hit is required either as a homozygous hit in *NPHS1* together with a heterozygous hit in *NPHS2*, or vice versa for manifestation of disease. The importance of this third event is underscored by the finding that straightforward bi-allelic hit in either *NPHS1* or *NPHS2* results in CNF, and trans-heterozygote parents are phenotypically normal. Moreover, in view of the overlap in mutation phenotype between CNF and congenital FSGS, these disorders could be regarded as part of a spectrum, and the disease phenotype that develops may perhaps be partially determined by the genetic background of the patient, which could be explored further using transgenic strategies. The lack of mutations in the SRN1-like group was surprising, but confirms the profound genetic

diversity of FSGS despite in many cases the uniformity in clinical presentation and renal histology. No concurrent *NPHS1* mutations were detected in the case with a heterozygous R138Q *NPHS2* mutation and SRN1, which provides supporting evidence that the tri-allelic inheritance is a phenomenon specific to congenital rather than the later onset SRN1 disease.

### *4.9.5 Analysis of the –340 G to C base change suggests it is able to disrupt protein-DNA binding to the NPHS1 promoter*

One of the base substitutions detected within this study lay –340 base pairs upstream of the initiation codon, and was not detected in 100 ethnically matched control chromosomes. However, this did not exclude the possibility of a rare polymorphism, as the mutation did not lie within a documented transcription factor consensus binding sequence. Electromobility shift assay (EMSA) was used to analyse whether this change was able to interfere with protein-DNA binding to the *NPHS1* promoter. Preliminary EMSA analysis using wild type and mutated oligonucleotides showed diminished binding of kidney nuclear protein extract, suggesting that the mutation was functional and interfered with the binding of an unknown transcription factor. This did not appear to be kidney specific, as the mutated oligonucleotide was unable to bind liver nuclear protein extract to the same degree, and the EMSA experiments were reproducible in a variety of experimental conditions. Although the mutation lay immediately 3' of a predicted NF1 site, this did not appear to be a suitable candidate on the basis of competition assays and the lack of a supershift. Further experiments are currently in progress to identify the transcription factor in question, which will provide an important insight into the transcriptional regulation of nephrin.

### *4.9.6 Summary of findings*

Genotype phenotype correlation of *NPHS1*/nephrin mutations indicates that the majority result in a severe congenital nephrotic syndrome, and that intact extracellular and cytosolic domains are required. Furthermore, immunoglobulin domains 2, 4 and 7, are likely to be particularly important for gene function and form a target for diagnostic tests. Moreover, a specific nonsense mutation within the cytosolic tail is associated with a variably severe clinical phenotype, apparently influenced by gender. This remains unexplained but might result from the co-inheritance of a disease allele in another gene, or compensation by a genetic or other determinant, such as through functional redundancy. *NPHS1* and *NPHS2* mutations can both result in the CNF phenotype, and identify a specific di-genic inheritance, resulting in three affected alleles able to modify the disease phenotype from CNF to congenital FSGS. These findings can be added to a growing body of data (Katsanis *et al*, 2001), which demonstrates that inheritance of different alleles at independent genetic loci may contribute to disease phenotype. In addition, the importance of a molecular diagnosis confirms observations made through the study of Denys Drash and Frasier syndromes (Chapter 3), that the clinical phenotype may not necessarily be indicative of the underlying molecular defect, or even whether different diseases are truly represented. The findings together with an overlap in mutation phenotype with other forms of FSGS clearly substantiate a wider functional role for nephrin and podocin reaching outside congenital nephrotic disease. This data also provided the first evidence for a functional inter-relationship between nephrin and podocin, underscoring the critical role these genes play in regulating glomerular protein filtration and in the pathogenesis of proteinuria. This apparent interplay provided the basis for a hypothesis that nephrin and podocin may form part of a multimeric complex activating or residing within intracellular pathways essential for podocyte function and slit diaphragm integrity, and that both genes are important mediators of the typical podocyte dysfunction seen universally in nephrotic disease. Preliminary data supporting this hypothesis is now emerging, through the identification of nephrin, podocin and CD2AP as potential binding partners within the podocyte (Schwartz *et al*, 2001; Shih *et al*, 2001). Finally, the presence of a functional mutation –340 base pairs upstream of the initiation codon, seemingly able to result in nephrotic disease, underlines the critical importance of the correct transcriptional regulation of the *NPHS1* promoter.

## Concluding remarks and future directions

The aim of this study was to investigate the role of three glomerular genes *WT1*, *NPHS1* and *NPHS2* in the pathogenesis of childhood nephrotic syndrome, through the mutational analysis of selected cases of inherited nephrotic syndrome and limited functional experiments. The work has contributed to the understanding of the basic processes of podocyte damage, although these remain poorly understood. The damage seen undoubtedly results from disruption of more than a single protein or pathway, making the basis of these diseases complex and difficult to define.

A number of the mutations detected in the *NPHS1* and *NPHS2* genes did not disrupt protein expression, suggesting that the loss of glomerular permselectivity is due to malfunction of the protein product within the podocyte rather than its absence. This has provided the basis for further experiments to determine intracellular protein binding partners for both proteins, which have suggested that nephrin has the potential to activate at least two different signalling pathways within the podocyte through interaction with proteins other than CD2AP (Shih *et al*, 2001). In addition, further studies of the *NPHS1* promoter have identified potential candidate transcription factors that may bind the region of the mutation detected in this study. Data on the role of the *WT1* gene in glomerular function remains confusing, but it is likely that it plays an important role in both glomerular development and podocyte homeostasis.

The common theme in all types of nephrotic syndrome is the appearance of gross morphological changes in podocyte phenotype, characterised predominantly by foot process fusion, and thought to be caused by disruption of the sub-membranous actin cytoskeleton. Since this structure forms the common link between the slit diaphragm and the podocyte foot process, it is tempting to speculate that indiscriminate damage of podocyte membrane proteins, and/or the disruption of their transcriptional control funnels into a final common pathway which by destabilising the actin cytoskeleton, induces foot process fusion, disruption of the GFB and proteinuria.

## APPENDIX I: Clinical Features of congenital and early onset nephrotic syndrome cases analysed for *NPHS1* and *NPHS2* mutations

| Case | Ethnic Origin | Sex | Family History? | Clinical Presentation | Renal histology | Outcome at time of study |
|---|---|---|---|---|---|---|
| *Congenital CNF (n=41 patients)* | | | | | | |
| 1 | England | F | no | severe nephrotic syndrome from 2 weeks of life | CNF | mild proteinuria |
| 2 | England | F | no | prematurity; severe nephrotic syndrome from birth | CNF | renal transplant |
| 4 | England | M | no | prematurity; severe nephrotic syndrome from birth | CNF | dialysis |
| 5 | England | M | no | prematurity; severe nephrotic syndrome from birth | CNF | severe proteinuria |
| 6 | Middle East | M | no | prematurity; severe nephrotic syndrome from birth | CNF | dialysis |
| 7 | Pakistan | F | no | prematurity; severe nephrotic syndrome from birth | CNF | deceased |
| 8 | Turkey | F | no | prematurity; severe nephrotic syndrome from birth | CNF | deceased |

| Case | Ethnic Origin | Sex | Family History? | Clinical Presentation | Renal histology | Outcome at time of study |
|---|---|---|---|---|---|---|
| 9 | England/India | M | no | prematurity; severe nephrotic syndrome from birth | CNF | Dialysis |
| 10 | India | M | no | prematurity; severe nephrotic syndrome from birth | CNF | Dialysis |
| 11 | Middle East | F | no | prematurity; severe nephrotic syndrome from birth | CNF | severe proteinuria |
| 15 | Turkey | F | no | severe nephrotic syndrome from birth | CNF | deceased |
| 20 | India | M | no | prematurity; severe nephrotic syndrome from birth | CNF | Transplant |
| 25 | England | F | no | prematurity; severe nephrotic syndrome from birth | CNF | Transplant |
| 26 | Bangladesh | F | yes | prematurity; severe nephrotic syndrome from birth | CNF | mild proteinuria |
| 32 | England | M | yes | prematurity; severe nephrotic syndrome from birth | CNF | Transplant |

| Case | Ethnic Origin | Sex | Family History? | Clinical Presentation | Renal histology | Outcome at time of study |
|---|---|---|---|---|---|---|
| 47 | England | M | yes | prematurity; severe nephrotic syndrome from birth | CNF | deceased |
| 50 | Middle East | M | yes | prematurity; severe nephrotic syndrome from birth | CNF | transplant |
| 54 | England | M | no | severe nephrotic syndrome from birth | CNF | transplant |
| 62 | India | F | no | prematurity; severe nephrotic syndrome from birth | CNF | dialysis |
| 63 | India | F | no | prematurity; severe nephrotic syndrome from birth | CNF | dialysis |
| 64 | Middle East | M | no | severe nephrotic syndrome from 2 months | CNF | ? |
| 65 | England | F | no | prematurity; severe nephrotic syndrome from birth | CNF | deceased |
| 72 | England | F | no | prematurity; severe nephrotic syndrome from birth | CNF | dialysis |

| Case | Ethnic Origin | Sex | Family History? | Clinical Presentation | Renal histology | Outcome at time of study |
|---|---|---|---|---|---|---|
| 73 | England | M | no | prematurity; severe nephrotic syndrome from birth | CNF | transplant |
| 80 | India | M | no | prematurity; severe nephrotic syndrome from birth | CNF with tubular atrophy | deceased |
| 81 | Malta | M | no | prematurity; severe nephrotic syndrome from 2 months | CNF | transplant |
| 82 | Malta | F | yes:83 | severe nephrotic syndrome from birth at term | CNF | Dialysis; failed transplant |
| 83 | Malta | M | yes:82 | severe nephrotic syndrome from birth at term | CNF | deceased |
| 84 | Malta | M | no | severe nephrotic syndrome from birth | - | Severe proteinuria |
| 85 | India | M | no | prematurity; severe nephrotic syndrome from birth | CNF | deceased |
| 86 | Malta | M | yes:92 | Severe nephrotic syndrome from 12 days | - | deceased |

| Case | Ethnic Origin | Sex | Family History? | Clinical Presentation | Renal histology | Outcome at time of study |
|---|---|---|---|---|---|---|
| 87 | Malta | M | yes:88 | Prematurity; severe nephrotic syndrome from birth | CNF | deceased |
| 88 | Malta | M | yes:87 | Prematurity; severe nephrotic syndrome from birth | - | deceased |
| 89 | Malta | M | yes:94 | severe nephrotic syndrome from 2 weeks of age | CNF | deceased |
| 90 | Malta | F | no | severe nephrotic syndrome from birth | - | remission |
| 91 | Malta | F | no | severe nephrotic syndrome from birth | - | mild proteinuria |
| 92 | Malta | F | yes:86 | severe nephrotic syndrome from birth | - | mild proteinuria |
| 93 | Malta | F | no | severe nephrotic syndrome from birth at term | CNF | remission |
| 94 | Malta | M | yes:89 | severe nephrotic syndrome from birth at term | - | mild proteinuria |

| Case | Ethnic Origin | Sex | Family History? | Clinical Presentation | Renal histology | Outcome at time of study |
|---|---|---|---|---|---|---|
| 96 | South Africa | M | no | severe nephrotic syndrome from birth at term | CNF | remission |
| 97 | England | F | no | nephrotic syndrome at ?8 weeks | CNF | Remission |
| *Congenital FSGS (n=4 patients)* | | | | | | |
| 23 | India | F | yes:24 | severe nephrotic syndrome from birth | - | dialysis |
| 24 | India | M | yes:23 | severe nephrotic syndrome from birth | FSGS | transplant |
| 39 | England | M | no | severe nephrotic syndrome from birth | initial histology: minimal change; subsequently FSGS | transplant |
| 49 | England | M | no | severe nephrotic syndrome from birth | FSGS | transplant |
| *Early onset FSGS* | | | | | | |
| 1 | England | F | no | severe nephrotic syndrome from 9 months of age | FSGS | dialysis |
| 19 | England | F | no | severe nephrotic syndrome from 7 months | FSGS | transplant |

| Case | Ethnic Origin | Sex | Family History? | Clinical Presentation | Renal histology | Outcome at time of study |
|---|---|---|---|---|---|---|
| 21 | Middle East | F | yes: 22 | severe nephrotic syndrome from 1year | FSGS | ? |
| 22 | Middle East | F | yes: 21 | severe nephrotic syndrome from 8 months | FSGS | ? |
| 99 | England | M | yes | severe nephrotic syndrome from 9 months of age | FSGS | transplant |
| *Congenital DMS* | | | | | | |
| 16 | England | F | yes | severe nephrotic syndrome since birth | DMS | transplant |
| 40 | India | F | yes | severe nephrotic syndrome since birth | DMS | dialysis |
| *Early onset DMS* | | | | | | |
| 55 | England | M | no | onset of severe nephrotic syndrome at 2 years | DMS | dialysis |
| 80 | England | M | no | onset of severe nephrotic syndrome at 18 months | DMS | dialysis |

**APPENDIX II: Family trees of CNF families tested for allelic association to the *NPHS1* locus (Parent were heterozygotes; affecteds homozygous as shown).**

**A) Families originating from the island of Malta**

**Family 1: cases 82 and 83**

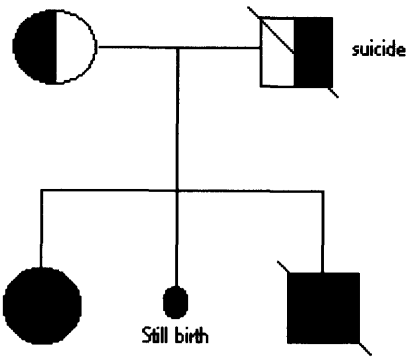


**Family 2: case 81**

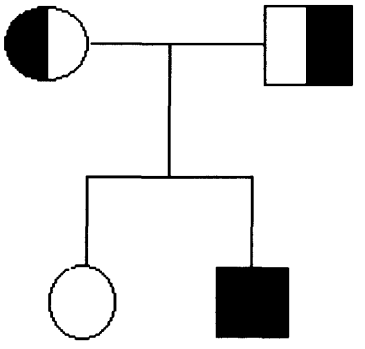

**Family 3: case 91**

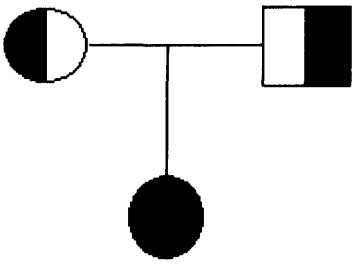

**Family 4: case 86 and 82**

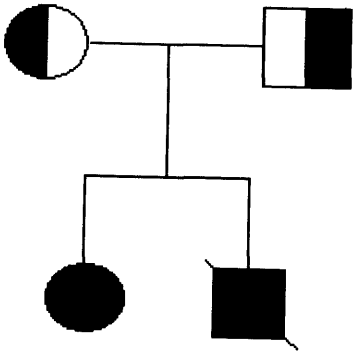

**Family 5: case 93**

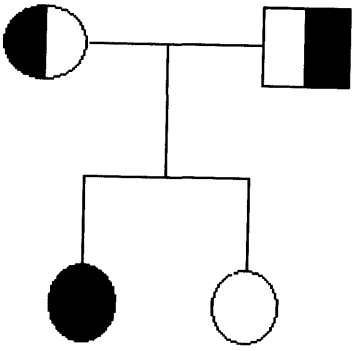

**Family 6: case 94 and 89**

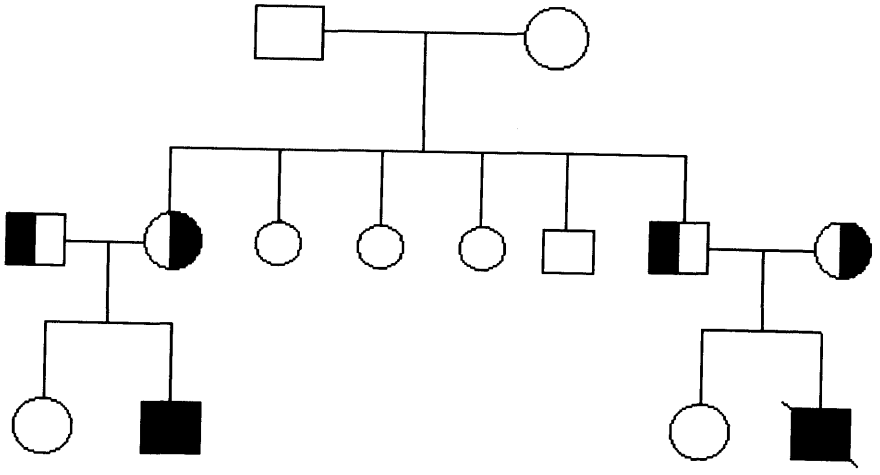

↑

**94**

↑

**89**

**(B) Consanguineous families originating from the Bangladesh (26), Pakistan (7), India (10, 20, 62, 63, 80), Turkey (8, 15) and the Middle East (11, 50)**

**Family 7: case 26**

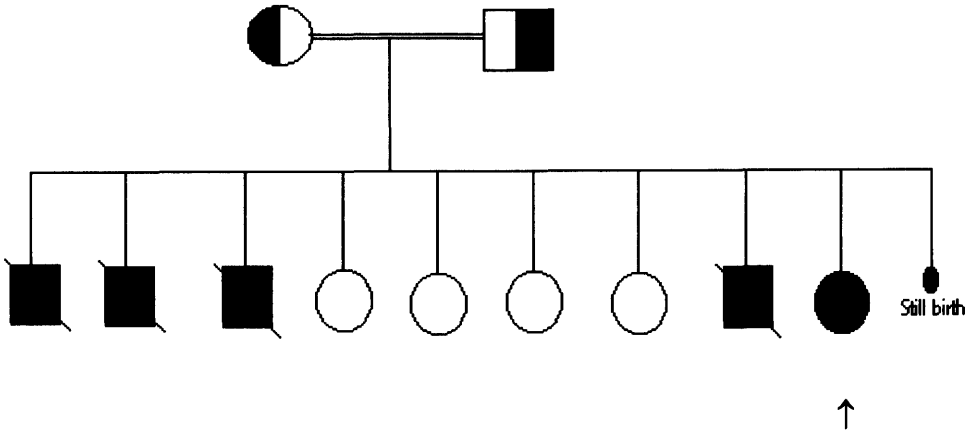


**Family 8: case 80**

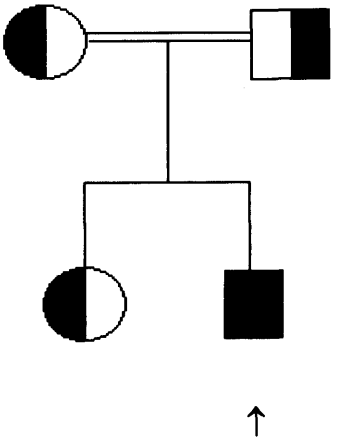

**Family 9: 11**

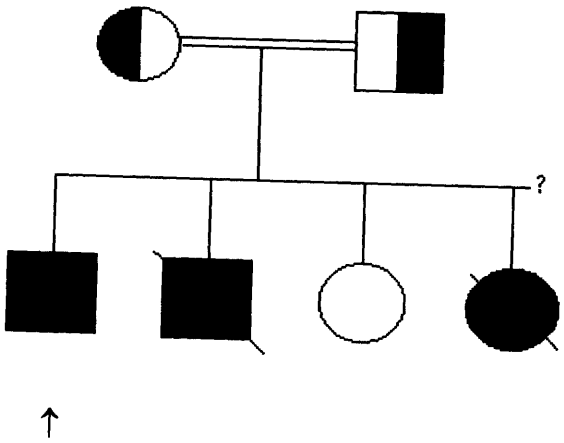


**Family 10: 20**

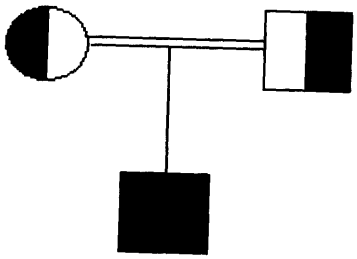

**Family 11: 50**

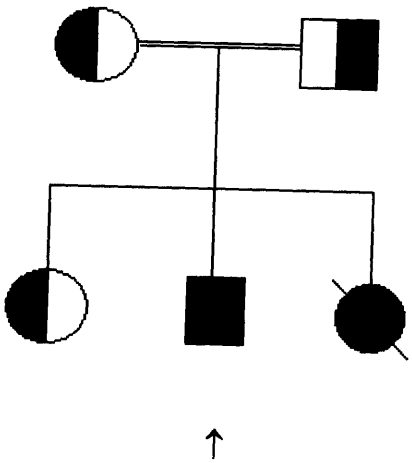

**Family 12: 8**

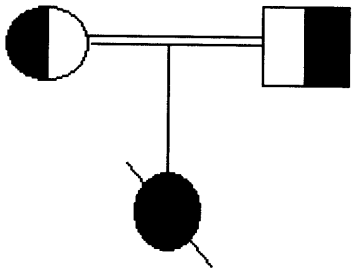

**Family 13: 15**

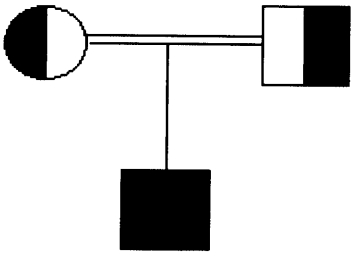

**Family 14: 10**

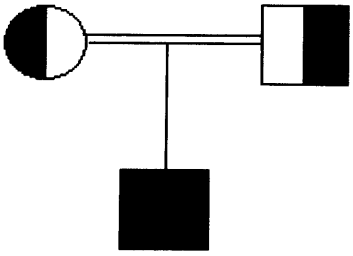

**Family 15: 7**

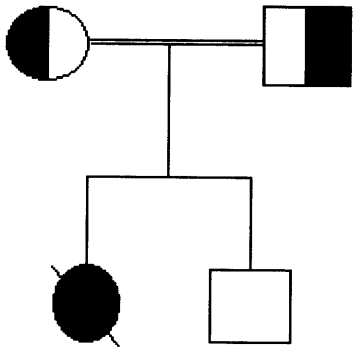

**Family 16:62**

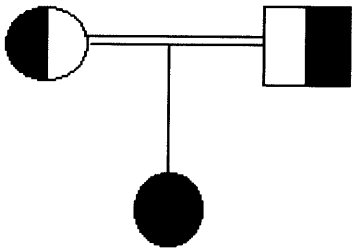

**Family 17: 63**

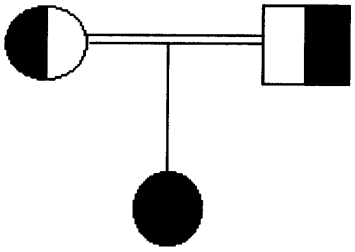

## References


Aaltonen, P., Luimula, P., Astrom, E., Palmen, T., Gronholm, T., Palojoki, E., Jaakkola, I., Ahola, H., Tikkanen, I., and Holthofer, H. (2001). Changes in the expression of nephrin gene and protein in experimental diabetic nephropathy. Lab.Invest. *81*, 1185-1190.

Abrahamson, D.R. and Perry, E.W. (1986). Evidence for splicing new basement membrane into old during glomerular development in newborn rat kidneys. J.Cell Biol. *103*, 2489-2498.

Abrahamson, D.R. (1987). Structure and development of the glomerular capillary wall and basement membrane. Am.J.Physiol. *253*, F783-F794

Abrahamson, D.R., Woods, A., Couchman, J.R., Chatham, W.W., and Heck, L.W. (1988). Cell surface receptors for kidney basement membranes. Am.J.Kidney Dis. *12*, 78-83.

Adler, S. (1992). Integrin receptors in the glomerulus: potential role in glomerular injury. Am.J.Physiol. *262*, F697-F704

Ahola, H., Wang, S.X., Luimula, P., Solin, M.L., Holzman, L.B., and Holthofer, H. (1999). Cloning and expression of the rat nephrin homolog. Am.J.Pathol. *155*, 907-913.

Akasaka, Y., Kikuchi, H., Nagai, T., Hiraoka, N., Kato, S., and Hata, J. (1993). A point mutation found in the WT1 gene in a sporadic Wilms' tumor without genitourinary abnormalities is identical with the most frequent point mutation in Denys-Drash syndrome. FEBS Lett. *317*, 39-43.

Albright, S.G., Warner, A.A., Seeds, J.W., and Burton, B.K. (1990). Congenital nephrosis as a cause of elevated alpha-fetoprotein. Obstet.Gynecol. *76*, 969-971.

Alexander, F. and Campbell, W.A. (1971). Congenital nephrotic syndrome and renal vein thrombosis in infancy. J.Clin.Pathol. *24*, 27-40.

Altay, C., Oner, C., Oner, R., Mesci, L., Balkan, H., Tuzmen, S., Basak, A.N., Gumruk, F., and Gurgey, A. (1997). Genotype-phenotype analysis in HbS-beta-thalassemia. Hum.Hered. *47*, 161-164.

Altschul, S.F., Gish, W., Miller, W., Myers, E.W., and Lipman, D.J. (1990). Basic local alignment search tool. J.Mol.Biol. *215*, 403-410.

Antikainen, M., Holmberg, C., and Taskinen, M.R. (1992). Growth, serum lipoproteins and apoproteins in infants with congenital nephrosis. Clin.Nephrol. *38*, 254-263.

Antikainen, M., Sariola, H., Rapola, J., Taskinen, M.R., Holthofer, H., and Holmberg, C. (1994). Pathology of renal arteries of dyslipidemic children with congenital nephrosis. APMIS *102*, 129-134.

Armstrong, J.F., Pritchard-Jones, K., Bickmore, W.A., Hastie, N.D., and Bard, J.B. (1993). The expression of the Wilms' tumour gene, WT1, in the developing mammalian embryo. Mech.Dev. *40*, 85-97.

Ars, E., Serra, E., Garcia, J., Kruyer, H., Gaona, A., Lazaro, C., and Estivill, X. (2000). Mutations affecting mRNA splicing are the most common molecular defects in patients with neurofibromatosis type 1. Hum.Mol.Genet. *9*, 237-247.

Autio-Harmainen, H., Vaananen, R., and Rapola, J. (1981). Scanning electron microscopic study of normal human glomerulogenesis and of fetal glomeruli in congenital nephrotic syndrome of the Finnish type. Kidney Int. *20*, 747-752.

Autio-Harmainen, H. and Rapola, J. (1981). Renal pathology of fetuses with congenital nephrotic syndrome of the Finnish type. A qualitative and quantitative light microscopic study. Nephron *29*, 158-163.

Aya, K., Tanaka, H., and Seino, Y. Novel mutation in the nephrin gene of a Japanese patient with congenital nephrotic syndrome of the Finnish type. (2000). Kidney Int. *57*, 401-404.

Bachmann, S., Kriz, W., Kuhn, C., and Franke, W.W. (1983). Differentiation of cell types in the mammalian kidney by immunofluorescence microscopy using antibodies to intermediate filament proteins and desmoplakins. Histochemistry *77*, 365-394.

Baird, P.N., Santos, A., Groves, N., Jadresic, L., and Cowell, J.K. (1992). Constitutional mutations in the WT1 gene in patients with Denys-Drash syndrome. Hum.Mol.Genet. *1*, 301-305.

Baird, P.N. and Cowell, J.K. (1993). A novel zinc finger mutation in a patient with Denys-Drash syndrome. Hum.Mol.Genet. *2*, 2193-2194.

Banton, C.R., Thalayasingam, B., and Coulthard, M.G. (1990). Spontaneous resolution of congenital nephrotic syndrome in a neonate. Arch.Dis.Child *65*, 992-993.

Barakat, A.Y., Papadopoulou, Z.L., Chandra, R.S., Hollerman, C.E., and Calcagno, P.L. (1974). Pseudohermaphroditism, nephron disorder and wilms' tumor: a unifying concept. Pediatrics *54*, 366-369.

Barakat, A.Y., Khoury, L.A., Allam, C.K., and Najjar, S.S. (1982). Diffuse mesangial sclerosis and ocular abnormalities in two siblings. Int.J.Pediatr.Nephrol. *3*, 33-35.

Barasch, J., Qiao, J., McWilliams, G., Chen, D., Oliver, J.A., and Herzlinger, D. (1997). Ureteric bud cells secrete multiple factors, including bFGF, which rescue renal progenitors from apoptosis. Am.J.Physiol. *273*, F757-F767

Barbaux, S., Niaudet, P., Gubler, M.C., Grunfeld, J.P., Jaubert, F., Kuttenn, F., Fekete, C.N., Souleyreau-Therville, N., Thibaud, E., Fellous, M., and McElreavey, K. (1997). Donor splice-site mutations in WT1 are responsible for Frasier syndrome. Nat.Genet. *17*, 467-470.

Barbosa, A.S., Hadjiathanasiou, C.G., Theodoridis, C., Papathanasiou, A., Tar, A., Merksz, M., Gyorvari, B., Sultan, C., Dumas, R., Jaubert, F., Niaudet, P., Moreira-Filho, C.A., Cotinot, C., and Fellous, M. (1999). The same mutation affecting the splicing of WT1 gene is present on Frasier syndrome patients with or without Wilms' tumor. Hum.Mutat. *13*, 146-153.

Bard, J.B., Gordon, A., Sharp, L., and Sellers, W.I. (2001). Early nephron formation in the developing mouse kidney. *199*, 385-392.

Bard, J.B., McConnell, J.E., and Davies, J.A. (1994). Towards a genetic basis for kidney development. Mech.Dev. *48*, 3-11.

Bardeesy, N., Zabel, B., Schmitt, K., and Pelletier, J. (1994). WT1 mutations associated with incomplete Denys-Drash syndrome define a domain predicted to behave in a dominant-negative fashion. Genomics *21*, 663-664.

Barisoni, L., Mokrzycki, M., Sablay, L., Nagata, M., Yamase, H., and Mundel, P. (2000) Podocyte cell cycle regulation and proliferation in collapsing glomerulopathies. Kidney Int. *58*, 137-143.

Barnes, J.D., Crosby, J.L., Jones, C.M., Wright, C.V., and Hogan, B.L. (1994). Embryonic expression of Lim-1, the mouse homolog of Xenopus Xlim-1, suggests a role in lateral mesoderm differentiation and neurogenesis. Dev.Biol. *161*, 168-178.

Beckwith, J.B., Kiviat, N.B., and Bonadio, J.F. (1990). Nephrogenic rests, nephroblastomatosis, and the pathogenesis of Wilms' tumor. Pediatr.Pathol. *10*, 1-36.

Beckwith, J.B. (1993). Precursor lesions of Wilms tumor: clinical and biological implications. Med.Pediatr.Oncol. *21*, 158-168.

Beltcheva, O., Martin, P., Lenkkeri, U., and Tryggvason, K. (2001). Mutation spectrum in the nephrin gene (*NPHS1*) in congenital nephrotic syndrome. Hum.Mutat. *17*, 368-373.

Benigni, A., Tomasoni, S., Gagliardini, E., Zoja, C., Grunkemeyer, J.A., Kalluri, R., and Remuzzi, G. (2001). Blocking angiotensin ii synthesis/activity preserves glomerular nephrin in rats with severe nephrosis. J.Am.Soc.Nephrol. *12*, 941-948.

Benson, D., Lipman, D.J., and Ostell, J. (1993). GenBank. Nucleic.Acids.Res. *21*, 2963-2965.

Bickmore, W.A., Oghene, K., Little, M.H., Seawright, A., van, H., V, and Hastie, N.D. (1992). Modulation of DNA binding specificity by alternative splicing of the Wilms tumor wt1 gene transcript. Science *257*, 235-237.

Binder, C.J., Weiher, H., Exner, M., and Kerjaschki, D. (1999). Glomerular overproduction of oxygen radicals in Mpv17 gene-inactivated mice causes podocyte foot process flattening and proteinuria: A model of steroid-resistant nephrosis sensitive to radical scavenger therapy. Am.J.Pathol. *154*, 1067-1075.

Blantz, R.C., Gabbai, F.B., Tucker, B.J., Yamamoto, T., and Wilson, C.B. (1993). Role of mesangial cell in glomerular response to volume and angiotensin II. Am.J.Physiol. *264*, F158-F165

Borel, F., Barilla, K.C., Hamilton, T.B., Iskandar, M., and Romaniuk, P.J. (1996). Effects of Denys-Drash syndrome point mutations on the DNA binding activity of the Wilms' tumor suppressor protein WT1. Biochemistry *35*, 12070-12076.

Boute, N., Gribouval, O., Roselli, S., Benessy, F., Lee, H., Fuchshuber, A., Dahan, K., Gubler, M.C., Niaudet, P., and Antignac, C. (2000) NPHS2, encoding the glomerular protein podocin, is mutated in autosomal recessive steroid-resistant nephrotic syndrome. Nat.Genet. *24*, 349-354.

Brandli, A.W. (1999). Towards a molecular anatomy of the Xenopus pronephric kidney. Int.J.Dev.Biol. *43*, 381-395.

Brdicka, R. (1995). [The human genome--chromosome 11]. Cas.Lek.Cesk. *134*, 353-355.

Brenner, B.M., Hostetter, T.H., and Humes, H.D. (1978). Glomerular permselectivity: barrier function based on discrimination of molecular size and charge. Am.J.Physiol. *234*, F455-F460

Breslow, N.E., Takashima, J.R., Ritchey, M.L., Strong, L.C., and Green, D.M. (2000). Renal failure in the Denys-Drash and Wilms' tumor-aniridia syndromes. Cancer Res. *60*, 4030-4032.

Briggs, J., Kriz, W., and Schnermann, J. (1998). Overview of renal structure and function. In Primer of kidney diseases. a. Greenberg, ed. (Sna Diego, USA: Academic Press),

Brown, D.A. and London, E. (1998). Functions of lipid rafts in biological membranes. Annu.Rev.Cell Dev.Biol. *14:111-36.*, 111-136.

Bruce, S.R. and Peterson, M.L. (2001. Multiple features contribute to efficient constitutive splicing of an unusually large exon. Nucleic.Acids.Res. *29*, 2292-2302.

Bruce, S.R., Kaetzel, C.S., and Peterson, M.L. (1999). Cryptic intron activation within the large exon of the mouse polymeric immunoglobulin receptor gene: cryptic splice sites correspond to protein domain boundaries. Nucleic.Acids.Res. *27*, 3446-3454.

Bruening, W., Bardeesy, N., Silverman, B.L., Cohn, R.A., Machin, G.A., Aronson, A.J., Housman, D., and Pelletier, J. (1992). Germline intronic and exonic mutations in the Wilms' tumour gene (WT1) affecting urogenital development. Nat.Genet. *1*, 144-148.

Bruening, W. and Pelletier, J. (1996). A non-AUG translational initiation event generates novel WT1 isoforms. J.Biol.Chem. *271*, 8646-8654.

Bruening, W., Moffett, P., Chia, S., Heinrich, G., and Pelletier, J. (1996). Identification of nuclear localization signals within the zinc fingers of the WT1 tumor suppressor gene product. FEBS Lett. *393*, 41-47.

Brummendorf, T. and Rathjen, F.G. (1994). Cell adhesion molecules. 1: immunoglobulin superfamily. Protein Profile. *1*, 951-1058.

Buckler, A.J., Pelletier, J., Haber, D.A., Glaser, T., and Housman, D.E. (1991). Isolation, characterization, and expression of the murine Wilms' tumor gene (WT1) during kidney development. Mol.Cell Biol. *11*, 1707-1712.

Buzi, F., Mella, P., Pilotta, A., Felappi, B., Camerino, G., and Notarangelo, L.D. (2001) Frasier syndrome with childhood-onset renal failure. Horm.Res. *55*, 77-80.

Call, K.M., Glaser, T., Ito, C.Y., Buckler, A.J., Pelletier, J., Haber, D.A., Rose, E.A., Kral, A., Yeger, H., and Lewis, W.H. (1990). Isolation and characterization of a zinc finger polypeptide gene at the human chromosome 11 Wilms' tumor locus. Cell *60*, 509-520.

Caricasole, A., Duarte, A., Larsson, S.H., Hastie, N.D., Little, M., Holmes, G., Todorov, I., and Ward, A. (1996). RNA binding by the Wilms tumor suppressor zinc finger proteins. Proc.Natl.Acad.Sci.U.S.A. *93*, 7562-7566.

Carroll, T.J. and Vize, P.D. (1996). Wilms' tumor suppressor gene is involved in the development of disparate kidney forms: evidence from expression in the Xenopus pronephros. Dev.Dyn. *206*, 131-138.

Caulfield, J.P., Reid, J.J., and Farquhar, M.G. (1976). Alterations of the glomerular epithelium in acute aminonucleoside nephrosis. Evidence for formation of occluding junctions and epithelial cell detachment. Lab.Invest. *34*, 43-59.

Cetinkaya, E., Ocal, G., Berberoglu, M., Adiyaman, P., Ekim, M., Yalcinkaya, F., and Orun, E. (2001). Association of partial gonadal dysgenesis, nephropathy and WT1 gene mutation without Wilms' tumor: incomplete Denys-Drash syndrome. J.Pediatr.Endocrinol.Metab. *14*, 561-564.

Chevalier, G., Yeger, H., Martinerie, C., Laurent, M., Alami, J., Schofield, P.N., and Perbal, B. (1998). novH: differential expression in developing kidney and Wilm's tumors. Am.J.Pathol. *152*, 1563-1575.

Cho, C.R., Lumsden, C.J., and Whiteside, C.I. (1993). Epithelial cell detachment in the nephrotic glomerulus: a receptor co-operativity model. J.Theor.Biol. *160*, 407-426.

Cho, E.A., Patterson, L.T., Brookhiser, W.T., Mah, S., Kintner, C., and Dressler, G.R. (1998). Differential expression and function of cadherin-6 during renal epithelium development. Development *125*, 803-812.

Clarkson, P.A., Davies, H.R., Williams, D.M., Chaudhary, R., Hughes, I.A., and Patterson, M.N. (1993). Mutational screening of the Wilms's tumour gene, WT1, in males with genital abnormalities. J.Med.Genet. *30*, 767-772.

Cleper, R., Davidovitz, M., Krause, I., Bar, N.N., Ash, S., Schwarz, M., Mor, C., and Eisenstein, B. (1999). Unexpected Wilms' tumor in a pediatric renal transplant recipient: suspected Denys-Drash syndrome. Transplant.Proc. *31*, 1907-1909.

Clericuzio, C.L. (1993). Clinical phenotypes and Wilms tumor. Med.Pediatr.Oncol. *21*, 182-187.

Combs, H.L., Shankland, S.J., Setzer, S.V., Hudkins, K.L., and Alpers, C.E. (1998). Expression of the cyclin kinase inhibitor, p27kip1, in developing and mature human kidney. Kidney Int. *53*, 892-896.

Cook, D.M., Hinkes, M.T., Bernfield, M., and Rauscher, F.J. (1996). Transcriptional activation of the syndecan-1 promoter by the Wilms' tumor protein WT1. Oncogene *13*, 1789-1799.

Coppes, M.J., de Kraker, J., van Dijken, P.J., Perry, H.J., Delemarre, J.F., Tournade, M.F., Lemerle, J., and Voute, P.A. (1989). Bilateral Wilms' tumor: long-term survival and some epidemiological features. J.Clin.Oncol. *7*, 310-315.

Coppes, M.J., Liefers, G.J., Higuchi, M., Zinn, A.B., Balfe, J.W., and Williams, B.R. (1992). Inherited WT1 mutation in Denys-Drash syndrome. Cancer Res. *52*, 6125-6128.

Coppes, M.J., Campbell, C.E., and Williams, B.R. (1993). The role of WT1 in Wilms tumorigenesis. FASEB J. *7*, 886-895.

Coppes, M.J., Liefers, G.J., Paul, P., Yeger, H., and Williams, B.R. (1993). Homozygous somatic Wt1 point mutations in sporadic unilateral Wilms tumor. Proc.Natl.Acad.Sci.U.S.A. *90*, 1416-1419.

Coppes, M.J., Huff, V., and Pelletier, J. (1993). Denys-Drash syndrome: relating a clinical disorder to genetic alterations in the tumor suppressor gene WT1. J.Pediatr. *123*, 673-678.

Coppes, M.J. and Clericuzio, C.L. (1994). "Molecular genetic analysis of the WT1 gene in patients suspected to have the Denys-Drash syndrome". Med.Pediatr.Oncol. *23*, 390

Coze, C., Gentet, J.C., Chapuis, E., Picon, G., Guys, J.M., Panuel, M., Scheiner, C., and Raybaud, C. (1992). [Drash syndrome]. Pediatrie. *47*, 757-760.

Cunningham, B.A., Hemperly, J.J., Murray, B.A., Prediger, E.A., Brackenbury, R., and Edelman, G.M. (1987). Neural cell adhesion molecule: structure, immunoglobulin-like domains, cell surface modulation, and alternative RNA splicing. Science *236*, 799-806.

Dagert, M. and Ehrlich, S.D. (1979). Prolonged incubation in calcium chloride improves the competence of Escherichia coli cells. Gene *6*, 23-28.

Davies, J.A. (1996). Mesenchyme to epithelium transition during development of the mammalian kidney tubule. Acta Anat.(Basel.) *156*, 187-201.

Davies, R.C., Calvio, C., Bratt, E., Larsson, S.H., Lamond, A.I., and Hastie, N.D. (1998). WT1 interacts with the splicing factor U2AF65 in an isoform-dependent manner and can be incorporated into spliceosomes. Genes Dev. *12*, 3217-3225.

Dechsukhum, C., Ware, J.L., Ferreira-Gonzalez, A., Wilkinson, D.S., and Garrett, C.T. (2000). Detection of a novel truncated WT1 transcript in human neoplasia. Mol.Diagn. *5*, 117-128.

Deen, W.M., Lazzara, M.J., and Myers, B.D. (2001). Structural determinants of glomerular permeability. Am.J.Physiol.Renal Physiol. *281*, F579-F596

Dehbi, M. and Pelletier, J. (1996). PAX8-mediated activation of the wt1 tumor suppressor gene. EMBO J. *15*, 4297-4306.

Demmer, L., Primack, W., Loik, V., Brown, R., Therville, N., and McElreavey, K. (1999). Frasier syndrome: a cause of focal segmental glomerulosclerosis in a 46,XX female. J.Am.Soc.Nephrol. *10*, 2215-2218.

Denamur, E., Andre, J.L., Niaudet, P., and Loirat, C. (2000). Absence of correlation between genotype and the severity of diffuse mesangial sclerosis in Denys-Drash syndrome. Pediatr.Nephrol. *14*, 439-440.

Denamur, E., Bocquet, N., Mougenot, B., Da Silva, F., Martinat, L., Loirat, C., Elion, J., Bensman, A., and Ronco, P.M. (1999). Mother-to-child transmitted WT1 splice-site mutation is responsible for distinct glomerular diseases. J.Am.Soc.Nephrol. *10*, 2219-2223.

Denis, C.L., Ferguson, J., and Young, E.T. (1983). mRNA levels for the fermentative alcohol dehydrogenase of Saccharomyces cerevisiae decrease upon growth on a nonfermentable carbon source. J.Biol.Chem. *258*, 1165-1171.

Denys, P., Malvaux, P., Van Den Berghe, H., Tanghe, W., and Proesmans, W. (1967). [Association of an anatomo-pathological syndrome of male pseudohermaphroditism, Wilms' tumor, parenchymatous nephropathy and XX/XY mosaicism]. Arch.Fr.Pediatr. *24*, 729-739.

Devriendt, K., van den Berghe, K., Moerman, P., and Fryns, J.P. (1996). Elevated maternal serum and amniotic fluid alpha-fetoprotein levels in the Denys-Drash syndrome. Prenat Diagn *16*:455-7

Devriendt, K., Deloof, E., Moerman, P., Legius, E., Vanhole, C., de Zegher, F., Proesmans, W., and Devlieger, H. (1995). Diaphragmatic hernia in Denys-Drash syndrome. Am.J.Med.Genet. *57*, 97-101.

Dharnidharka, V.R., Ruteshouser, E.C., Rosen, S., Kozakewich, H., Harris, H.W.J., Herrin, J.T., and Huff, V. Pulmonary dysplasia, Denys-Drash syndrome and Wilms tumor 1 gene mutation in twins. (2001). Pediatr.Nephrol. *16*, 227-231.

Di Benedetto, G., Erguven, A., Stenico, M., Castri, L., Bertorelle, G., Togan, I., and Barbujani, G. (2001). DNA diversity and population admixture in Anatolia. Am.J.Phys.Anthropol. *115*, 144-156.

Diamond, J.R. and Karnovsky, M.J. (1986). Focal and segmental glomerulosclerosis following a single intravenous dose of puromycin aminonucleoside. Am.J.Pathol. *122*, 481-487.

Donovan, M.J., Natoli, T.A., Sainio, K., Amstutz, A., Jaenisch, R., Sariola, H., and Kreidberg, J.A. (1999). Initial differentiation of the metanephric mesenchyme is independent of WT1 and the ureteric bud. Dev.Genet. *24*, 252-262.

Donoviel, D.B., Freed, D.D., Vogel, H., Potter, D.G., Hawkins, E., Barrish, J.P., Mathur, B.N., Turner, C.A., Geske, R., Montgomery, C.A., Starbuck, M., Brandt, M., Gupta, A., Ramirez-Solis, R., Zambrowicz, B.P., and Powell, D.R. (2001). Proteinuria and perinatal lethality in mice lacking NEPH1, a novel protein with homology to NEPHRIN. Mol.Cell Biol.2001. *21*, 4829-4836.

Doray, B., Salomon, R., Amiel, J., Pelet, A., Touraine, R., Billaud, M., Attie, T., Bachy, B., Munnich, A., and Lyonnet, S. (1998). Mutation of the RET ligand, neurturin, supports multigenic inheritance in Hirschsprung disease. Hum.Mol.Genet. *7*, 1449-1452.

Doublier, S., Ruotsalainen, V., Salvidio, G., Lupia, E., Biancone, L., Conaldi, P.G., Reponen, P., Tryggvason, K., and Camussi, G. (2001). Nephrin redistribution on podocytes is a potential mechanism for proteinuria in patients with primary acquired nephrotic syndrome. *158*, 1723-1731.

Doyonnas, R., Kershaw, D.B., Duhme, C., Merkens, H., Chelliah, S., Graf, T., and McNagny, K.M. (2001). Anuria, omphalocele, and perinatal lethality in mice lacking the CD34-related protein podocalyxin. Exp.Med. *194*, 13-27.

Drash, A., Sherman, F., Hartmann, W.H., and Blizzard, R.M. (1970). A syndrome of pseudohermaphroditism, Wilms' tumor, hypertension, and degenerative renal disease. J.Pediatr. *76*, 585-593.

Drenckhahn, D. and Franke, R.P. (1988). Ultrastructural organization of contractile and cytoskeletal proteins in glomerular podocytes of chicken, rat, and man. Lab.Invest. *59*, 673-682.

Dressler, G.R., Deutsch, U., Chowdhury, K., Nornes, H.O., and Gruss, P. (1990). Pax2, a new murine paired-box-containing gene and its expression in the developing excretory system. Development *109*, 787-795.

Dressler, G.R., Wilkinson, J.E., Rothenpieler, U.W., Patterson, L.T., Williams-Simons, L., and Westphal, H. (1993). Deregulation of Pax-2 expression in transgenic mice generates severe kidney abnormalities. Nature *362*, 65-67.

Drummond, I.A., Madden, S.L., Rohwer-Nutter, P., Bell, G.I., Sukhatme, V.P., and Rauscher, F.J. (1992). Repression of the insulin-like growth factor II gene by the Wilms tumor suppressor WT1. Science *257* , 674-678.

Drummond, I.A., Rupprecht, H.D., Rohwer-Nutter, P., Lopez-Guisa, J.M., Madden, S.L., Rauscher, F.J., and Sukhatme, V.P. (1994). DNA recognition by splicing variants of the Wilms' tumor suppressor, WT1. Mol.Cell Biol. *14*, 3800-3809.

Duarte, A., Caricasole, A., Graham, C.F., and Ward, A. (1998). Wilms' tumour-suppressor protein isoforms have opposite effects on Igf2 expression in primary embryonic cells, independently of p53 genotype. Br.J.Cancer *77*, 253-259.

Dudley, A.T., Godin, R.E., and Robertson, E.J. (1999). Interaction between FGF and BMP signaling pathways regulates development of metanephric mesenchyme. Genes Dev. *13*, 1601-1613.

Dustin, M.L., Olszowy, M.W., Holdorf, A.D., Li, J., Bromley, S., Desai, N., Widder, P., Rosenberger, F., van der Merwe, P.A., Allen, P.M., and Shaw, A.S. (1998). A novel adaptor protein orchestrates receptor patterning and cytoskeletal polarity in T-cell contacts. Cell *94*, 667-677.

Eddy, A.A. and Mauer, S.M. (1985). Pseudohermaphroditism, glomerulopathy, and Wilms tumor (Drash syndrome): frequency in end-stage renal failure. J.Pediatr. *106*, 584-587.

Edidin, D.V. (1985). Pseudohermaphroditism, glomerulopathy, and Wilms tumor (Drash syndrome). J.Pediatr. *107*, 988

Edwards, A., Daniels, B.S., and Deen, W.M. (1999). Ultrastructural model for size selectivity in glomerular filtration. Am.J.Physiol. *276*, F892-F902

Ekblom, P. (1993). Basement membranes in development. In Molecular and Cellular Aspects of Basement Membranes. D.H.a.T.R. Rohrbach, ed. (New York: Academic Press), pp. 359-383.

Emmert, D.B., Stoehr, P.J., Stoesser, G., and Cameron, G.N. (1994). The European Bioinformatics Institute (EBI) databases. Nucleic.Acids.Res. *22*, 3445-3449.

Englert, C., Vidal, M., Maheswaran, S., Ge, Y., Ezzell, R.M., Isselbacher, K.J., and Haber, D.A. (1995). Truncated WT1 mutants alter the subnuclear localization of the wild-type protein. Proc.Natl.Acad.Sci.U.S.A. *92*, 11960-11964.

Englert, C., Hou, X., Maheswaran, S., Bennett, P., Ngwu, C., Re, G.G., Garvin, A.J., Rosner, M.R., and Haber, D.A. (1995). WT1 suppresses synthesis of the epidermal growth factor receptor and induces apoptosis. EMBO J. *14*, 4662-4675.

Fahrig, T., Landa, C., Pesheva, P., Kuhn, K., and Schachner, M. (1987). Characterization of binding properties of the myelin-associated glycoprotein to extracellular matrix constituents. EMBO J. *6*, 2875-2883.

Farquhar, M.G., Vernier, R.L., and Good, R.A. (1957). An electronmicroscopic study of the glomerulus in nephrosis, glomerulonephritis and lupus erythematosus. Journal of Experimental Medicine *106*, 649-660.

Fields, S. and Song, O. (1989). A novel genetic system to detect protein-protein interactions. Nature *340*, 245-246.

Francke, U., Holmes, L.B., Atkins, L., and Riccardi, V.M. (1979). Aniridia-Wilms' tumor association: evidence for specific deletion of 11p13. Cytogenet.Cell Genet. *24*, 185-192.

Frasier, S. D. Gonadoblastoma associated with pure gonadal dysgenesis in monozygous twins. Bashore, R. A. and Mosier H. D. (1964) Journal of Pediatrics *64*, 740-745.

Friedman, A.L. and Finlay, J.L. (1987). The Drash syndrome revisited: diagnosis and follow-up. Am.J.Med.Genet.Suppl. *3:293-6.*, 293-296.

Frishberg, Y., Rinat, C., Megged, O., Shapira, E., Feinstein, S., and Raas-Rothschild, A. (2002) Mutations in NPHS2 encoding podocin are a prevalent cause of steroid-resistant nephrotic syndrome among Israeli-Arab children. J.Am.Soc.Nephrol. *13*, 400-405.

Fuchshuber, A., Jean, G., Gribouval, O., Gubler, M.C., Broyer, M., Beckmann, J.S., Niaudet, P., and Antignac, C. (1995). Mapping a gene (SRN1) to chromosome 1q25-q31 in idiopathic nephrotic syndrome confirms a distinct entity of autosomal recessive nephrosis. Hum.Mol.Genet. *4*, 2155-2158.

Fuchshuber, A., Niaudet, P., Gribouval, O., Jean, G., Gubler, M.C., Broyer, M., and Antignac, C. (1996). Congenital nephrotic syndrome of the Finnish type: linkage to the locus in a non-Finnish population. Pediatr.Nephrol. *10*, 135-138.

Furness, P.N., Hall, L.L., Shaw, J.A., and Pringle, J.H. (1999). Glomerular expression of nephrin is decreased in acquired human nephrotic syndrome. Nephrol.Dial.Transplant. *14*, 1234-1237.

Furukawa, T., Ohno, S., Oguchi, H., Hora, K., Tokunaga, S., and Furuta, S. (1991). Morphometric study of glomerular slit diaphragms fixed by rapid-freezing and freeze-substitution. Kidney Int. *40*, 621-624.

Gallo, G.E. and Chemes, H.E. (1987). The association of Wilms' tumor, male pseudohermaphroditism and diffuse glomerular disease (Drash syndrome): report of eight cases with clinical and morphologic findings and review of the literature. Pediatr.Pathol. *7*, 175-189.

Garrod, D.R. and Fleming, S. (1990). Early expression of desmosomal components during kidney tubule morphogenesis in human and murine embryos. Development *108*, 313-321.

Geijsen, N., Spaargaren, M., Raaijmakers, J.A., Lammers, J.W., Koenderman, L., and Coffer, P.J. (1999). Association of RACK1 and PKCbeta with the common beta-chain of the IL-5/IL-3/GM-CSF receptor. Oncogene *18*, 5126-5130.

Gelberg, H., Healy, L., Whiteley, H., Miller, L.A., and Vimr, E. (1996). In vivo enzymatic removal of alpha 2-->6-linked sialic acid from the glomerular filtration barrier results in podocyte charge alteration and glomerular injury. Lab.Invest. *74*, 907-920.

Georgakopoulos, T., Koutroubas, G., Vakonakis, I., Tzermia, M., Prokova, V., Voutsina, A., and Alexandraki, D. (2001) Functional analysis of the Saccharomyces cerevisiae YFR021w/YGR223c/YPL100w ORF family suggests relations to mitochondrial/peroxisomal functions and amino acid signalling pathways. Yeast. *18*, 1155-1171.

Gertner, J.M., Kauschansky, A., Giesker, D.W., Siegel, N.J., Breg, W.R., and Genel, M. (1980). XY gonadal dysgenesis associated with the congenital nephrotic syndrome. Obstet.Gynecol. *55*, 66S-69S.

Gessler, M., Poustka, A., Cavenee, W., Neve, R.L., Orkin, S.H., and Bruns, G.A. (1990). Homozygous deletion in Wilms tumours of a zinc-finger gene identified by chromosome jumping. Nature *343*, 774-778.

Gessler, M., Konig, A., and Bruns, G.A. (1992). The genomic organization and expression of the WT1 gene. Genomics *12*, 807-813.

Gessler, M., Konig, A., Arden, K., Grundy, P., Orkin, S., Sallan, S., Peters, C., Ruyle, S., Mandell, J., and Li, F. (1994). Infrequent mutation of the WT1 gene in 77 Wilms' Tumors. Hum.Mutat. *3*, 212-222.

Ghahremani, M., Chan, C.B., Bistritzer, T., Aladjem, M.M., Tieder, M., and Pelletier, J. (1996). A novel mutation H373Y in the Wilms' tumor suppressor gene, WT1, associated with Denys-Drash syndrome. Hum.Hered. *46*, 336-338.

Gibbons, R.J. and Higgs, D.R. (1996). The alpha-thalassemia/mental retardation syndromes. Medicine (Baltimore.) *75*, 45-52.

Giordano, P.C., Harteveld, C.L., Haak, H.L., Batelaan, D., van Delft, P., Plug, R.J., Emonts, M., Zanardini, R., and Bernini, L.F. (1998). A case of non-beta-globin gene linked beta thalassaemia in a Dutch family with two additional alpha-gene

defects: the common -alpha3.7 deletion and the rare IVS1-116 (A-->G) acceptor splice site mutation. Br.J.Haematol. *103*, 370-376.

Goldman, S.M., Garfinkel, D.J., Oh, K.S., and Dorst, J.P. (1981). The Drash syndrome: male pseudohermaphroditism, nephritis, and Wilms tumor. Radiology *141*, 87-91.

Goto, S., Yaoita, E., Matsunami, H., Kondo, D., Yamamoto, T., Kawasaki, K., Arakawa, M., and Kihara, I. (1998). Involvement of R-cadherin in the early stage of glomerulogenesis. J.Am.Soc.Nephrol. *9*, 1234-1241.

Groves, N., Baird, P.N., Hogg, A., and Cowell, J.K. (1992). A single base pair polymorphism in the WT1 gene detected by single-strand conformation polymorphism analysis. Hum.Genet. *90*, 440-442.

Guez, S., Giani, M., Melzi, M.L., Antignac, C., and Assael, B.M. (1998). Adequate clinical control of congenital nephrotic syndrome by enalapril. Pediatr.Nephrol. *12*, 130-132.

Guglielmino, C.R., De Silvestri, A., and Beres, J. (2000). Probable ancestors of Hungarian ethnic groups: an admixture analysis. Ann.Hum.Genet. *64*, 145-159.

Gumbiner, B. and Simons, K. (1987). The role of uvomorulin in the formation of epithelial occluding junctions. Ciba.Found.Symp. *125:168-86.*, 168-186.

Haber, D.A., Sohn, R.L., Buckler, A.J., Pelletier, J., Call, K.M., and Housman, D.E. (1991). Alternative splicing and genomic structure of the Wilms tumor gene WT1. Proc.Natl.Acad.Sci.U.S.A. *88*, 9618-9622.

Habib, R. and Kleinknecht, C. (1971). The primary nephrotic syndrome of childhood. Classification and clinicopathologic study of 406 cases. Pathol.Annu. *6:417-74.*, 417-474.

Habib, R. and Bois, E. (1973). [Heterogeneity of early onset nephrotic syndromes in infants (nephrotic syndrome "in infants"). Anatomical, clinical and genetic study of 37 cases]. Helv.Paediatr.Acta *28*, 91-107.

Habib, R. (1993). Nephrotic syndrome in the 1st year of life. Pediatr.Nephrol. *7*, 347-353.

Hallman, N., Hjelt, l., and Ahvenainen, E.K. (1956). Nephrotic syndrome in newborn and young infants. Ann.Paediatr.Fenn. *2*, 227-241.

Hallman, N., Norio, R., and Kouvalainen, K. (1967). Main features of the congenital nephrotic syndrome. Acta Paediatr.Scand. *:Suppl 172:75-8.*, Suppl-8

Haltia, A., Solin, M.L., Holmberg, C., Reivinen, J., Miettinen, A., and Holthofer, H. (1998). Morphologic changes suggesting abnormal renal differentiation in congenital nephrotic syndrome. Pediatr.Res. *43*, 410-414.

Hamed, R.M. and Shomaf, M. (2001). Congenital nephrotic syndrome: a clinico-pathologic study of thirty children. J.Nephrol. *14*, 104-109.

Hammes, A., Guo, J.K., Lutsch, G., Leheste, J.R., Landrock, D., Ziegler, U., Gubler, M.C., and Schedl, A. (2001). Two splice variants of the Wilms' tumor 1 gene have distinct functions during sex determination and nephron formation. Cell *106*, 319-329.

Harris, H.W.J., Umetsu, D., Geha, R., and Harmon, W.E. (1986). Altered immunoglobulin status in congenital nephrotic syndrome. Clin.Nephrol. *25*, 308-313.

Hartwig, A. (2001). Zinc finger proteins as potential targets for toxic metal ions: differential effects on structure and function. Antioxid.Redox.Signal. *3*, 625-634.

Harvey Lodish, Arnold Berk, Lawrence Zipursky, Paul Matsudaira, David Baltimore, and James Darnell (1999). Molecular Cell Biology (New York: W.H.Freeman and Co).

Hastie, N.D. (1992). Dominant negative mutations in the Wilms tumour (WT1) gene cause Denys-Drash syndrome--proof that a tumour-suppressor gene plays a crucial role in normal genitourinary development. Hum.Mol.Genet. *1*, 293-295.

Hausladen, J., Granahan, E., and Bockenhauer, D. (2001). Case report: Teenage girl with proteinuria and amenorrhea. Curr.Opin.Pediatr. *13*, 150-153.

Haws, R.M., Weinberg, A.G., and Baum, M. (1992). Spontaneous remission of congenital nephrotic syndrome: a case report and review of the literature. Pediatr.Nephrol. *6*, 82-84.

Heaton, P.A., Smales, O., and Wong, W. (1999). Congenital nephrotic syndrome responsive to captopril and indometacin. Arch.Dis.Child *81*, 174-175.

Heller, N. and Brandli, A.W. (1997). Xenopus Pax-2 displays multiple splice forms during embryogenesis and pronephric kidney development. Mech.Dev. *69*, 83-104.

Henikoff, S., Greene, E.A., Pietrokovski, S., Bork, P., Attwood, T.K., and Hood, L. (1997). Gene families: the taxonomy of protein paralogs and chimeras. Science *278*, 609-614.

Heymann,W., Hackel, D.B., Harwood, S., Wilson, S.F.G., Hunter, J.L.P. (1959). Production fo the nephritic syndrome in rats by Freund's adjuvants and rat kidney suspensions. Proc. Soc. Exp. Biol. Med. *100*, 660-664.

Hiromura, K., Haseley, L.A., Zhang, P., Monkawa, T., Durvasula, R., Petermann, A.T., Alpers, C.E., Mundel, P., and Shankland, S.J. (2001). Podocyte expression of the CDK-inhibitor p57 during development and disease. Kidney Int.2001.Dec.;60.(6.):2235.-46. *60*, 2235-2246.

Hirose, M. (1999). The role of Wilms' tumor genes. J.Med.Invest. *46*, 130-140.

Hollenberg, S.M., Sternglanz, R., Cheng, P.F., and Weintraub, H. (1995). Identification of a new family of tissue-specific basic helix-loop-helix proteins with a two-hybrid system. Mol.Cell Biol. *15*, 3813-3822.

Holmes, G., Boterashvili, S., English, M., Wainwright, B., Licht, J., and Little, M. (1997). Two N-terminal self-association domains are required for the dominant negative transcriptional activity of WT1 Denys-Drash mutant proteins. Biochem.Biophys.Res.Commun. *233*, 723-728.

Holthofer, H., Miettinen, A., Lehto, V.P., Lehtonen, E., and Virtanen, I. (1984). Expression of vimentin and cytokeratin types of intermediate filament proteins in developing and adult human kidneys. Lab.Invest. *50*, 552-559.

Holthofer, H., Ahola, H., Solin, M.L., Wang, S., Palmen, T., Luimula, P., Miettinen, A., and Kerjaschki, D. (1999). Nephrin localizes at the podocyte filtration slit area and is characteristically spliced in the human kidney. Am.J.Pathol. *155*, 1681-1687.

Holzman, L.B., St John, P.L., Kovari, I.A., Verma, R., Holthofer, H., and Abrahamson, D.R. (1999). Nephrin localizes to the slit pore of the glomerular epithelial cell. Kidney Int. *56*, 1481-1491.

Honda, K., Yamada, T., Endo, R., Ino, Y., Gotoh, M., Tsuda, H., Yamada, Y., Chiba, H., and Hirohashi, S. (1998). Actinin-4, a novel actin-bundling protein associated with cell motility and cancer invasion. J.Cell Biol. *140*, 1383-1393.

Hora, K. (1991). Ultrastructural study of normal rat glomeruli by the quick-freezing and deep-etching method. Nippon.Jinzo.Gakkai.Shi. *33*, 839-848.

Hossain, A. and Saunders, G.F. (2001). The human sex-determining gene SRY is a direct target of WT1. J.Biol.Chem. *276*, 16817-16823.

Huang, M., Gu, G., Ferguson, E.L., and Chalfie, M. (1995). A stomatin-like protein necessary for mechanosensation in C. elegans. Nature *378*, 292-295.

Huber, T.B., Kottgen, M., Schilling, B., Walz, G., and Benzing, T. (2001). Interaction with podocin facilitates nephrin signaling. J.Biol.Chem. *276*, 41543-41546.

Huttunen, N.P. (1976). Congenital nephrotic syndrome of Finnish type. Study of 75 patients. Arch.Dis.Child *51*, 344-348.

Huttunen, N.P., Rapola, J., Vilska, J., and Hallman, N. (1980). Renal pathology in congenital nephrotic syndrome of Finnish type: a quantitative light microscopic study on 50 patients. Int.J.Pediatr.Nephrol. *1*, 10-16.

Ichimura, T., Bonventre, J.V., Bailly, V., Wei, H., Hession, C.A., Cate, R.L., and Sanicola, M. (1998). Kidney injury molecule-1 (KIM-1), a putative epithelial cell adhesion molecule containing a novel immunoglobulin domain, is up-regulated in renal cells after injury. J.Biol.Chem. *273*, 4135-4142.

Igakura, T., Kadomatsu, K., Kaname, T., Muramatsu, H., Fan, Q.W., Miyauchi, T., Toyama, Y., Kuno, N., Yuasa, S., Takahashi, M., Senda, T., Taguchi, O., Yamamura, K., Arimura, K., and Muramatsu, T. (1998). A null mutation in basigin, an immunoglobulin superfamily member, indicates its important roles in peri-implantation development and spermatogenesis. Dev.Biol. *194*, 152-165.

Inkyo-Hayasaka, K., Sakai, T., Kobayashi, N., Shirato, I., and Tomino, Y. (1996). Three-dimensional analysis of the whole mesangium in the rat. Kidney Int. *50*, 672-683.

Inoue, T., Yaoita, E., Kurihara, H., Shimizu, F., Sakai, T., Kobayashi, T., Ohshiro, K., Kawachi, H., Okada, H., Suzuki, H., Kihara, I., and Yamamoto, T. (2001). FAT is a component of glomerular slit diaphragms. Kidney Int.2001. *59*, 1003-1012.

Ito, K., Ger, Y.C., and Kawamura, S. (1986). Actin filament alterations in glomerular epithelial cells of adriamycin-induced nephrotic rats. Acta Pathol.Jpn. *36*, 253-260.

Ito, S., Takata, A., Hataya, H., Ikeda, M., Kikuchi, H., Hata, J., and Honda, M. (2001). Isolated diffuse mesangial sclerosis and Wilms tumor suppressor gene. J.Pediatr. *138*, 425-427.

Ito, S., Ikeda, M., Takata, A., Kikuchi, H., Hata, J., and Honda, M. (1999). Nephrotic syndrome and end-stage renal disease with WT1 mutation detected at 3 years. Pediatr.Nephrol. *13*, 790-791.

Itoh, M., Nagafuchi, A., Moroi, S., and Tsukita, S. (1997). Involvement of ZO-1 in cadherin-based cell adhesion through its direct binding to alpha catenin and actin filaments. J.Cell Biol. *138*, 181-192.

Jadresic, L., Leake, J., Gordon, I., Dillon, M.J., Grant, D.B., Pritchard, J., Risdon, R.A., and Barratt, T.M. (1990). Clinicopathologic review of twelve children with nephropathy, Wilms tumor, and genital abnormalities (Drash syndrome). J.Pediatr. *117*, 717-725.

Jeanpierre, C., Beroud, C., Niaudet, P., and Junien, C. (1998). Software and database for the analysis of mutations in the human WT1 gene. Nucleic.Acids.Res. *26*, 271-274.

Jeanpierre, C., Denamur, E., Henry, I., Cabanis, M.O., Luce, S., Cecille, A., Elion, J., Peuchmaur, M., Loirat, C., Niaudet, P., Gubler, M.C., and Junien, C. (1998). Identification of constitutional WT1 mutations, in patients with isolated diffuse mesangial sclerosis, and analysis of genotype/phenotype correlations by use of a computerized mutation database. Am.J.Hum.Genet. *62*, 824-833.

Jin, D.K., Kang, S.J., Kim, S.J., Bang, E.H., Hwang, H.Z., Tadokoro, K., Yamada, M., and Kohsaka, T. (1999). Transcriptional regulation of PDGF-A and TGF-beta by +KTS WT1 deletion mutants and a mutant mimicking Denys-Drash syndrome. Ren.Fail. *21*, 685-694.

Johnstone, R.W., See, R.H., Sells, S.F., Wang, J., Muthukkumar, S., Englert, C., Haber, D.A., Licht, J.D., Sugrue, S.P., Roberts, T., Rangnekar, V.M., and Shi, Y. (1996). A novel repressor, par-4, modulates transcription and growth suppression functions of the Wilms' tumor suppressor WT1. Mol.Cell Biol. *16*, 6945-6956.

Johnstone, R.W., Wang, J., Tommerup, N., Vissing, H., Roberts, T., and Shi, Y. (1998). Ciao 1 is a novel WD40 protein that interacts with the tumor suppressor protein WT1. J.Biol.Chem. *273*, 10880-10887.

Kanwar, Y.S., Linker, A., and Farquhar, M.G. (1980). Increased permeability of the glomerular basement membrane to ferritin after removal of glycosaminoglycans (heparan sulfate) by enzyme digestion. J.Cell Biol. *86*, 688-693.

Kanwar, Y.S. and Rosenzweig, L.J. (1982). Altered glomerular permeability as a result of focal detachment of the visceral epithelium. Kidney Int. *21*, 565-574.

Kanwar, Y.S., Veis, A., Kimura, J.H., and Jakubowski, M.L. (1984). Characterization of heparan sulfate-proteoglycan of glomerular basement membranes. Proc.Natl.Acad.Sci.U.S.A. *81*, 762-766.

Kanwar, Y.S., Liu, Z.Z., Kashihara, N., and Wallner, E.I. (1991). Current status of the structural and functional basis of glomerular filtration and proteinuria. Semin.Nephrol. *11*, 390-413.

Kaplan, J. and Pollak, M.R.(2001). Familial focal segmental glomerulosclerosis. Curr.Opin.Nephrol.Hypertens. *10*, 183-187.

Kaplan, J.M., Kim, S.H., North, K.N., Rennke, H., Correia, L.A., Tong, H.Q., Mathis, B.J., Rodriguez-Perez, J.C., Allen, P.G., Beggs, A.H., and Pollak, M.R. (2000) Mutations in ACTN4, encoding alpha-actinin-4, cause familial focal segmental glomerulosclerosis. Nat.Genet. *24*, 251-256.

Karle, S.M., Uetz, B., Ronner, V., Glaeser, L., Hildebrandt, F., and Fuchshuber, A. (2002). Novel mutations in NPHS2 detected in both familial and sporadic steroid-resistant nephrotic syndrome. J.Am.Soc.Nephrol. *13*, 388-393.

Karnovsky, M.J. and Ainsworth, S.K. (1972). The structural basis of glomerular filtration. Adv.Nephrol.Necker.Hosp. *2:35-60.*, 35-60.

Katsanis, N., Ansley, S.J., Badano, J.L., Eichers, E.R., Lewis, R.A., Hoskins, B.E., Scambler, P.J., Davidson, W.S., Beales, P.L., and Lupski, J.R. (2001). Triallelic inheritance in Bardet-Biedl syndrome, a Mendelian recessive disorder. Science *293*, 2256-2259.

Keegan, L., Gill, G., and Ptashne, M. (1986). Separation of DNA binding from the transcription-activating function of a eukaryotic regulatory protein. Science *231*, 699-704.

Kennedy, D., Ramsdale, T., Mattick, J., and Little, M. (1996). An RNA recognition motif in Wilms' tumour protein (WT1) revealed by structural modelling. Nat.Genet. *12*, 329-331.

Kent, J., Coriat, A.M., Sharpe, P.T., Hastie, N.D., and van, H., V (1995). The evolution of WT1 sequence and expression pattern in the vertebrates. Oncogene *11*, 1781-1792.

Kerjaschki, D., Ojha, P.P., Susani, M., Horvat, R., Binder, S., Hovorka, A., Hillemanns, P., and Pytela, R. (1989). A beta 1-integrin receptor for fibronectin in human kidney glomeruli. Am.J.Pathol. *134*, 481-489.

Kerjaschki, D., Ullrich, R., Exner, M., Orlando, R.A., and Farquhar, M.G. (1996). Induction of passive Heymann nephritis with antibodies specific for a synthetic peptide derived from the receptor-associated protein. J.Exp.Med. *183*, 2007-2015.

Kerkhoffs, J.L., Harteveld, C.L., Wijermans, P., van Delft, P., Haak, H.L., Bernini, L.F., and Giordano, P.C. (2000). Very mild pathology in a case of Hb S/beta0-thalassemia in combination with a homozygosity for the alpha-thalassemia 3.7 kb deletion. Hemoglobin 2000. *24*, 259-263.

Kestila, M., Mannikko, M., Holmberg, C., Gyapay, G., Weissenbach, J., Savolainen, E.R., Peltonen, L., and Tryggvason, K. (1994). Congenital nephrotic syndrome of the Finnish type maps to the long arm of chromosome 19. Am.J.Hum.Genet. *54*, 757-764.

Kestila, M., Lenkkeri, U., Mannikko, M., Lamerdin, J., McCready, P., Putaala, H., Ruotsalainen, V., Morita, T., Nissinen, M., Herva, R., Kashtan, C.E., Peltonen, L., Holmberg, C., Olsen, A., and Tryggvason, K. (1998). Positionally cloned gene for a novel glomerular protein--nephrin--is mutated in congenital nephrotic syndrome. Mol.Cell *1*, 575-582.

Kikuchi, H., Akasaka, Y., Kurosawa, Y., Yoneyama, H., Kato, S., and Hata, J. (1995). A critical mutation in both WT1 alleles is not sufficient to cause Wilms' tumor. FEBS Lett. *360*, 26-28.

Kikuchi, H., Takata, A., Akasaka, Y., Fukuzawa, R., Yoneyama, H., Kurosawa, Y., Honda, M., Kamiyama, Y., and Hata, J. (1998). Do intronic mutations affecting splicing of WT1 exon 9 cause Frasier syndrome? J.Med.Genet. *35*, 45-48.

Kim, J., Prawitt, D., Bardeesy, N., Torban, E., Vicaner, C., Goodyer, P., Zabel, B., and Pelletier, J. (1999). The Wilms' tumor suppressor gene (wt1) product regulates Dax-1 gene expression during gonadal differentiation. Mol.Cell Biol. *19*, 2289-2299.

Kim, Y.G., Alpers, C.E., Brugarolas, J., Johnson, R.J., Couser, W.G., and Shankland, S.J. (1999). The cyclin kinase inhibitor p21CIP1/WAF1 limits glomerular epithelial cell proliferation in experimental glomerulonephritis. Kidney Int. *55*, 2349-2361.

Kiselyov, V.V., Berezin, V., Maar, T.E., Soroka, V., Edvardsen, K., Schousboe, A., and Bock, E. (1997). The first immunoglobulin-like neural cell adhesion molecule (NCAM) domain is involved in double-reciprocal interaction with the second

immunoglobulin-like NCAM domain and in heparin binding. J.Biol.Chem. *272*, 10125-10134.

Kispert, A., Vainio, S., and McMahon, A.P. (1998). Wnt-4 is a mesenchymal signal for epithelial transformation of metanephric mesenchyme in the developing kidney. Development *125*, 4225-4234.

Klamt, B., Koziell, A., Poulat, F., Wieacker, P., Scambler, P., Berta, P., and Gessler, M. (1998). Frasier syndrome is caused by defective alternative splicing of WT1 leading to an altered ratio of WT1 +/-KTS splice isoforms. Hum.Mol.Genet. *7*, 709-714.

Knudson, A.G.J. and Strong, L.C. (1972). Mutation and cancer: a model for Wilms' tumor of the kidney. J.Natl.Cancer Inst. *48*, 313-324.

Kobayashi, N., Reiser, J., Schwarz, K., Sakai, T., Kriz, W., and Mundel, P. (2001). Process formation of podocytes: morphogenetic activity of microtubules and regulation by protein serine/threonine phosphatase PP2A. Histochem.Cell Biol. *115*, 255-266.

Kohler, B., Schumacher, V., Schulte-Overberg, U., Biewald, W., Lennert, T., l'Allemand, D., Royer-Pokora, B., and Gruters, A. (1999). Bilateral Wilms tumor in a boy with severe hypospadias and cryptochidism due to a heterozygous mutation in the WT1 gene. Pediatr.Res. *45*, 187-190.

Kohsaka, T., Suzuki, T., and Yamada, M. (1997). [Denys-Drash syndrome]. Ryoikibetsu.Shokogun.Shirizu. 599-604.

Kohsaka, T., Tagawa, M., Takekoshi, Y., Yanagisawa, H., Tadokoro, K., and Yamada, M. (1999). Exon 9 mutations in the WT1 gene, without influencing KTS splice isoforms, are also responsible for Frasier syndrome. Hum.Mutat. *14*, 466-470.

Kondo, Y. and Shigematsu, H. (1972). Cellular aspects of rabbit Masugi nephritis. I. Cell kinetics in recoverable glomerulonephritis. Virchows Arch.B.Cell Pathol. *10*, 40-50.

Konig, A., Jakubiczka, S., Wieacker, P., Schlosser, H.W., and Gessler, M. (1993). Further evidence that imbalance of WT1 isoforms may be involved in Denys-Drash syndrome. Hum.Mol.Genet. *2*, 1967-1968.

Korhonen, M., Ylanne, J., Laitinen, L., and Virtanen, I. (1990). The alpha 1-alpha 6 subunits of integrins are characteristically expressed in distinct segments of developing and adult human nephron. J.Cell Biol. *111*, 1245-1254.

Koziell, A., Grech, V., Hussain, S., Lee, G., Lenkkeri, U., Tryggvason, K., and Scambler, P. (2002). Genotype/phenotype correlations of *NPHS1* and NPHS2 mutations in nephrotic syndrome advocate a functional inter-relationship in glomerular filtration. Hum.Mol.Genet. *11*, 379-388.

Koziell, A., Charmandari, E., Hindmarsh, P.C., Rees, L., Scambler, P., and Brook, C.G. (2000). Frasier syndrome, part of the Denys Drash continuum or simply a WT1

gene associated disorder of intersex and nephropathy? Clin.Endocrinol.(Oxf.) *52*, 519-524.

Koziell, A. and Grundy, R. (1999). Frasier and Denys-Drash syndromes: different disorders or part of a spectrum? Arch.Dis.Child *81*, 365-369.

Koziell, A.B., Grundy, R., Barratt, T.M., and Scambler, P. (1999). Evidence for the genetic heterogeneity of nephropathic phenotypes associated with Denys-Drash and Frasier syndromes. Am.J.Hum.Genet. *64*, 1778-1781.

Krawczak, M., Reiss, J., and Cooper, D.N. (1992). The mutational spectrum of single base-pair substitutions in mRNA splice junctions of human genes: causes and consequences. Hum.Genet. *90*, 41-54.

Kreidberg, J.A., Sariola, H., Loring, J.M., Maeda, M., Pelletier, J., Housman, D., and Jaenisch, R. (1993). WT-1 is required for early kidney development. Cell *74*, 679-691.

Kriz, W. (1996). Progressive renal failure--inability of podocytes to replicate and the consequences for development of glomerulosclerosis. Nephrol.Dial.Transplant. *11*, 1738-1742.

Kriz, W., Kretzler, M., Provoost, A.P., and Shirato, I. (1996). Stability and leakiness: opposing challenges to the glomerulus. Kidney Int. *49*, 1570-1574.

Kriz, W., Kretzler, M., Nagata, M., Provoost, A.P., Shirato, I., Uiker, S., Sakai, T., and Lemley, K.V. (1996). A frequent pathway to glomerulosclerosis: deterioration of tuft architecture-podocyte damage-segmental sclerosis. Kidney Blood Press.Res. *19*, 245-253.

Kriz, W., Gretz, N., and Lemley, K.V. (1998). Progression of glomerular diseases: is the podocyte the culprit? Kidney Int. *54*, 687-697.

Kurihara, H., Anderson, J.M., and Farquhar, M.G. (1992). Diversity among tight junctions in rat kidney: glomerular slit diaphragms and endothelial junctions express only one isoform of the tight junction protein ZO-1. Proc.Natl.Acad.Sci.U.S.A. *89*, 7075-7079.

Kurihara, H., Anderson, J.M., and Farquhar, M.G. (1995). Increased Tyr phosphorylation of ZO-1 during modification of tight junctions between glomerular foot processes. Am.J.Physiol. *268*, F514-F524

Kuure, S., Vuolteenaho, R., and Vainio, S. (2000). Kidney morphogenesis: cellular and molecular regulation. Mech.Dev. *92*, 31-45.

Ladomery, M.R., Slight, J., Mc, G.S., and Hastie, N.D. (1999). Presence of WT1, the Wilm's tumor suppressor gene product, in nuclear poly(A)(+) ribonucleoprotein. J.Biol.Chem. *274*, 36520-36526.

Laity, J.H., Dyson, H.J., and Wright, P.E. (2000). Molecular basis for modulation of biological function by alternate splicing of the Wilms' tumor suppressor protein. Proc.Natl.Acad.Sci.U.S.A. *97*, 11932-11935.

Larsson, S.H., Charlieu, J.P., Miyagawa, K., Engelkamp, D., Rassoulzadegan, M., Ross, A., Cuzin, F., van, H., V, and Hastie, N.D. (1995). Subnuclear localization of WT1 in splicing or transcription factor domains is regulated by alternative splicing. Cell *81*, 391-401.

Latta, H. (1970). The glomerular cappillary wall. J.Ultrastruct.Res. *32*, 526-544.

Laurie, G.W., Leblond, C.P., Inoue, S., Martin, G.R., and Chung, A. (1984). Fine structure of the glomerular basement membrane and immunolocalization of five basement membrane components to the lamina densa (basal lamina) and its extensions in both glomeruli and tubules of the rat kidney. Am.J.Anat. *169*, 463-481.

Leahey, A.M., Charnas, L.R., and Nussbaum, R.L. (1993). Nonsense mutations in the OCRL-1 gene in patients with the oculocerebrorenal syndrome of Lowe. Hum.Mol.Genet. *2*, 461-463.

Lee, S.B. and Haber, D.A. (2001). Wilms tumor and the WT1 gene. Exp.Cell Res. *264*, 74-99.

Lee, S.B., Huang, K., Palmer, R., Truong, V.B., Herzlinger, D., Kolquist, K.A., Wong, J., Paulding, C., Yoon, S.K., Gerald, W., Oliner, J.D., and Haber, D.A. (1999). The Wilms tumor suppressor WT1 encodes a transcriptional activator of amphiregulin. Cell *98*, 663-673.

Lee, T.H. and Pelletier, J. (2001). Functional characterization of WT1 binding sites within the human vitamin D receptor gene promoter. Physiol.Genomics *7*, 187-200.

Lenkkeri, U., Mannikko, M., McCready, P., Lamerdin, J., Gribouval, O., Niaudet, P.M., Antignac, C.K., Kashtan, C.E., Homberg, C., Olsen, A., Kestila, M., and Tryggvason, K. (1999). Structure of the gene for congenital nephrotic syndrome of the finnish type (*NPHS1*) and characterization of mutations. Am.J.Hum.Genet. *64*, 51-61.

Li, C., Ruotsalainen, V., Tryggvason, K., Shaw, A.S., and Miner, J.H. (2000). CD2AP is expressed with nephrin in developing podocytes and is found widely in mature kidney and elsewhere. Am.J.Physiol.Renal Physiol. *279*, F785-F792

Li, F.P., Breslow, N.E., Morgan, J.M., Ghahremani, M., Miller, G.A., Grundy, P.E., Green, D.M., Diller, L.R., and Pelletier, J. (1996). Germline WT1 mutations in Wilms' tumor patients: preliminary results. Med.Pediatr.Oncol. *27*, 404-407.

Lim, H.N., Hughes, I.A., and Ross, H.J. (2001). Clinical and molecular evidence for the role of androgens and WT1 in testis descent. Mol.Cell Endocrinol. *185*, 43-50.

Lindahl, P., Hellstrom, M., Kalen, M., Karlsson, L., Pekny, M., Pekna, M., Soriano, P., and Betsholtz, C. (1998). Paracrine PDGF-B/PDGF-Rbeta signaling controls mesangial cell development in kidney glomeruli. Development *125*, 3313-3322.

Little, M., Carman, G., and Donaldson, E. (2000). Novel WT1 exon 9 mutation (D396Y) in a patient with early onset Denys Drash syndrome. Hum.Mutat. *15*, 389

Little, M., Holmes, G., Bickmore, W., van, H., V, Hastie, N., and Wainwright, B. (1995). DNA binding capacity of the WT1 protein is abolished by Denys-Drash syndrome WT1 point mutations. Hum.Mol.Genet. *4* , 351-358.

Little, M. and Wells, C. (1997). A clinical overview of WT1 gene mutations. Hum.Mutat. *9*, 209-225.

Little, M.H., Prosser, J., Condie, A., Smith, P.J., van, H., V, and Hastie, N.D. (1992). Zinc finger point mutations within the WT1 gene in Wilms tumor patients. Proc.Natl.Acad.Sci.U.S.A. *89*, 4791-4795.

Little, M.H., Williamson, K.A., Mannens, M., Kelsey, A., Gosden, C., Hastie, N.D., and van, H., V (1993). Evidence that WT1 mutations in Denys-Drash syndrome patients may act in a dominant-negative fashion. Hum.Mol.Genet. *2*, 259-264.

Little, M.H., Holmes, G., Pell, L., Caricasole, A., Duarte, A., Law, M., Ward, A., and Wainwright, B. (1996). A novel target for the Wilms' tumour suppressor protein (WT1) is bound by a unique combination of zinc fingers. Oncogene *13*, 1461-1469.

Little, N.A., Hastie, N.D., and Davies, R.C. (2000). Identification of WTAP, a novel Wilms' tumour 1-associating protein. Hum.Mol.Genet. *9*, 2231-2239.

Liu, L., Aya, K., Tanaka, H., Shimizu, J., Ito, S., and Seino, Y.(2001). Nephrin is an important component of the barrier system in the testis. Acta Med.Okayama. *55*, 161-165.

Liu, L., Done, S.C., Khoshnoodi, J., Bertorello, A., Wartiovaara, J., Berggren, P.O., and Tryggvason, K. (2001). Defective nephrin trafficking caused by missense mutations in the *NPHS1* gene: insight into the mechanisms of congenital nephrotic syndrome. Hum.Mol.Genet. *10*, 2637-2644.

Lobbert, R.W., Klemm, G., Gruttner, H.P., Harms, D., Winterpacht, A., and Zabel, B.U. (1998). Novel WT1 mutation, 11p LOH, and t(7;12) (p22;q22) chromosomal translocation identified in a Wilms' tumor case. Genes Chromosomes.Cancer *21*, 347-350.

Luimula, P., Ahola, H., Wang, S.X., Solin, M.L., Aaltonen, P., Tikkanen, I., Kerjaschki, D., and Holthofer, H. (2000). Nephrin in experimental glomerular disease. Kidney Int. *58*, 1461-1468.

Maalouf, E.F., Ferguson, J., van, H., V, and Modi, N. (1998). In utero nephropathy, Denys-Drash syndrome and Potter phenotype. Pediatr.Nephrol. *12*, 449-451.

Maas, R.L., Jepeal, L.I., Elfering, S.L., Holcombe, R.F., Morton, C.C., Eddy, R.L., Byers, M.G., Shows, T.B., and Leder, P. (1991). A human gene homologous to the formin gene residing at the murine limb deformity locus: chromosomal location and RFLPs. Am.J.Hum.Genet. *48*, 687-695.

Machin, G.A. (1996). Atypical presentation of Denys-Drash syndrome in a female with a novel Wt1 gene mutation. Birth Defects Orig.Artic.Ser. *30*, 269-286.

MacLean, H.E., Warne, G.L., and Zajac, J.D. (1997). Intersex disorders: shedding light on male sexual differentiation beyond SRY. Clin.Endocrinol.(Oxf.) *46*, 101-108.

Maddox, D.A., Deen, W.M., and Brenner, B.M. (1974). Dynamics of glomerular ultrafiltration. VI. Studies in the primate. Kidney Int. *5*, 271-278.

Mahan, J.D., Mauer, S.M., Sibley, R.K., and Vernier, R.L. (1984). Congenital nephrotic syndrome: evolution of medical management and results of renal transplantation. J.Pediatr. *105*, 549-557.

Maheswaran, S., Englert, C., Lee, S.B., Ezzel, R.M., Settleman, J., and Haber, D.A. (1998). E1B 55K sequesters WT1 along with p53 within a cytoplasmic body in adenovirus-transformed kidney cells. Oncogene *16*, 2041-2050.

Maheswaran, S., Englert, C., Zheng, G., Lee, S.B., Wong, J., Harkin, D.P., Bean, J., Ezzell, R., Garvin, A.J., McCluskey, R.T., DeCaprio, J.A., and Haber, D.A. (1998). Inhibition of cellular proliferation by the Wilms tumor suppressor WT1 requires association with the inducible chaperone Hsp70. Genes Dev. *12*, 1108-1120.

Majumdar, A. and Drummond, I.A. (2000).The zebrafish floating head mutant demonstrates podocytes play an important role in directing glomerular differentiation. Dev.Biol. *222*, 147-157.

Majumdar, A. and Drummond, I.A. (1999). Podocyte differentiation in the absence of endothelial cells as revealed in the zebrafish avascular mutant, cloche. Dev.Genet. *24*, 220-229.

Manivel, J.C., Sibley, R.K., and Dehner, L.P. (1987). Complete and incomplete Drash syndrome: a clinicopathologic study of five cases of a dysontogenetic-neoplastic complex. Hum.Pathol. *18*, 80-89.

Mannikko, M., Kestaila, M., Holmberg, C., Norio, R., Ryynanen, M., Olsen, A., Peltonen, L., and Tryggvason, K. (1995). Fine mapping and haplotype analysis of the locus for congenital nephrotic syndrome on chromosome 19q13.1. Am.J.Hum.Genet. *57*, 1377-1383.

Mannikko, M., Lenkkeri, U., Kashtan, C.E., Kestila, M., Holmberg, C., and Tryggvason, K. (1996). Haplotype analysis of congenital nephrotic syndrome of the Finnish type in non-Finnish families. J.Am.Soc.Nephrol. *7*, 2700-2703.

Mannikko, M., Kestila, M., Lenkkeri, U., Alakurtti, H., Holmberg, C., Leisti, J., Salonen, R., Aula, P., Mustonen, A., Peltonen, L., and Tryggvason, K. (1997). Improved prenatal diagnosis of the congenital nephrotic syndrome of the Finnish type based on DNA analysis. Kidney Int. *51*, 868-872.

Mathias, R., Stecklein, H., Guay-Woodford, L., Harmon, W.E., and Harris, H.W.J. (1989). Gamma globulin deficiency in newborns with congenital nephrotic syndrome. N.Engl.J.Med. *320*, 398-399.

Mathis, B.J., Kim, S.H., Calabrese, K., Haas, M., Seidman, J.G., Seidman, C.E., and Pollak, M.R. (1998). A locus for inherited focal segmental glomerulosclerosis maps to chromosome 19q13. Kidney Int. *53*, 282-286.

Mattoo, T.K., Giangreco, A.B., Afzal, M., and Akhtar, M. (1990). Cystic lymphangiectasia of the kidneys in an infant with nephrotic syndrome. Pediatr.Nephrol. *4*, 228-232.

Mayo, M.W., Wang, C.Y., Drouin, S.S., Madrid, L.V., Marshall, A.F., Reed, J.C., Weissman, B.E., and Baldwin, A.S. (1999). WT1 modulates apoptosis by transcriptionally upregulating the bcl-2 proto-oncogene. EMBO J. *18*, 3990-4003.

McClung, J.K., Danner, D.B., Stewart, D.A., Smith, J.R., Schneider, E.L., Lumpkin, C.K., Dell'Orco, R.T., and Nuell, M.J. (1989). Isolation of a cDNA that hybrid selects antiproliferative mRNA from rat liver. Biochem.Biophys.Res.Commun. *164*, 1316-1322.

McLean, R.H., Kennedy, T.L., Rosoulpour, M., Ratzan, S.K., Siegel, N.J., Kauschansky, A., and Genel, M. (1982). Hypothyroidism in the congenital nephrotic syndrome. J.Pediatr. *101*, 72-75.

McMaster, M.L., Gessler, M., Stanbridge, E.J., and Weissman, B.E. (1995). WT1 expression alters tumorigenicity of the G401 kidney-derived cell line. Cell Growth Differ. *6*, 1609-1617.

McTaggart, S.J., Algar, E., Chow, C.W., Powell, H.R., and Jones, C.L. (2001). Clinical spectrum of Denys-Drash and Frasier syndrome. Pediatr.Nephrol. *16*, 335-339.

Messina, A., Davies, D.J., Dillane, P.C., and Ryan, G.B. (1987). Glomerular epithelial abnormalities associated with the onset of proteinuria in aminonucleoside nephrosis. Am.J.Pathol. *126*, 220-229.

Meyer, T.W., Bennett, P.H., and Nelson, R.G. (1999). Podocyte number predicts long-term urinary albumin excretion in Pima Indians with Type II diabetes and microalbuminuria. Diabetologia *42*, 1341-1344.

Miyamoto, N., Yoshida, M., Kuratani, S., Matsuo, I., and Aizawa, S. (1997). Defects of urogenital development in mice lacking Emx2. Development *124*, 1653-1664.

Moffett, P., Bruening, W., Nakagama, H., Bardeesy, N., Housman, D., Housman, D.E., and Pelletier, J. (1995). Antagonism of WT1 activity by protein self-association. Proc.Natl.Acad.Sci.U.S.A. *92*, 11105-11109.

Montgomery, B.T., Kelalis, P.P., Blute, M.L., Bergstralh, E.J., Beckwith, J.B., Norkool, P., Green, D.M., and D'Angio, G.J. (1991). Extended followup of bilateral Wilms tumor: results of the National Wilms Tumor Study. J.Urol. *146*, 514-518.

Moore, A.W., Schedl, A., McInnes, L., Doyle, M., Hecksher-Sorensen, J., and Hastie, N.D. (1998). YAC transgenic analysis reveals Wilms' tumour 1 gene activity in the proliferating coelomic epithelium, developing diaphragm and limb. Mech.Dev. *79*, 169-184.

Moorthy, A.V., Chesney, R.W., and Lubinsky, M. (1987). Chronic renal failure and XY gonadal dysgenesis: "Frasier" syndrome--a commentary on reported cases. Am.J.Med.Genet.Suppl. *3:297-302.*, 297-302.

Moos, M., Tacke, R., Scherer, H., Teplow, D., Fruh, K., and Schachner, M. (1988). Neural adhesion molecule L1 as a member of the immunoglobulin superfamily with binding domains similar to fibronectin. Nature *334*, 701-703.

Morris, J.F., Madden, S.L., Tournay, O.E., Cook, D.M., Sukhatme, V.P., and Rauscher, F.J. (1991). Characterization of the zinc finger protein encoded by the WT1 Wilms' tumor locus. Oncogene *6*, 2339-2348.

Mrowka, C. and Schedl, A. (2000). Wilms' tumor suppressor gene WT1: from structure to renal pathophysiologic features. J.Am.Soc.Nephrol. *11* Suppl 16: S106-S115

Mueller, R.F. (1994). The Denys-Drash syndrome. J.Med.Genet. *31*, 471-477.

Myers, B.D. and Guasch, A. (1994). Mechanisms of proteinuria in nephrotic humans. Pediatr.Nephrol. *8*, 107-112.

Nachtigal, M.W., Hirokawa, Y., Enyeart-VanHouten, D.L., Flanagan, J.N., Hammer, G.D., and Ingraham, H.A. (1998). Wilms' tumor 1 and Dax-1 modulate the orphan nuclear receptor SF-1 in sex-specific gene expression. Cell *93*, 445-454.

Nadimpalli, R., Yalpani, N., Johal, G.S., and Simmons, C.R. (2000). Prohibitins, stomatins, and plant disease response genes compose a protein superfamily that controls cell proliferation, ion channel regulation, and death. J.Biol.Chem. *275*, 29579-29586.

Nagata, M., Yamaguchi, Y., Komatsu, Y., and Ito, K. (1995). Mitosis and the presence of binucleate cells among glomerular podocytes in diseased human kidneys. Nephron *70*, 68-71.

Nagata, M., Nakayama, K., Terada, Y., Hoshi, S., and Watanabe, T. (1998). Cell cycle regulation and differentiation in the human podocyte lineage. Am.J.Pathol. *153*, 1511-1520.

Nagata, M., Shibata, S., Shigeta, M., Yu-Ming, S., and Watanabe, T. (1999). Cyclin-dependent kinase inhibitors: p27kip1 and p57kip2 expression during human podocyte differentiation. Nephrol.Dial.Transplant. *14 Suppl 1:48-51.*, 48-51.

Nakagama, H., Heinrich, G., Pelletier, J., and Housman, D.E. (1995). Sequence and structural requirements for high-affinity DNA binding by the WT1 gene product. Mol.Cell Biol. *15*, 1489-1498.

Neri, G. and Opitz, J. (1999). Syndromal (and nonsyndromal) forms of male pseudohermaphroditism. Am.J.Med.Genet. *89*, 201-209.

Neufeld, G., Cohen, T., Gengrinovitch, S., and Poltorak, Z. (1999). Vascular endothelial growth factor (VEGF) and its receptors. FASEB J. *13*, 9-22.

Neugarten, J., Medve, I., Lei, J., and Silbiger, S.R. (1999). Estradiol suppresses mesangial cell type I collagen synthesis via activation of the MAP kinase cascade. Am.J.Physiol. *277*, F875-F881

Neuhaus, T.J., Wadhwa, M., Callard, R., and Barratt, T.M. (1995). Increased IL-2, IL-4 and interferon-gamma (IFN-gamma) in steroid-sensitive nephrotic syndrome. Clin.Exp.Immunol. *100*, 475-479.

Neuhaus, T.J., Shah, V., Callard, R.E., and Barratt, T.M. (1995). T-lymphocyte activation in steroid-sensitive nephrotic syndrome in childhood. Nephrol.Dial.Transplant. *10*, 1348-1352.

Ng, P.C. and Henikoff, S. (2001). Predicting deleterious amino acid substitutions. Genome Res. *11*, 863-874.

Noakes, P.G., Miner, J.H., Gautam, M., Cunningham, J.M., Sanes, J.R., and Merlie, J.P. (1995). The renal glomerulus of mice lacking s-laminin/laminin beta 2: nephrosis despite molecular compensation by laminin beta 1. Nat.Genet. *10*, 400-406.

Nordenskjold, A., Friedman, E., and Anvret, M. (1994). WT1 mutations in patients with Denys-Drash syndrome: a novel mutation in exon 8 and paternal allele origin. Hum.Genet. *93*, 115-120.

Nordenskjold, A., Fricke, G., and Anvret, M. (1995). Absence of mutations in the WT1 gene in patients with XY gonadal dysgenesis. Hum.Genet. *96*, 102-104.

Norio, R. (1966). Heredity in the congenital nephrotic syndrome. A genetic study of 57 finnish families with a review of reported cases. Ann.Paediatr.Fenn. *12:Suppl 27:1-94.*, Suppl-94

Norio, R. (1974). Congenital nephrotic syndrome of Finnish type and other types of early familial nephrotic syndromes. Birth Defects Orig.Artic.Ser. *10*, 69-72.

Novak, A., Hsu, S.C., Leung-Hagesteijn, C., Radeva, G., Papkoff, J., Montesano, R., Roskelley, C., Grosschedl, R., and Dedhar, S. (1998). Cell adhesion and the

integrin-linked kinase regulate the LEF-1 and beta-catenin signaling pathways. Proc.Natl.Acad.Sci.U.S.A. *95*, 4374-4379.

Nussbaum, R.L., Orrison, B.M., Janne, P.A., Charnas, L., and Chinault, A.C. (1997). Physical mapping and genomic structure of the Lowe syndrome gene OCRL1. Hum.Genet. *99*, 145-150.

O'Driscoll, L., Kennedy, S., McDermott, E., Kelehan, P., and Clynes, M. (1996). Multiple drug resistance-related messenger RNA expression in archival formalin-fixed paraffin-embedded human breast tumour tissue. Eur.J.Cancer *32A*, 128-133.

O'Neill, J.P., Rogan, P.K., Cariello, N., and Nicklas, J.A. (1998). Mutations that alter RNA splicing of the human HPRT gene: a review of the spectrum. Mutat.Res. *411*, 179-214.

Obrink, B. (1997). CEA adhesion molecules: multifunctional proteins with signal-regulatory properties. Curr.Opin.Cell Biol. *9*, 616-626.

Ogawa, O., Eccles, M.R., Yun, K., Mueller, R.F., Holdaway, M.D., and Reeve, A.E. (1993). A novel insertional mutation at the third zinc finger coding region of the WT1 gene in Denys-Drash syndrome. Hum.Mol.Genet. *2*, 203-204.

Ogura, H., Agata, H., Xie, M., Odaka, T., and Furutani, H. (1997). A study of learning splice sites of DNA sequence by neural networks. Comput.Biol.Med. *27*, 67-75.

Ohno, S., Hora, K., Furukawa, T., and Oguchi, H. (1992). Ultrastructural study of the glomerular slit diaphragm in fresh unfixed kidneys by a quick-freezing method. Virchows Arch.B.Cell Pathol.Incl.Mol.Pathol. *61*, 351-358.

Ohta, S., Ozawa, T., Shiraga, H., and Fuse, H. (2000). Genetic analysis of two female patients with incomplete Denys-Drash syndrome. Endocr.J. *47*, 683-687.

Ohta, S., Ozawa, T., Izumino, K., Sakuragawa, N., and Fuse, H. (2000). A novel missense mutation of the Wt1 gene causing Denys-Drash syndrome with exceptionally mild renal manifestations. J.Urol.2000. *163*, 1857-1858.

Okuhara, K., Tajima, S., Nakae, J., Sasaki, S., Tochimaru, H., Abe, S., and Fujieda, K. (1999). A Japanese case with Frasier syndrome caused by the splice junction mutation of WT1 gene. Endocr.J. *46*, 639-642.

Olsen, A.S., Georgescu, A., Johnson, S., and Carrano, A.V. (1996). Assembly of a 1-Mb restriction-mapped cosmid contig spanning the candidate region for Finnish congenital nephrosis (*NPHS1*) in 19q13.1. Genomics *34*, 223-225.

Oosterwijk, E., Van Muijen, G.N., Oosterwijk-Wakka, J.C., and Warnaar, S.O. (1990). Expression of intermediate-sized filaments in developing and adult human kidney and in renal cell carcinoma. J.Histochem.Cytochem. *38*, 385-392.

Ophascharoensuk, V., Fero, M.L., Hughes, J., Roberts, J.M., and Shankland, S.J. (1998). The cyclin-dependent kinase inhibitor p27Kip1 safeguards against inflammatory injury. Nat.Med. *4*, 575-580.

Orlando, R.A., Takeda, T., Zak, B., Schmieder, S., Benoit, V.M., McQuistan, T., Furthmayr, H., and Farquhar, M.G. (2001). The glomerular epithelial cell anti-adhesin podocalyxin associates with the actin cytoskeleton through interactions with ezrin. J.Am.Soc.Nephrol. *12*, 1589-1598.

Pagani, F., Buratti, E., Stuani, C., Bendix, R., Dork, T., and Baralle, F.E. (2002). A new type of mutation causes a splicing defect in ATM. Nat.Genet. *30*, 426-429.

Palmer, R.E., Kotsianti, A., Cadman, B., Boyd, T., Gerald, W., and Haber, D.A. (2001). WT1 regulates the expression of the major glomerular podocyte membrane protein Podocalyxin. Curr.Biol. *11*, 1805-1809.

Patek, C.E., Little, M.H., Fleming, S., Miles, C., Charlieu, J.P., Clarke, A.R., Miyagawa, K., Christie, S., Doig, J., Harrison, D.J., Porteous, D.J., Brookes, A.J., Hooper, M.L., and Hastie, N.D. (1999). A zinc finger truncation of murine WT1 results in the characteristic urogenital abnormalities of Denys-Drash syndrome. Proc.Natl.Acad.Sci.U.S.A. *96*, 2931-2936.

Patrakka, J., Kestila, M., Wartiovaara, J., Ruotsalainen, V., Tissari, P., Lenkkeri, U., Mannikko, M., Visapaa, I., Holmberg, C., Rapola, J., Tryggvason, K., and Jalanko, H. (2000). Congenital nephrotic syndrome (*NPHS1*): features resulting from different mutations in Finnish patients. Kidney Int. *58*, 972-980.

Pei, Y., Paterson, A.D., Wang, K.R., He, N., Hefferton, D., Watnick, T., Germino, G.G., Parfrey, P., Somlo, S., and St George-Hyslop, P. (2001). Bilineal disease and trans-heterozygotes in autosomal dominant polycystic kidney disease. Am.J.Hum.Genet. *68*, 355-363.

Pelletier, J., Bruening, W., Kashtan, C.E., Mauer, S.M., Manivel, J.C., Striegel, J.E., Houghton, D.C., Junien, C., Habib, R., and Fouser, L. (1991). Germline mutations in the Wilms' tumor suppressor gene are associated with abnormal urogenital development in Denys-Drash syndrome. Cell *67*, 437-447.

Perotti, D., Mondini, P., Giardini, R., Ferrari, A., Massimino, M., Gambirasio, F., Pierotti, M.A., Fossati-Bellani, F., and Radice, P. (1998). No evidence of WT1 involvement in a Burkitt's lymphoma in a patient with Denys-Drash syndrome. Ann.Oncol. *9*, 627-631.

Piscione, T.D. and Rosenblum, N.D. (1999). The malformed kidney: disruption of glomerular and tubular development. Clin.Genet. *56*, 341-356.

Plisov, S.Y., Yoshino, K., Dove, L.F., Higinbotham, K.G., Rubin, J.S., and Perantoni, A.O. (2001). TGF beta 2, LIF and FGF2 cooperate to induce nephrogenesis. Development *128*, 1045-1057.

Poulat, F., Morin, D., Konig, A., Brun, P., Giltay, J., Sultan, C., Dumas, R., Gessler, M., and Berta, P. (1993). Distinct molecular origins for Denys-Drash and Frasier syndromes. Hum.Genet. *91*, 285-286.

Pritchard-Jones, K., Fleming, S., Davidson, D., Bickmore, W., Porteous, D., Gosden, C., Bard, J., Buckler, A., Pelletier, J., and Housman, D. (1990). The candidate Wilms' tumour gene is involved in genitourinary development. Nature *346*, 194-197.

Putaala, H., Soininen, R., Kilpelainen, P., Wartiovaara, J., and Tryggvason, K. (2001). The murine nephrin gene is specifically expressed in kidney, brain and pancreas: inactivation of the gene leads to massive proteinuria and neonatal death. Hum.Mol.Genet. *10*, 1-8.

Putaala, H., Sainio, K., Sariola, H., and Tryggvason, K. (2000). Primary structure of mouse and rat nephrin cDNA and structure and expression of the mouse gene. J.Am.Soc.Nephrol. *11*, 991-1001.

Quaggin, S.E., Schwartz, L., Cui, S., Igarashi, P., Deimling, J., Post, M., and Rossant, J. (1999). The basic-helix-loop-helix protein pod1 is critically important for kidney and lung organogenesis. Development *126*, 5771-5783.

Raats, C.J., Van Den Born, J., and Berden, J.H. (2000). Glomerular heparan sulfate alterations: mechanisms and relevance for proteinuria. Kidney Int. *57*, 385-400.

Rackley, R.R., Flenniken, A.M., Kuriyan, N.P., Kessler, P.M., Stoler, M.H., and Williams, B.R. (1993). Expression of the Wilms' tumor suppressor gene WT1 during mouse embryogenesis. Cell Growth Differ. *4* , 1023-1031.

Ramos, R.G., Igloi, G.L., Lichte, B., Baumann, U., Maier, D., Schneider, T., Brandstatter, J.H., Frohlich, A., and Fischbach, K.F. (1993). The irregular chiasm C-roughest locus of Drosophila, which affects axonal projections and programmed cell death, encodes a novel immunoglobulin-like protein. Genes Dev. *7*, 2533-2547.

Rauscher, F.J., Morris, J.F., Tournay, O.E., Cook, D.M., and Curran, T. (1990). Binding of the Wilms' tumor locus zinc finger protein to the EGR-1 consensus sequence. Science *250*, 1259-1262.

Rauscher, F.J. (1993). The WT1 Wilms tumor gene product: a developmentally regulated transcription factor in the kidney that functions as a tumor suppressor. FASEB J. *7*, 896-903.

Rayl, E.A., Moroson, B.A., and Beardsley, G.P. (1996). The human purH gene product, 5-aminoimidazole-4-carboxamide ribonucleotide formyltransferase/IMP cyclohydrolase. Cloning, sequencing, expression, purification, kinetic analysis, and domain mapping. J.Biol.Chem. *271*, 2225-2233.

Reddy, J.C., Morris, J.C., Wang, J., English, M.A., Haber, D.A., Shi, Y., and Licht, J.D. (1995). WT1-mediated transcriptional activation is inhibited by dominant negative mutant proteins. J.Biol.Chem. *270*, 10878-10884.

Reeves, W., Caulfield, J.P., and Farquhar, M.G. (1978). Differentiation of epithelial foot processes and filtration slits: sequential appearance of occluding junctions, epithelial polyanion, and slit membranes in developing glomeruli. Lab.Invest. *39*, 90-100.

Regele, H.M., Fillipovic, E., Langer, B., Poczewki, H., Kraxberger, I., Bittner, R.E., and Kerjaschki, D. (2000). Glomerular expression of dystroglycans is reduced in minimal change nephrosis but not in focal segmental glomerulosclerosis. J.Am.Soc.Nephrol. *11*, 403-412.

Reiser, J., Kriz, W., Kretzler, M., and Mundel, P. (2000). The glomerular slit diaphragm is a modified adherens junction. J.Am.Soc.Nephrol. *11*, 1-8.

Renshaw, J., King-Underwood, L., and Pritchard-Jones, K. (1997). Differential splicing of exon 5 of the Wilms tumour (WTI) gene. Genes Chromosomes.Cancer *19*, 256-266.

Ricardo, S.D., Bertram, J.F., and Ryan, G.B. (1994). Reactive oxygen species in puromycin aminonucleoside nephrosis: in vitro studies. Kidney Int. *45*, 1057-1069.

Richard, D.J., Schumacher, V., Royer-Pokora, B., and Roberts, S.G. (2001). Par4 is a coactivator for a splice isoform-specific transcriptional activation domain in WT1. Genes Dev. *15*, 328-339.

Rodewald, R. and Karnovsky, M.J. (1974). Porous substructure of the glomerular slit diaphragm in the rat and mouse. J.Cell Biol. *60*, 423-433.

Roselli, S., Gribouval, O., Boute, N., Sich, M., Benessy, F., Attie, T., Gubler, M.C., and Antignac, C. (2002). Podocin localizes in the kidney to the slit diaphragm area. Am.J.Pathol. *160*, 131-139.

Rothenpieler, U.W. and Dressler, G.R. (1993). Pax-2 is required for mesenchyme-to-epithelium conversion during kidney development. Development *119*, 711-720.

Rudin, C., Pritchard, J., Fernando, O.N., Duffy, P.G., and Trompeter, R.S. (1998). Renal transplantation in the management of bilateral Wilms' tumour (BWT) and of Denys-Drash syndrome (DDS). Nephrol.Dial.Transplant. *13*, 1506-1510.

Ruotsalainen, V., Patrakka, J., Tissari, P., Reponen, P., Hess, M., Kestila, M., Holmberg, C., Salonen, R., Heikinheimo, M., Wartiovaara, J., Tryggvason, K., and Jalanko, H. (2000). Role of nephrin in cell junction formation in human nephrogenesis. Am.J.Pathol. *157*, 1905-1916.

Ryan, G., Steele-Perkins, V., Morris, J.F., Rauscher, F.J., and Dressler, G.R. (1995). Repression of Pax-2 by WT1 during normal kidney development. Development *121*, 867-875.

Saiki, R.K., Scharf, S., Faloona, F., Mullis, K.B., Horn, G.T., Erlich, H.A., and Arnheim, N. (1985). Enzymatic amplification of beta-globin genomic sequences and restriction site analysis for diagnosis of sickle cell anemia. Science *230*, 1350-1354.

Saiki, R.K., Gelfand, D.H., Stoffel, S., Scharf, S.J., Higuchi, R., Horn, G.T., Mullis, K.B., and Erlich, H.A. (1988). Primer-directed enzymatic amplification of DNA with a thermostable DNA polymerase. Science *239*, 487-491.

Sakai, A., Tadokoro, K., Yanagisawa, H., Nagafuchi, S., Hoshikawa, N., Suzuki, T., Kohsaka, T., Hasegawa, T., Nakahori, Y., and Yamada, M. (1993). A novel mutation of the WT1 gene (a tumor suppressor gene for Wilms' tumor) in a patient with Denys-Drash syndrome. Hum.Mol.Genet. *2*, 1969-1970.

Sakamoto, Y., Yoshida, M., Semba, K., and Hunter, T. (1997). Inhibition of the DNA-binding and transcriptional repression activity of the Wilms' tumor gene product, WT1, by cAMP-dependent protein kinase-mediated phosphorylation of Ser-365 and Ser-393 in the zinc finger domain. Oncogene *15*, 2001-2012.

Sakazume, S. (2001). Wilms tumor-pseudohermaphroditism-glomerulopathy, Denys-Drash type. Ryoikibetsu.Shokogun.Shirizu. *(34.Pt.2.)*, 813-814.

Salomon, R., Gubler, M.C., and Niaudet, P. (2000). Genetics of the nephrotic syndrome. Curr.Opin.Pediatr. *12*, 129-134.

Salzer, U. and Prohaska, R. (2001). Stomatin, flotillin-1, and flotillin-2 are major integral proteins of erythrocyte lipid rafts. Blood *97*, 1141-1143.

Sambrook, J., Fritsch, E., and Maniatis, T. (1989). Molecular Cloning, a laboratory manual (Cold Spring Harbour Laboratory Press).

Sariola, H. (1984). Incomplete fusion of the epithelial and endothelial basement membranes in interspecies hybrid glomeruli. Cell Differ. *14*, 189-195.

Saxen, L. (1987). Organogenesis of the Kidney. (Cambridge, UK: Cambridge Univ. Press).

Scharnhorst, V., van der Eb, A.J., and Jochemsen, A.G. (2001). WT1 proteins: functions in growth and differentiation. Gene *273*, 141-161.

Scharnhorst, V., Dekker, P., van der Eb, A.J., and Jochemsen, A.G. (2000). Physical interaction between Wilms tumor 1 and p73 proteins modulates their functions. J.Biol.Chem. *275*, 10202-10211.

Scharnhorst, V., Dekker, P., van der Eb, A.J., and Jochemsen, A.G. (1999). Internal translation initiation generates novel WT1 protein isoforms with distinct biological properties. J.Biol.Chem. *274*, 23456-23462.

Schedl, A. and Hastie, N.D. (2000). Cross-talk in kidney development. Curr.Opin.Genet.Dev. *10*, 543-549.

Schmitt, K., Zabel, B., Tulzer, G., Eitelberger, F., and Pelletier, J. (1995). Nephropathy with Wilms tumour or gonadal dysgenesis: incomplete Denys-Drash syndrome or separate diseases? Eur.J.Pediatr. *154*, 577-581.

Schnabel, E., Dekan, G., Miettinen, A., and Farquhar, M.G. (1989). Biogenesis of podocalyxin--the major glomerular sialoglycoprotein--in the newborn rat kidney. Eur.J.Cell Biol. *48*, 313-326.

Schnabel, E., Anderson, J.M., and Farquhar, M.G. (1990). The tight junction protein ZO-1 is concentrated along slit diaphragms of the glomerular epithelium. J.Cell Biol. *111*, 1255-1263.

Schneider, S., Wildhardt, G., Ludwig, R., and Royer-Pokora, B. (1993). Exon skipping due to a mutation in a donor splice site in the WT-1 gene is associated with Wilms' tumor and severe genital malformations. Hum.Genet. *91*, 599-604.

Schultz, J., Milpetz, F., Bork, P., and Ponting, C.P. (1998). SMART, a simple modular architecture research tool: identification of signaling domains. Proc.Natl.Acad.Sci.U.S.A. *95*, 5857-5864.

Schumacher, V., Scharer, K., Wuhl, E., Altrogge, H., Bonzel, K.E., Guschmann, M., Neuhaus, T.J., Pollastro, R.M., Kuwertz-Broking, E., Bulla, M., Tondera, A.M., Mundel, P., Helmchen, U., Waldherr, R., Weirich, A., and Royer-Pokora, B. (1998). Spectrum of early onset nephrotic syndrome associated with WT1 missense mutations. Kidney Int. *53*, 1594-1600.

Schwarz, K., Simons, M., Reiser, J., Saleem, M.A., Faul, C., Kriz, W., Shaw, A.S., Holzman, L.B., and Mundel, P. (2001). Podocin, a raft-associated component of the glomerular slit diaphragm, interacts with CD2AP and nephrin. J.Clin.Invest. *108*, 1621-1629.

Seiler, M.W., Venkatachalam, M.A., and Cotran, R.S. (1975). Glomerular epithelium: structural alterations induced by polycations. Science *189*, 390-393.

Seppala, M., Rapola, J., Huttunen, N.P., Aula, P., Karjalainen, O., and Ruoslahti, E. (1976). Congenital nephrotic syndrome: prenatal diagnosis and genetic counselling by estimation of aminotic-fluid and maternal serum alpha-fetoprotein. Lancet *2*, 123-125.

Serluca, F.C. and Fishman, M.C. (2001). Pre-pattern in the pronephric kidney field of zebrafish. Development *128*, 2233-2241.

Shankland, S.J., Eitner, F., Hudkins, K.L., Goodpaster, T., D'Agati, V., and Alpers, C.E. (2000). Differential expression of cyclin-dependent kinase inhibitors in human glomerular disease: role in podocyte proliferation and maturation. Kidney Int. *58*, 674-683.

Shankland, S.J. (1999). Cell cycle regulatory proteins in glomerular disease. Kidney Int. *56*, 1208-1215.

Sharma, P.M., Bowman, M., Madden, S.L., Rauscher, F.J., and Sukumar, S. (1994). RNA editing in the Wilms' tumor susceptibility gene, WT1. Genes Dev. *8*, 720-731.

Shigemoto, K., Brennan, J., Walls, E., Watson, C.J., Stott, D., Rigby, P.W., and Reith, A.D. (2001). Identification and characterisation of a developmentally regulated mammalian gene that utilises -1 programmed ribosomal frameshifting. Nucleic.Acids.Res. *29*, 4079-4088.

Shih, N.Y., Li, J., Cotran, R., Mundel, P., Miner, J.H., and Shaw, A.S. (2001). CD2AP localizes to the slit diaphragm and binds to nephrin via a novel C-terminal domain. Am.J.Pathol. *159*, 2303-2308.

Shih, N.Y., Li, J., Karpitskii, V., Nguyen, A., Dustin, M.L., Kanagawa, O., Miner, J.H., and Shaw, A.S. (1999). Congenital nephrotic syndrome in mice lacking CD2-associated protein. Science *286*, 312-315.

Shimamura, R., Fraizer, G.C., Trapman, J., Lau, Y., and Saunders, G.F. (1997). The Wilms' tumor gene WT1 can regulate genes involved in sex determination and differentiation: SRY, Mullerian-inhibiting substance, and the androgen receptor. Clin.Cancer Res. *3*, 2571-2580.

Sibley, R.K., Mahan, J., Mauer, S.M., and Vernier, R.L. (1985). A clinicopathologic study of forty-eight infants with nephrotic syndrome. Kidney Int. *27*, 544-552.

Siegel, J.F., Delakas, D., Rai, S., and Kushner, L. (1996). Unilateral nephrectomy induces the expression of the Wilms tumor gene in the contralateral kidney of the adult rat. J.Urol. *156*, 688-692.

Silbiger, S., Lei, J., and Neugarten, J. (1999). Estradiol suppresses type I collagen synthesis in mesangial cells via activation of activator protein-1. Kidney Int. *55*, 1268-1276.

Simons, K. and Toomre, D. (2000). Lipid rafts and signal transduction. Nat.Rev.Mol.Cell Biol. *1*, 31-39.

Simons, K. and Ikonen, E. (1997). Functional rafts in cell membranes. Nature *387*, 569-572.

Simons, M., Schwarz, K., Kriz, W., Miettinen, A., Reiser, J., Mundel, P., and Holthofer, H. Involvement of lipid rafts in nephrin phosphorylation and organization of the glomerular slit diaphragm. (2001). Am.J.Pathol.2001. *159*, 1069-1077.

Smeets, H.J., Knoers, V.V., van de Heuvel, L.P., Lemmink, H.H., Schroder, C.H., and Monnens, L.A. (1996). Hereditary disorders of the glomerular basement membrane. Pediatr.Nephrol. *10*, 779-788.

Smith, G., Winterborn, M., and White, R.H. (1991). Spontaneous resolution of congenital nephrotic syndrome in a neonate. Arch.Dis.Child *66*, 752-753.

Smoyer, W.E. and Mundel, P. (1998). Regulation of podocyte structure during the development of nephrotic syndrome. J.Mol.Med. *76*, 172-183.

Somlo, S. and Mundel, P. (2000). Getting a foothold in nephrotic syndrome. Nat.Genet. *24*, 333-335.

Sonderegger, P. and Rathjen, F.G. (1992). Regulation of axonal growth in the vertebrate nervous system by interactions between glycoproteins belonging to two subgroups of the immunoglobulin superfamily. J.Cell Biol. *119*, 1387-1394.

Stallmach, T., Neuhaus, T.J., Kosters, R., and Hailemariam, S. (1998). [Glomerulopathy in Denys-Drash syndrome. Case report of a model disease]. Pathologe. *19*, 230-234.

Stewart, G.W., Hepworth-Jones, B.E., Keen, J.N., Dash, B.C., Argent, A.C., and Casimir, C.M. (1992). Isolation of cDNA coding for an ubiquitous membrane protein deficient in high Na+, low K+ stomatocytic erythrocytes. Blood *79*, 1593-1601.

Stewart, G.W. (1993). The membrane defect in hereditary stomatocytosis. Baillieres.Clin.Haematol. *6*, 371-399.

Stockand, J.D. and Sansom, S.C. (1998). Glomerular mesangial cells: electrophysiology and regulation of contraction. Physiol.Rev. *78*, 723-744.

Stump, T. and Garett, R. (1954). Bilateral Wilms' tumour in a male pseudohermaphrodite. Journal of Urology *72:11*, 1146-1152.

Sukhatme, V.P., Cao, X.M., Chang, L.C., Tsai-Morris, C.H., Stamenkovich, D., Ferreira, P.C., Cohen, D.R., Edwards, S.A., Shows, T.B., and Curran, T. (1988). A zinc finger-encoding gene coregulated with c-fos during growth and differentiation, and after cellular depolarization. Cell *53*, 37-43.

Suri, M., Kabra, M., Kataria, A., Singh, G.R., Sharma, S., Gupta, A.K., Menon, P.S., and Verma, I.C. (1995). Denys-Drash syndrome. Indian Pediatr. *32*, 1310-1313.

Swiatecka-Urban, A., Mokrzycki, M.H., Kaskel, F., Da Silva, F., and Denamur, E. (2001). Novel WT1 mutation (C388Y) in a female child with Denys-Drash syndrome. Pediatr.Nephrol. *16*, 627-630.

Tajinda, K., Carroll, J., and Roberts, C.T.J. (1999). Regulation of insulin-like growth factor I receptor promoter activity by wild-type and mutant versions of the WT1 tumor suppressor. Endocrinology *140* , 4713-4724.

Takahashi, T., Takahashi, K., Gerety, S., Wang, H., Anderson, D.J., and Daniel, T.O. (2001). Temporally compartmentalized expression of ephrin-B2 during renal glomerular development. J.Am.Soc.Nephrol. *12*, 2673-2682.

Tapon, N., Nagata, K., Lamarche, N., and Hall, A. (1998). A new rac target POSH is an SH3-containing scaffold protein involved in the JNK and NF-kappaB signalling pathways. EMBO J. *17*, 1395-1404.

Tavernarakis, N. and Driscoll, M. (1997). Molecular modeling of mechanotransduction in the nematode Caenorhabditis elegans. Annu.Rev.Physiol. *59:659-89.*, 659-689.

Taylor, G.M., Neuhaus, T.J., Shah, V., Dillon, S., and Barratt, T.M. (1997). Charge and size selectivity of proteinuria in children with idiopathic nephrotic syndrome. Pediatr.Nephrol. *11*, 404-410.

Tisher C and Madsen K (1991). Anatomy of the Kidney. In Kideny. B.M. Brenner and F. Rector, eds. (Philadelphia, USA: W.B. Saunders company),

Topham, P.S., Kawachi, H., Haydar, S.A., Chugh, S., Addona, T.A., Charron, K.B., Holzman, L.B., Shia, M., Shimizu, F., and Salant, D.J. (1999). Nephritogenic mAb 5-1-6 is directed at the extracellular domain of rat nephrin. J.Clin.Invest. *104*, 1559-1566.

Troyanovsky, B., Levchenko, T., Mansson, G., Matvijenko, O., and Holmgren, L. (1902). Angiomotin: an angiostatin binding protein that regulates endothelial cell migration and tube formation. J.Cell Biol.2001.Mar. *152*, 1247-1254.

Tryggvason, K. and Wartiovaara, J. (2001). Molecular basis of glomerular permselectivity. Curr.Opin.Nephrol.Hypertens. *10*, 543-549.

Tryggvason, K. (1978). Morphometric studies on glomeruli in the congenital nephrotic syndrome. Nephron *22*, 544-550.

Tryggvason, K. (1999). Unraveling the mechanisms of glomerular ultrafiltration: nephrin, a key component of the slit diaphragm. J.Am.Soc.Nephrol. *10*, 2440-2445.

Tsuchida, Y., Yokomori, K., and Choi, S.H. (1995). [Hereditary renal tumors: Wilms' tumor--congenital anomalies' syndrome]. Nippon.Rinsho. *53*, 2742-2748.

Tsuda, M., Sakiyama, T., Kitagawa, T., Watanabe, S., Watanabe, T., Takahashi, S., Kawaguchi, H., and Ito, K. (1993). Molecular analysis of two Japanese cases of Denys-Drash syndrome. J.Inherit.Metab.Dis. *16*, 876-880.

Tsuda, M., Sakiyama, T., Owada, M., and Chiba, Y. (1996). A newly identified exonic mutation of the WT1 gene in a patient with Denys-Drash syndrome. Acta Paediatr.Jpn. *38*, 265-266.

Tsukaguchi, H., Abreu, P., Pereira, A., and Pollak, M. (2000). Missense Mutations in Podocin in a Family with Adult Onset FSGS. J.Am.Soc.Nephrol. (Abstract)

Tsukamoto, Y., Matsumoto, T., Taira, E., Kotani, T., Yamate, J., Takaha, N., Tatesaki, R., Namikawa, T., Miki, N., and Sakuma, S. (1998). Adhesive activity of gicerin, a cell-adhesion molecule, in kidneys and nephroblastomas of chickens. Cell Tissue Res. *292*, 137-142.

van den Heuvel, L.P., Westenend, P.J., Van Den Born, J., Assmann, K.J., Knoers, N., and Monnens, L.A. (1995). Aberrant proteoglycan composition of the

glomerular basement membrane in a patient with Denys-Drash syndrome. Nephrol.Dial.Transplant. *10*, 2205-2211.

Venkatachalam, M.A. and Rennke, H.G. (1978). The structural and molecular basis of glomerular filtration. Circ.Res. *43*, 337-347.

Verloes, A., Massart, B., Dehalleux, I., Langhendries, J.P., and Koulischer, L. (1995). Clinical overlap of Beckwith-Wiedemann, Perlman and Simpson-Golabi-Behmel syndromes: a diagnostic pitfall. Clin.Genet. *47*, 257-262.

Vicanek, C., Ferretti, E., Goodyer, C., Torban, E., Moffett, P., Pelletier, J., and Goodyer, P. (1997). Regulation of renal EGF receptor expression is normal in Denys-Drash syndrome. Kidney Int. *52*, 614-619.

Vollrath, D., Jaramillo-Babb, V.L., Clough, M.V., McIntosh, I., Scott, K.M., Lichter, P.R., and Richards, J.E. (1998). Loss-of-function mutations in the LIM-homeodomain gene, LMX1B, in nail-patella syndrome. Hum.Mol.Genet. *7*, 1091-1098.

Wagner, K.J., Patek, C.E., Miles, C., Christie, S., Brookes, A.J., and Hooper, M.L. (2001). Truncation of WT1 results in downregulation of cyclin G1 and IGFBP-4 expression. Biochem.Biophys.Res.Commun. *287*, 977-982.

Wang, Z.Y., Qiu, Q.Q., Enger, K.T., and Deuel, T.F. (1993). A second transcriptionally active DNA-binding site for the Wilms tumor gene product, WT1. Proc.Natl.Acad.Sci.U.S.A. *90*, 8896-8900.

Wang, Z.Y., Qiu, Q.Q., Gurrieri, M., Huang, J., and Deuel, T.F. (1995). WT1, the Wilms' tumor suppressor gene product, represses transcription through an interactive nuclear protein. Oncogene *10*, 1243-1247.

Wang, Z.Y., Qiu, Q.Q., Seufert, W., Taguchi, T., Testa, J.R., Whitmore, S.A., Callen, D.F., Welsh, D., Shenk, T., and Deuel, T.F. (1996). Molecular cloning of the cDNA and chromosome localization of the gene for human ubiquitin-conjugating enzyme 9. J.Biol.Chem. *271*, 24811-24816.

Ward, A., Pooler, J.A., Miyagawa, K., Duarte, A., Hastie, N.D., and Caricasole, A. (1995). Repression of promoters for the mouse insulin-like growth factor II-encoding gene (Igf-2) by products of the Wilms' tumour suppressor gene wt1. Gene *167*, 239-243.

Watanabe, H., Sakai, T., Kobayashi, N., Fukuda, Y., and Yabuta, K. (1996). Glomerular basement membrane outpockets and glomerular growth in the postnatal development of the rat kidney. Pediatr.Nephrol. *10*, 461-466.

Watnick, T., He, N., Wang, K., Liang, Y., Parfrey, P., Hefferton, D., St George-Hyslop, P., Germino, G., and Pei, Y. (2000). Mutations of PKD1 in ADPKD2 cysts suggest a pathogenic effect of trans-heterozygous mutations. Nat.Genet. *25*, 143-144.

Webster, N.J., Kong, Y., Sharma, P., Haas, M., Sukumar, S., and Seely, B.L. (1997). Differential effects of Wilms tumor WT1 splice variants on the insulin receptor promoter. Biochem.Mol.Med. *62*, 139-150.

Weiher, H., Noda, T., Gray, D.A., Sharpe, A.H., and Jaenisch, R. (1990). Transgenic mouse model of kidney disease: insertional inactivation of ubiquitously expressed gene leads to nephrotic syndrome. Cell *62*, 425-434.

Wharram, B.L., Goyal, M., Gillespie, P.J., Wiggins, J.E., Kershaw, D.B., Holzman, L.B., Dysko, R.C., Saunders, T.L., Samuelson, L.C., and Wiggins, R.C. (2000). Altered podocyte structure in GLEPP1 (Ptpro)-deficient mice associated with hypertension and low glomerular filtration rate. J.Clin.Invest. *106*, 1281-1290.

White, R.H. (1973). The familial nephrotic syndrome. I. A European survey. Clin.Nephrol. *1*, 215-219.

Whiteside, C., Prutis, K., Cameron, R., and Thompson, J. (1989). Glomerular epithelial detachment, not reduced charge density, correlates with proteinuria in adriamycin and puromycin nephrosis. Lab.Invest. *61*, 650-660.

Winn, M.P., Conlon, P.J., Lynn, K.L., Howell, D.N., Slotterbeck, B.D., Smith, A.H., Graham, F.L., Bembe, M., Quarles, L.D., Pericak-Vance, M.A., and Vance, J.M. (1999). Linkage of a gene causing familial focal segmental glomerulosclerosis to chromosome 11 and further evidence of genetic heterogeneity. Genomics *58*, 113-120.

Xiao, S., Gillespie, D.G., Baylis, C., Jackson, E.K., and Dubey, R.K. (2001). Effects of estradiol and its metabolites on glomerular endothelial nitric oxide synthesis and mesangial cell growth. Hypertension *37*, 645-650.

Xu, P.X., Adams, J., Peters, H., Brown, M.C., Heaney, S., and Maas, R. (1999). Eya1-deficient mice lack ears and kidneys and show abnormal apoptosis of organ primordia. Nat.Genet. *23*, 113-117.

Yan, K., Khoshnoodi, J., Ruotsalainen, V., and Tryggvason, K. (2002). N-linked glycosylation is critical for plasma membrane localisation of nephrin. J.Am.Soc Nephrol. *13*, 1385-1389

Yang, Y., Zhang, S.Y., Sich, M., Beziau, A., van den Heuvel, L.P., and Gubler, M.C. (2001). Glomerular extracellular matrix and growth factors in diffuse mesangial sclerosis. Pediatr.Nephrol. *16*, 429-438.

Yang, Y., Jeanpierre, C., Dressler, G.R., Lacoste, M., Niaudet, P., and Gubler, M.C. (1999). WT1 and PAX-2 podocyte expression in Denys-Drash syndrome and isolated diffuse mesangial sclerosis. Am.J.Pathol. *154*, 181-192.

Yaoita, E., Kawasaki, K., Yamamoto, T., and Kihara, I. (1990). Variable expression of desmin in rat glomerular epithelial cells. Am.J.Pathol. *136*, 899-908.

Ye, Y., Raychaudhuri, B., Gurney, A., Campbell, C.E., and Williams, B.R. (1996). Regulation of WT1 by phosphorylation: inhibition of DNA binding, alteration of transcriptional activity and cellular translocation. EMBO J. *15*, 5606-5615.

Yu, Y., Leng, C.G., Kato, Y., and Ohno, S. (1997). Ultrastructural study of glomerular capillary loops at different perfusion pressures as revealed by quick-freezing, freeze-substitution and conventional fixation methods. Nephron *76*, 452-459.

Yuan, H., Takeuchi, E., and Salant, D.J. (2002). Podocyte slit-diaphragm protein nephrin is linked to the actin cytoskeleton. Am.J.Physiol.Renal Physiol. *282*, F585-F591

Zatz, M., Vainzof, M., and Passos-Bueno, M.R. (2000). Limb-girdle muscular dystrophy: one gene with different phenotypes, one phenotype with different genes. Curr.Opin.Neurol. *13*, 511-517.

Zdravkovic, D., Milenkovic, T., Sedlecki, K., Guc-Scekic, M., Rajic, V., and Banicevic, M. (2001). Causes of ambiguous external genitalia in neonates. Srp.Arh.Celok.Lek. *129*, 57-60.

Zeis, P.M., Sotsiou, F., and Sinaniotis, C. (1996). Congenital nephrotic syndrome, diffuse mesangial sclerosis, and bilateral cataract. Pediatr.Nephrol. *10*, 732-733.

Zhai, G., Iskandar, M., Barilla, K., and Romaniuk, P.J. (2001). Characterization of RNA aptamer binding by the Wilms' tumor suppressor protein WT1. Biochemistry *40*, 2032-2040.

Zhan, Q., Chen, I.T., Antinore, M.J., and Fornace, A.J.J. (1998). Tumor suppressor p53 can participate in transcriptional induction of the GADD45 promoter in the absence of direct DNA binding. Mol.Cell Biol. *18*, 2768-2778.

Zhang, J., Ofevrstedt, L., Khoshnoodi, J., Skoglund, U., and Tryggvason, K. (2001). Molecular structure of recombinant nephrin by electron tomography. ASN abstract A2179: paper presented at the ASN/ISN World Congress of Nephrology, San Francisco, CA, USA